DISS. ETH NO. 27377

Identification of the TRPV4 ion channel as a mechanotransducer and therapeutic target in low back pain

A thesis submitted to attain the degree of

DOCTOR OF SCIENCES of ETH ZURICH

(Dr. sc. ETH Zurich)

presented by

Elena Cambria

MSc in Bioengineering, Ecole polytechnique fédérale de Lausanne (EPFL)

born on 02.12.1989

citizen of

Switzerland (Bagnes, VS) and Italy

accepted on the recommendation of

Prof. Dr. Stephen J. Ferguson, examiner

Prof. Dr. Karin Wuertz-Kozak, co-examiner

Prof. Dr. Mauro Alini, co-examiner

2021

Dedicated to those who believed in me and supported me
during the realization of this doctoral project

Table of contents

Acknowledgements

Summary

Low back pain (LBP) is the leading cause of disability worldwide and a huge global socio-economic burden. The costs related to LBP are projected to further increase in the coming decades due to the growth and aging of the global population. Degenerative disc disease, which is characterized by intervertebral disc (IVD) degeneration, inflammation, and nerve ingrowth, principally contributes to LBP. One of the main contributors to IVD degeneration is excessive or aberrant mechanical loading. Current treatments of LBP, including physical, psychological, pharmacological, and surgical approaches, have unclear mechanisms of action, low effect sizes, and are not beneficial in the long term. Targeted therapeutic strategies in preclinical development, such as molecular and gene therapy, selectively address the biological changes that occur in IVD degeneration. Nevertheless, despite the mechanical nature of LBP, mechanotransduction pathways are currently not targeted. This is mainly due to the very limited information on mechanosensing and mechanotransduction mechanisms in the IVD. Transient receptor potential (TRP) ion channels are promising therapeutic targets to treat LBP, as they can sense and transduce a variety of signals, including mechanical stress. The TRP vanilloid 4 (TRPV4) channel is especially interesting, as it was shown to mediate mechanical, inflammatory and pain signals. Its clinical potential is further highlighted by ongoing preclinical and clinical trials. The overall goal of this thesis was to investigate the potential role of TRPV4 in mediating hyperphysiological mechanical signals in the IVD, and its relevance as a therapeutic target to treat LBP.

As a first step towards the investigation of TRPV4, we developed a novel in vitro compression model for mechanotransduction studies. Agarose-collagen composite hydrogels were fabricated and characterized in terms of material and mechanical properties. Bovine nucleus pulposus (NP) cell phenotype and mechanotransduction ability after dynamic compression were further analyzed. Agarose-collagen composite hydrogels combined the mechanical strength of agarose with the biofunctionality of collagen, which enhanced cell adhesion and the activation of focal adhesion kinases. Moreover, agarose-collagen scaffolds recapitulated the extracellular matrix (ECM) of the IVD, with their non-fibrillar matrix and collagen fibers, and allowed the exploration of mechanotransduction mechanisms in a reproducible system.

In a second study, NP cell-laden agarose-collagen hydrogels and a mouse model were used to investigate the role of TRPV4 in transducing hyperphysiological dynamic compression. Degenerative changes and the expression of the inflammatory mediator cyclooxygenase 2 (COX2) were examined in mouse IVDs that were dynamically compressed at a hyperphysiological regime (versus sham). Cell damage and inflammation (prostaglandin E2 (PGE2) release) were measured in bovine NP cells embedded in agarose-collagen hydrogels and dynamically compressed at a hyperphysiological regime with or without TRPV4 inhibition. The activation of the mitogen-activated protein kinase (MAPK) pathways was analyzed. Finally, degenerative changes and COX2 expression were further evaluated in the IVDs of trpv4 knockout (KO) mice (versus wild-type). TRPV4 was shown to regulate the COX2/PGE2 inflammatory factors and mediate cell damage induced by hyperphysiological dynamic compression, possibly via the extracellular signal-regulated kinases 1/2 (ERK) pathway.

In a final step, we investigated the role of TRPV4 as a transducer of hyperphysiological cyclic stretching and a potential therapeutic target. Human primary annulus fibrosus (AF) cells were seeded on silicone chambers and cyclically stretched at a hyperphysiological magnitude in the presence or absence of a TRPV4 inhibitor. Clustered regularly interspaced short palindromic repeats (CRISPR)-Cas9 TRPV4 KO AF cells were generated, hyperphysiologically stretched, and compared to control cells. Gene and protein expression of inflammatory and catabolic mediators, as well as activation of MAPK pathways, were analyzed. This study identified TRPV4 as a mediator of stretch-induced inflammation in human AF cells. Moreover, it revealed TRPV4 pharmacological inhibition and gene editing as potential future therapeutic approaches to rescue mechanoflammation.

In this thesis, in vitro and in vivo models of hyperphysiological compression and stretching were established and used to identify TRPV4 as mechanotransducer and therapeutic target in the IVD. A novel in vitro compression model was developed to mimic the ECM of the IVD and other native tissues composed of non-fibrillar matrix and collagens, and to investigate their mechanotransduction mechanisms. This system was instrumental to investigate the function of TRPV4 in IVD cells. The novel findings obtained with this model, together with those obtained in the mouse compression model and the stretching system demonstrate that TRPV4 mediates a mechanism leading from mechanical hyperphysiological loading to IVD degeneration and inflammation, which eventually lead to chronic LBP. TRPV4 modulation might thus constitute a promising therapeutic strategy to treat patients suffering from IVD pathologies caused by aberrant mechanical stress. Future studies should clarify the exact mechanism of action of TRPV4 inhibition and gene editing and examine their potential to mitigate chronic inflammation and LBP in preclinical and clinical trials.

Résumé

La lombalgie est la principale cause d'invalidité dans le monde et représente un énorme fardeau socio-économique. Les coûts liés à la lombalgie vont encore augmenter dans les prochaines décennies en raison de la croissance et du vieillissement de la population mondiale. La discopathie dégénérative, qui se caractérise par la dégénérescence du disque intervertébral (DIV), l'inflammation et la croissance des nerfs dans le DIV, contribue principalement à la lombalgie. Un des principaux facteurs de dégénérescence discale est une sollicitation mécanique excessive ou aberrante. Les traitements actuels de la lombalgie, y compris les approches physiques, psychologiques, pharmacologiques et chirurgicales, ont des mécanismes d'action peu clairs, des effets de faible ampleur et ne sont pas bénéfiques à long terme. Des stratégies thérapeutiques ciblées en développement préclinique, telles que la thérapie moléculaire et génique, s'attaquent de manière sélective aux changements biologiques qui se produisent dans la dégénérescence discale. Néanmoins, malgré la nature mécanique de la lombalgie, les voies de mécanotransduction ne sont actuellement pas ciblées. Cela est principalement dû au fait que les informations sur les mécanismes de mécanodétection et de mécanotransduction dans le DIV sont très limitées. Les canaux ioniques TRP (de l'anglais *transient receptor potential*) sont des cibles thérapeutiques prometteuses pour traiter la lombalgie, car ils peuvent détecter et transduire divers signaux, y compris le stress mécanique. Le canal TRP vanilloïde 4 (TRPV4) est particulièrement intéressant, car il a été démontré qu'il transmet des signaux mécaniques, inflammatoires et de douleur. Son potentiel clinique est encore mis en évidence par des essais précliniques et cliniques en cours. L'objectif général de cette thèse était d'étudier le rôle potentiel de TRPV4 dans la médiation des signaux mécaniques hyperphysiologiques dans le DIV et sa pertinence en tant que cible thérapeutique pour traiter la lombalgie.

Dans une première étape vers l'étude de TRPV4, nous avons développé un nouveau modèle de compression in vitro pour les études de mécanotransduction. Des hydrogels composites agarose-collagène ont été fabriqués et caractérisés en termes de propriétés matérielles et mécaniques. Le phénotype de cellules bovines de noyau pulpeux (NP) et la capacité de mécanotransduction après compression dynamique ont aussi été analysés. Les hydrogels composites agarose-collagène ont combiné la résistance mécanique de l'agarose avec la biofonctionnalité du collagène, ce qui a permis d'améliorer l'adhésion cellulaire et l'activation de la protéine FAK (de l'anglais *focal adhesion kinase*). De plus, les hydrogels agarose-collagène ont récapitulé la matrice extracellulaire du DIV, avec leur matrice non fibrillaire et leurs fibres de collagène, et ont permis l'exploration des mécanismes de mécanotransduction dans un système reproductible.

Dans une seconde étude, les hydrogels d'agarose-collagène chargés de cellules NP et un modèle de souris ont été utilisés pour étudier le rôle de TRPV4 dans la transduction de la compression dynamique hyperphysiologique. Les changements dégénératifs et l'expression du médiateur inflammatoire cyclooxygénase 2 (COX2) ont été examinés dans des DIV de souris qui ont été comprimés dynamiquement à un régime hyperphysiologique (en comparaison à des contrôles négatifs). Les dommages cellulaires et l'inflammation (libération de prostaglandine E2 (PGE2)) ont été mesurés dans des cellules bovines de NP

incorporées dans des hydrogels d'agarose-collagène et comprimées dynamiquement à un régime hyperphysiologique avec ou sans inhibition de TRPV4. L'activation des voies MAPK (de l'anglais *mitogen-activated protein kinase*) a été analysée. Enfin, les changements dégénératifs et l'expression de COX2 ont été évalués dans les DIV de souris knockout (KO) pour le gène trpv4 (par rapport au type sauvage). Nous avons démontré que TRPV4 régule les facteurs inflammatoires COX2/PGE2 et est un médiateur des dommages cellulaires induits par la compression dynamique hyperphysiologique, probablement par la voie ERK (de l'anglais *extracellular signal-regulated kinases 1/2*).

Dans une dernière étape, nous avons étudié le rôle de TRPV4 comme transducteur de l'étirement cyclique hyperphysiologique et comme cible thérapeutique potentielle. Des cellules humaines de l'anneau fibreux (AF) ont été cultivées sur des chambres de silicone et étirées cycliquement à une magnitude hyperphysiologique en présence ou en l'absence d'un inhibiteur de TRPV4. Des cellules de l'AF KO pour le gène TRPV4 ont été générées par la technique CRISPR-Cas9 (de l'anglais *clustered regularly interspaced short palindromic repeats Cas9),* étirées de façon hyperphysiologique, et comparées à des cellules témoins. L'expression des gènes et des protéines des médiateurs inflammatoires et cataboliques, ainsi que l'activation des voies MAPK, ont été analysées. Cette étude a identifié TRPV4 comme un médiateur de l'inflammation induite par étirement dans les cellules d'AF humaines. De plus, elle a révélé que l'inhibition pharmacologique et la modification du gène de TRPV4 sont des approches thérapeutiques potentielles futures pour réduire la mécanoflammation.

Dans cette thèse, des modèles in vitro et in vivo de compression et d'étirement hyperphysiologiques ont été établis et utilisés pour identifier TRPV4 comme mécanotransducteur et cible thérapeutique dans le DIV. Un nouveau modèle de compression in vitro a été développé pour imiter la matrice extracellulaire du DIV et d'autres tissus natifs composés de matrice non fibrillaire et de collagènes et pour étudier leurs mécanismes de mécanotransduction. Ce système a permis d'étudier la fonction de TRPV4 dans les cellules du DIV. Les nouvelles découvertes obtenues avec ce modèle, ainsi que celles obtenues dans le modèle de compression de DIV de la souris et le système d'étirement, démontrent que TRPV4 intervient dans un mécanisme qui mène de la sollicitation mécanique hyperphysiologique à la dégénérescence et à l'inflammation des DIV, qui finissent par entraîner une lombalgie chronique. La modulation de TRPV4 pourrait donc constituer une stratégie thérapeutique prometteuse pour traiter les patients souffrant de pathologies des DIV causées par un stress mécanique aberrant. Les études futures devraient clarifier le mécanisme d'action exact de l'inhibition de TRPV4 et de la modification des gènes et examiner leur potentiel pour atténuer l'inflammation chronique et la lombalgie dans les essais précliniques et cliniques.

Chapter 1

Introduction

1.1 Thesis motivation

Low back pain and impact on society

Low back pain (LBP) is a very frequent condition with a lifetime prevalence of up to 84% [1, 2]. It spans low- to high-income countries, and although uncommon in the first decade of life, affects people from all age groups [3]. The highest prevalence of LBP is observed among women and people between 40-80 years of age [4]. LBP is the leading cause of invalidity worldwide [5]. It is estimated that years lived with disability caused by LBP have augmented by 54% between 1990 and 2015, globally [3, 5]. This change is mainly due to the growth and aging of the global population [4]. While most LBP episodes resolve within weeks, recurrence is common [3]. The prevalence of chronic low back pain is about 23%, with 11–12% of the population being disabled by it [1]. LBP is the most frequent cause of medically certified sick leave and early retirement in Europe [6]. Consequently, LBP generates enormous expenses, including direct (healthcare) and indirect (productivity loss and work absence) costs. These costs differ between countries according to the local culture, social norms, and healthcare methods [3]. In Switzerland, direct costs of LBP were estimated at 2.6 billion €, and productivity losses between 2.2 and 4.1 billion € for 5.7 million individuals over the age of 20 in 2005 [7]. Costs related to LBP are projected to further increase in the coming decades. Intensified research efforts are thus sorely needed to tackle LBP as a public health and societal issue.

Current treatments of low back pain

Existing treatments of LBP are divided into physical, psychological, and pharmacological therapies, as well as surgical interventions. As the first line of management, the patient should be reassured, educated about the nature of LBP, and advised to remain active. Although early referral to physical therapy was shown to reduce healthcare use and total costs [8, 9], there is variable evidence for specific physical approaches [8, 10]. Exercise therapy appears to be as effective as no treatment or other treatment in acute LBP and to be slightly effective at reducing pain and improving function in chronic LBP [8, 11]. Guidelines further recommend considering the use of psychological therapies, such as cognitive behavioral therapy and mindfulness-based stress reduction, and combined physical and psychosocial approaches especially for patients who do not respond to first-line treatments [10]. Pharmacotherapy should be applied only in case of a lack of response to first-line non-pharmacological approaches. Current pharmacological treatments have unclear mechanisms of action, low effect sizes [1], and can provoke side effects in the long term. The use of paracetamol is no longer recommended due to evidence of absence of effectiveness and potential harm [10, 12]. Non-steroidal anti-inflammatory drugs (NSAIDs) should be administered after taking into account risks such as gastrointestinal, liver, and cardiorenal toxicity [10]. Routine use of opioids is not recommended due to the small benefit and risk of misuse, abuse, and dependence [10]. Clinical guidelines regarding surgical interventions vary. These are not only more costly and prone to adverse events compared to non-surgical approaches, but their (long-term) benefit is also challenged [8, 10]. Considering the variable evidence in

favor of physical therapy and the high risks associated with surgery, efforts should be deployed to improve pharmacological therapies.

Mechanical loading as a contributor to low back pain

Key contributors to LBP include comorbidities, genetic, psychological, social, and biophysical factors that are generally inter-related [3]. The term LBP is usually accompanied by the adjectives "non-specific" or "mechanical" [8]. This is due to the fact that it is often impossible to identify a specific nociceptive cause, such as a vertebral fracture, malignancy, or infection [3]. Non-specific/mechanical LBP stems intrinsically from the spine, IVDs, or surrounding soft tissues [8]. The spine is constantly subjected to muscle activation, as well as flexion, extension, and torsion motions during daily activities [13]. Therefore, the IVDs are continuously mechanically stimulated. The central gel-like nucleus pulposus (NP) sustains compressive loads, hydrostatic and osmotic pressures, while tensile stress predominates in the ring-shaped annulus fibrosus (AF) [13]. A physiological level of mechanical loading is beneficial for IVD homeostasis, as it promotes solute transport and cell metabolism [14]. However, hyperphysiological mechanical stressors, such as impact, heavy lifting, muscle activations, and work/lifestyle factors (e.g., vibration exposure, gait, and posture) [15], contribute to IVD degeneration, characterized by increased cell death, reduced anabolic gene expression, increased catabolism and extracellular matrix degradation [13, 14]. IVD degeneration can ultimately lead to IVD structural failure and cause degenerative disc disease (DDD), which is accompanied by inflammation and nociception [16]. DDD can further cause nerve ingrowth and compression, which principally contribute to LBP [17, 18]. Despite the mechanical nature of LBP, current drugs do not specifically target mediators of mechanosensing and mechanotransduction pathways, as these are poorly understood. A better understanding of the molecular mechanisms leading from hyperphysiological mechanical loading to IVD degeneration, inflammation, and nociception would reveal novel, and possibly more effective, therapeutic targets.

Transient receptor potential channels as therapeutic targets

Transient receptor potential (TRP) channels have recently emerged as potential therapeutic targets to treat several diseases [19]. They are a super-family of non-selective calcium-permeable transmembrane channels composed of six subfamilies in mammals: TRPC (canonical), TRPV (vanilloid), TRPM (melastatin), TRPP (polycystin), TRPML (mucolipin), and TRPA (ankyrin) [20]. TRP channels have sparked interest among researchers due to their polymodal nature. They can sense various stimuli, including changes in temperature, pH, osmolarity, as well as oxidative and mechanical stress [20]. The mechanosensitive member 4 of the vanilloid subfamily (TRPV4) is especially intriguing for the study of IVD degeneration and LBP. TRPV4 is known to transduce mechanical, inflammatory and pain signals in joint tissues [21] but is poorly explored in the IVD. TRPV4 was shown to mediate dynamic compression in chondrocytes [22]. Moreover, cartilage-specific TRPV4 knockout in mice reduced age-related osteoarthritis [23]. In the IVD, reduced osmolarity increased the expression of TRPV4 and pro-inflammatory cytokines [24]. The potential of TRPV4 as a therapeutic target is further

highlighted by several preclinical trials using TRPV4 inhibitors as a treatment for diverse conditions [25-27]. Furthermore, a selective antagonist of TRPV4 was recently administered to healthy volunteers and heart failure patients without any safety concern [28]. Nevertheless, the role of TRPV4 as a potential mechanotransducer and therapeutic target has never been investigated in the context of DDD and LBP. This thesis aims to fill this knowledge gap in the IVD field.

1.2 Thesis aims

The overall goal of this thesis was to investigate the potential role of the TRPV4 ion channel in mediating hyperphysiological mechanical signals in the IVD, and as therapeutic target. To this end, several in vitro and vivo models, as well as different types of mechanical loading, were established and applied. The specific aims of the thesis are described below.

Aim 1: To develop a novel 3D hydrogel that combines mechanical strength and biofunctionality for mechanotransduction studies

Mechanotransduction studies with physiological relevance require 3D in vitro models that: (i) recapitulate the in vivo environment of the tissue of interest; (ii) allow a reliable and reproducible application of the mechanical signals (e.g. dynamic compression); and (iii) allow the conduction of cellular and molecular assays. Agarose hydrogels have often been used to encapsulate chondrocytes and to study the effect of compression due to their strong mechanical properties [29, 30]. However, agarose is a bio-inert material that does not present any cell-adhesion motifs and therefore does not recapitulate the cell-matrix interactions that are crucial for mechanotransduction. We aimed to develop novel agarose-collagen composite hydrogels that: (i) mimic native tissues constituted of non-fibrillar matrix and collagens; (ii) combine the mechanical properties of agarose and the biofunctionality of collagen I; and (iii) allow the exploration of mechanical loading and cellular mechanotransduction. Specifically, we hypothesized that the physical blending of collagen I into agarose would enhance the biofunctionality of the construct by promoting cell adhesion and the activation of focal adhesion kinases (FAK). Agarose, collagen, and agarose-collagen composite hydrogels were compared in terms of structural homogeneity, rheological properties, and size stability. Bovine NP cell viability, proliferation, morphology, gene expression, glycosaminoglycan (GAG) production, adhesion, and FAK phosphorylation after dynamic compression were analyzed.

Aim 2: To investigate the role of TRPV4 in transducing hyperphysiological dynamic compression

Mechanical loading is a known contributor to IVD degeneration and LBP. However, current treatments of LBP do not target IVD mechanosensors and mechanotransducers, as they are poorly understood. The mechanosensitive TRPV4 ion channel is an interesting therapeutic target in the context of joint diseases, as it transduces mechanical,

inflammatory, and pain signals [21]. TRPV4 was shown to mediate the transduction of dynamic compressive loading in chondrocytes [22]. Moreover, reduced osmolarity was shown to increase TRPV4 expression and pro-inflammatory cytokines in bovine NP cells [24]. We aimed to investigate the potential role of TRPV4 in hyperphysiological dynamic compression of NP cells in vitro and IVDs in vivo. We hypothesized that: (i) hyperphysiological dynamic compression induces IVD degeneration, cell damage, and increased cyclooxygenase 2 (COX2) and prostaglandin E2 (PGE2) expression; and that (ii) TRPV4 mediates these effects. To test these hypotheses, mouse IVDs were dynamically compressed at a short repetitive hyperphysiological regime, and degenerative changes and the expression of the inflammatory mediator COX2 were examined (versus sham). Bovine NP cells were embedded in our previously developed agarose-collagen hydrogels and dynamically compressed at a hyperphysiological regime with or without selective TRPV4 inhibition. Lactate dehydrogenase (LDH) and PGE2 release, as well as phosphorylation of mitogen-activated protein kinases (MAPKs), were analyzed. Degenerative changes and COX2 expression were further evaluated in the IVDs of trpv4-deficient mice (versus wild-type).

Aim 3: To investigate the role of TRPV4 in transducing hyperphysiological cyclic stretching

AF disruption is commonly linked to LBP [31]. While the NP sustains hydrostatic and osmotic pressures generated by compressive forces from the body weight and spinal motions, the AF is subjected to tensile stresses [13] that could lead to AF disruption. We aimed to investigate the role of TRPV4 as a mechanotransducer and a potential therapeutic target in a more clinically relevant model by analyzing human primary AF cells that were cyclically stretched at a hyperphysiological strain. We hypothesized that: (i) hyperphysiological cyclic stretching induces inflammation; and that (ii) TRPV4 inhibition and knockout (KO) reduce stretch-induced inflammation. TRPV4 pharmacological inhibition and gene editing were thus tested as potential therapeutic approaches to rescue the induced mechanoflammation. To test our hypotheses, human AF cells were stretched at a 20% hyperphysiological cyclic strain. TRPV4 was either inhibited with the selective TRPV4 antagonist GSK2193874 or knocked out via CRISPR-Cas9 gene editing. The gene expression, inflammatory mediator release and MAPK pathway activation were analyzed.

1.3 Thesis outline

This thesis is divided into seven chapters and an appendix. The content of each chapter is described below.

Chapter 1 introduces the clinical and economical motivations for this thesis and presents the aims and the outline of the thesis.

Chapter 2 provides background information on the anatomy of the IVD, IVD pathologies, and state-of-the-art therapeutic approaches. It further summarizes the

current knowledge on biomechanics and mechanobiology of the IVD, as well as TRP channels.

Chapter 3 addresses the first aim of the thesis and introduces novel agarose-collagen composite hydrogels as 3D in vitro models for mechanotransduction studies. We showed that agarose-collagen hydrogels retain strong mechanical properties while outperforming agarose hydrogels in terms of matrix production, cell adhesion, and mechanotransduction ability. This unique composite hydrogel scaffold thus mimics the natural extracellular matrix of the IVD, allowing the direct exploration of the influence of mechanical loading in a highly biomimetic and reproducible model system. This system can further be used to model other native tissues composed of non-fibrillar matrix and collagens and to investigate their mechanotransduction mechanisms.

Chapter 4 addresses the second aim of the thesis and describes a study that explores the role of TRPV4 in transducing hyperphysiological dynamic compression in NP cells in vitro and mouse IVDs in vivo. We identified TRPV4 as a regulator of the COX2/PGE2 inflammatory factors and as a mediator of cell damage induced by hyperphysiological dynamic compression, possibly via the extracellular signal-regulated kinases 1/2 (ERK) pathway. Targeted TRPV4 modulation might thus constitute a promising therapeutic strategy to treat patients suffering from IVD pathologies caused by aberrant mechanical stress.

Chapter 5 addresses the third aim of the thesis and presents a study that further investigates the role of TRPV4 in transducing hyperphysiological cyclic stretching in human AF cells in vitro. We first developed a model with an inflammatory response to hyperphysiological stretching representative of early-stage annulus fibrosus injury. Moreover, we established the first successful CRISPR-Cas9 KO in degenerated human AF cells (TRPV4 KO). Through CRISPR-Cas9 gene editing and selective pharmacological inhibition experiments, we identified TRPV4 as a mediator of stretch-induced inflammation in human AF cells. This study and the one described in Chapter 4 highlight a novel link between mechanical hyperphysiological loading and injury mechanisms leading to degeneration of the IVD and elucidate an important pathway in the complex process that eventually leads to chronic LBP.

Chapter 6 expands on the use of the CRISPR-Cas9 gene editing technology in the IVD field and presents a review on this topic. This chapter provides an overview of the relevant recent advances, proposes potential treatment strategies for DDD and LBP, and discusses the current limitations that may hamper the clinical translation of the CRISPR-Cas9 technology.

Chapter 7 concludes the thesis by highlighting the contributions to the field and discussing the limitations and futures perspectives of this work.

In the **Appendix**, the reader will find a list of abbreviations, the curriculum vitae, and an additional study that investigates the TRP canonical 6 (TRPC6) ion channel in simulated microgravity of human IVD cells. In this study, we showed that simulated microgravity and TRPC channel inhibition led to reduced proliferation and increased senescence. Furthermore, simulated microgravity reduced TRPC6 expression. IVD cell

senescence and mechanotransduction may hence potentially be regulated by TRPC6 expression.

1.4 References

1.   Balague, F., et al., Non-specific low back pain. Lancet, 2012. 379(9814): p. 482-91.

2.   Airaksinen, O., et al., Chapter 4. European guidelines for the management of chronic nonspecific low back pain. Eur Spine J, 2006. 15 Suppl 2: p. S192-300.

3.   Hartvigsen, J., et al., What low back pain is and why we need to pay attention. Lancet, 2018. 391(10137): p. 2356-2367.

4.   Hoy, D., et al., A systematic review of the global prevalence of low back pain. Arthritis Rheum, 2012. 64(6): p. 2028-37.

5.   Vos, T., et al., Global, regional, and national incidence, prevalence, and years lived with disability for 310 diseases and injuries, 1990-2015: a systematic analysis for the Global Burden of Disease Study 2015. Lancet, 2016. 388(10053): p. 1545-1602.

6.   Bevan, S., et al., Fit for work. Musculoskeletal disorders in the European workforce. London: The work foundation, 2009. 2009.

7.   Wieser, S., et al., Cost of low back pain in Switzerland in 2005. Eur J Health Econ, 2011. 12(5): p. 455-67.

8.   Will, J.S., D.C. Bury, and J.A. Miller, Mechanical Low Back Pain. Am Fam Physician, 2018. 98(7): p. 421-428.

9.   Childs, J.D., et al., Implications of early and guideline adherent physical therapy for low back pain on utilization and costs. BMC Health Serv Res, 2015. 15: p. 150.

10.   Foster, N.E., et al., Prevention and treatment of low back pain: evidence, challenges, and promising directions. Lancet, 2018. 391(10137): p. 2368-2383.

11.   Hayden, J.A., et al., Exercise therapy for treatment of non-specific low back pain. Cochrane Database Syst Rev, 2005(3): p. CD000335.

12.   Qaseem, A., et al., Noninvasive Treatments for Acute, Subacute, and Chronic Low Back Pain: A Clinical Practice Guideline From the American College of Physicians. Ann Intern Med, 2017. 166(7): p. 514-530.

13.   Fearing, B.V., et al., Mechanotransduction and cell biomechanics of the intervertebral disc. JOR Spine, 2018. 1(3).

14.   Chan, S.C., S.J. Ferguson, and B. Gantenbein-Ritter, The effects of dynamic loading on the intervertebral disc. Eur Spine J, 2011. 20(11): p. 1796-812.

15.   Setton, L.A. and J. Chen, Cell mechanics and mechanobiology in the intervertebral disc. Spine (Phila Pa 1976), 2004. 29(23): p. 2710-23.

16.   Adams, M.A. and P.J. Roughley, What is intervertebral disc degeneration, and what causes it? Spine (Phila Pa 1976), 2006. 31(18): p. 2151-61.

17. Freemont, A.J., et al., Nerve ingrowth into diseased intervertebral disc in chronic back pain. Lancet, 1997. 350(9072): p. 178-181.

18. Kos, N., L. Gradisnik, and T. Velnar, A Brief Review of the Degenerative Intervertebral Disc Disease. Med Arch, 2019. 73(6): p. 421-424.

19. Moran, M.M., et al., Transient receptor potential channels as therapeutic targets. Nat Rev Drug Discov, 2011. 10(8): p. 601-20.

20. Krupkova, O., J. Zvick, and K. Wuertz-Kozak, The Role of Transient Receptor Potential Channels in Joint Diseases. European Cells & Materials, 2017. 34: p. 180-201.

21. McNulty, A.L., et al., TRPV4 as a therapeutic target for joint diseases. Naunyn Schmiedebergs Arch Pharmacol, 2015. 388(4): p. 437-50.

22. O'Conor, C.J., et al., TRPV4-mediated mechanotransduction regulates the metabolic response of chondrocytes to dynamic loading. Proc Natl Acad Sci U S A, 2014. 111(4): p. 1316-21.

23. O'Conor, C.J., et al., Cartilage-Specific Knockout of the Mechanosensory Ion Channel TRPV4 Decreases Age-Related Osteoarthritis. Sci Rep, 2016. 6: p. 29053.

24. Walter, B.A., et al., Reduced tissue osmolarity increases TRPV4 expression and pro-inflammatory cytokines in intervertebral disc cells. Eur Cell Mater, 2016. 32: p. 123-36.

25. Dong, Q., et al., Blockage of transient receptor potential vanilloid 4 alleviates myocardial ischemia/reperfusion injury in mice. Sci Rep, 2017. 7: p. 42678.

26. Michalick, L., et al., Transient Receptor Potential Vanilloid 4 and Serum Glucocorticoid-regulated Kinase 1 Are Critical Mediators of Lung Injury in Overventilated Mice In Vivo. Anesthesiology, 2017. 126(2): p. 300-311.

27. Thorneloe, K.S., et al., An orally active TRPV4 channel blocker prevents and resolves pulmonary edema induced by heart failure. Sci Transl Med, 2012. 4(159): p. 159ra148.

28. Goyal, N., et al., Clinical Pharmacokinetics, Safety, and Tolerability of a Novel, First-in-Class TRPV4 Ion Channel Inhibitor, GSK2798745, in Healthy and Heart Failure Subjects. Am J Cardiovasc Drugs, 2019. 19(3): p. 335-342.

29. Anderson, D.E. and B. Johnstone, Dynamic Mechanical Compression of Chondrocytes for Tissue Engineering: A Critical Review. Frontiers in Bioengineering and Biotechnology, 2017. 5(76).

30. Bougault, C., et al., Investigating conversion of mechanical force into biochemical signaling in three-dimensional chondrocyte cultures. Nature Protocols, 2009. 4(6): p. 928-938.

31. Torre, O.M., et al., Annulus fibrosus cell phenotypes in homeostasis and injury: implications for regenerative strategies. Ann N Y Acad Sci, 2019. 1442(1): p. 61-78.

Chapter 2

Background

2.1 Anatomy of the intervertebral disc

The human spine is composed of 32 to 34 vertebrae, 23 intervertebral discs (IVDs), ligaments, the rib cage, and the spinal musculature [1]. The functions of the spine include: (i) housing and protecting the spinal cord and the efferent and afferent nerves; (ii) supporting the body mass and withstanding external forces; and (iii) allowing for mobility and flexibility. The spine is divided into 5 distinctive regions: cervical (with 7 vertebrae numbered C1 to C7), thoracic (T1-T12), lumbar (L1-L5), sacrum (S1-S5), and the coccyx (3 to 5 vertebrae) (**Figure 1**) [2]. Vertebrae in the cervical, thoracic, and lumbar regions are separated by IVDs, while the vertebrae of the sacrum and the coccyx are fused (**Figure 1**) [2].
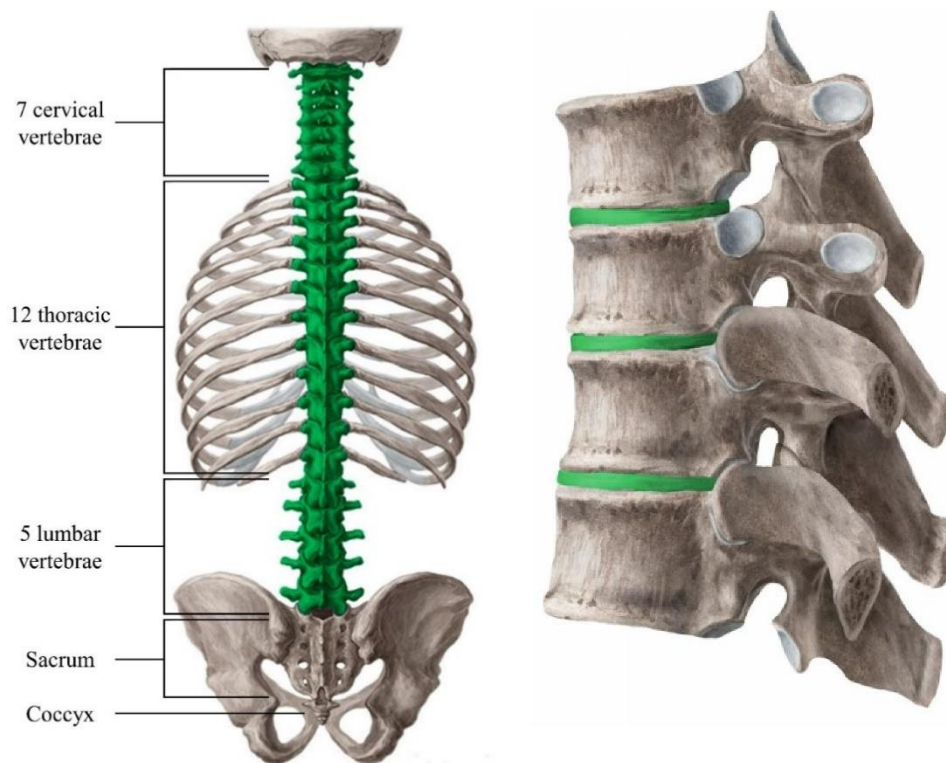
Figure 1: Left: The human spine and its 5 regions. The green section highlights the part of the spine that contains individual vertebrae and IVDs. **Right:** Structure of the vertebrae with the IVDs in green. Reprinted from [2] with permission from the Multidisciplinary Digital Publishing Institute (MDPI) and Kenhub. Originally adapted from © Kenhub (www.kenhub.com); illustrator: Begoña Rodriguez.

The IVD is composed of 3 main structures: the cartilaginous endplates (CEPs) at the superior and inferior faces of the IVD, the gelatinous nucleus pulposus (NP) in the center, and the fibrous and highly structured ring called annulus fibrous (AF) at the outer periphery (**Figure 2 A, B**) [3].
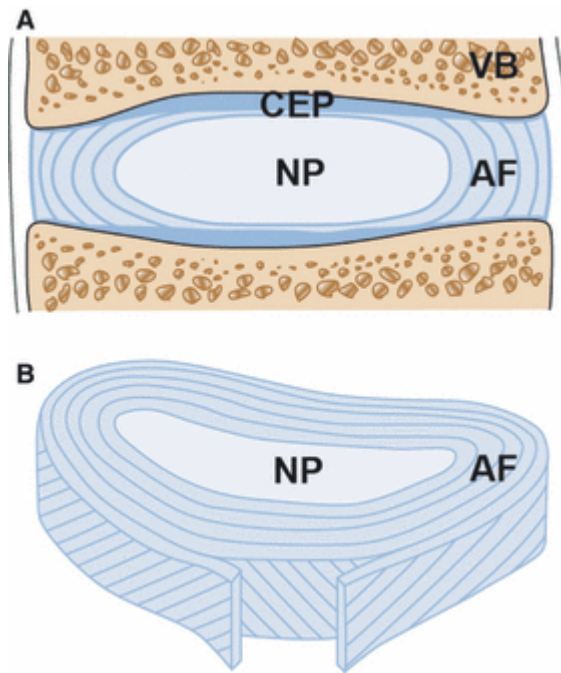
Figure 2: A) Schematic representation of the sagittal section of an IVD with the adjacent vertebrae (VB) and cartilaginous endplates (CEPs) at the superior and inferior faces, and the annulus fibrosus (AF) surrounding the nucleus pulposus (NP). **B)** Transverse section showing the structure of the lamellae and the alignment of the fibers of the AF. Reprinted from [4] with permission from John Wiley and Sons.

Cartilaginous endplates

The CEPs are thin, strong, and porous structures that separate the IVD from the adjacent vertebrae. They keep the NP pressurized and prevent it to bulge into the relatively soft center of the vertebrae [2]. Moreover, the CEPs are vascularized and ensure nutrient and fluid transport via diffusion between the vertebrae and the IVD [2]. The CEPs consist of hyaline cartilage composed of chondrocytes, proteoglycans, and a network of thin and closely packed fibrils of collagen (mainly type II) [2].

Nucleus pulposus

The NP is found in the center of the IVD. This highly hydrated (80-90% water [2]) and incompressible structure sustains compressive loads, as well as hydrostatic and osmotic pressures [3]. The NP is composed of a loose network of randomly distributed collagen II fibers (15–20% dry weight), radially dispersed elastin fibers, and proteoglycans (50% dry weight) [2]. Proteoglycans, like the abundantly present aggrecan, carry negative electric charges on their sulfated glycosaminoglycans (GAGs), which provide the NP with its osmotic and swelling properties [3]. NP cells are round chondrocyte-like cells that are interspersed in the NP at a low cellular density of around 4000 cells/mm^3 [5]. The microenvironment at the center of the IVD is characterized by low oxygen tension, leading to anaerobic metabolism and low pH [6]. NP cells maintain tissue homeostasis by synthesizing and degrading large amounts of extracellular matrix (ECM) composed of collagens and proteoglycans [2]. Large vacuolated notochordal cells

can be present in young IVDs, but they are almost all completely replaced by chondrocyte-like cells in adulthood in humans [2].

Annulus fibrosus

The AF is a highly organized fibrocartilaginous structure that surrounds the NP. It is often subdivided into inner and outer AF. The main functions of the AF are to confine the relatively fluid NP, withstand compressive and tensile stress, and allow joint mobility [2]. The AF is composed of 15-25 concentric lamellae made of 20-60 collagen fiber bundles aligned at angles ranging from 55° to 20° that alternate direction at every layer (**Figure 2 B**) [2]. The ECM of the AF varies radially and mainly consists of water (70–78% inner and 55–65% outer wet weight), collagens (type I and type II collagen, 25–40% inner and 60–70% outer dry weight), and proteoglycans (11–20% inner and 5–8% outer dry weight) [2]. The collagen types I and II further substitute each other in a radial gradient, transitioning from 100% type II in the innermost lamellae to 100% type I in the outermost lamella [2]. The outermost layers of the AF are superficially vascularized and innervated by afferent and efferent branches of the spinal nerves [2]. While cells of the inner AF tend to be rounder, outer AF cells display an elongated morphology and align with the fibers of the lamellae [3].

2.2 Aging and pathologies of the intervertebral disc

Intervertebral disc aging

Compared to the young healthy IVD, the aging IVD undergoes natural metabolic, biochemical, and structural changes, which do not necessarily provoke any symptoms [7, 8]. These changes usually start in the CEPs and sequentially affect the NP and the AF [6, 8]. The blood supply to the CEPs and the IVD cellularity start decreasing already during childhood [6]. The ECM synthesis is reduced, leading to a loss in NP hydration due to the decrease in proteoglycan and hence in osmolarity [6]. ECM turnover decreases as well, causing an increase in collagen content and cross-linking [6]. Moreover, collagen type II in the inner AF tends to be replaced by collagen I [6]. Microstructural defects, such as cleft and tears, are already visible in the CEPs and NP by the age of 15 years, further extending into the AF with increasing age [6, 9].

Intervertebral disc degeneration

Pathological IVD degeneration is defined as an accelerated aging process including structural failure [6]. Causes of IVD degeneration are various and include genetics, aging, scarce metabolite diffusion, and loading history [6]. They all cumulatively contribute to weakening the IVD. However, mechanical loading is thought to precipitate IVD degeneration [6]. Excessive mechanical loading causes structural defects and cellular catabolic and inflammatory responses that strongly affect the matrix composition of the IVD and its biomechanical properties [6]. This, in turn, induces further aberrant mechanical loading [8], thus triggering a vicious circle [10].

IVD degeneration mostly affects lower lumbar IVDs [6]. Their bigger size impairs an efficient nutrient diffusion and they are subjected to the highest mechanical load. The degenerated IVD is characterized by several structural defects, such as annular tears, height loss, and disruption (**Figure 3**) [8]. Moreover, the CEPs become calcified and sclerotic (**Figure 3**) [8].
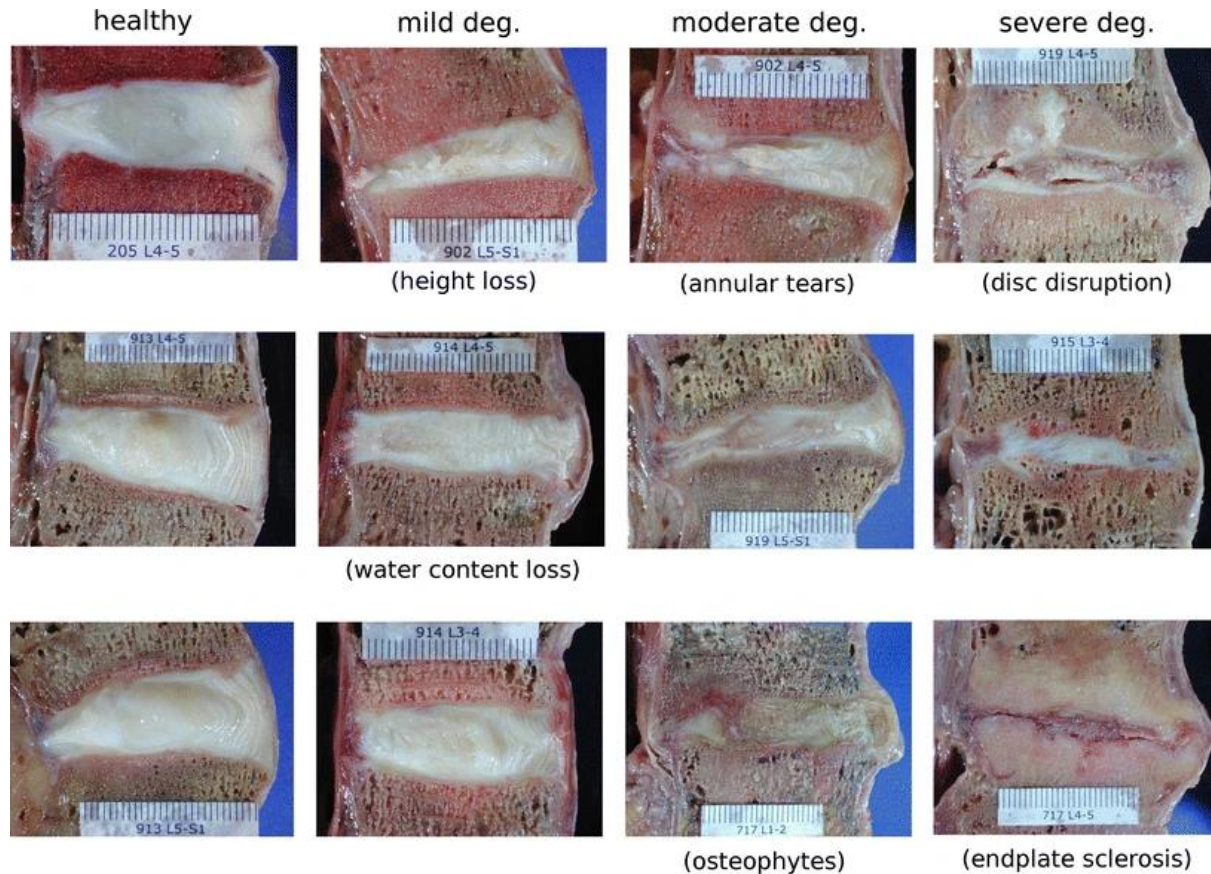
Figure 3: Various stages of IVD degeneration observed in sagittal sections of human lumbar IVDs. Reprinted from [8] with permission from Springer Nature.

Structural changes are believed to alter the mechanical properties of the IVD and, consequently, the way it withstands mechanical loading [8]. Abnormal mechanical stress causes increased cell death [11, 12]. IVD cell senescence and death are thought to play an important role in the pathogenesis of IVD degeneration [12, 13]. Moreover, aberrant mechanical loading initiates catabolic and inflammatory cascades [10]. Degenerated IVDs show increased levels of matrix-degrading enzymes, such as matrix metalloproteinases (MMP 1, 3, 13) [14], "a disintegrin and metalloproteinase with thrombospondin motifs" (ADAMTS 4) [14], and (pro-)inflammatory mediators, such as interleukins (IL 1β, 6, 8, 15), as well as cyclooxygenase 2 (COX2) and its enzymatic product prostaglandin E2 (PGE2), to name a few [15, 16]. Catabolic and inflammatory responses might be mediated by the nuclear factor-kappa B (NF-κB) and mitogen-activated protein kinase (MAPK: extracellular signal-regulated kinases 1/2 (ERK 1/2), p38 and Jun-N-terminal kinase (JNK)) signaling pathways [17]. Detrimental cell-mediated responses further result in reduced ECM synthesis and proteoglycan content, and thus loss of osmotic and swelling

pressure in the NP [8]. Moreover, increased ECM degradation and inflammation exacerbate structural defects, leading to IVD collapse and structural failure [6, 8].

Intervertebral disc herniation

When radial fissures in the AF allow the bulging of the NP into the AF, herniation arises [6]. Depending on the level of NP bulging, it may result in protrusion, when the NP migrates through the lamellae of the AF, or extrusion, when the NP exits the AF [6]. Extrusion of the nuclear material can further cause inflammation and/or compression of a spinal nerve or its root, thus provoking so-called radicular pain [6, 18].

Degenerative disc disease and low back pain

Like IVD physiological aging, IVD degeneration is not necessarily symptomatic [8]. Degenerative disc disease (DDD) is characterized by IVD degeneration accompanied by pain [6]. Pain mechanisms can start with IVD degeneration, which induces anatomical and functional changes, such as NP prolapse, which further cause the irritation or compression of spinal nerves [18]. This is for example the case of radicular pain stemming from IVD herniation, as explained above. Alternatively, pain can arise from the IVD itself and can stem from the structural defects and inflammation that characterize IVD degeneration [18]. During severe disc disruption, the blood vessels and nerves that normally populate the surface of the AF grow into the diseased IVD [19]. Ingrown nerves express substance P, a nociceptive neurotransmitter, and are associated with pain [19]. It is believed that noxious inflammatory stimuli from the degenerated disc environment, as well as mechanical stimulation of ingrown (or superficial) nociceptors, provoke nerve sensitization and pain [18].

2.3 Current treatments of low back pain

Current treatments of LBP aim to manage pain but do not address the causes of the condition. Treatment strategies are divided into physical, psychological, and pharmacological therapies, as well as surgical interventions. Clinical guidelines have recently changed based on novel evidence and recommend against routine use of imaging as a diagnostic method, pharmacotherapy, and surgery [20]. However, there is an enormous gap between evidence-based recommendations and the current practice [20]. For example, IVD imaging including radiography and magnetic resonance imaging (MRI) is still frequently used, generating high direct costs [20]. Nevertheless, its use should be limited to cases where specific serious conditions, such as vertebral fracture, malignancy, or infection, are suspected [20]. The MRI-based Pfirrmann scale, which grades IVD degeneration from grade 1 (healthy IVD) to grade 5 (highly degenerated and collapsed IVD) [21] is useful to compare data in basic and clinical research. However, imaging findings do not correlate with pain [22] and patients with degenerative changes can be asymptomatic [23].

In a first consultation, the patient should be physically examined and questioned about occupational and psychosocial factors, as well as the severity and duration of pain [24]. Acute LBP is defined by a duration below 6 weeks and becomes chronic when it lasts over 12 weeks [20]. The results of this first evaluation will allow to rule out specific serious causes of LBP and select the appropriate treatment strategies in case of non-specific pain [24].

Physical and psychological therapies

As the first line of management, the patient should be reassured and told that LBP is not a serious condition and the prognosis is good in most of the cases [20]. The patient should also be advised to remain physically active and resume professional activities [20]. Early referral to physical therapy was shown to reduce healthcare use and total costs [24, 25]. Recommended physical therapies, especially for chronic LBP, include a graded exercise program aiming for functional improvement [20]. However, there is variable evidence for specific physical approaches [20, 24]. Exercise therapy appears to be as effective as no treatment or other treatment in acute LBP and to be slightly effective at reducing pain and improving function in chronic LBP [24, 26]. Passive therapies, such as acupuncture, massage, and spinal manipulation, are either optional or not recommended depending on the guidelines [20]. Despite insufficient evidence, guidelines further recommend considering the use of psychological therapies, such as cognitive behavioral therapy and mindfulness-based stress reduction, and combined physical and psychosocial approaches especially for patients who do not respond to first-line treatments [20].

Pharmacological therapies

Current guidelines recommend the use of pharmacotherapy only in case of a lack of response to first-line non-pharmacological approaches [20]. This recommendation is based on the fact that current pharmacological treatments have unclear mechanisms of action, low effect sizes [27], and can provoke side effects in the long term. The most common pharmacological therapies for LBP include paracetamol, non-steroidal anti-inflammatory drugs (NSAIDs), and opioids.

Paracetamol

 Paracetamol (also called acetaminophen) used to be a first-line medicine for the management of LBP [20]. It is an analgesic with an unclear mechanism of action that does not possess anti-inflammatory properties [28]. Today, the use of paracetamol is no longer recommended for LBP due to evidence of absence of effectiveness and potential harm [20, 29].

Non-steroidal anti-inflammatory drugs

NSAIDs, such as ibuprofen and aspirin, inhibit the COX2 enzyme [28]. They were shown to be slightly effective at providing short-term relief in acute and chronic LBP without radicular pain [24, 30]. However, there was no significant difference between

NSAID treatment and placebo in the case of radiculopathy [30]. Moreover, NSAIDs were not more effective than paracetamol or other drugs [30]. NSAIDs should be administered after taking into account risks like gastrointestinal, liver, and cardiorenal toxicity [20].

Opioids

Opioids, typified by morphine, are potent analgesics that act on neuronal receptors in the central nervous system and peripheral nerves [28]. There is evidence of moderate short-term efficacy of opioids in treating chronic LBP compared to placebo [31]. However, rates of misuse average between 21% and 29%, and rates of addiction between 8% and 12% [32]. Routine use of opioids is therefore not recommended due to the small benefit and risk of misuse, abuse, and dependence [20].

Interventional therapies and surgery

Clinical guidelines regarding interventional therapies and surgery vary [20]. Increasingly invasive procedures can be applied based on the condition of the patient. They range from epidural injections to microdiscectomy, spinal fusion, and total disc replacement (TDR). Surgery should be used as a last resort in disabling chronic LBP in case of failure of conservative therapies, as it is more costly and prone to adverse events compared to non-surgical approaches [20].

Epidural injections

The first more invasive approach involves injections of drugs, such as corticosteroids or anesthetics, into the epidural space that surrounds the spinal cord and nerve roots. Epidural injections are not recommended by recent guidelines for LBP, but rather for severe radicular pain [20]. They alleviate pain by delivering an increased drug concentration locally, but their effect is short-lived (<4 weeks) and there is no effect on long-term surgery risk [20, 33]. Moreover, epidural injections can cause rare but serious adverse events, including loss of vision, stroke, paralysis, and death [20].

Microdiscectomy

Microdiscectomy is a minimally invasive surgical procedure aimed to relieve pain stemming from disc herniation. The herniated tissue is surgically removed to relieve the pressure on the spinal nerves. Early surgery is associated with faster pain relief compared to initial conservative treatment and delayed surgery, but benefits decrease with longer follow-up (>1 year) [20, 34].

Spinal fusion

Spinal fusion is a surgical procedure that consists in the complete removal of the diseased IVD, replacement with a titanium fusion cage or a bone-like material, and connection of the two adjacent vertebrae with titanium pedicle screws and rods [2]. The aim is to prevent motion between the fused vertebrae. The benefits of spinal fusion for discogenic LBP are similar to those of intense rehabilitation and only slightly higher than non-surgical treatments [20, 35]. Long-term issues can further arise because spinal fusion

changes the biomechanical behavior of the spine, which may cause degeneration of the adjacent spinal segments [2].

<u>Total disc replacement</u>

In contrast to spinal fusion, TDR aims to preserve the motion of the diseased segment by removing the diseased IVD and replacing it with a synthetic implant. TDR is a relatively recent type of surgery compared to spinal fusion, with only a few disc implants approved so far for the lumbar level [2]. There is low-quality evidence that there are no clinically relevant differences between TDR and fusion techniques, with small overall success rates in both groups [36]. The safety and effectiveness of TDR need to be further evaluated in high-quality randomized controlled trials with long-term follow-up [36].

2.4 Preclinical therapeutic strategies

Considering the variable evidence in favor of physical therapy and the high risks and costs associated with surgery, efforts are currently deployed to develop targeted pharmacological and biological regenerative therapies with a clear mechanism of action and limited side effects. Targeted therapeutic strategies mainly include molecular and gene therapy. They may complement other promising but broader therapeutic approaches such as IVD tissue engineering and cell therapy.

Tissue engineering

Tissue engineering aims to replace either a part (the NP or AF) or the whole degenerated IVD with engineered scaffolds that may or not contain cells. Both natural and synthetic biomaterials are investigated and several state-of-the-art manufacturing techniques, such as electrospinning, composite hydrogel fabrication, and three-dimensional (3D) bioprinting, are applied [2]. Hurdles that need to be overcome by tissue-engineered scaffolds include scalability, integration with the native tissue, as well as sufficient load-bearing capacity [2].

Cell therapy

In cell therapy, cells are transplanted in the degenerated IVD with the aim of repairing the deteriorated environment. The current strategies are mainly directed at regenerating the NP, with only a few approaches targeting the AF or the CEPs [37]. Several issues remain open, including the choice of cell source and type (e.g. autologous or allogeneic; differentiated cells or mesenchymal stem cells), the delivery mode (e.g. in suspension or embedded in a biomaterial), and the selection of patients (e.g. early or later stages of IVD degeneration) [37]. The main challenge faced by cell therapy is the survival of the transplanted cells in the harsh and inflamed microenvironment of the degenerated IVD, which is characterized by low nutrient transport, oxygen and, pH, as well as high mechanical stress [37].

Molecular therapy

The goal of molecular therapy is to selectively address the biological changes that occur in IVD degeneration and DDD via the administration of specific molecules. Molecular therapeutic approaches can be divided into those that promote IVD anabolism and regeneration (mainly via growth factors) and those that inhibit catabolic and inflammatory processes.

Growth factors

Growth factors are proteins that target specific cell receptors and play a role in cell proliferation, differentiation, and ECM synthesis [38]. The potential of several growth factors (bone morphogenic proteins (BMP 2 and 7), transforming growth factor beta (TGFβ), epidermal growth factor (EGF), basic fibroblast growth factor (bFGF), growth/differentiation factor 5 (GDF5), and insulin-like growth factor 1 (IGF1)) for IVD regeneration has been tested in vitro and in vivo with positive outcomes including the increase of ECM synthesis (studies reviewed in [38]). However, the main disadvantage of growth factors, besides their high cost, is their short half-life, which limits the duration of their therapeutic effects and requires multiple injections [38].

Anti-catabolic and anti-inflammatory approaches

Two of the major signaling pathways that are targeted by anti-catabolic and anti-inflammatory molecular therapies to treat DDD are the NF-κB and MAPK pathways [39]. Local administration of NF-κB decoy oligodeoxynucleotides to the DRG in a rat lumbar disc herniation model was shown to significantly suppress pain [40]. Systemic inhibition of NF-κB activity via pharmacological inhibition with the Nemo Binding Domain (8K-NBD) peptide was shown to mitigate age-associated IVD degeneration in a mouse model of accelerated aging by increasing proteoglycan synthesis and improving the loss of cellularity [41]. Modulation of the MAPK pathways, especially of the p38 MAPK, has further yielded promising results. Inhibition of p38 in cytokine-activated rabbit NP cells reduced gene expression and production of factors associated with ECM catabolism, inflammation, and pain [42]. Moreover, IL1-induced downregulation of ECM gene expression and proteoglycan synthesis were reversed [42].

Gene therapy

Gene therapy is an experimental technique that aims to modify genes in order to treat a disease. This approach is interesting in the context of DDD, as genetic inheritance is one of the multiple factors that can cause IVD degeneration. Gene polymorphisms affecting genes such as aggrecan, collagen 1, 9, and 11, MMP 1, 2 and 3, IL 1 and 6, and COX2 have been associated with IVD degeneration [43]. Gene therapy can not only correct unfavorable gene polymorphisms, but also control the dysregulated molecular pathways in DDD by activating anabolic genes and growth factors and repressing catabolic and inflammatory genes [44]. Several gene therapy studies targeting genes like osteogenic protein-1 (OP1), sex-determining region Y box 9 (SOX9), TGFβ1, IGF1, BMP2, and IL1 receptor antagonist (IL1Ra) have been performed in vitro and in vivo with encouraging

regenerative results [45-47]. Gene therapy can complement cell therapy by editing cells to be transplanted ex vivo so that they can survive the harsh environment of the degenerated IVD and secrete reparatory molecules. Another approach is to perform gene editing in vivo by delivering the transduction agents locally to IVD cells or dorsal root ganglion (DRG) neurons [48]. Cells can be transduced via non-viral (e.g. liposomes) or viral vectors (e.g. lentivirus, adenovirus, or adeno-associated-virus) [38]. Non-viral vectors have low transduction efficiency, while viral vectors are very efficient but raise the issue of immunogenicity [39]. Although promising, gene therapy needs to overcome technical, safety, and ethical issues before it can be applied in clinics in the future.

<u>CRISPR-Cas9</u>

The most recent gene editing technique is the Nobel prize-winning clustered regularly interspaced short palindrome repeats (CRISPR)-Cas9 technique (explained in detail in Chapter 6). The CRISPR-Cas9 system is composed of a Cas9 endonuclease that is directed to the target deoxyribonucleic acid (DNA) sequence by a single-guide ribonucleic acid (sgRNA) [48]. It can be used to perform gene knockout, editing, as well as transcriptional regulation (gene activation or interference) [48]. Recently, CRISPR-Cas9 was used for epigenome editing to repress the inflammatory cytokine receptors tumor necrosis factor receptor 1 (TNFR1) and IL 1 receptor 1 (IL1R1) in human adipose tissue-derived stem cells to improve cell therapy for musculoskeletal diseases [49]. This technique was further used to modulate the A-kinase anchoring protein 150 (AKAP150) in DRG neurons and abolish the nociceptive neuron activity as a targeted strategy for LBP [50].

<u>RNA interference</u>

Another recent form of gene therapy is RNA interference (RNAi). RNAi aims to silence genes by interfering with their transcription or translation via small non-coding RNAs like small interfering RNAs (siRNAs) and microRNAs (miRNAs) [38]. siRNA approaches aiming to silence ADAMTS5 and caspase 3, an enzyme that plays a role in apoptosis, have yielded promising results in rabbit models of IVD degeneration [51-53].

2.5 Biomechanics and mechanobiology of the intervertebral disc

Despite the mechanical nature of LBP, current drugs and biological therapies do not specifically target mediators of mechanosensing and mechanotransduction pathways, as these are poorly understood. A better understanding of the molecular mechanisms leading from hyperphysiological mechanical loading to IVD degeneration, inflammation, and nociception might reveal novel, and possibly more effective, therapeutic targets.

Biomechanics

The spine is constantly subjected to muscle activation, as well as flexion, extension, and torsion motions during daily activities [3]. As the shock absorbers of the spine, the IVDs are well-adapted to withstand motions and mechanical loads. Due to its well-hydrated matrix that is rich in aggrecan, the NP sustains high osmotic and hydrostatic pressures during loading (**Figure 4**) [3]. Axial compression and swelling effects in the NP further generate bulging and deformation of the AF, resulting in radial and circumferential tension (**Figure 4**) [3]. The organized collagen type I bundles in the outer AF allow to withstand tensile stress and restrict the overall IVD expansion in the transverse plane [3]. Depending on their anatomical region (NP or AF), IVD cells are subjected to different combinations of hydrostatic, shear, compressive, or tensile stress (**Figure 4**) [3, 54, 55].
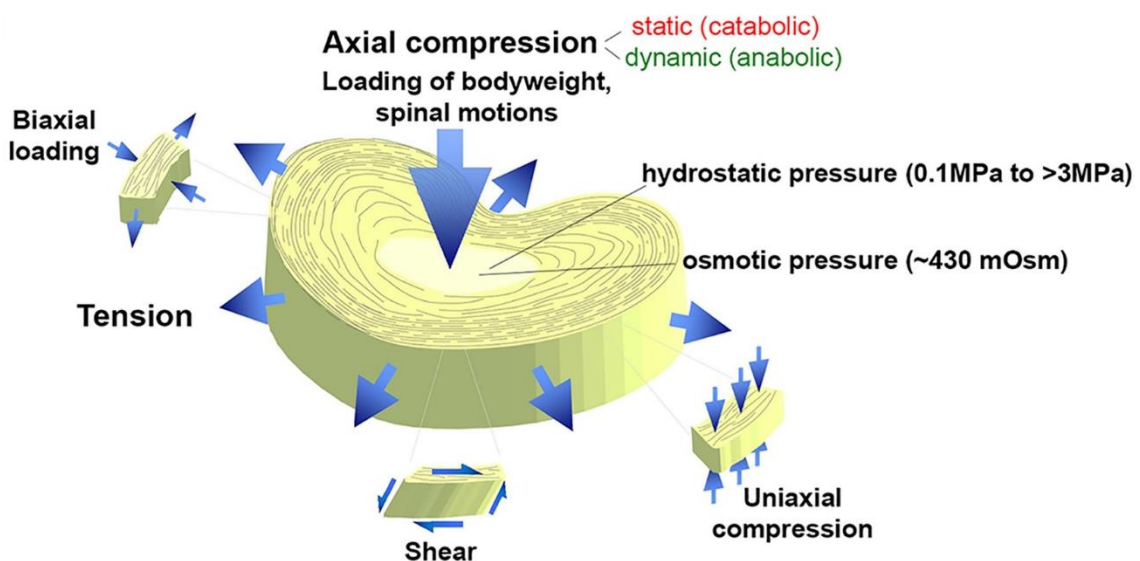
Figure 4: Schematic representation of the mechanical deformation of the IVD. Adapted from [3] with permission from John Wiley and Sons.

Mechanobiology

Mechanical stimuli elicit cellular responses in the IVD that depend on the magnitude, frequency, and duration of the loading [56]. In general, a physiological level of mechanical loading is beneficial for IVD homeostasis, as it promotes solute transport and cell metabolism [11]. However, hyperphysiological mechanical stressors, such as impact, heavy lifting, muscle activations, and work/lifestyle factors (e.g., vibration exposure, gait, and posture) [57], contribute to cell death, catabolism, and inflammation leading to IVD degeneration [3, 11].

<u>Hydrostatic and osmotic pressures</u>

Hydrostatic pressures in the IVD vary between 0.1 and over 3 MPa depending on the posture and activity [3, 58, 59]. Studies that apply a physiological range (0.3 to 1 MPa) of hydrostatic pressure on IVD cells have yielded different results, with some studies

reporting anabolic responses and others reporting catabolism [3]. However, hydrostatic pressures above 3 MPa seem to induce degenerative changes more consistently, although species-specific variations were observed [3].

The osmolality in the IVD is ~430 mOsm/kg and varies during loading with proteoglycan density and hydration [60]. While physiologic osmolality promotes ECM production [61], hypo- or hyperosmolarity affect IVD cell proliferation [62, 63].

<u>Compression</u>

Most mechanical loading studies have investigated compressive stimuli. Static loading was shown to induce detrimental changes including downregulation of ECM genes, protease activation, and cell death both in vitro and in vivo [64-70], supposedly via inhibition of nutrient transport and gas exchange [3]. Physiological dynamic loading (with a magnitude between 0.2 and 1 MPa) was reported to elicit anabolic responses with promotion of cell metabolism and maintenance of ECM synthesis depending on magnitude and frequency [71-73]. On the contrary, hyperphysiological dynamic compression (at high magnitude (> 1.3 MPa), frequency, or duration) causes cell death [74-76], decreased expression of anabolic genes (collagens and proteoglycans) [77-79], as well as increased expression of matrix-degrading enzymes (MMPs, ADAMTS) [72, 77, 79-81] and pro-inflammatory cytokines [75].

<u>Tension</u>

Similar patterns were observed in tensile stress studies. During flexion and extension, the outer AF was shown to experience biaxial stretching with magnitudes between 4% and 6% and negligible biological responses [82, 83]. A study with isolated AF cells stretched at low magnitude (1%) and physiological frequency (1 Hz) showed maintenance of proteoglycan production [84]. However, outside of this physiologic window, stretching can provoke detrimental biological responses. Cyclic stretching of IVD (mostly AF) cells at a high strain of 8 to 20% was shown to induce downregulation of anabolic markers (aggrecan, collagen II) [85] and upregulation of catabolic (MMP 1, 3, 9, 13, ADAMTS 4, 5) [56, 85] and (pro-)inflammatory (COX2, PGE2, IL 1β, 6, 8, 15, toll-like receptors (TLR) 2, 4, nerve growth factor (NGF), TNFα, monocyte chemoattractant protein (MCP) 1, 3, monokine induced by gamma interferon (MIG)) [56, 85-88] mediators.

Mechanosensing and mechanotransduction

Mechanosensing is defined as the process by which cells detect mechanical signals, while mechanotransduction is the process used by the cells to convert mechanical signals into biochemical responses. While many studies have reported biological responses to mechanical signals in the IVD, the investigation and knowledge of the underlying mechanosensing and mechanotransduction mechanisms are very limited. The response of cells to mechanical loading depends on cell morphology, cell-cell interactions, and cell-ECM interactions [3]. Mechanosensing in the IVD is thought to occur via purinergic receptors, integrins, and ion channels including transient receptor potential (TRP) channels [3].

Purinergic receptors

Purinergic receptors in the plasma membrane are indirectly activated by mechanical loading via the production of adenosine triphosphate (ATP). Compressive mechanical loading of NP and AF cells embedded in an agarose hydrogel was shown to increase glucose consumption as well as the production of lactate and ATP [89]. ATP functions as an energy source and building block for proteoglycan synthesis [90]. Moreover, ATP and its breakdown products adenosine diphosphate (ADP) and adenosine regulate different cellular responses via purinergic receptors (P1, P2Y, and P2X) [91]. P1 and P2Y are G-couples protein receptors, while P2X are ligand-gated ion channels [91]. Both NP and AF cells were shown to express P2X4 purinergic receptors [92].

Integrins and cytoskeleton

Integrins are transmembrane heterodimers composed of α and β subunits that can bind specific ECM ligands depending on their subunits [3]. NP cells express the integrin subunits α1, α2, α3, α5, α6, αv, β1, β3, β5, β6, and β8, while AF cells express α1, α5, αv, β1, β3, β5, and β6 [93]. There is currently little information on mechanotransduction pathways through integrin binding. Interestingly, integrin-mediated mechanotransduction was shown to be altered in degenerated IVD cells compared to healthy controls [94].

Integrins are part of focal adhesions, which connect the ECM to the cytoskeleton. The cytoskeleton is mainly composed of actin filaments, tubulin microtubules, and intermediate filaments. In NP cells, F-actin is expressed as short dispersed filaments mainly at the periphery of the cell, while AF cells display organized fibers throughout the cytoplasm, especially in the outer AF [3]. Outer AF cells also express higher levels of β-actin compared to NP cells [95]. On the contrary, NP cells have a higher expression of tubulin compared to outer AF cells [95]. The following intermediate filaments are present in IVD cells and constitute NP and AF cell-specific markers: keratins 8, 18, and 19, vimentin, and nuclear lamins [3]. Both NP and AF cells possess cytoplasmic protrusions called processes. In AF cells, processes spread between lamellar spaces giving them a stellate morphology [96].

The cytoskeleton mediates the cellular response to substrate stiffness. AF cells seeded on a stiff substrate display an elongated morphology and clear actin fibers, while they are round with less clear actin fibers on soft substrates [96]. NP cells tend to form clusters on soft substrates with cell-substrate and cell-cell interactions mediated by cadherins [96]. Moreover, cytoskeletal reorganization is one of the mechanisms by which IVD cells respond to mechanical signals. An example is given by IVD cells stretched in silicone chambers. Cells realign perpendicular to the direction of stretching [97] and express more actin filaments compared to controls [98]. Another example of cytoskeletal reorganization is the cellular response to hypo- and hyperosmolarity and the resulting change in cell volume, which is mediated by F-actin remodeling [3]. In the context of IVD degeneration, inflammation was shown the disrupt the F-actin network and osmotic stress-induced cell volume change in NP cells [99]. Moreover, degenerated IVD cells were shown to be more prone to respond to mechanical stimuli with inflammation compared to healthy cells [3].

Actin formation and organization are mediated by the RhoA/Rho-associated kinase (ROCK) signaling pathway [100]. Interestingly, ROCK inhibition abolished cell-cell interactions and the formation of clusters in NP cells [101]. Cytoskeletal regulation of NP and AF cells has further been associated with the yes-associated protein (YAP) and transcriptional coactivator with PDZ-binding motif (TAZ) signaling [3].

Transient receptor potential channels

Mechanical stress or the cell volume changes caused by osmotic stress provoke conformational changes and deformations of the cellular membrane that might open mechanosensitive ion channels [3]. Candidate ion channels that are expressed differentially between NP and AF cells were identified via proteomic analysis and included sodium, potassium, and calcium channels [3]. Our group has recently investigated the expression of TRP channels in IVD cells [102]. TRP channels are non-selective calcium-permeable transmembrane channels that can be activated by several different stimuli, including changes in temperature, pH, osmolarity, as well as oxidative and mechanical stress [103]. Six subfamilies of TRP channels exist in mammals: TRPC (canonical), TRPV (vanilloid), TRPM (melastatin), TRPP (polycystin), TRPML (mucolipin), and TRPA (ankyrin) [103]. TRP channels can be activated either directly by mechanical forces applied to the cell membrane or indirectly via multistep signaling cascades that induce conformational changes, which in turn apply mechanical force on the cell membrane [104].

A very limited number of studies have investigated TRP channels in the IVD [102, 105-108]. Our group recently reported that 26 out of 28 currently known TRP channels are expressed in the IVD on the mRNA level [102]. Moreover, gene and protein expression of TRPC6, TRPM2 and TRPML1 were higher in degenerated IVDs compared to healthy controls [102]. We also showed that TRPC6 is regulated in simulated microgravity of human IVD cells (See the Chapter " TRPC6 in simulated microgravity of intervertebral disc cells" in the Appendix). Reduced osmolarity was further shown to increase the expression of TRPV4 and pro-inflammatory cytokines in IVD cells [105].

TRPV4 is especially intriguing for the study of IVD degeneration and LBP, as it is known to transduce mechanical, inflammatory and pain signals in joint tissues [109]. TRPV4 was originally described in 2000 as a non-selective calcium-permeable osmosensor [110, 111]. The cryogenic electron microscopy (cryo-EM) and X-ray structures of TRPV4 were reported in 2018 [112]. TRPV4 has a symmetric tetramer architecture (**Figure 5 a, b**). Each subunit has a transmembrane domain composed of 6 membrane-spanning segments S1 to S6 (**Figure 5 c**) [112]. The intracellular domains contain an N-terminal ankyrin repeat domain (ARD) followed by a linker domain (**Figure 5 c**) [112]. A helix-turn-helix (HTH) motif and a pre-S1 helix accommodate the C-terminal TRP domain, a conserved sequence motif among TRP channels that regulates channel activity (**Figure 5 c**) [112]. TRPV4 is constitutively expressed throughout the body and is activated by various stimuli that are also present in the degenerated IVD, such as mechanical and osmotic stress, as well as inflammation under the form of increased tissue temperature and reduced pH [113]. TRPV4 interacts with a multitude of other proteins, including integrins, cytoskeletal proteins, and other ion channels [113]. It mediates physiological functions but also contributes to pain sensations [113]. Deficiency or

23

malfunction of this channel lead to various diseases, including skeletal dysplasias and neuromuscular diseases [113].
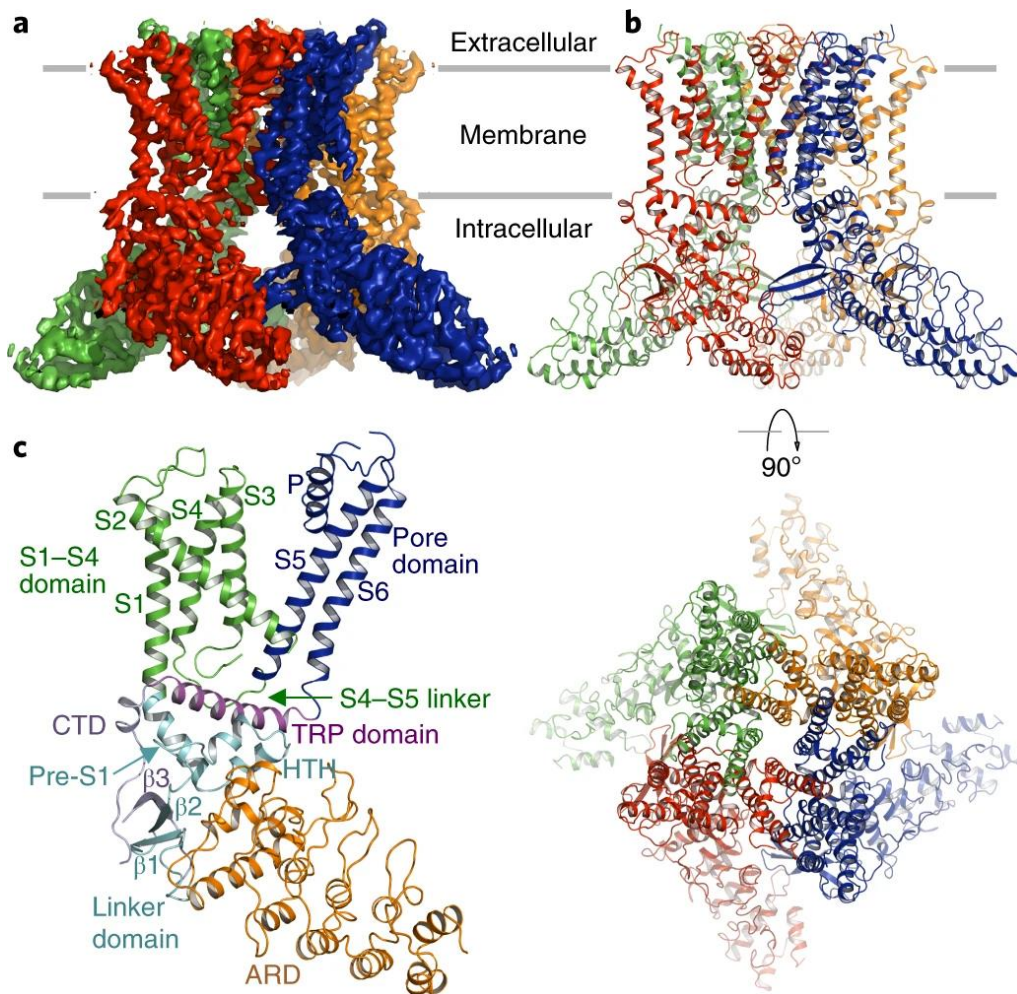
Figure 5: a) Cryo-EM reconstruction of the tetrameric TRPV4 channel. Each subunit is in a different color. **b)** Orthogonal view. **c)** Structure of a single subunit. Each domain is labeled and in a different color. Reprinted from [112] with permission from Springer Nature.

TRPV4 was shown to mediate dynamic compression in chondrocytes [114]. Moreover, cartilage-specific TRPV4 knockout in mice reduced age-related osteoarthritis [115]. The potential of TRPV4 as a therapeutic target is further highlighted by several preclinical trials using TRPV4 inhibitors as a treatment for diverse conditions such as myocardial ischemia/reperfusion injury, ventilator-induced lung injury, and pulmonary edema [116-118]. Furthermore, a selective antagonist of TRPV4 was recently administered to healthy volunteers and heart failure patients without any safety concern [119]. Nevertheless, the role of TRPV4 as a potential mechanotransducer and therapeutic target has never been investigated in the context of DDD and LBP.

2.6 References

1. Oxland, T.R., Fundamental biomechanics of the spine--What we have learned in the past 25 years and future directions. J Biomech, 2016. 49(6): p. 817-832.

2. Frost, B.A., S. Camarero-Espinosa, and E.J. Foster, Materials for the Spine: Anatomy, Problems, and Solutions. Materials (Basel), 2019. 12(2). https://doi.org/10.3390/ma12020253

3. Fearing, B.V., et al., Mechanotransduction and cell biomechanics of the intervertebral disc. JOR Spine, 2018. 1(3). https://doi.org/10.1002/jsp2.1026

4. Pattappa, G., et al., Diversity of intervertebral disc cells: phenotype and function. J Anat, 2012. 221(6): p. 480-96. https://doi.org/10.1111/j.1469-7580.2012.01521.x

5. Maroudas, A., et al., Factors involved in the nutrition of the human lumbar intervertebral disc: cellularity and diffusion of glucose in vitro. J Anat, 1975. 120(Pt 1): p. 113-30.

6. Adams, M.A. and P.J. Roughley, What is intervertebral disc degeneration, and what causes it? Spine (Phila Pa 1976), 2006. 31(18): p. 2151-61.

7. Haefeli, M., et al., The course of macroscopic degeneration in the human lumbar intervertebral disc. Spine (Phila Pa 1976), 2006. 31(14): p. 1522-31.

8. Galbusera, F., et al., Ageing and degenerative changes of the intervertebral disc and their impact on spinal flexibility. European Spine Journal, 2014. 23: p. S324-S332. https://doi.org/10.1007/s00586-014-3203-4

9. Boos, N., et al., Classification of age-related changes in lumbar intervertebral discs: 2002 Volvo Award in basic science. Spine (Phila Pa 1976), 2002. 27(23): p. 2631-44.

10. Vergroesen, P.P., et al., Mechanics and biology in intervertebral disc degeneration: a vicious circle. Osteoarthritis Cartilage, 2015. 23(7): p. 1057-70.

11. Chan, S.C., S.J. Ferguson, and B. Gantenbein-Ritter, The effects of dynamic loading on the intervertebral disc. Eur Spine J, 2011. 20(11): p. 1796-812.

12. Rannou, F., et al., Intervertebral disc degeneration: the role of the mitochondrial pathway in annulus fibrosus cell apoptosis induced by overload. Am J Pathol, 2004. 164(3): p. 915-24.

13. Le Maitre, C.L., A.J. Freemont, and J.A. Hoyland, Accelerated cellular senescence in degenerate intervertebral discs: a possible role in the pathogenesis of intervertebral disc degeneration. Arthritis Res Ther, 2007. 9(3): p. R45.

14. Le Maitre, C.L., A.J. Freemont, and J.A. Hoyland, Localization of degradative enzymes and their inhibitors in the degenerate human intervertebral disc. Journal of Pathology, 2004. 204(1): p. 47-54.

15. Molinos, M., et al., Inflammation in intervertebral disc degeneration and regeneration. Journal of the Royal Society Interface, 2015. 12(104).

16. Wuertz, K. and L. Haglund, Inflammatory mediators in intervertebral disk degeneration and discogenic pain. Global Spine J, 2013. 3(3): p. 175-84.

17. Wuertz, K., et al., Inflammatory and catabolic signalling in intervertebral discs: the roles of NF-kappaB and MAP kinases. Eur Cell Mater, 2012. 23: p. 103-19; discussion 119-20.

18. Ito, K. and L. Creemers, Mechanisms of intervertebral disk degeneration/injury and pain: a review. Global Spine J, 2013. 3(3): p. 145-52.

19. Freemont, A.J., et al., Nerve ingrowth into diseased intervertebral disc in chronic back pain. Lancet, 1997. 350(9072): p. 178-181.

20. Foster, N.E., et al., Prevention and treatment of low back pain: evidence, challenges, and promising directions. Lancet, 2018. 391(10137): p. 2368-2383.

21. Pfirrmann, C.W., et al., Magnetic resonance classification of lumbar intervertebral disc degeneration. Spine (Phila Pa 1976), 2001. 26(17): p. 1873-8.

22. Videman, T., et al., Associations between back pain history and lumbar MRI findings. Spine, 2003. 28(6): p. 582-588.

23. Hasz, M.W., Diagnostic Testing for Degenerative Disc Disease. Advances in Orthopedics, 2012. 2012.

24. Will, J.S., D.C. Bury, and J.A. Miller, Mechanical Low Back Pain. Am Fam Physician, 2018. 98(7): p. 421-428.

25. Childs, J.D., et al., Implications of early and guideline adherent physical therapy for low back pain on utilization and costs. BMC Health Serv Res, 2015. 15: p. 150.

26. Hayden, J.A., et al., Exercise therapy for treatment of non-specific low back pain. Cochrane Database Syst Rev, 2005(3): p. CD000335.

27. Balague, F., et al., Non-specific low back pain. Lancet, 2012. 379(9814): p. 482-91.

28. McKay, G. and M. Walters, Non-Opioid Analgesics. Lecture Notes Clinical Pharmacology and Therapeutics (9th ed.). Hoboken: Wiley. ISBN 9781118344897, 2013.

29. Qaseem, A., et al., Noninvasive Treatments for Acute, Subacute, and Chronic Low Back Pain: A Clinical Practice Guideline From the American College of Physicians. Ann Intern Med, 2017. 166(7): p. 514-530.

30. Roelofs, P.D., et al., Non-steroidal anti-inflammatory drugs for low back pain. Cochrane Database Syst Rev, 2008(1): p. CD000396.

31. Chaparro, L.E., et al., Opioids compared with placebo or other treatments for chronic low back pain: an update of the Cochrane Review. Spine (Phila Pa 1976), 2014. 39(7): p. 556-63.

32. Vowles, K.E., et al., Rates of opioid misuse, abuse, and addiction in chronic pain: a systematic review and data synthesis. Pain, 2015. 156(4): p. 569-76.

33. Chou, R., et al., Epidural Corticosteroid Injections for Radiculopathy and Spinal Stenosis: A Systematic Review and Meta-analysis. Ann Intern Med, 2015. 163(5): p. 373-81.

34. Deyo, R.A. and S.K. Mirza, CLINICAL PRACTICE. Herniated Lumbar Intervertebral Disk. N Engl J Med, 2016. 374(18): p. 1763-72.

35. Chou, R., et al., Surgery for low back pain: a review of the evidence for an American Pain Society Clinical Practice Guideline. Spine (Phila Pa 1976), 2009. 34(10): p. 1094-109.

36. van den Eerenbeemt, K.D., et al., Total disc replacement surgery for symptomatic degenerative lumbar disc disease: a systematic review of the literature. Eur Spine J, 2010. 19(8): p. 1262-80.

37.   Bendtsen, M., et al., Biological challenges for regeneration of the degenerated disc using cellular therapies. Acta Orthopaedica, 2016. 87: p. 39-46.

38.   Sampara, P., et al., Understanding the molecular biology of intervertebral disc degeneration and potential gene therapy strategies for regeneration: a review. Gene Ther, 2018. 25(2): p. 67-82.

39.   Sakai, D. and S. Grad, Advancing the cellular and molecular therapy for intervertebral disc disease. Adv Drug Deliv Rev, 2015. 84: p. 159-71.

40.   Suzuki, M., et al., Nuclear factor-kappa B decoy suppresses nerve injury and improves mechanical allodynia and thermal hyperalgesia in a rat lumbar disc herniation model. Eur Spine J, 2009. 18(7): p. 1001-7.

41.   Nasto, L.A., et al., ISSLS prize winner: inhibition of NF-kappaB activity ameliorates age-associated disc degeneration in a mouse model of accelerated aging. Spine (Phila Pa 1976), 2012. 37(21): p. 1819-25.

42.   Studer, R.K., et al., p38 MAPK inhibition modulates rabbit nucleus pulposus cell response to IL-1. J Orthop Res, 2008. 26(7): p. 991-8.

43.   Mayer, J.E., et al., Genetic polymorphisms associated with intervertebral disc degeneration. Spine J, 2013. 13(3): p. 299-317.

44.   Fontana, G., E. See, and A. Pandit, Current trends in biologics delivery to restore intervertebral disc anabolism. Advanced Drug Delivery Reviews, 2015. 84: p. 146-158.

45.   Ren, S., et al., Treatment of rabbit intervertebral disc degeneration with co-transfection by adeno-associated virus-mediated SOX9 and osteogenic protein-1 double genes in vivo. Int J Mol Med, 2013. 32(5): p. 1063-8.

46.   Moon, S.H., et al., Biologic response of human intervertebral disc cells to gene therapy cocktail. Spine (Phila Pa 1976), 2008. 33(17): p. 1850-5.

47.   Le Maitre, C.L., A.J. Freemont, and J.A. Hoyland, A preliminary in vitro study into the use of IL-1Ra gene therapy for the inhibition of intervertebral disc degeneration. International Journal of Experimental Pathology, 2006. 87(1): p. 17-28.

48.   Krupkova, O., et al., The potential of CRISPR/Cas9 genome editing for the study and treatment of intervertebral disc pathologies. JOR Spine, 2018. 1(1): p. e1003.

49.   Farhang, N., et al., (*) CRISPR-Based Epigenome Editing of Cytokine Receptors for the Promotion of Cell Survival and Tissue Deposition in Inflammatory Environments. Tissue Eng Part A, 2017. 23(15-16): p. 738-749.

50.   Stover, J.D., et al., CRISPR Epigenome Editing of AKAP150 in DRG Neurons Abolishes Degenerative IVD-Induced Neuronal Activation. Mol Ther, 2017. 25(9): p. 2014-2027.

51.   Seki, S., et al., Effect of small interference RNA (siRNA) for ADAMTS5 on intervertebral disc degeneration in the rabbit anular needle-puncture model. Arthritis Res Ther, 2009. 11(6): p. R166.

52.   Sudo, H. and A. Minami, Caspase 3 as a Therapeutic Target for Regulation of Intervertebral Disc Degeneration in Rabbits. Arthritis and Rheumatism, 2011. 63(6): p. 1648-1657.

53.   Yamada, K., et al., Caspase 3 Silencing Inhibits Biomechanical Overload-Induced Intervertebral Disk Degeneration. American Journal of Pathology, 2014. 184(3): p. 753-764.

54. Chan, S.C., et al., Region specific response of intervertebral disc cells to complex dynamic loading: an organ culture study using a dynamic torsion-compression bioreactor. PLoS One, 2013. 8(8): p. e72489.

55. Iatridis, J.C., et al., Region-Dependent Aggrecan Degradation Patterns in the Rat Intervertebral Disc Are Affected by Mechanical Loading In Vivo. Spine, 2011. 36(3): p. 203-209.

56. Sowa, G., et al., Determination of Annulus Fibrosus Cell Response to Tensile Strain as a Function of Duration, Magnitude, and Frequency. Journal of Orthopaedic Research, 2011. 29(8): p. 1275-1283.

57. Setton, L.A. and J. Chen, Cell mechanics and mechanobiology in the intervertebral disc. Spine (Phila Pa 1976), 2004. 29(23): p. 2710-23.

58. Wilke, H.J., et al., ISSLS prize winner: A novel approach to determine trunk muscle forces during flexion and extension: a comparison of data from an in vitro experiment and in vivo measurements. Spine (Phila Pa 1976), 2003. 28(23): p. 2585-93.

59. Sato, K., S. Kikuchi, and T. Yonezawa, In vivo intradiscal pressure measurement in healthy individuals and in patients with ongoing back problems. Spine (Phila Pa 1976), 1999. 24(23): p. 2468-74.

60. Ishihara, H., et al., Proteoglycan synthesis in the intervertebral disk nucleus: the role of extracellular osmolality. Am J Physiol, 1997. 272(5 Pt 1): p. C1499-506.

61. O'Connell, G.D., I.B. Newman, and M.A. Carapezza, Effect of long-term osmotic loading culture on matrix synthesis from intervertebral disc cells. Biores Open Access, 2014. 3(5): p. 242-9.

62. Mavrogonatou, E. and D. Kletsas, High osmolality activates the G1 and G2 cell cycle checkpoints and affects the DNA integrity of nucleus pulposus intervertebral disc cells triggering an enhanced DNA repair response. DNA Repair (Amst), 2009. 8(8): p. 930-43.

63. Mavrogonatou, E. and D. Kletsas, Effect of varying osmotic conditions on the response of bovine nucleus pulposus cells to growth factors and the activation of the ERK and Akt pathways. J Orthop Res, 2010. 28(10): p. 1276-82.

64. Hsieh, A.H. and J.C. Lotz, Prolonged spinal loading induces matrix metalloproteinase-2 activation in intervertebral discs. Spine (Phila Pa 1976), 2003. 28(16): p. 1781-8.

65. Lotz, J.C., et al., Compression-induced degeneration of the intervertebral disc: an in vivo mouse model and finite-element study. Spine (Phila Pa 1976), 1998. 23(23): p. 2493-506.

66. Lotz, J.C. and J.R. Chin, Intervertebral disc cell death is dependent on the magnitude and duration of spinal loading. Spine, 2000. 25(12): p. 1477-1482.

67. Iatridis, J.C., et al., Compression-induced changes in intervertebral disc properties in a rat tail model. Spine (Phila Pa 1976), 1999. 24(10): p. 996-1002.

68. Chen, J., W. Yan, and L.A. Setton, Static compression induces zonal-specific changes in gene expression for extracellular matrix and cytoskeletal proteins in intervertebral disc cells in vitro. Matrix Biol, 2004. 22(7): p. 573-83.

69. Hutton, W.C., et al., The effect of compressive force applied to the intervertebral disc in vivo. A study of proteoglycans and collagen. Spine (Phila Pa 1976), 1998. 23(23): p. 2524-37.

70. Ohshima, H., J.P. Urban, and D.H. Bergel, Effect of static load on matrix synthesis rates in the intervertebral disc measured in vitro by a new perfusion technique. J Orthop Res, 1995. 13(1): p. 22-9.

71. Korecki, C.L., J.J. MacLean, and J.C. Iatridis, Dynamic compression effects on intervertebral disc mechanics and biology. Spine (Phila Pa 1976), 2008. 33(13): p. 1403-9.

72. Maclean, J.J., et al., Anabolic and catabolic mRNA levels of the intervertebral disc vary with the magnitude and frequency of in vivo dynamic compression. J Orthop Res, 2004. 22(6): p. 1193-200.

73. Neidlinger-Wilke, C., et al., A three-dimensional collagen matrix as a suitable culture system for the comparison of cyclic strain and hydrostatic pressure effects on intervertebral disc cells. J Neurosurg Spine, 2005. 2(4): p. 457-65.

74. Walsh, A.J. and J.C. Lotz, Biological response of the intervertebral disc to dynamic loading. J Biomech, 2004. 37(3): p. 329-37.

75. Wang, D.L., S.D. Jiang, and L.Y. Dai, Biologic response of the intervertebral disc to static and dynamic compression in vitro. Spine (Phila Pa 1976), 2007. 32(23): p. 2521-8.

76. Illien-Junger, S., et al., The combined effects of limited nutrition and high-frequency loading on intervertebral discs with endplates. Spine (Phila Pa 1976), 2010. 35(19): p. 1744-52.

77. MacLean, J.J., et al., Effects of immobilization and dynamic compression on intervertebral disc cell gene expression in vivo. Spine (Phila Pa 1976), 2003. 28(10): p. 973-81.

78. Ching, C.T., et al., Changes in nuclear composition following cyclic compression of the intervertebral disc in an in vivo rat-tail model. Med Eng Phys, 2004. 26(7): p. 587-94.

79. Korecki, C.L., et al., Intervertebral Disc Cell Response to Dynamic Compression Is Age and Frequency Dependent. Journal of Orthopaedic Research, 2009. 27(6): p. 800-806.

80. MacLean, J.J., et al., The effects of short-term load duration on anabolic and catabolic gene expression in the rat tail intervertebral disc. J Orthop Res, 2005. 23(5): p. 1120-7.

81. Wuertz, K., et al., In vivo remodeling of intervertebral discs in response to short- and long-term dynamic compression. J Orthop Res, 2009. 27(9): p. 1235-42.

82. Li, S.Y., et al., The Effects of Cyclic Tensile Strain on the Organisation and Expression of Cytoskeletal Elements in Bovine Intervertebral Disc Cells: An in Vitro Study. European Cells & Materials, 2011. 21: p. 508-522.

83. Stokes, I.A., Surface strain on human intervertebral discs. J Orthop Res, 1987. 5(3): p. 348-55.

84. Rannou, F., et al., Cyclic tensile stretch modulates proteoglycan production by intervertebral disc annulus fibrosus cells through production of nitrite oxide. J Cell Biochem, 2003. 90(1): p. 148-57.

85. Shengjie, W., et al., High amplitude and low frequency cyclic mechanical strain promotes degeneration of human nucleus pulposus cells via the NF-κB p65 pathway. Journal of Cellular Physiology, 2018. 233(9): p. 7206-7216.

86. Miyamoto, H., et al., Effects of cyclic mechanical stress on the production of inflammatory agents by nucleus pulposus and anulus fibrosus derived cells in vitro. Spine, 2006. 31(1): p. 4-9.

87. Gawri, R., et al., High mechanical strain of primary intervertebral disc cells promotes secretion of inflammatory factors associated with disc degeneration and pain. Arthritis Res Ther, 2014. 16(1): p. R21.

88. Pratsinis, H., et al., Cyclic tensile stress of human annulus fibrosus cells induces MAPK activation: involvement in proinflammatory gene expression. Osteoarthritis Cartilage, 2016. 24(4): p. 679-87.

89. Fernando, H.N., et al., Mechanical loading affects the energy metabolism of intervertebral disc cells. J Orthop Res, 2011. 29(11): p. 1634-41.

90. Hirschberg, C.B., P.W. Robbins, and C. Abeijon, Transporters of nucleotide sugars, ATP, and nucleotide sulfate in the endoplasmic reticulum and Golgi apparatus. Annu Rev Biochem, 1998. 67: p. 49-69.

91. Burnstock, G., Pathophysiology and therapeutic potential of purinergic signaling. Pharmacol Rev, 2006. 58(1): p. 58-86.

92. Gonzales, S., et al., Measurement of ATP-Induced Membrane Potential Changes in IVD cells. Cell Mol Bioeng, 2014. 7(4): p. 598-606.

93. Nettles, D.L., W.J. Richardson, and L.A. Setton, Integrin expression in cells of the intervertebral disc. J Anat, 2004. 204(6): p. 515-20.

94. Le Maitre, C.L., et al., Altered integrin mechanotransduction in human nucleus pulposus cells derived from degenerated discs. Arthritis Rheum, 2009. 60(2): p. 460-9.

95. Li, S., V.C. Duance, and E.J. Blain, Zonal variations in cytoskeletal element organization, mRNA and protein expression in the intervertebral disc. J Anat, 2008. 213(6): p. 725-32.

96. Molladavoodi, S., J. McMorran, and D. Gregory, Mechanobiology of annulus fibrosus and nucleus pulposus cells in intervertebral discs. Cell Tissue Res, 2020. 379(3): p. 429-444.

97. Abbott, R.D., et al., Live free or die: stretch-induced apoptosis occurs when adaptive reorientation of annulus fibrosus cells is restricted. Biochem Biophys Res Commun, 2012. 421(2): p. 361-6.

98. Li, S., et al., The effects of cyclic tensile strain on the organisation and expression of cytoskeletal elements in bovine intervertebral disc cells: an in vitro study. Eur Cell Mater, 2011. 21: p. 508-22.

99. Maidhof, R., et al., Inflammation induces irreversible biophysical changes in isolated nucleus pulposus cells. PLoS One, 2014. 9(6): p. e99621.

100. Amano, M., M. Nakayama, and K. Kaibuchi, Rho-kinase/ROCK: A key regulator of the cytoskeleton and cell polarity. Cytoskeleton (Hoboken), 2010. 67(9): p. 545-54.

101. Hwang, P.Y., et al., The role of extracellular matrix elasticity and composition in regulating the nucleus pulposus cell phenotype in the intervertebral disc: a narrative review. J Biomech Eng, 2014. 136(2): p. 021010.

102. Sadowska, A., et al., Differential regulation of TRP channel gene and protein expression by intervertebral disc degeneration and back pain. Sci Rep, 2019. 9(1): p. 18889.

103. Krupkova, O., J. Zvick, and K. Wuertz-Kozak, The Role of Transient Receptor Potential Channels in Joint Diseases. European Cells & Materials, 2017. 34: p. 180-201.

104. Liu, C. and C. Montell, Forcing open TRP channels: Mechanical gating as a unifying activation mechanism. Biochem Biophys Res Commun, 2015. 460(1): p. 22-5.

105. Walter, B.A., et al., Reduced tissue osmolarity increases TRPV4 expression and pro-inflammatory cytokines in intervertebral disc cells. Eur Cell Mater, 2016. 32: p. 123-36.

106. Sadowska, A., et al., Inflammaging in cervical and lumbar degenerated intervertebral discs: analysis of proinflammatory cytokine and TRP channel expression. Eur Spine J, 2018. 27(3): p. 564-577.

107. Kameda, T., et al., Expression and Activity of TRPA1 and TRPV1 in the Intervertebral Disc: Association with Inflammation and Matrix Remodeling. Int J Mol Sci, 2019. 20(7).

108. Franco-Obregon, A., et al., TRPC6 in simulated microgravity of intervertebral disc cells. Eur Spine J, 2018. 27(10): p. 2621-2630.

109. McNulty, A.L., et al., TRPV4 as a therapeutic target for joint diseases. Naunyn Schmiedebergs Arch Pharmacol, 2015. 388(4): p. 437-50.

110. Strotmann, R., et al., OTRPC4, a nonselective cation channel that confers sensitivity to extracellular osmolarity. Nat Cell Biol, 2000. 2(10): p. 695-702.

111. Liedtke, W., et al., Vanilloid receptor-related osmotically activated channel (VR-OAC), a candidate vertebrate osmoreceptor. Cell, 2000. 103(3): p. 525-35.

112. Deng, Z.Q., et al., Cryo-EM and X-ray structures of TRPV4 reveal insight into ion permeation and gating mechanisms. Nature Structural & Molecular Biology, 2018. 25(3): p. 252-+. https://doi.org/10.1038/s41594-018-0037-5

113. White, J.P.M., et al., TRPV4: Molecular Conductor of a Diverse Orchestra. Physiological Reviews, 2016. 96(3): p. 911-973.

114. O'Conor, C.J., et al., TRPV4-mediated mechanotransduction regulates the metabolic response of chondrocytes to dynamic loading. Proc Natl Acad Sci U S A, 2014. 111(4): p. 1316-21.

115. O'Conor, C.J., et al., Cartilage-Specific Knockout of the Mechanosensory Ion Channel TRPV4 Decreases Age-Related Osteoarthritis. Sci Rep, 2016. 6: p. 29053.

116. Dong, Q., et al., Blockage of transient receptor potential vanilloid 4 alleviates myocardial ischemia/reperfusion injury in mice. Sci Rep, 2017. 7: p. 42678.

117. Michalick, L., et al., Transient Receptor Potential Vanilloid 4 and Serum Glucocorticoid-regulated Kinase 1 Are Critical Mediators of Lung Injury in Overventilated Mice In Vivo. Anesthesiology, 2017. 126(2): p. 300-311.

118. Thorneloe, K.S., et al., An orally active TRPV4 channel blocker prevents and resolves pulmonary edema induced by heart failure. Sci Transl Med, 2012. 4(159): p. 159ra148.

119. Goyal, N., et al., Clinical Pharmacokinetics, Safety, and Tolerability of a Novel, First-in-Class TRPV4 Ion Channel Inhibitor, GSK2798745, in Healthy and Heart Failure Subjects. Am J Cardiovasc Drugs, 2019. 19(3): p. 335-342.

Chapter 3

Cell-laden agarose-collagen composite hydrogels for mechanotransduction studies

Cell-laden agarose-collagen composite hydrogels for mechanotransduction studies

Elena Cambria[1], Silvio Brunner[1†], Sally Heusser[1†], Philipp Fisch[1], Wolfgang Hitzl[2,3,4], Stephen J. Ferguson[1] and Karin Wuertz-Kozak[1,5,6]

[1] Institute for Biomechanics, ETH Zurich, Zurich, Switzerland

[2] Research Office (Biostatistics), Paracelsus Medical University, Salzburg, Austria

[3] Department of Ophthalmology and Optometry, Paracelsus Medical University, Salzburg, Austria

[4] Research Program Experimental Ophthalmology and Glaucoma Research, Paracelsus Medical University, Salzburg, Austria

[5] Department of Biomedical Engineering, Rochester Institute of Technology, Rochester, NY, United States

[6] Spine Center, Schön Klinik München Harlaching, Academic Teaching Hospital and Spine Research Institute of the Paracelsus Private Medical University Salzburg (Austria), Munich, Germany

[†] These authors contributed equally.

3.1 Abstract

The increasing investigation of cellular mechanotransduction mechanisms requires biomaterials combining biofunctionality and suitable mechanical properties. Agarose is a standard biomaterial for cartilage and intervertebral disc mechanobiology studies but lacks adhesion motifs and the necessary cell-matrix interaction for mechanotransduction. Here, collagen type I was blended at two concentrations (2 and 4.5 mg/mL) with agarose 2% wt/vol. The composite hydrogels were characterized in terms of structural homogeneity, rheological properties and size stability. Nucleus pulposus (NP) cell viability, proliferation, morphology, gene expression, GAG production, adhesion and mechanotransduction ability were further tested. Blended hydrogels presented a homogenous network of the two polymers. While the addition of 4.5 mg/mL collagen significantly decreased the storage modulus and increased the loss modulus of the gels, blended gels containing 2 mg/mL collagen displayed similar mechanical properties to agarose. Hydrogel size was conserved over 21 days for all agarose-based gels. Embedded cells were viable (> 80%) and presented reduced proliferation and a round morphology typical of NP cells in vivo. Gene expression of collagen type I and II and aggrecan significantly increased in blended hydrogels from day 1 to 7, further resulting in a significantly superior GAG/DNA ratio compared to agarose gels at day 7. Agarose-collagen hydrogels not only promoted cell adhesion, contrary to agarose gels, but also showed a 5.36-fold higher focal adhesion kinase phosphorylation (pFAK/β-tubulin) when not compressed, and increased pFAK/FAK values 10 min after compression. Agarose-collagen thus outperforms agarose, mimics native tissues constituted of non-fibrillar matrix and collagens, and allows exploring complex loading in a highly reproducible system.

Keywords: blended hydrogels, agarose, collagen, mechanobiology, extracellular matrix, dynamic compression, focal adhesion kinase

3.2 Introduction

As many degenerative and regenerative processes are related to mechanical loading, the field of mechanobiology is widely expanding. The interest in understanding how mechanical signals influence cell behavior is in fact shared across disciplines as diverse as cancer and developmental biology, regenerative medicine, tissue engineering, and clinical disciplines such as pulmonology and orthopedics [1; 2; 3]. As an example, mechanical loading is a known contributor to intervertebral disc (IVD) degeneration, which when associated with pain and inflammation, is defined as degenerative disc disease [4]. Degenerative disc disease is a leading source of low back pain, which is itself the first cause of disability worldwide with a lifetime prevalence of 84% [5].

While physiological mechanical loading promotes the metabolic balance of the IVD [6], hyperphysiological loading provokes cell catabolism, inflammation and reduced cell viability [7]. Partly due to poor knowledge about the underlying molecular mechanisms, current treatments, such as anti-inflammatory drugs, are not targeted and have low effect

sizes [5]. Therefore, studies aiming at unlocking mechanotransduction mechanisms in the IVD are needed.

Mechanotransduction in vivo takes place in a three-dimensional (3D) microenvironment with instructive biochemical cues and specific mechanical stimuli [2]. Conducting mechanotransduction studies with in vivo relevance thus requires advanced 3D culture systems that possess both the biofunctionality of native extracellular matrix (ECM) proteins, and tunable mechanical properties. However, such biomaterials are rare. Agarose has established itself as a gold standard biomaterial for dynamic compression studies, primarily in the field of cartilage tissue engineering [8]. Agarose is a linear polysaccharide derived from red algae and consisting of β-1,3-linked-D-galactose and α-1,4-linked 3,6-anhydro-L-galactose units [9]. The gelling mechanism of agarose resides in the formation and aggregation of double helices by intermolecular hydrogen-bonds upon cooling [9]. Agarose offers biocompatibility, retention of round cell morphology, homogeneity and strong mechanical properties [10]. The elastic modulus of agarose ranges from ~1 to a few thousand kPa, depending on polymer concentration and molecular weight [11]. However, agarose is bio-inert and does not present any cell adhesion motifs. This characteristic is a shortcoming in the investigation of mechanotransduction, where most of the mechanisms are thought to originate from the ability of mechanosensors, such as integrins, to interact with the surrounding ECM [12]. In fact, the positive effects of mechanical loading on cell-laden agarose constructs seem to become apparent only after a pre-culture period aiming to increase pericelluar matrix production [8].

To enhance the biofunctionality of agarose, covalent modifications with adhesive peptides or proteins have been achieved through 1'1, carbonyldiimidazole (CDI) chemistry [13; 14; 15], reaction with S-2-nitrobenzyl cysteine (S-NBC) [16], crosslinking with sulfosuccinimidyl 6-(4'-azido-2'-nitrophenylamino)hexanoate (sulfo-SANPAH) [17; 18; 19; 20; 21], and carboxylation and EDC (1-ethyl-3-(3-dimethylaminopropyl) carbodiimide) condensation [22]. Interestingly, in a 3D covalently crosslinked collagen type IV-agarose system, the effect of high rate shear deformation aiming to mimic traumatic injury on neurons was enhanced by increasing collagen concentration [23]. Nevertheless, covalent modifications are time-consuming and involve cytotoxic reagents that need to be extensively washed out.

In order to improve the mechanical properties of natural ECM protein hydrogels, it is possible to physically blend-in agarose at low concentrations [24; 25; 26]. Ulrich et al. found that adding agarose into collagen I 3D hydrogels largely increased their elasticity and reduced cell migration [24]. Similar collagen-agarose co-gels were mechanically tested under uniaxial tension [25] and indentation [26]. Conversely, and as an alternative to covalent modifications, the polymer blending technique can also be used to incorporate peptides and proteins in agarose to improve its bioactivity. Yamada and colleagues have blended laminin active peptides in 2D agarose gels and have shown enhanced cell adhesion based on substrate stiffness [27]. Composite agarose-based microbeads blended with collagen or fibrinogen/ hydroxyapatite have been produced by emulsification [28; 29] and used for osteogenic differentiation [30] and vasculogenesis [29], respectively. Nevertheless, the concentrations of agarose used in these studies were relatively low (up to 1% wt/vol), while the typical concentration to enable suitable mechanical stability and

load transmission in dynamic compression studies is equal or above 2% wt/vol [8]. In this study, the final agarose concentration was kept constant to 2% wt/vol and collagen I was physically blended at two final concentrations of 2 and 4.5 mg/mL.

We aimed to develop novel agarose-collagen composite hydrogels that: i) simultaneously combine the mechanical qualities of 2% wt/vol agarose and the biofunctionality of collagen I; ii) mimic native tissues constituted of non-fibrillar matrix and collagens; and iii) allow the investigation of complex loading and cellular mechanotransduction. To this end, we characterized hydrogels in terms of homogeneity, mechanical properties, size stability, and assessed their effect on IVD cell viability, proliferation, gene expression and glycosaminoglycans (GAG) content. Furthermore, we tested the hypothesis that agarose-collagen hydrogels display enhanced cell adhesion and mechanotransduction capacity compared to agarose hydrogels, as measured by focal adhesion kinase (FAK) phosphorylation after dynamic compression.

3.3 Materials and methods

Cell isolation and culture

Tails from 18-24-month-old cows were obtained from the local slaughterhouse and carefully dissected to expose the IVDs. Nucleus pulposus (NP) biopsies were minced and digested overnight at 37°C, 5% CO_2, using 0.4% collagenase NB4 (17454.01, Serva) and 0.2% dispase II (04942078001, Roche) dissolved in PBS 1X with 5% Antibiotic-Antimycotic (Anti-Anti; 15240-062, Gibco). The next day, the tissue digest was filtered through a cell strainer and the cell suspension was centrifuged at 1000 rpm for 5 min. The pellet was washed with culture medium (Dulbecco's modified Eagle medium/F-12 Nutrient Mixture (DMEM/F12; 31330-038, Gibco), 10% fetal calf serum (FCS; F7524, Sigma-Aldrich) and 1% Anti-Anti). After centrifugation and resuspension in culture medium, cells were seeded in fibronectin-coated (0.01 mg/mL human plasma fibronectin; FC010, Merck Millipore) culture flasks (150 cm^2). Cells were expanded to passage 1-2 at 37°C, 5% CO_2, and the medium was changed twice per week.

Hydrogel fabrication and culture

Agarose hydrogels: Agarose 4% wt/vol (1.6 g agarose powder; 50101, SeaPlaque low-gelling temperature, Lonza; dissolved in 40 mL PBS 1X and autoclaved at 120°C) was first heated in the microwave and cooled down to 40°C. Cells were trypsinized and resuspended at a density of 8×10^6 cells/mL in PBS 1X at 4°C. The agarose solution was then mixed 1:1 with the cell suspension and vortexed to obtain a final cell concentration of 4×10^6 cells/mL in agarose 2% wt/vol. Using a positive displacement pipette, 160 µL of the mixture were molded in a silicon ring (inner Ø: 8 mm, outer Ø: 12 mm, height: 3 mm) placed between two microscope glass slides. Agarose hydrogels gelled within 1-2 minutes at room temperature (RT).

Collagen hydrogels: Bovine collagen I (6 mg/mL; 5010, Advanced BioMatrix) was mixed on ice with UltraPure Distilled Water (Invitrogen), PBS 10X and 1 M NaOH

according to the manufacturer protocol to obtain a 5 mg/mL collagen solution. Pelleted cells were resuspended and vortexed with the collagen solution to obtain a concentration of 4×10^6 cells/mL. Hydrogels were molded as described above and incubated for 30 min at 37°C until complete gelation.

Agarose-collagen hydrogels: Agarose 4% wt/vol was heated and kept at 60°C. In parallel, bovine collagen I (10 mg/mL; 5133, Advanced BioMatrix) was mixed with UltraPure Distilled Water according to the manufacturer protocol to obtain a 9 mg/mL or 4 mg/mL collagen solution. Pelleted cells were resuspended in the collagen solution to obtain an 8×10^6 cells/mL suspension. The solution was then mixed 1:1 and vortexed with the agarose 4% wt/vol solution to obtain a final concentration of 4×10^6 cells/mL in agarose 2% wt/vol and collagen 4.5 mg/mL or 2 mg/mL. Hydrogels were molded as described above, incubated for 10 min at RT, and for 30 min at 37°C until complete gelation.

Hydrogels were demolded and cultured in 12-well plates in culture medium at 37°C, 5% CO_2 for up to 21 days. The medium was changed every other day.

Confocal reflection microscopy of collagen I

One day after hydrogel fabrication, cell-free hydrogels were incubated for 1 h in PBS 1X and imaged with a confocal microscope (Leica TCS SP8). Images were acquired in the reflection mode with a 488 nm laser and a 25X water objective. The reflected light was detected in the range from 475 to 795 nm. Images were stitched in order to image a whole gel.

Rheometry

Oscillatory measurements were performed on an Anton Paar MCR301 Rheometer (Anton Paar, Switzerland), equipped with a 20 mm diameter parallel plate geometry (PP20; Anton Paar, Switzerland) and a peltier element with hood (H-PTD 200; Anton Paar, Switzerland). To avoid slipping of the hydrogels during oscillation, the plate and the probe of the rheometer were coated with 330 μL 0.1 mg/mL PLL at 60°C. A wet tissue was placed inside the hood to avoid evaporation of the hydrogels. Rheometry was performed with cell-free hydrogels at a gap of 1 mm, with a deflection angle of 1% and a frequency of 1 Hz. The measurement was performed in several intervals with temperatures ranging from 24 to 37°C depending on the hydrogel type (**Table 1**).

Table 1: Duration and temperature of rheometry intervals depending on hydrogel type

Gel	Interval 1	Interval 2	Interval 3	Interval 4	Interval 5	Interval 6
Agarose	3.6 min, 33°C→24°C	240 min 24°C	5.3 min 24°C→37°C	210 min 37°C	5.3 min 27°C→24°C	210 min 24°C
Agarose-Collagen	3.6 min, 33°C→24°C	300 min 24°C	5.3 min 24°C→37°C	270 min 37°C	5.3 min 27°C→24°C	270 min 24°C
Collagen	10 min, 13°C→37°C	240 min 37°C	5.3 min 37°C→24°C	215.3 min 24°C		

Hydrogel dimension measurement

At days 1, 7 and 21 after fabrication, cell-laden hydrogels were placed under a camera positioned at constant height. Pictures were acquired and the hydrogel diameter was evaluated with the distance measurement function of the ImageJ software. The height of the hydrogels was measured with a mechanical tester (TA.XTplus Texture Analyser, Stable Micro System), with a 5 kg load cell.

Viability assay

At days 1, 7 and 21 after fabrication, hydrogels were incubated in NucBlue Live Cell Stain (R37605, Thermo Fisher Scientific) and 2 µM ethidium homodimer (46043, Sigma-Aldrich) in culture medium for 1 h at 37°C in the dark. Hydrogels were washed with PBS 1X and imaged with a confocal microscope (Leica TCS SP8) and a 20X dry objective. Six images per gel from 20 to 120 µm from the bottom of the gel (Z-stack) were acquired. Automated cell counting based on particle size and circularity was performed for each image using the ImageJ software. The cell viability percentage was calculated as the difference between the number of NucBlue-stained cells and the number of ethidium homodimer-stained cells, divided by the number of NucBlue-stained cells.

Proliferation assay

At days 1, 7 and 21 after fabrication, hydrogels were incubated for 24 h in 1 µM EdU in culture medium at 37°C (Click-iT EdU Imaging Kit Alexa-Fluor 488, C10337, Thermo Fisher Scientific) and washed 3 x 5 min with PBS 1X. Hydrogels were then fixed with 4% formaldehyde for 30 min at RT and washed 3 x 5 min with blocking solution (3% BSA (A6588, AppliChem) in PBS 1X). Cells were permeabilized with 0.25% Triton X-100 (A4975, AppliChem) in blocking solution for 30 min and hydrogels were washed 3 x 5 min with blocking solution. The reagents of the kit were mixed according to the manufacturer protocol except for the Alexa Fluor azide, which was used at half of the recommended concentration. Hydrogels were incubated for 45 min in Click-IT reaction cocktail in the dark, washed three times with blocking solution, and incubated for 30 min in 2 µg/mL DAPI (62248, Thermo Fisher Scientific) in PBS 1X. After 3 x 5 min washes in PBS 1X, hydrogels were imaged with a confocal microscope (Leica TCS SP8), using a 20X dry objective and a 488 nm laser to visualize the proliferating cells. Automated cell counting based on particle size and circularity was performed using the ImageJ software. The proliferating cell percentage was calculated as the number of Alexa-Fluor 488-stained cells divided by the number of DAPI-stained cells.

3D cell morphology imaging

At days 1, 7 and 21 after fabrication, hydrogels were washed three times with PBS 1X and fixed with 4% formaldehyde (252549, Sigma-Aldrich) for 30 min at RT. After incubation in blocking solution (3% BSA, 0.5% TWEEN 20 (P1379, Sigma-Aldrich) in PBS 1X) for 3 x 5 min, cells were permeabilized with 0.25% Triton X-100 in blocking solution for 30 min. Hydrogels were washed for 3 x 5 min with blocking solution and then incubated in the dark for 2 h in 6.6 nM Alexa Fluor 568 phalloidin (A12380, Thermo Fisher

Scientific) in blocking solution. After 3 washes in blocking solution, hydrogels were incubated for 30 min in 2 μg/mL DAPI diluted in PBS 1X. Hydrogels were finally washed 3 x 5 min in PBS 1X and imaged with a confocal microscope (Leica TCS SP8), using a 40X water objective and a DPSS 561 nm laser to visualize the phalloidin-stained F-actin filaments.

RNA extraction and RT-qPCR

At days 1, 7 and 21 after fabrication, hydrogels were washed in PBS 1X. Following the protocol of Bougault et al. [10], hydrogels were dissolved in solubilization buffer (1.5 mL QG buffer (19063, Qiagen), 2 mL RLT lysis buffer (79216, Qiagen), 20 μL 2-mercaptoethanol) and RNA was extracted using the RNeasy Mini Kit (74106, Qiagen). RNA was eluted in 30 μL RNase-free water and the RNA yield and purity were assessed with a NanoDrop 1000 Spectrophotometer (Thermo Fisher Scientific). RNA (100 ng to 1 μg) was reverse-transcribed into cDNA in a 60 μL volume using the TaqMan Reverse Transcription kit (N8080234, Applied Biosystems). For each qPCR reaction, 10 ng of cDNA was mixed with TaqMan primers (COL1A2: Bt03214883_m1; COL2A1: Bt03251861_m1; ACAN: Bt03212186_m1; YWHAZ: Bt01122444_g1), TaqMan Fast Universal PCR Master Mix (2X) (4352042, Applied Biosystems) and RNAse-free water to a total volume of 10 μL. Gene expression was measured in duplicates with the CFX96 Touch Detection System (Bio-Rad). YWHAZ was used as a reference gene. Results are shown as $2^{-\Delta Ct}$ values (i.e. relative to YWHAZ).

GAG and DNA quantification

At days 1, 7 and 21 after fabrication, hydrogels were snap-frozen in liquid nitrogen and lyophilized overnight. Hydrogels and GAG standards (bovine chondroitin sulfate, C6737, Sigma-Aldrich) ranging from 0.78 μg/mL to 50 μg/mL were digested for 16 h at 60°C in 140 μg/mL papain in 100 mM phosphate buffer pH 6.5, 5 mM L-cysteine•HCl and 5 mM Na2EDTA. After digestion, the samples and the standards were centrifuged for 10 min at 12'000 rpm and 40 μL of the supernatant were pipetted in duplicate in a 96-well plate. Dimethylmethylene blue solution [31] was added (150 μL/well) and absorbance was measured immediately at 540 nm with a reference at 595 nm using a plate reader (Infinite M200 PRO, TECAN). The Quant-iT PicoGreen™ dsDNA Assay Kit (P7589, Thermo Fisher Scientific) was used for DNA quantification according to the manufacturer protocol. For each sample, the GAG quantity (μg) was normalized to the DNA quantity (μg).

2D cell adhesion assay

Hydrogel solutions were prepared as described above and 10 μL were cast in a 96-well angiogenesis plate (89646, ibidi). Bovine NP cells were seeded on top of the hydrogels at a density of 60'000 cells/cm^2 in 50 μL/well culture medium and incubated overnight at 37°C, 5% CO2. The next day, hydrogels were washed three times with PBS 1X, fixed and stained with Alexa-Fluor 568 phalloidin and DAPI as described above. A confocal microscope (Leica TCS SP8) with 10X and 20X dry objectives and a DPSS 561 nm laser

was used to image the cells on the hydrogels. Automated counting of the DAPI-stained cells was performed with the ImageJ software.

Cell-laden hydrogel dynamic compression

Agarose and 2 mg/mL agarose-collagen hydrogels were pre-cultured in the silicon rings used for molding for 7 days at 37°C, 5% CO_2, in DMEM/F-12 without phenol red (11039-021, Gibco) supplemented with 10% FCS and 0.1% ampicillin (A0839, AppliChem). Two hours before compression, the medium was replaced with serum-free medium. For dynamic compression, the hydrogels in silicon rings were transferred to the wells of a commercial compression device (MCTR, CellScale) in 1 mL of serum-free medium. Hydrogels were dynamically compressed for 5, 10 or 20 min with a sine wave function at 0.5 Hz with a nominal force of 73 N and 3 N of pre-load (corresponding to a 20% strain ratio) at 37°C, 5% CO_2. Non-compressed hydrogels were kept in identical conditions in a 12-well plate. Immediately after mechanical loading, hydrogels were processed for protein analysis.

Protein extraction and Western blot

Hydrogels were cut into 4 pieces, washed with PBS 1X, snap-frozen in liquid nitrogen and lyophilized overnight. RIPA buffer supplemented with protease and phosphatase inhibitor cocktails (78430; 78428, Thermo Fisher Scientific) was used to lyse the hydrogels on ice (100 μL/gel) for 1 h. The lysates and the soaked hydrogels were then transferred to NucleoSpin filter columns (740606, Macherey-Nagel) and centrifuged for 1 h at 4°C at 12'000 rpm. For all samples, 22.5 μL of lysate were mixed with 4X Laemmli buffer (1610747, Bio-Rad), heated for 5 min at 95°C, and loaded onto a 4-20% gradient gel (4568093, Bio-Rad). Proteins were separated by electrophoresis in a Mini-PROTEAN Tetra Cell (Bio-Rad) and transferred to a PVDF membrane (1704156, Bio-Rad). The membrane was washed 3 x 10 min with Tris Buffered Saline with 0.05% TWEEN 20 (TBS-T) and blocked for 2 h at RT with 5% skim milk diluted in TBS-T. Primary antibodies (FAK: 3285; phospho-FAK (Tyr397): 3283; β-tubulin: 2146; Cell Signaling Technology) were applied 1:1000 in 3% BSA in TBS-T overnight at 4°C on a rocker. The next day, the membrane was washed 3 x 10 min with TBS-T and incubated for 1 h at RT on a rocker with the secondary antibody (anti-rabbit IgG HRP: 7074, Cell Signaling Technology) diluted 1:1000 in 5% skim milk in TBS-T. After washing 3 x 10 min with TBS-T, proteins were detected with a chemiluminescence substrate (34076, Thermo Fisher Scientific) on a ChemiDocTouch Imaging System (Bio-Rad). The density of the bands was semi-quantified using the Volume Tools of the ImageLab software (Bio-Rad) and by fitting a rectangular shape of same area to each band. For each blot, the density of each band was normalized by the one of the agarose non-compressed control. Phospho-FAK and FAK were each expressed relative to the β-tubulin loading control and the pFAK/FAK ratio was calculated.

Statistical analysis

For each experimental condition, cells from 3-4 different animals were used. Cell-free experiments were conducted in triplicates. Data consistency was checked and data

were screened for outliers and normal, Gamma, Log-normal and Tweedie distributions by using quantile plots. Continuous variables were also tested for these distributions by using Kolmogorov-Smirnov test. Due to the small sample size, independent and dependent bootstrap-t tests were used based on 5000 Monte Carlo simulations. Additionally, generalized estimation equation models (GEE) were used to analyze data and corresponding LSD tests for pairwise comparisons. Independent and unstructured working correlation matrices were used for modelling. All reported tests were two-sided, and p-values < 0.05 were considered as statistically significant. Results are shown as means ± standard deviation (SD). All statistical analyses were performed with STATISTICA 13 (Hill, T. & Lewicki, P. Statistics: Methods and Applications. StatSoft, Tulsa, OK) and PASW 21 (IBM SPSS Statistics for Windows, Version 21.0., Armonk, NY).

3.4 Results

Hydrogel homogeneity

Although agarose and collagen I are both hydrophilic materials, it is challenging to mix them homogenously due to their different gelling temperatures and mechanisms. While low gelling temperature agarose is liquid above 65°C and gels at around 26-30°C, collagen I is liquid at 4°C and gels at 37°C. It was therefore crucial to first test whether mixing by vortexing produced a homogenous distribution of these materials. As expected, reflection microscopy of collagen I revealed no signal in agarose hydrogels (**Figure 1 A**), while a strong signal was detected in collagen hydrogels (**Figure 1 B**). In comparison, both the 2 mg/mL and 4.5 mg/mL agarose-collagen hydrogels displayed an intermediate signal, with collagen I fibrillar structures appearing homogenously distributed throughout the agarose matrix (**Figure 1 C, D**).

Hydrogel rheological properties

Gel formation of agarose and agarose-collagen 2 mg/mL and 4.5 mg/mL hydrogels started immediately after lowering the temperature to 24°C. The storage modulus (G') reached a plateau at 20.7 ± 0.3, 21.6 ± 0.4 and 20.8 ± 0.7 kPa, respectively, after 240 or 300 min (**Figure 2 A**). This gelation process is governed by the formation of hydrogen bonds resulting in the aggregation of double helices [9]. To promote collagen fibril formation, the temperature was then increased to 37°C, at which G' dropped to 13.0 ± 0.2, 14.8 ± 0.3 and 10.5 ± 0.6 kPa, respectively (**Figure 2 A**). The temperature was subsequently decreased again to 24°C in order to evaluate the rheological properties of the formed hydrogels at room temperature. At this final 24°C temperature, G' increased to 16.5 ± 0.2, 18.8 ± 0.4 and 13.3 ± 0.6 kPa for the agarose, agarose-collagen 2 mg/mL and 4.5 mg/mL hydrogels, respectively (**Figure 2 A**). The loss modulus (G'') of the agarose-based hydrogels varied with temperature similarly to the G', but displayed values about one order of magnitude lower (**Figure 2 A**). This highlights the mainly elastic nature of the agarose-based hydrogels.

Formation of collagen hydrogels started after increasing the temperature to 37°C. The G' reached a plateau at 0.7 ± 0.1 kPa after 240 min (**Figure 2 A**). Upon decrease of the temperature to 24°C, a decrease in G' to 0.4 ± 0.1 kPa was observed (**Figure 2 A**).

Collagen hydrogels were significantly softer than agarose or agarose-collagen hydrogels at both 37 and 24°C (**Figure 2 B**). While agarose and agarose-collagen 2 mg/mL hydrogels had a similar G' at both 37 and 24°C, agarose-collagen 4.5 mg/mL hydrogels displayed a significantly lower G' compared to agarose-collagen 2 mg/mL hydrogels at both temperatures (**Figure 2 B**). Additionally, the G'' of agarose-collagen 4.5 mg/mL hydrogels was significantly higher compared to agarose hydrogels at 37°C (**Figure 2 B**).
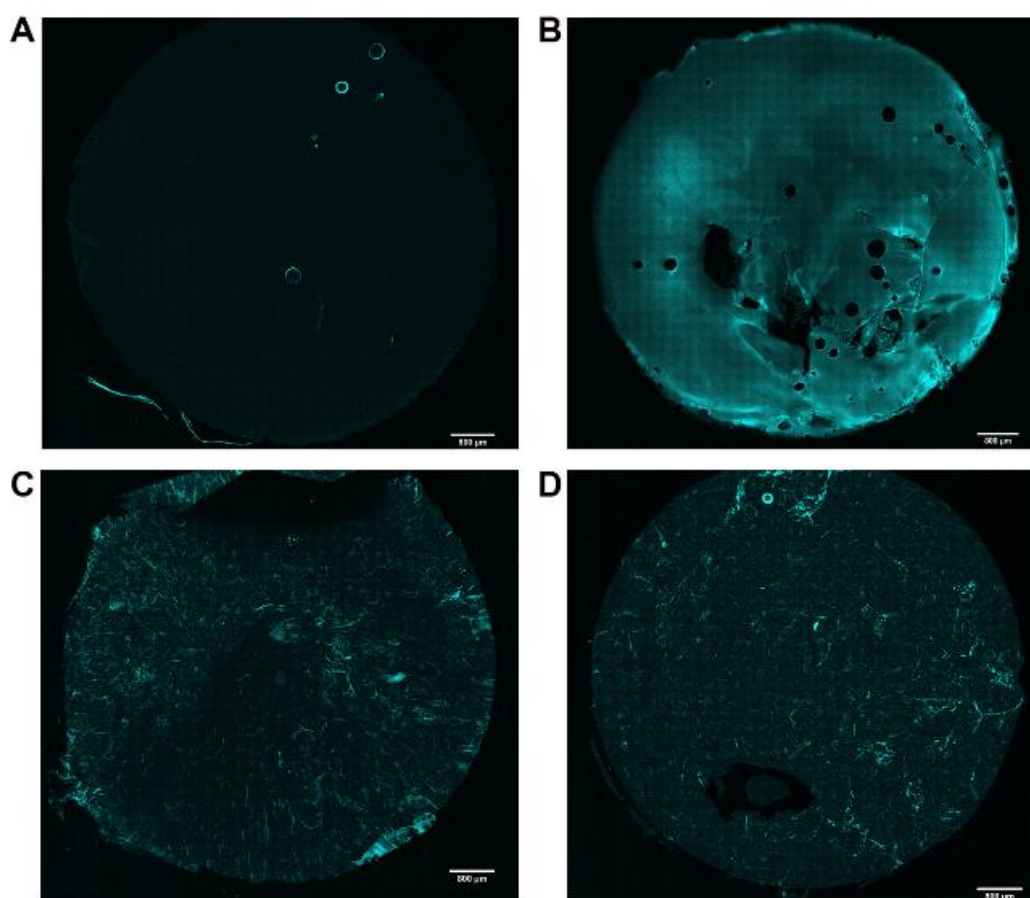
Figure 1: Representative images of confocal reflection microscopy of collagen I in **A)** agarose; **B)** collagen; **C)** agarose-collagen 2 mg/mL; and **D)** agarose-collagen 4.5 mg/mL hydrogels. Scale bar = 800 μm.

Hydrogel dimensional stability

Another important feature of biomaterials intended for dynamic compression, and mechanobiology studies in general, is size stability. Cell-laden agarose-based hydrogels showed unaltered height and diameter at days 1, 7 and 21 (**Figure 3 A, B**). In comparison, collagen hydrogels displayed compaction, with a significantly reduced height and diameter at all time-points (**Figure 3 A, B**). Within the collagen group, hydrogels significantly shrunk over time in both height and diameter (**Figure 3 A, B**).
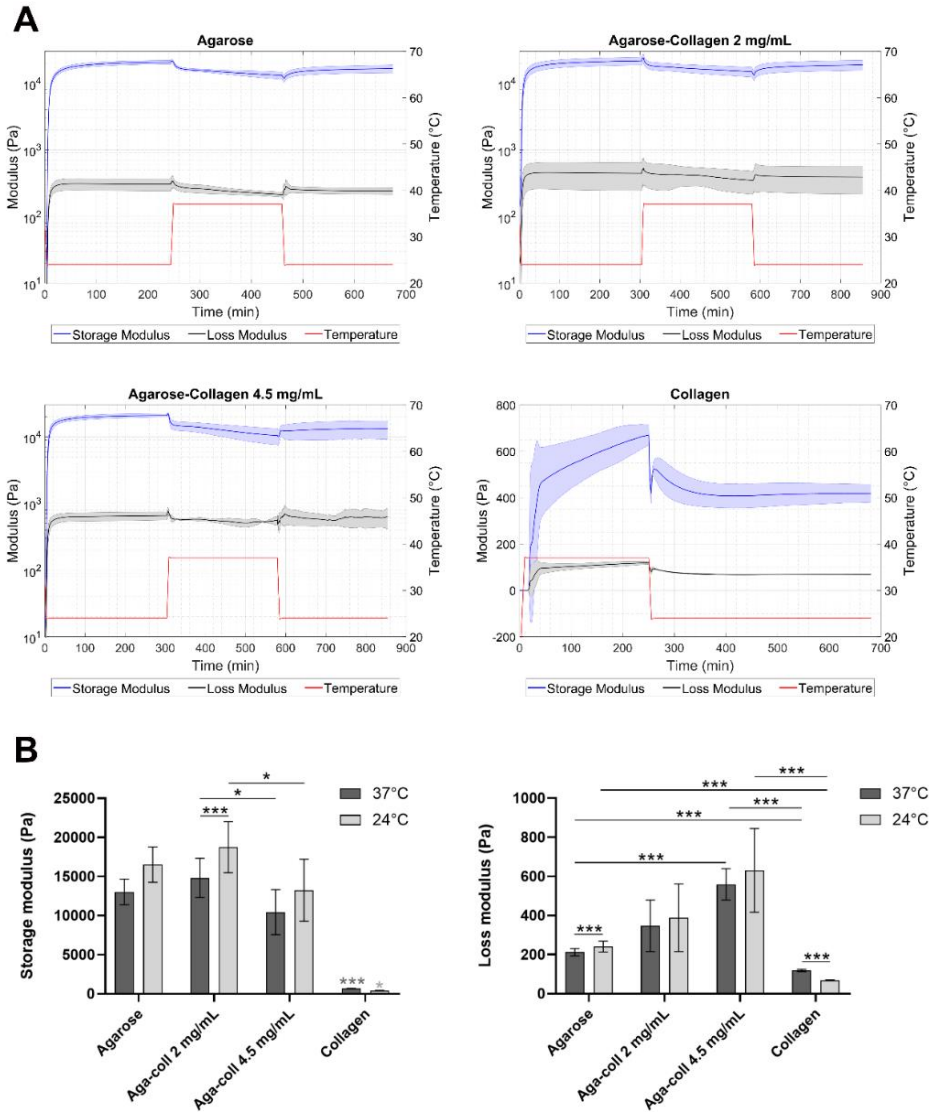
Figure 2: A) Rheological properties of agarose, agarose-collagen 2 mg/mL, agarose-collagen 4.5 mg/mL, and collagen hydrogels with temperature variation over time. **B)** Extracted storage and loss moduli at 37 and 24°C. n=3 independent replicates, mean ± SD; *p<0.05, ***p<0.001; light grey asterisks on bars indicate a statistically significant difference compared to all other hydrogel types at the same temperature.
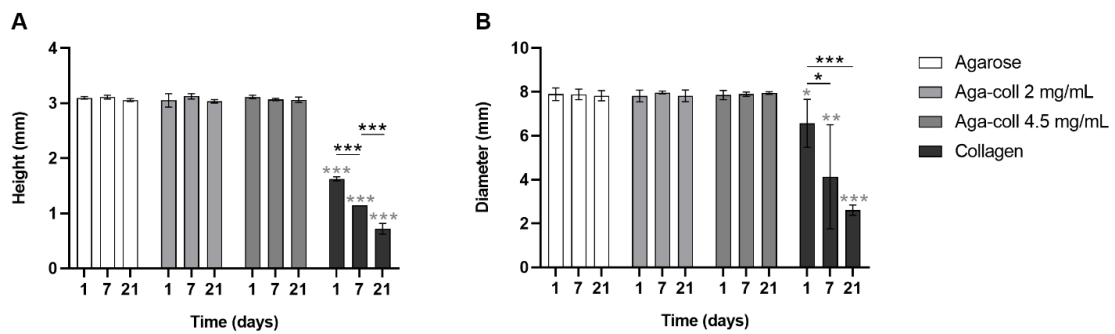
Figure 3: A) Height and **B)** diameter of agarose, agarose-collagen 2 mg/mL, agarose-collagen 4.5 mg/mL, and collagen hydrogels at day 1, 7 and 21 after fabrication. n=3 biological replicates, mean ± SD; *p<0.05, **p<0.01, ***p<0.001; light grey asterisks on bars indicate a statistically significant difference compared to all other hydrogel types at the same day.

Cell viability and proliferation

As cells were briefly subjected to mechanical and thermal stress during hydrogel fabrication due to vortexing and non-physiological temperatures, cell viability was tested. Viability ranged from 80 to 95% and was slightly higher for collagen hydrogels at days 1 and 7 (**Figure 4 A**). The cell viability in agarose-based hydrogels marginally decreased at day 7, then increased at day 21 (**Figure 4 A).**

The proliferation rate of IVD cells in vivo is relatively low, with only 4-5% cells positively stained for Ki67 in human samples [32]. A high proliferation rate is therefore undesired, as it might promote cell de-differentiation. The percentage of cells in the S phase was generally variable and low (<10%) in all experimental groups, except for collagen hydrogels at day 7, which displayed a significantly higher proliferation percentage of 45.8% (**Figure 4 B**). The proliferation rate of agarose-collagen 2 mg/mL decreased between day 1 and 21 (**Figure 4 B**).
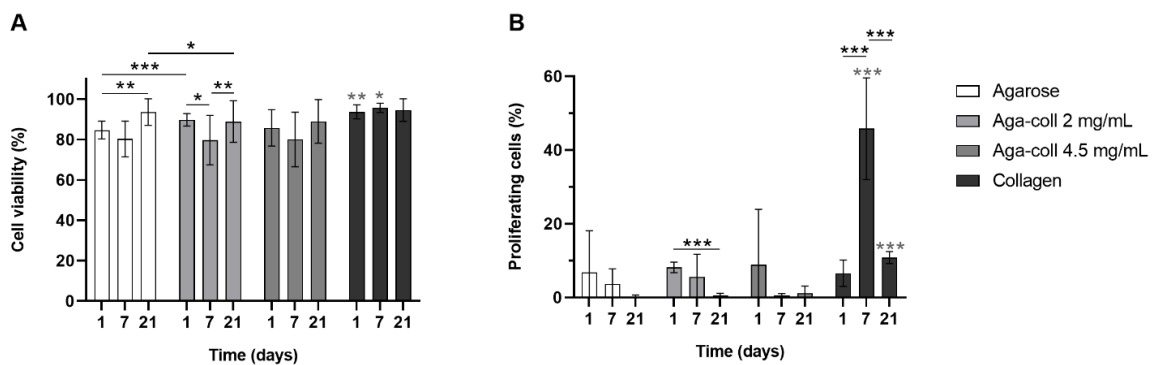
Figure 4: A) Cell viability percentage and **B)** percentage of proliferating cells of agarose, agarose-collagen 2 mg/mL, agarose-collagen 4.5 mg/mL, and collagen hydrogels at day 1, 7 and 21 after fabrication. n=3 biological replicates, mean ± SD; *p<0.05, **p<0.01, ***p<0.001; light grey asterisks on bars indicate a statistically significant difference compared to all other hydrogel types at the same day.

3D cell morphology

In order to understand the interaction between cells and the different hydrogels, cells encapsulated in 3D hydrogels were stained and imaged over time. The 3D cell morphology in all agarose-based hydrogels remained round at all time-points, while cells in collagen hydrogels displayed an elongated morphology and a higher cell density at days 7 and 21 (**Figure 5**).
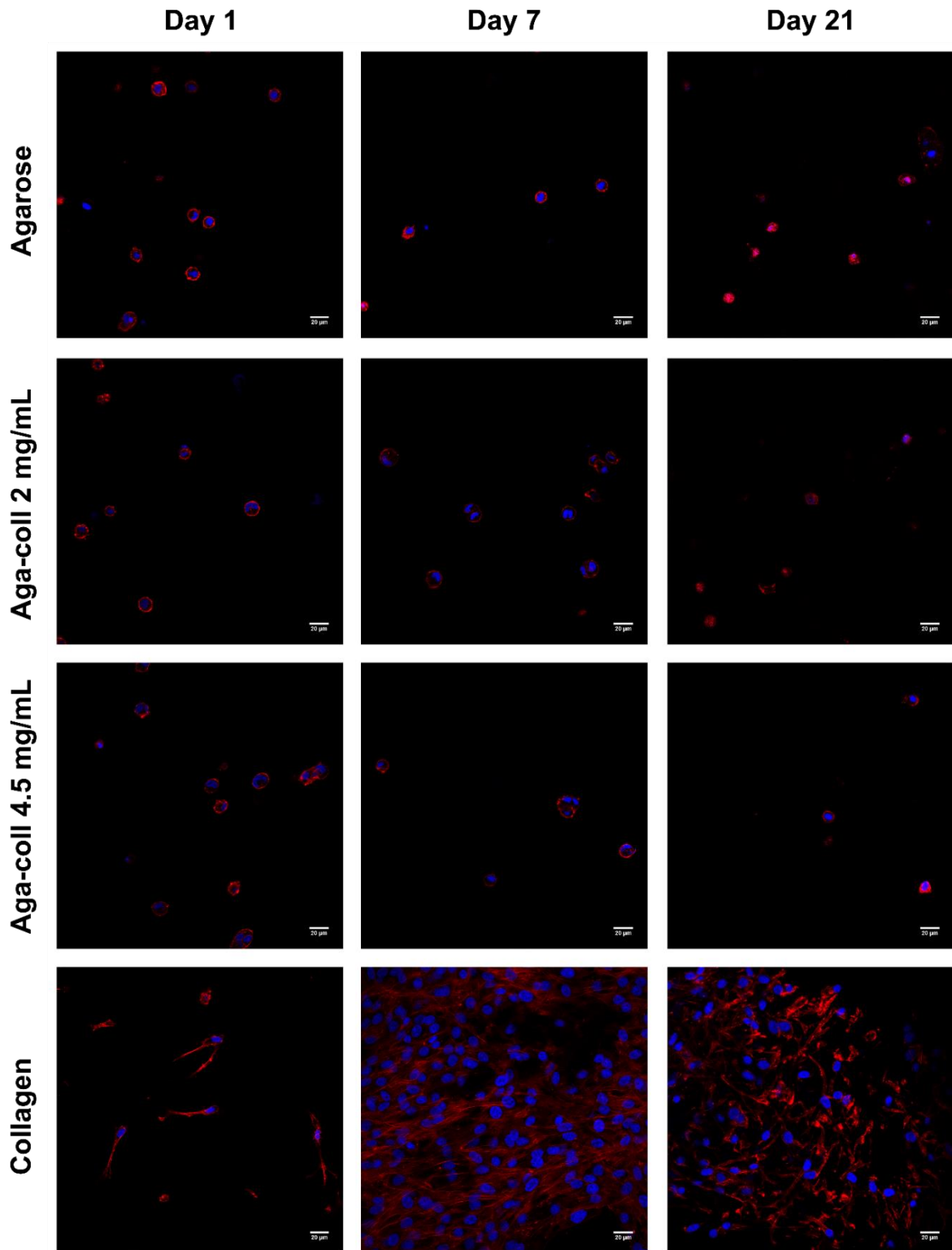
Figure 5: Representative images of cell morphology (red = phalloidin, blue = DAPI) of agarose, agarose-collagen 2 mg/mL, agarose-collagen 4.5 mg/mL, and collagen hydrogels at day 1, 7 and 21 after fabrication. Scale bar = 20 μm.

ECM gene expression and GAG production

We investigated the mRNA expression of collagen I (COL1A2), collagen II (COL2A1) and aggrecan (ACAN), as the main components of the ECM of the IVD. The gene expression of COL1A2, COL2A1 and ACAN significantly increased between day 1 and 7 in composite agarose-collagen hydrogels at both collagen concentrations (**Figure 6 A, B, C**). This change was also noted for COL2A1 and ACAN in agarose hydrogels (**Figure 6 B, C**). ACAN was additionally significantly increased between day 1 and 21 in agarose hydrogels (**Figure 6 C**). This increase over time was confirmed when measuring the GAG/DNA content. At day 1, the GAG/DNA ratio was significantly higher in collagen hydrogels compared to other gels (**Figure 6 D**). Nevertheless, an increase over time (between day 1 and day 7, and between day 7 and day 21) was observed in all agarose-based hydrogels, which finally surpassed collagen hydrogels at day 21 (**Figure 6 D**). Interestingly, the GAG/DNA content was significantly higher in both blended agarose-collagen hydrogels compared to the agarose group at day 7 (**Figure 6 D**).
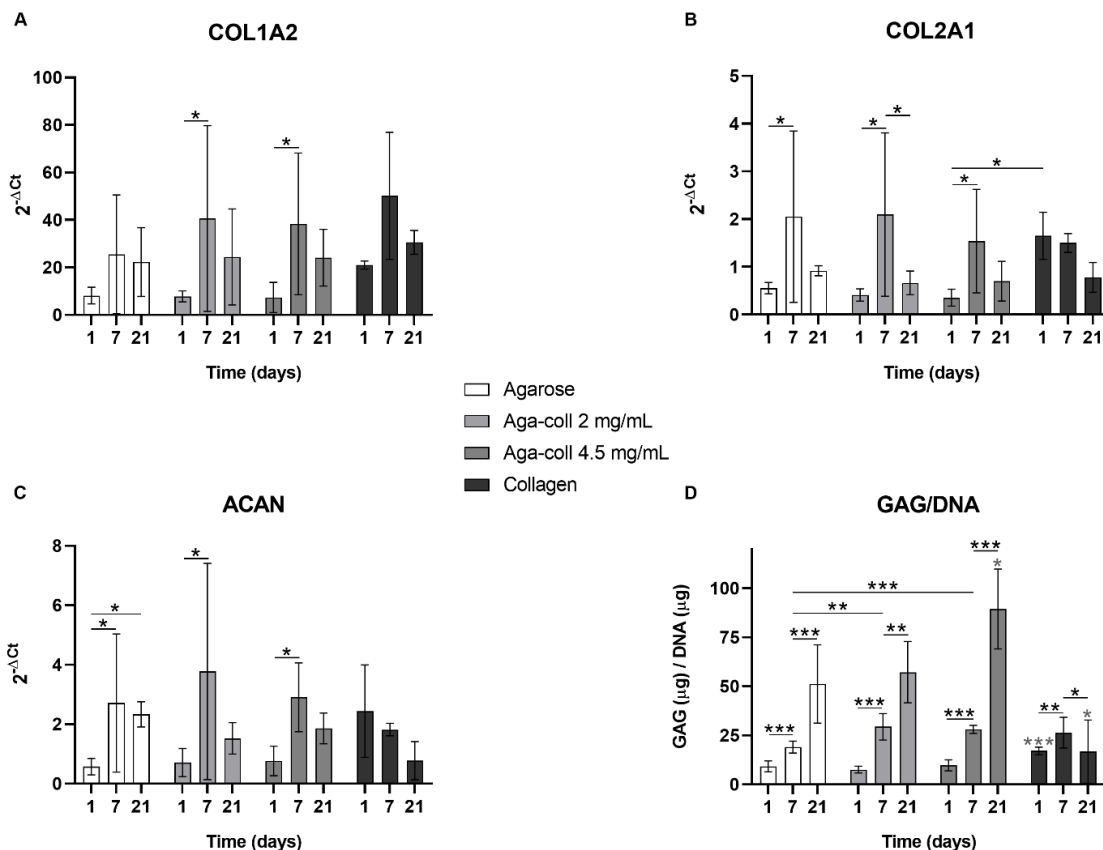
Figure 6: Gene expression of **A)** COL1A2, **B)** COL2A1, **C)** ACAN, and **D)** GAG/DNA quantification of agarose, agarose-collagen 2 mg/mL, agarose-collagen 4.5 mg/mL, and collagen hydrogels at day 1, 7 and 21 after fabrication. n=3 biological replicates, mean ± SD; *p<0.05, **p<0.01, ***p<0.001; light grey asterisks on bars indicate a statistically significant difference compared to all other hydrogel types at the same day.

## 2D cell adhesion

As expected, no cells could adhere to agarose 2D hydrogels (**Figure 7 A, E**). In comparison, all substrates containing collagen displayed a significantly higher number of cells (**Figure 7 B, C, D**): 1'728 ± 671 cells on the 2 mg/mL agarose-collagen gels; 314 ± 220 on the 4.5 mg/mL agarose-collagen gels; and 6'381 ± 2017 cells on the collagen gels (**Figure 7 E**). Surprisingly, the number of cells adhering to the 4.5 mg/mL agarose-collagen gels was significantly reduced compared to the 2 mg/mL and the collagen groups (**Figure 7 E**). The morphology of the cells seeded on the 4.5 mg/mL agarose-collagen hydrogels was also slightly rounder (inset of Figure 7 C) compared to the more elongated polygonal shape of cells seeded on 2 mg/mL agarose-collagen and collagen hydrogels (insets of **Figure 7 B, D**).
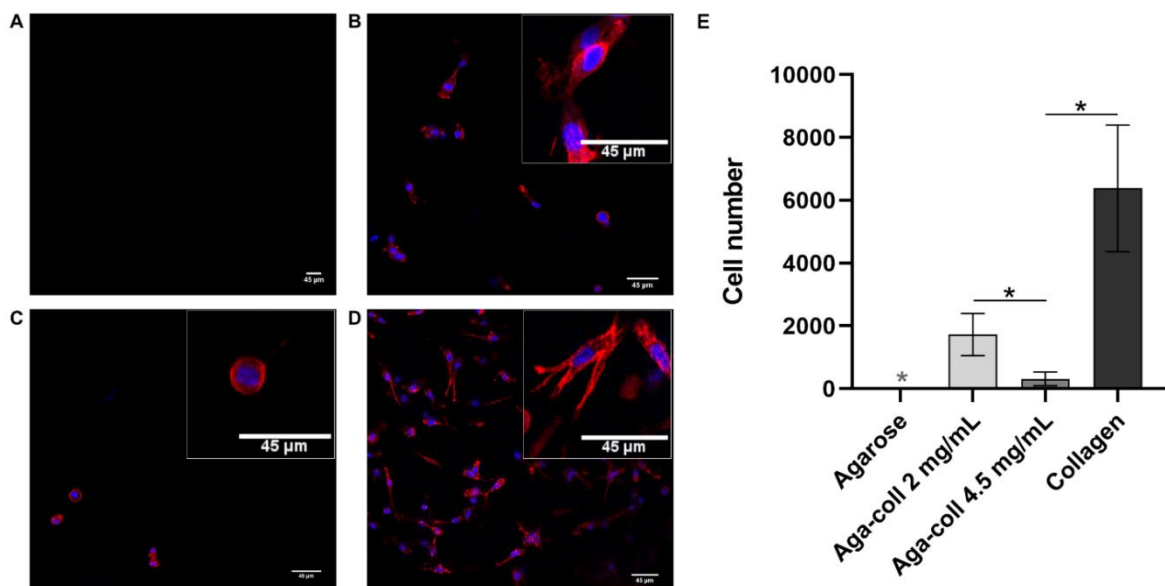
Figure 7: Representative images and enlarged insets of cells (red = phalloidin, blue = DAPI) seeded on **A)** agarose, **B)** agarose-collagen 2 mg/mL, **C)** agarose-collagen 4.5 mg/mL, and **D)** collagen 2D hydrogels at day 1 after fabrication. Scale bars = 45 μm. **E)** Cell count per hydrogel type. n=3 biological replicates, mean ± SD; *p<0.05; the light grey asterisks on the agarose bar indicates a statistically significant difference compared to all other hydrogel types.

FAK phosphorylation in dynamic compression

Based on their superior mechanical and adhesive properties, the agarose-collagen 2 mg/mL hydrogels were selected to test the capacity to transmit mechanical load to cells. Agarose and 2 mg/mL agarose-collagen gels were pre-cultured for 7 days and FAK expression and phosphorylation was semi-quantified after hydrogel dynamic compression for 0, 5, 10 or 20 min (**Figure 8 A**). No statistically significant difference was found across conditions in the expression of FAK relative to β-tubulin (**Figure 8 B**). Both hydrogel types did not show any significant change in FAK phosphorylation between compressed and non-compressed samples (**Figure 8 C, D**). However, pFAK levels relative to β-tubulin were considerably higher (5.36-fold) in 2 mg/mL agarose-collagen gels compared to agarose gels in non-compressed samples (**Figure 8 C**).The composite gels

further displayed a slight but significant increase in pFAK/FAK values compared to the agarose gels 10 min after compression (**Figure 8 D**).
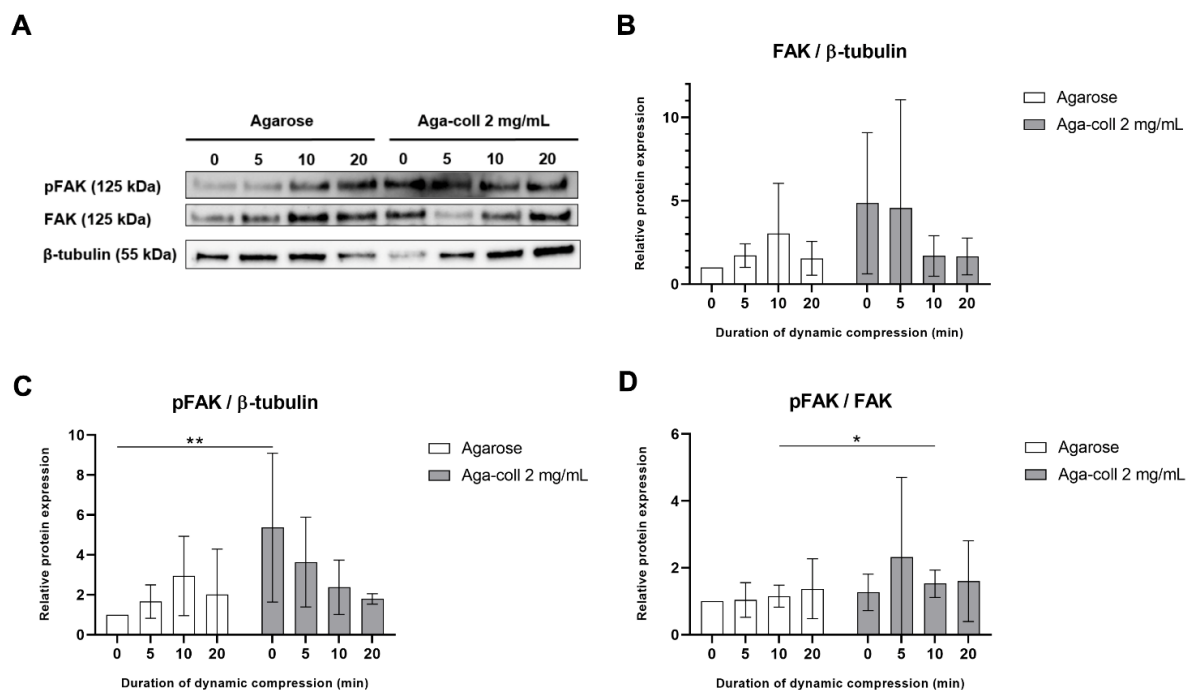
Figure 8: A) Western blot of agarose and agarose-collagen 2 mg/mL hydrogels dynamically compressed for 0, 5, 10 or 20 min. Densitometry analysis of **B)** relative FAK, **C)** pFAK, and **D)** pFAK/FAK protein expression, n=4 biological replicates, mean ± SD; *p<0.05, **p<0.01.

3.5 Discussion

Biomaterials combining strong and tunable mechanical properties with the biological cues of natural ECM proteins are in demand for mechanotransduction studies. This study aimed to introduce agarose-collagen composite hydrogels as a simple, inexpensive and effective option in the context of IVD mechanobiology investigations. While the typical agarose concentration for dynamic compression studies of 2% wt/vol was kept constant, collagen I was physically blended into agarose at two final concentrations of 2 and 4.5 mg/mL. Reflection microscopy showed that mixing by vortexing the two polymers was an effective method to achieve a homogenous distribution of collagen throughout the gels. Previous studies involving scanning electron microscopy observed the formation of an intricate network between the two materials, where fine "web-like" agarose intercalated between larger entangled collagen fibers [24; 25]. While adding collagen at 4.5 mg/mL decreased the elasticity and increased the viscosity of the hydrogels, blending 2 mg/mL collagen did not affect the rheological properties of the gels. The blending of collagen I at the higher concentration might impair the formation of hydrogen bonds in agarose and the resulting formation and aggregation of double helices that govern agarose gelling mechanism. The collagen fibers might thus create macroscopic defects in the agarose non-fibrillar matrix. This might also explain why the decrease in storage modulus of the 4.5 mg/mL hydrogels was only observed after

49

the hydrogel was heated to 37°C, which triggered the formation of collagen fibers. Despite the introduction of degradable collagen I, agarose-collagen hydrogels presented suitable dimensional stability, contrary to collagen hydrogels that underwent cell-mediated contraction [33]. This feature represents an advantage, especially in the case where these hydrogels need to be subjected to mechanical loading with a displacement-controlled bioreactor. NP cells were viable and their proliferation was low in all agarose-based hydrogels, approaching proliferation rates of IVD cells in vivo. Interestingly, the presence of collagen did not alter the round 3D morphology of cells embedded in blended hydrogels. This suggests a dense matrix mainly composed of agarose. The gene expression of collagen I and II, as well as aggrecan increased at day 7 in blended hydrogels, and the GAG/DNA content was also increased compared the agarose hydrogels at this time-point. A similar increase in GAG/DNA was also observed in chondrocyte-laden agarose-poly(ethylene glycol) diacrylate (PEGDA) interpenetrating networks when aggrecan was physically blended in [34]. While collagen I blending increased cell adhesion, the effect was surprisingly stronger for the lower concentration of collagen at 2 mg/mL. We attribute this finding to the difference in mechanical properties between the 2 and 4.5 mg/mL hydrogels. In this case, the lower stiffness of the 4.5 mg/mL hydrogels might over-rule their increased adhesion ligand density, thus resulting in reduced cell adhesion. This phenomenon suggests a non-linear response, similar to the one observed for the spread area of cells on gels [35]. This stiffness-dependent cell adhesion behavior was already observed with human dermal fibroblasts seeded on laminin peptide-agarose gels in the study of Yamada et al [27]. Enhanced cell adhesion due to collagen blending at 2 mg/mL was further confirmed by higher levels of FAK phosphorylation relative to β-tubulin in non-compressed samples, and higher pFAK/FAK values 10 min after compression. While FAK activation is usually associated with cell seeding on stiff 2D substrates [12], little is known about the effect of stiffness in 3D materials. No significant difference in mechanical properties was observed between agarose and 2 mg/mL agarose-collagen gels. Therefore, FAK phosphorylation was likely induced by the interaction of cells with the collagen present in the matrix via integrin receptors [12]. The fact that dynamic compression of the hydrogels did not influence the level of FAK phosphorylation additionally suggests an effect inherently driven by the composite biomaterial. In fact, the fibrillar nature of the collagen introduced in the composite network might guide the promotion of focal adhesion formation, as this phenomenon has only been shown in fibrillar 3D scaffolds so far [36; 37; 38]. Recently, it has been shown that focal adhesion formation plays an important role in the response of NP cells to their surrounding matrix and the presence or absence of integrin binding sites [39].

Our agarose-collagen gels composed of 2% wt/vol agarose and 2 mg/mL collagen contain approximatively 10% fibrillar collagen (collagen/agarose wt/wt), thus mimicking the NP matrix well [25]. However, the ratio of collagen and agarose can be tuned in order to mimic other native tissues such as ligaments, tendons and cartilage. On the biological level, IVDs and cartilage share several characteristics such as a relatively stiff ECM, high collagen II and proteoglycan content, low proliferation and round cell morphology. The use of blended agarose-collagen could therefore be extended to the embedding of chondrocytes and the study of their mechanotransduction mechanisms. Such studies would be beneficial to shed light on the pathways leading to osteoarthritis, one of the great health challenges of the increasingly aging population. With a similar focus, blended

agarose-collagen hydrogels might constitute promising substrates for mesenchymal stem cells chondrogenic differentiation.

3.6 Conclusion

Agarose-collagen blended hydrogels are easy to produce, inexpensive and do not require cytotoxic reagents. We showed that they constitute a valid 3D culture model for dynamic compression and investigation of IVD cell mechanotransduction. Using physical blending, a homogenous interconnected network was formed, presenting both the biofunctionality of collagen I and the mechanical strength and stability of agarose. In fact, the addition of collagen type I at 2 mg/mL conserved many qualities of agarose: non-degradability, strong elastic properties, ability to promote ECM gene expression, and low proliferation and round morphology of embedded cells. Furthermore, blended agarose-collagen hydrogels not only enhanced the production of GAG at day 7 compared to agarose gels, but also increased cell adhesion and FAK activation, one of the first steps in the integrin-mediated mechanotransduction mechanisms. In light of the described findings, agarose-collagen hydrogels represent an improved alternative to agarose gels for the exploration of cell-matrix interaction and mechanotransduction mechanisms of native tissues constituted of a non-fibrillar matrix (such as proteoglycans and GAGs) and collagens. In this context, they could further be used to explore stem cell chondrogenic differentiation.

3.7 References

1. D.E. Jaalouk, and J. Lammerding, Mechanotransduction gone awry. Nature Reviews Molecular Cell Biology 10 (2009) 63-73.

2. F. Martino, A.R. Perestrelo, V. Vinarský, S. Pagliari, and G. Forte, Cellular Mechanotransduction: From Tension to Function. 9 (2018).

3. A.E. Miller, P. Hu, and T.H. Barker, Feeling Things Out: Bidirectional Signaling of the Cell-ECM Interface, Implications in the Mechanobiology of Cell Spreading, Migration, Proliferation, and Differentiation. Advanced healthcare materials (2020) e1901445.

4. M.A. Adams, and P.J. Roughley, What is intervertebral disc degeneration, and what causes it? Spine (Phila Pa 1976) 31 (2006) 2151-61.

5. F. Balague, A.F. Mannion, F. Pellise, and C. Cedraschi, Non-specific low back pain. Lancet 379 (2012) 482-91.

6. S.C. Chan, J. Walser, P. Kappeli, M.J. Shamsollahi, S.J. Ferguson, and B. Gantenbein-Ritter, Region specific response of intervertebral disc cells to complex dynamic loading: an organ culture study using a dynamic torsion-compression bioreactor. PLoS One 8 (2013) e72489.

7. S.C. Chan, S.J. Ferguson, and B. Gantenbein-Ritter, The effects of dynamic loading on the intervertebral disc. Eur Spine J 20 (2011) 1796-812.

8. D.E. Anderson, and B. Johnstone, Dynamic Mechanical Compression of Chondrocytes for Tissue Engineering: A Critical Review. Frontiers in Bioengineering and Biotechnology 5 (2017).

9. D. Velasco, E. Tumarkin, and E. Kumacheva, Microfluidic encapsulation of cells in polymer microgels. Small 8 (2012) 1633-42.

10. C. Bougault, A. Paumier, E. Aubert-Foucher, and F. Mallein-Gerin, Investigating conversion of mechanical force into biochemical signaling in three-dimensional chondrocyte cultures. Nat Protoc 4 (2009) 928-938.

11. V. Normand, D.L. Lootens, E. Amici, K.P. Plucknett, and P. Aymard, New insight into agarose gel mechanical properties. Biomacromolecules 1 (2000) 730-8.

12. J.-H. Lee, D.-H. Kim, H.-H. Lee, and H.-W. Kim, Role of nuclear mechanosensitivity in determining cellular responses to forces and biomaterials. Biomaterials 197 (2019) 60-71.

13. R. Bellamkonda, J.P. Ranieri, and P. Aebischer, Laminin oligopeptide derivatized agarose gels allow three-dimensional neurite extension in vitro. J Neurosci Res 41 (1995) 501-9.

14. M. Borkenhagen, J.F. Clemence, H. Sigrist, and P. Aebischer, Three-dimensional extracellular matrix engineering in the nervous system. J Biomed Mater Res 40 (1998) 392-400.

15. X. Yu, G.P. Dillon, and R.B. Bellamkonda, A laminin and nerve growth factor-laden three-dimensional scaffold for enhanced neurite extension. Tissue Eng 5 (1999) 291-304.

16. Y. Luo, and M.S. Shoichet, A photolabile hydrogel for guided three-dimensional cell growth and migration. Nature Materials 3 (2004) 249-253.

17. M.C. Dodla, and R.V. Bellamkonda, Anisotropic scaffolds facilitate enhanced neurite extension in vitro. J Biomed Mater Res A 78 (2006) 213-21.

18. J.T. Connelly, A.J. Garcia, and M.E. Levenston, Interactions between integrin ligand density and cytoskeletal integrity regulate BMSC chondrogenesis. J Cell Physiol 217 (2008) 145-54.

19. J.T. Connelly, T.A. Petrie, A.J. Garcia, and M.E. Levenston, Fibronectin- and collagen-mimetic ligands regulate bone marrow stromal cell chondrogenesis in three-dimensional hydrogels. Eur Cell Mater 22 (2011) 168-76; discussion 176-7.

20. E. Schuh, S. Hofmann, K. Stok, H. Notbohm, R. Muller, and N. Rotter, Chondrocyte redifferentiation in 3D: the effect of adhesion site density and substrate elasticity. J Biomed Mater Res A 100 (2012) 38-47.

21. A.Y. Au, J.M. Hasenwinkel, and C.G. Frondoza, Micropatterned agarose scaffolds covalently modified with collagen for culture of normal and neoplastic hepatocytes. J Biomed Mater Res A 100 (2012) 342-52.

22. Y.X. Su, B. Chu, Y. Gao, C.X. Wu, L.M. Zhang, P. Chen, X.Y. Wang, and S.Q. Tang, Modification of agarose with carboxylation and grafting dopamine for promotion of its cell-adhesiveness. Carbohyd Polym 92 (2013) 2245-2251.

23. D.K. Cullen, M.C. Lessing, and M.C. LaPlaca, Collagen-dependent neurite outgrowth and response to dynamic deformation in three-dimensional neuronal cultures. Ann Biomed Eng 35 (2007) 835-46.

24. T.A. Ulrich, A. Jain, K. Tanner, J.L. MacKay, and S. Kumar, Probing cellular mechanobiology in three-dimensional culture with collagen-agarose matrices. Biomaterials 31 (2010) 1875-1884.

25. S.P. Lake, and V.H. Barocas, Mechanical and Structural Contribution of Non-Fibrillar Matrix in Uniaxial Tension: A Collagen-Agarose Co-Gel Model. Ann Biomed Eng 39 (2011) 1891-1903.

26. S.P. Lake, E.S. Hald, and V.H. Barocas, Collagen-agarose co-gels as a model for collagen-matrix interaction in soft tissues subjected to indentation. J Biomed Mater Res A 99a (2011) 507-515.

27. Y. Yamada, K. Hozumi, A. Aso, A. Hotta, K. Toma, F. Katagiri, Y. Kikkawa, and M. Nomizu, Laminin active peptide/agarose matrices as multifunctional biomaterials for tissue engineering. Biomaterials 33 (2012) 4118-25.

28. A. Batorsky, J.H. Liao, A.W. Lund, G.E. Plopper, and J.P. Stegemann, Encapsulation of adult human mesenchymal stem cells within collagen-agarose microenvironments. Biotechnol Bioeng 92 (2005) 492-500.

29. A.Y. Rioja, E.L.H. Daley, J.C. Habif, A.J. Putnam, and J.P. Stegemann, Distributed vasculogenesis from modular agarose-hydroxyapatite-fibrinogen microbeads. Acta biomaterialia 55 (2017) 144-152.

30. A.W. Lund, J.A. Bush, G.E. Plopper, and J.P. Stegemann, Osteogenic differentiation of mesenchymal stem cells in defined protein beads. J Biomed Mater Res B Appl Biomater 87 (2008) 213-21.

31. R.W. Farndale, D.J. Buttle, and A.J. Barrett, Improved quantitation and discrimination of sulphated glycosaminoglycans by use of dimethylmethylene blue. Biochim Biophys Acta 883 (1986) 173-7.

32. H.E. Gruber, J.A. Ingram, D.E. Davis, and E.N. Hanley, Jr., Increased cell senescence is associated with decreased cell proliferation in vivo in the degenerating human annulus. The spine journal : official journal of the North American Spine Society 9 (2009) 210-5.

33. E. Bell, B. Ivarsson, and C. Merrill, Production of a tissue-like structure by contraction of collagen lattices by human fibroblasts of different proliferative potential in vitro. Proceedings of the National Academy of Sciences of the United States of America 76 (1979) 1274-8.

34. G.C. Ingavle, S.H. Gehrke, and M.S. Detamore, The bioactivity of agarose-PEGDA interpenetrating network hydrogels with covalently immobilized RGD peptides and physically entrapped aggrecan. Biomaterials 35 (2014) 3558-70.

35. D.E. Discher, P. Janmey, and Y.L. Wang, Tissue cells feel and respond to the stiffness of their substrate. Science 310 (2005) 1139-43.

36. E. Cukierman, R. Pankov, D.R. Stevens, and K.M. Yamada, Taking cell-matrix adhesions to the third dimension. Science 294 (2001) 1708-1712.

37. A.D. Doyle, F.W. Wang, K. Matsumoto, and K.M. Yamada, One-dimensional topography underlies three-dimensional fibrillar cell migration. The Journal of Cell Biology 184 (2009) 481.

38. S. Nam, K.H. Hu, M.J. Butte, and O. Chaudhuri, Strain-enhanced stress relaxation impacts nonlinear elasticity in collagen gels. Proceedings of the National Academy of Sciences 113 (2016) 5492.

39. A. Krouwels, F.P.W. Melchels, M.H.P. van Rijen, C.B.M. Ten Brink, W.J.A. Dhert, F. Cumhur Oner, M.A. Tryfonidou, and L.B. Creemers, Focal adhesion signaling affects regeneration by human nucleus pulposus cells in collagen- but not carbohydrate-based hydrogels. Acta biomaterialia 66 (2018) 238-247.

Chapter 4

TRPV4 mediates cell damage induced by hyperphysiological compression and regulates COX2/PGE2 in intervertebral discs

TRPV4 mediates cell damage induced by hyperphysiological compression and regulates COX2/PGE2 in intervertebral discs

Elena Cambria[1], Sally Heusser[1], Ariane C. Scheuren[1], Wai Kit Tam[2], Agnieszka A. Karol[3], Wolfgang Hitzl[4,5,6], Victor Y. Leung[2], Ralph Müller[1], Stephen J. Ferguson[1], Karin Wuertz-Kozak[1,7,8]

[1] Institute for Biomechanics, ETH Zurich, Zurich, Switzerland

[2] Department of Orthopaedics and Traumatology, The University of Hong Kong, Pokfulam, Hong Kong

[3] Musculoskeletal Research Unit (MSRU), Department of Molecular Mechanisms of Disease (DMMD), Vetsuisse Faculty, University of Zurich, Zurich, Switzerland

[4] Research Office (Biostatistics), Paracelsus Medical University, Salzburg, Austria

[5] Department of Ophthalmology and Optometry, Paracelsus Medical University, Salzburg, Austria

[6] Research Program Experimental Ophthalmology and Glaucoma Research, Paracelsus Medical University, Salzburg, Austria

[7] Department of Biomedical Engineering, Rochester Institute of Technology, Rochester NY, USA

[8] Spine Center, Schön Klinik München Harlaching, Academic Teaching Hospital and Spine Research Institute of the Paracelsus Private Medical University Salzburg (Austria), Munich, Germany

4.1 Abstract

Aberrant mechanical loading of the spine causes intervertebral disc (IVD) degeneration and low back pain. Current therapies do not target the mediators of the underlying mechanosensing and mechanotransduction pathways, as these are poorly understood. This study investigated the role of the mechanosensitive transient receptor potential vanilloid 4 (TRPV4) ion channel in dynamic compression of bovine nucleus pulposus (NP) cells in vitro and mouse IVDs in vivo. Degenerative changes and the expression of the inflammatory mediator cyclooxygenase 2 (COX2) were examined histologically in the IVDs of mouse tails that were dynamically compressed at a short repetitive hyperphysiological regime (versus sham). Bovine NP cells embedded in an agarose-collagen hydrogel were dynamically compressed at a hyperphysiological regime in the presence or absence of the selective TRPV4 antagonist GSK2193874. Lactate dehydrogenase (LDH) and prostaglandin E2 (PGE2) release, as well as phosphorylation of mitogen-activated protein kinases (MAPKs), were analyzed. Degenerative changes and COX2 expression were further evaluated in the IVDs of trpv4-deficient mice (versus wild-type; WT). Dynamic compression caused IVD degeneration in vivo as previously shown but did not affect COX2 expression. Dynamic compression significantly augmented LDH and PGE2 releases in vitro, which were significantly reduced by TRPV4 inhibition. Moreover, TRPV4 inhibition during dynamic compression activated the extracellular signal-regulated kinases 1/2 (ERK) MAPK pathway by 3.13-fold compared to non-compressed samples. Trpv4-deficient mice displayed mild IVD degeneration and decreased COX2 expression compared to WT mice. TRPV4 therefore regulates COX2/PGE2 and mediates cell damage induced by hyperphysiological dynamic compression, possibly via ERK. Targeted TRPV4 inhibition or knockdown might thus constitute promising therapeutic approaches to treat patients suffering from IVD pathologies caused by aberrant mechanical stress.

Keywords: dynamic compression, transient receptor potential channels, low back pain, mechanobiology, mechanosensing, mechanotransduction

4.2 Introduction

Intervertebral disc (IVD) degeneration, leading to IVD structural failure, causes degenerative disc disease (DDD) when it is accompanied and exacerbated by inflammation and nociception [1, 2]. DDD is the main cause of low back pain (LBP), which is the leading cause of disability globally [3, 4]. Aberrant mechanical loading of the spine is a recognized cause of IVD degeneration and LBP [5, 6]. However, at the molecular level, the underlying mechanosensing and mechanotransduction pathways are poorly understood. As a result, current treatments of LBP, such as anti-inflammatory drugs, do not specifically target mediators of mechanotransduction pathways. A better understanding of the molecular mechanisms leading from hyperphysiological mechanical loading to IVD degeneration and inflammation would reveal novel, and possibly more effective, therapeutic targets.

IVDs are continually subjected to mechanical stimulation via spinal flexion, extension, torsion, and muscle activation during daily activities [7]. The well-hydrated nucleus pulposus (NP) in the middle of the IVD primarily sustains compressive loads, hydrostatic and osmotic pressures, while the surrounding annulus fibrosus (AF) is mostly exposed to tensile stress [7]. IVD homeostasis is dependent on a physiological level of mechanical stimulation, which promotes solute transport and cell metabolism [5]. However, hyperphysiological mechanical stress induces harmful structural, cellular, and molecular changes in the IVDs [5, 7]. Several studies have focused on the investigation of compressive stimuli both in vivo and in vitro (reviewed in [5, 7]). It was shown that hyperphysiological dynamic compression (at high magnitude, frequency, or duration) causes cell death [8-10], decreased expression of anabolic genes (collagens and proteoglycans) [11-13], as well as increased expression of matrix-degrading enzymes (MMPs, ADAMTS) [11, 13-16] and pro-inflammatory cytokines [9]. These effects might be mediated by mitogen-activated protein kinase (MAPK: extracellular signal-regulated kinases 1/2 (ERK 1/2), p38 and Jun-N-terminal kinase (JNK)) signaling pathways [17, 18], while the initial mechanosensing mechanisms might involve integrins, purinergic signaling, and ion channels, including transient receptor potential (TRP) channels [7, 17]. Nevertheless, the exact mechanosensing and mechanotransductive mechanisms in IVD cells are currently unknown.

TRP ion channels are non-selective calcium-permeable transmembrane channels. They are of particular interest in the context of IVD research, as they sense variations in several factors that are altered during IVD degeneration: pH, oxidative and mechanical stress [19]. The TRP super-family is composed of six sub-families in mammals: TRPC (canonical), TRPV (vanilloid), TRPM (melastatin), TRPP (polycystin), TRPML (mucolipin) and TRPA (ankyrin) [19]. Several studies have recently investigated the expression and function of TRP channels in the IVD [20-24]. The mechanosensitive member 4 of the vanilloid subfamily (TRPV4) is especially intriguing for the study of load-mediated IVD degeneration and LBP. Reduced osmolarity was shown to increase TRPV4 expression and pro-inflammatory cytokines in bovine NP cells [20]. Moreover, our group has recently shown that TRPV4 transduces hyperphysiological mechanical loading into pro-inflammatory signals in human AF cells cyclically stretched in two dimensions (2D) [24].

Building on these results, we hypothesized that hyperphysiological dynamic compression induces IVD degeneration, cell damage and increased COX2/PGE2 expression, and that TRPV4 mediates these effects in murine IVDs and bovine NP cells embedded in a previously developed 3D matrix [25]. This agarose-collagen composite hydrogel mimics the composition of the IVD with its non-fibrillar matrix (proteoglycans and glycosaminoglycans) and collagen fibers, combines mechanical strength and biofunctionality, and is thus suitable for mechanotransduction studies [25].

4.3 Materials and methods

Compressed murine tails for histology

Sham and compressed mouse tails of 15-week-old female C57BL/6J mice (Charles River Laboratories, France) were provided by the Laboratory for Bone Biomechanics at ETH Zurich, Switzerland, as a by-product of another study [26]. The sixth caudal vertebra (C6) and the IVDs between C5 and C6, and C6 and C7 were dynamically compressed (8 N, 2 Hz, sine wave, 5 minutes, 3x per week over 4 weeks) via two stainless steel pins inserted in C5 and C7, as described elsewhere [26, 27]. Sham mice received pins and their tails were fixed in the loading device but were not dynamically compressed. Immediately after euthanasia, the tails were dissected, rinsed in phosphate buffered saline (PBS), and fixed in 4% paraformaldehyde solution for 24 h. The fixed tails were washed in PBS and decalcified in 12.5% ethylene-diamine-tetra-acetic acid (EDTA) in PBS at 4°C for 10 days. The decalcified samples were washed in PBS and placed into 70% ethanol at 4°C until paraffin embedding. Paraffin blocks were sectioned at 5 μm thickness. The experiments were carried out in strict accordance with the recommendations and regulations in the Animal Welfare Ordinance (TSchV 455.1) of the Swiss Federal Food Safety and Veterinary Office (license number 262/2016).

FAST histological staining

IVD degeneration was assessed via a multi-dye FAST (Fast Green, Alcian Blue, Safranin-O, and Tartrazine) histological staining, as previously described [28]. Briefly, paraffin sections were dewaxed in xylene and then rehydrated successively in 70% ethanol, 30% ethanol, and distilled water. The sections were first stained with 1% Alcian Blue 8GX (A3157, Sigma-Aldrich) at pH 1.0 for 2.5 min, followed by 0.1% Safranin-O (S8884, Sigma-Aldrich) for 3 min. Color differentiation was performed in 25% ethanol for 15 s. The sections were then stained with 0.08% Tartrazine (T0388, Sigma) in 0.25% acetic acid for 15 s and finally counterstained with 0.01% Fast Green (F7258, Sigma) solution for 5 min. Sections were air-dried, mounted in DePeX (BDH Laboratory; Poole, UK), and examined under a Nikon Eclipse 80i microscope (Tokyo, Japan). IVD degeneration was evaluated semi-quantitatively according to the criteria of Tam et al. [29].

COX2 immunohistochemistry

Histological sections were deparaffinized and a heat-mediated antigen retrieval was conducted (PT-Link, 95°C, 20 minutes, in citrate buffer pH 6.0). Subsequently, the sections were immunolabelled with a primary antibody recognizing COX2 protein expression (ab15191, abcam, LOT #GR299479-4, dilution 1:500) for 1 h at 37°C. Negative controls were performed by incubating sections with PBS instead of the primary antibody. Secondary anti-mouse/rabbit IgG (Dako EnVisionTM+ Dual Link System-HRP) was applied (1:200 dilution) for 30 min at room temperature (RT), followed by the amino-9-ethyl-carbazole (AEC) substrate kit (Dako) as a chromogen. Finally, the sections were counter-stained with Gill's hematoxylin for 3 min and cover-slipped with an aqueous

mounting medium (Glicerine, Sigma-Aldrich). Sections were evaluated semi-quantitatively for COX2 protein expression level according to immunohistochemical signal presence and intensity.

Bovine NP cell isolation and culture

Bovine NP cell isolation and culture were performed as described previously [25]. Briefly, tails from 18-24-month-old cows were purchased from the local slaughterhouse and carefully dissected to separate the NP from the AF of the IVDs. NP biopsies were minced and digested overnight at 37°C, 5% CO_2, using 0.4% collagenase NB4 (17454.01, Serva) and 0.2% dispase II (04942078001, Roche) dissolved in PBS 1X with 3% Antibiotic-Antimycotic (Anti-Anti; 15240-062, Gibco). The tissue digest was filtered, and NP cells were pelleted, washed with culture medium (Dulbecco's modified Eagle medium/F-12 Nutrient Mixture (DMEM/F12; 31330-038, Gibco), 10% fetal calf serum (FCS; F7524, Sigma-Aldrich) and 1% Anti-Anti), centrifuged, resuspended in culture medium and seeded in fibronectin-coated culture flasks. Cells were expanded to passage 1-2 at 37°C, 5% CO_2 and the medium was changed twice per week.

Agarose-collagen hydrogel fabrication and culture

Bovine NP cells were embedded and cultured in agarose-collagen hydrogels as described previously [25]. Briefly, after trypsinization, pelleted NP cells were resuspended in a 4 mg/ml collagen type I solution (5010, Advanced BioMatrix) prepared on ice at a density of $8x10^6$ cells/ml. The solution was then mixed 1:1 with a 4% wt/vol agarose solution (5010, Lonza) kept at 60°C to obtain a final concentration of $4x10^6$ cells/ml in agarose 2% wt/vol and collagen 2 mg/ml. Hydrogels (160 μl) were molded in silicon rings (inner Ø: 8 mm, outer Ø: 12 mm, height: 3 mm) for radial containment and placed between two microscope glass slides. Hydrogels were pre-cultured in 12-well plates at 37°C, 5% CO_2 in DMEM/F12 phenol red-free medium (11039, Gibco), supplemented with 10% FCS, 0.1% ampicillin (A0839, AppliChem) and 50 μg/ml L-ascorbic acid (A4544, Sigma-Aldrich) for 7 days before mechanical loading. The medium was changed every other day.

Cell-laden hydrogel dynamic compression

Four hours before compression, medium was changed to phenol red-free DMEM/F12 supplemented with 0.1% ampicillin, 50 μg/ml ascorbic acid, and 10 % charcoal-stripped FCS (A3382101, Gibco). For dynamic compression, the hydrogels in silicon rings were transferred to the wells of a commercial compression device (MCTR, CellScale) in 1 ml of medium. Hydrogels were dynamically compressed with a sine wave function at 0.5 Hz with a nominal force of 73 N and 13 N of pre-load for 1 h (unless otherwise stated) at 37°C, 5% CO_2. As the silicone ring dominates the stiffness, a strain of 20% can be inferred. Non-compressed hydrogels were kept in identical conditions in a 24-well plate.

Harvesting time-point: After compression, the hydrogels were transferred with their conditioned medium to a 24-well plate and further cultured for 24 or 48 h for analysis of the conditioned medium.

TRPV4 inhibition: Cell-laden hydrogels were pre-treated for 15 min with 0, 50, 100, or 200 nM of the selective TRPV4 antagonist GSK2193874 (17715, Cayman Chemical). The concentration of the vehicle (DMSO) was equalized in all chambers (0.002%). Hydrogels were subjected to dynamic compression for 1 h in the presence or absence of TRPV4 antagonist. After compression, the hydrogels were transferred with their conditioned medium to a 24-well plate and further cultured for 48 h for analysis of the conditioned medium.

MAPK phosphorylation: Hydrogels were pre-treated for 15 min with 0, 50, 100, or 200 nM of GSK2193874 and compressed for 30 min in the presence or absence of TRPV4 antagonist. Hydrogels were immediately processed for protein analysis. The lysates of two hydrogels per donor and per condition were pooled to reach sufficient protein amounts for Western blot.

Lactate dehydrogenase assay

Lactate dehydrogenase (LDH) is a cytosolic enzyme present in most cell types. When the cell membrane is damaged, LDH is released into the cell culture medium. Extracellular LDH was quantified using the colorimetric Pierce LDH Cytotoxicity Assay Kit (88954, Thermo Fisher Scientific) according to the manufacturer instructions. Samples (conditioned medium), blanks (medium used for compression), and the positive control of the kit were added in duplicates into a 96-well flat-bottom plate (50 µl/well). The reaction mixture was added (50 µl/well), and the plate was incubated at RT for 30 min protected from light. Stop solution was added (50 µl/well) and gently mixed. The absorbance was immediately measured at 490 nm with a reference at 680 nm using a plate reader (Infinite M200 PRO, TECAN). The average absorbance of the blanks was subtracted from the average absorbance of the samples.

PGE2 enzyme-linked immunosorbent assay

A competitive inhibition PGE2 enzyme-linked immunosorbent assay (ELISA) kit (RD-PGE2-Ge, Reddot Biotech) was used to quantify the levels of PGE2 in the conditioned medium according to the manufacturer instructions. Samples were used undiluted. PGE2 concentrations are expressed relative to the concentration of the non-compressed control.

Protein extraction and Western blot

Hydrogels were processed as described previously [25]. Briefly, hydrogels were cut into 4 pieces, washed with PBS 1X, snap-frozen in liquid nitrogen, and lyophilized overnight. RIPA buffer supplemented with protease and phosphatase inhibitor cocktails (78430; 78428, Thermo Fisher Scientific) was used to lyse the hydrogels on ice (100 µl/gel) for 1 h. The lysates and the soaked hydrogels were centrifuged in NucleoSpin filter columns (740606, Macherey-Nagel) for 1 h at 4°C at 12'000 rpm. For all samples, 22.5 µl

of lysate were mixed with 4X Laemmli buffer (1610747, Bio-Rad), heated at 95°C, and loaded onto a 4-20% gradient gel (4568093, Bio-Rad). Proteins were separated by electrophoresis in a Mini-PROTEAN Tetra Cell (Bio-Rad) and transferred to PVDF membranes (1704156, Bio-Rad). The membranes were washed with Tris Buffered Saline with 0.05% TWEEN 20 (TBS-T) and blocked for 2 h at RT with 5% skim milk in TBS-T. Primary antibodies (ERK1/2 (ERK): 9102; p-ERK: 9101; p38: 9212; p-p38: 9211; JNK: 9252; p-JNK: 9251; α-tubulin: 2144; Cell Signaling Technology) were applied 1:1000 in 5% BSA in TBS-T overnight at 4°C on a rocker. The membranes were washed with TBS-T and incubated for 1 h at RT on a rocker with the secondary antibody (anti-rabbit IgG HRP: 7074, Cell Signaling Technology) diluted 1:2000 in 5% skim milk in TBS-T. After washing with TBS-T, proteins were detected with a chemiluminescence substrate (34076, Thermo Fisher Scientific) on a ChemiDocTouch Imaging System (Bio-Rad). The density of the bands was semi-quantified on the ImageLab software (Bio-Rad). For each blot, the density of each band was normalized by the one of the non-compressed control. The ratio phosphorylated MAPKs/total MAPKs was calculated.

Trpv4 knockout murine tails for histology

Tails from unloaded wild-type (WT) and trpv4 knockout (KO) C57BL/6J mice were kindly provided by the Laboratory of Ion Channel Research at KU Leuven, Belgium. The trpv4 KO strain Trpv4tm1.1Ldtk [30] was backcrossed at least ten times into the C57BL/6J background, and C57BL/6J mice were used as WT controls. Mice of all genotypes were housed under identical conditions, with a maximum of four animals per cage on a 12-hour light-dark cycle and with food and water ad libitum. Fifteen-week-old male mice were euthanized and the tails were dissected, fixed, and washed as described above, and decalcified in Morse's solution at 4°C for 3 days. The decalcified samples were processed and sectioned as described above. The experiments were approved by the KULeuven Ethical Committee under the project "in vitro", license number LA1210202.

Statistical analysis

Data were checked for consistency and normality using skewness, kurtosis, and omnibus tests. Due to the small sample sizes, dependent bootstrap t-tests based on 10000 Monte Carlo samples were used. In addition, classical dependent t-tests and nonparametric tests (Wilcoxon Signed test) and Quantile Sign test were used. All reported tests were two-sided, and p-values < 0.05 were considered statistically significant. All statistical analyses were performed by using NCSS (NCSS 10, NCSS, LLC. Kaysville, UT) and PASW 24 (IBM SPSS Statistics for Windows, Version 21.0., Armonk, NY).

4.4 Results

Dynamic compression of murine IVDs causes mild degeneration in vivo

Dynamic compression was previously shown to induce IVD degeneration in vivo [8, 11, 12, 14, 16]. However, the expression of COX2 has not been investigated. In a first step,

we verified that dynamic compression causes structural and degenerative changes in mouse IVDs via a FAST histological staining. Sham IVDs showed a distinct and intact structure (**Figure 1 A**) with a single NP cell mass surrounded by matrix (**Figure 1 A, B**), a well-defined NP/AF boundary (**Figure 1 A, C**), and concentric lamellae in the AF (**Figure 1 A, C**). However, in dynamically compressed IVDs, the NP cell mass was mildly disrupted by matrix entering the NP (**Figure 1 D, E**). The NP/AF boundary was less clear (**Figure 1 D, F**) with a partial reversal of the AF lamellae into the NP (**Figure 1 D**), and disruption of the inner AF lamellae (**Figure 1 F**). The outer AF was rather intact, although rounder chondrocyte-like cells were present (**Figure 1 F**). Dynamic compression at 8 N, 2 Hz, 5 minutes 3x per week over 4 weeks, thus induces features of mild degeneration in mouse IVDs.
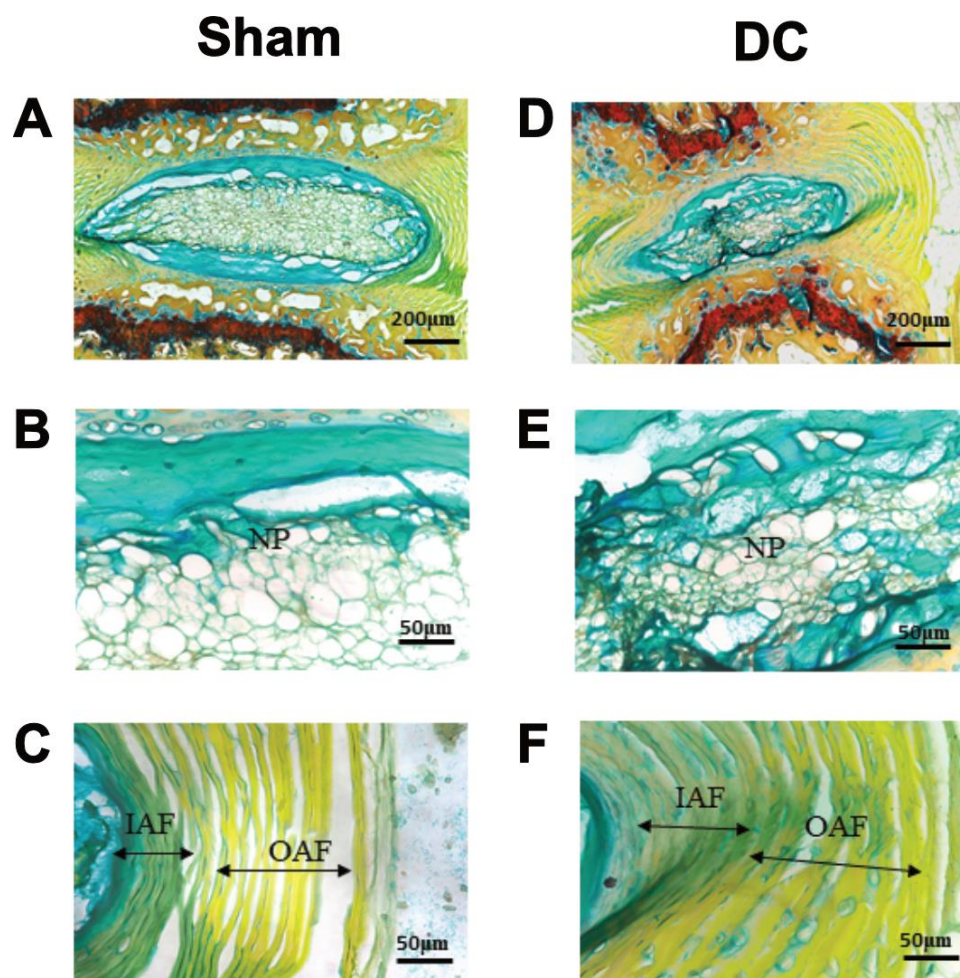
Figure 1: FAST staining of IVDs of sham **(A-C)** and dynamically compressed (DC; **D-F)** mouse tails. The nucleus pulposus (NP; **B, E),** inner and outer annulus fibrosus (IAF and OAF; **C, F)** are shown with a higher magnification. Scale bars: 200 μm in (A, D); 50 μm in **(B, E)** and **(C, F).** n = 2 in the sham group, n = 5 in the DC group.

Dynamic compression of murine IVDs does not affect COX2 expression in vivo

We previously showed that cyclic hyperphysiological stretching increases COX2 gene expression and the release of its product PGE2 in human AF cells [24]. In order to investigate the link between dynamic compression and inflammation, we performed

immunohistochemistry (IHC) to detect COX2 expression in sham and compressed mouse IVDs in vivo. COX2 was constitutively expressed in the NP of sham IVDs (**Figure 2 A**) and dynamic compression did not clearly affect COX2 expression (**Figure 2 B**).
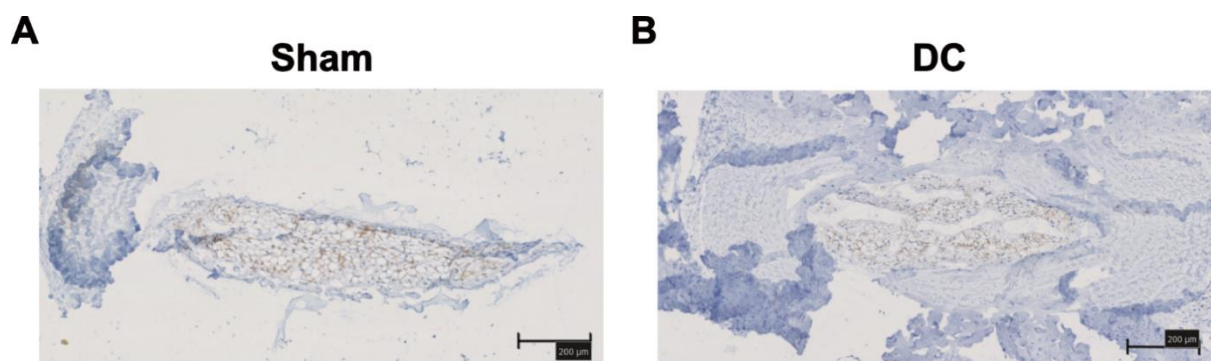
Figure 2: COX2 immunohistochemistry of IVDs of sham **(A)** and dynamically compressed (DC; **B)** mouse tails. Scale bars: 200 μm. n = 2 in the sham group, n = 3 in the DC group.

Hyperphysiological dynamic compression causes LDH and PGE2 release in vitro

In the second part of the study, we aimed to verify in vitro the effects of hyperphysiological dynamic compression observed in vivo, and to investigate the potential role of TRPV4. Bovine NP cells were isolated and cultured in 3D agarose-collagen hydrogels. Cell-laden hydrogels were dynamically compressed for 1 h at 0.5 Hz at a hyperphysiological regime of 73 N (corresponding to 20% strain). In order to test the effect of hyperphysiological dynamic compression on cell damage and inflammation, the release of LDH and PGE2 (a product of COX2) was measured 24 and 48 hours after the end of mechanical loading. No significant changes were observed after 24 h (**Figure 3 A, B**). However, LDH release considerably increased 48 h after compression compared to non-compressed cell-laden constructs (**Figure 3 A**). Furthermore, a slight but statistically significant 1.14-fold augmentation in PGE2 release was observed in compressed hydrogels compared to controls after 48 h (**Figure 3 B**). These data show that 1 h of hyperphysiological dynamic compression already induces NP cell damage and slight inflammation in vitro.
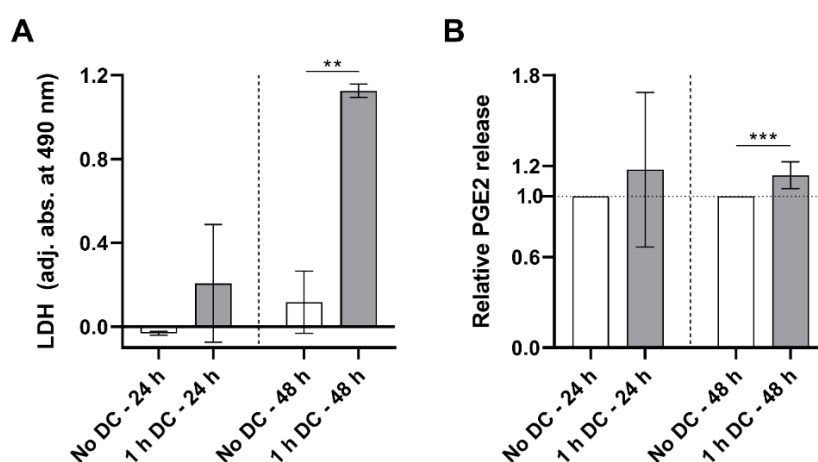
Figure 3: LDH **(A)** and relative PGE2 **(B)** release 24 or 48 h after no (white bars) or 1 h (grey bars) of dynamic compression (DC) at 73 N (corresponding to 20% strain) and 0.5 Hz. n = 3; mean ± SD; **p<0.01, ***p<0.001.

TRPV4 inhibition decreases compression-induced LDH and PGE2 release in vitro

To test whether compression-induced cell damage and inflammation were mediated by TRPV4, we blocked the ion channel with the selective antagonist GSK2193874 at different concentrations (50 to 200 nM) during dynamic compression and measured LDH and PGE2 release 48 h after mechanical loading. Once again, LDH release was significantly increased in compressed samples compared to controls (**Figure 4 A**). Interestingly, the compression-induced LDH release was partially but significantly reduced by TRPV4 inhibition at all GSK2193874 concentrations (**Figure 4 A**). In this data set, the small augmentation in PGE2 release induced by dynamic compression did not reach statistical significance ($p = 0.059$; **Figure 4 B**). Nevertheless, the TRPV4 inhibitor significantly decreased PGE2 release at 50 and 200 nM compared to the compressed condition without antagonist (**Figure 4 B**). The TRPV4 channel thus partially mediates compression-induced cell damage and inflammation, as measured by LDH and PGE2 release.
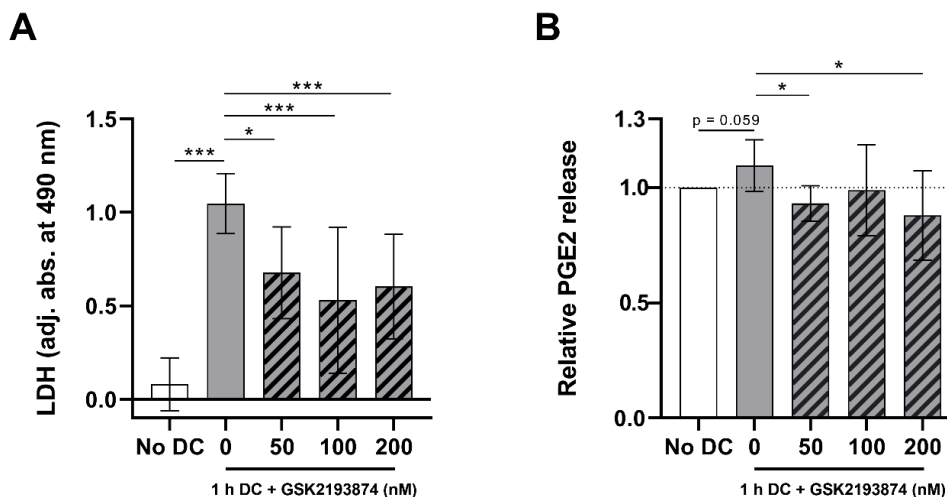
Figure 4: LDH **(A)** and relative PGE2 **(B)** release 48 h after no (white bars) or 1 h (grey bars) of dynamic compression (DC) at 73 N (corresponding to 20% strain) and 0.5 Hz in the absence or presence (hatched bars) of 50-200 nM of the TRPV4 antagonist GSK2193874. n = 4; mean ± SD; *p<0.05, ***p<0.001.

TRPV4 inhibition during dynamic compression activates the ERK MAPK pathway

MAPKs are known to play a role in apoptosis, survival, and inflammation in IVDs [18]. In order to test whether dynamic compression activates MAPKs and whether TRPV4 is involved in MAPK regulation, we measured the expression of total and phosphorylated MAPKs after 30 min of compression in the absence or presence of TRPV4 antagonist. Western blot bands for (p)-p38 and (p)-JNK were very faint or even absent and did not allow for densitometry analysis. However, (p)-ERK bands could be detected in all three tested cows. The expression of total ERK relative to the α-tubulin loading control remained similar across conditions (**Figure 5 A**). Samples dynamically compressed for 30 min without TRPV4 inhibitor displayed denser bands for p-ERK compared to non-compressed controls in all animals (**Figure 5 A, B**). However, upon densitometry analysis, the 1.88-fold increase in the p-ERK/ERK ratio compared to controls was not statistically

65

significant (**Figure 5 B**). Interestingly, blocking TRPV4 with 100 nM GSK2193874 during compression significantly increased ERK phosphorylation by 3.13-fold compared to non-compressed samples (**Figure 5 B**). Moreover, ERK phosphorylation with 100 nM TRPV4 antagonist was significantly higher than with 50 nM (**Figure 5 B**). These data show that TRPV4 inhibition during compression activates the ERK MAPK pathway.
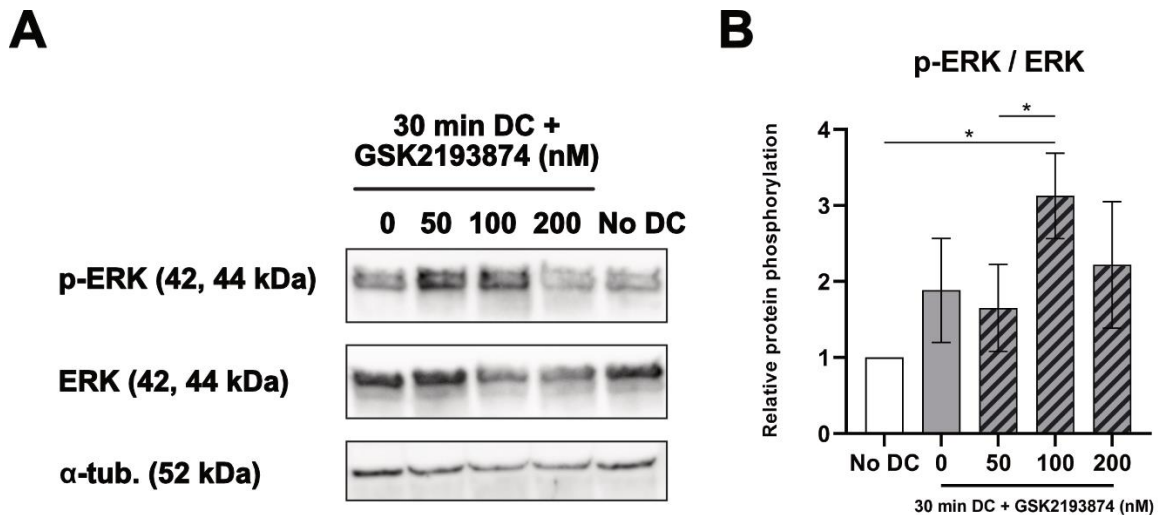
Figure 5: Representative Western blot **(A)** and densitometry analysis **(B)** of phosphorylated and total ERK 1/2 immediately after no (white bar) or 30 min (grey bars) of dynamic compression (DC) at 73 N (corresponding to 20% strain) and 0.5 Hz in the absence or presence (hatched bars) of 50-200 nM of the TRPV4 antagonist GSK2193874. α-tubulin bands are shown as a loading control in **(A)**. n = 3; mean ± SD; *$p < 0.05$.

Trpv4 KO murine IVDs show mild degeneration compared to WT IVDs

In the last part of the study, and as a proof-of-concept, we verified the observed roles of the TRPV4 ion channel in IVD homeostasis and COX2 regulation in murine IVDs that were not loaded. We first stained IVDs from WT and trpv4 KO mice with the FAST technique. The structure of WT IVDs was unaltered (**Figure 6 A**), with an intact NP (**Figure 6 B**) surrounded by concentric AF lamellae (**Figure 6 C**). Nevertheless, IVDs of trpv4 KO mice showed a mildly degenerated phenotype (**Figure 6 D**), characterized by a discontinued NP/AF boundary (**Figure 6 D, E**), partial reversals of the AF lamellae into the NP (**Figure 6 D, E**), and the presence of round chondrocyte-like cells at the transition between the NP and the inner AF (**Figure 6 E, F**). These images show that trpv4 KO promotes a mild degeneration in mouse IVDs, thus suggesting that TRPV4 plays a role in IVD homeostasis.
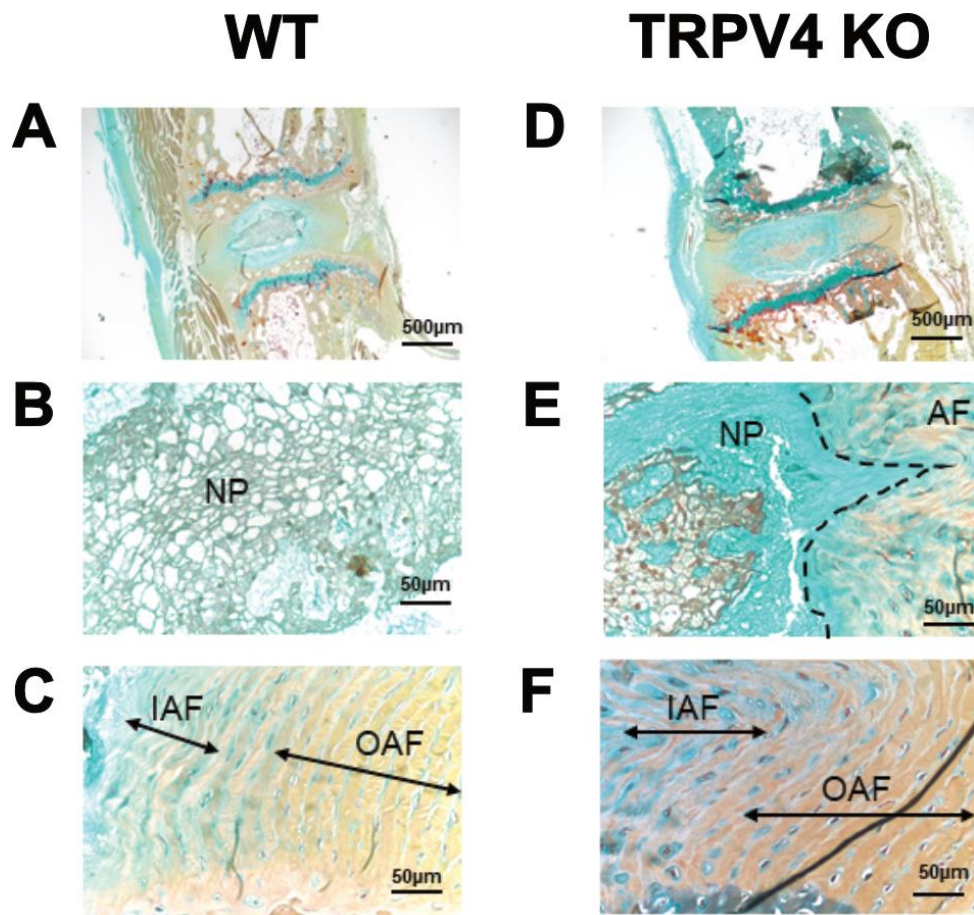
Figure 6: FAST staining of IVDs of wild-type (WT; **A-C)** and trpv4 knockout (KO; **D-F)** mouse tails. The nucleus pulposus (NP; **B, E)**, inner and outer annulus fibrosus (IAF and OAF; **C, F)** are shown with a higher magnification. Scale bars: 500 μm in **(A, D)**; 50 μm in **(B, E)** and **(C, F)**. n = 5.

Trpv4 KO murine IVDs show less COX2 expression in the NP compared to WT IVDs

We finally confirmed the link between TRPV4 and COX2 by performing IHC on WT and trpv4 KO mouse IVDs. COX2 was expressed in the NP of WT IVDs (**Figure 7 A**), similarly to sham IVDs (**Figure 2 A**). Interestingly, COX2 was not detected in trpv4 KO IVDs (**Figure 7 B**). TRPV4 thus regulates COX2 expression in murine IVDs in vivo.
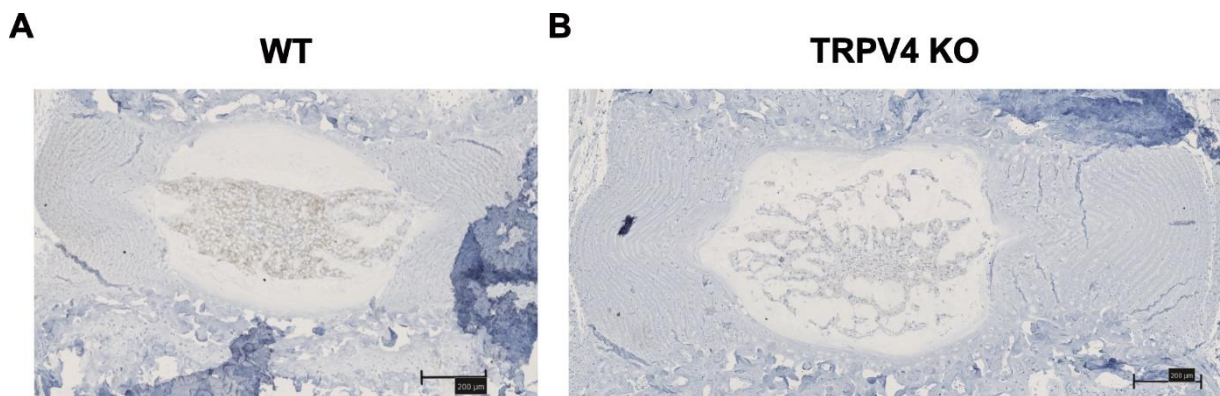
Figure 7: COX2 immunohistochemistry of IVDs of wild-type (WT; **A)** and trpv4 knockout (KO; **B)** mouse tails. Scale bars: 200 μm. n = 3.

4.5 Discussion

Aberrant mechanical loading is a contributor to IVD degeneration, which can cause DDD and LBP. However, the underlying mechanosensing and mechanotransduction mechanisms are poorly understood. This lack of understanding prevents the development of drugs that specifically target the molecular players that are involved in these pathways.

In this study, we investigated whether the mechanosensitive TRPV4 ion channel mediates the transduction of hyperphysiological dynamic compression in murine IVDs in vivo and bovine NP cells in vitro. We report novel evidence that compression-induced NP cell damage and inflammation are reduced by TRPV4 pharmacological inhibition, which might promote cell survival via the activation of the ERK MAPK pathway.

Our data show that hyperphysiological dynamic compression has degenerative effects both in vivo and in vitro. Short repetitive dynamic compression at 8 N, 2 Hz over 4 weeks provoked mild degeneration in murine caudal IVDs in vivo, as shown by FAST histological staining. These results agree with previous studies that showed that hyperphysiological dynamic compression (at high magnitude, frequency, or duration) causes IVD degeneration in rodent in vivo models [8, 11, 12, 14, 16]. Interestingly, dynamic compression did not affect COX2 expression in vivo. We speculate that this lack of change might be due to the short hyperphysiological loading of 5 minutes per day. The study should be repeated with a longer loading duration per day, and COX2 activity should be evaluated to determine the link between hyperphysiological dynamic compression and COX2 expression/activity. Our in vitro model, which is constituted of bovine NP cells embedded in a matrix-mimicking agarose-collagen hydrogel, recapitulated the detrimental changes induced by dynamic compression in vivo. Hyperphysiological dynamic compression of the cell-laden scaffolds caused a considerable increase in the release of LDH, an indicator of cell damage, and a slight augmentation in the release of PGE2, a product of COX2. We speculate that repetitive mechanical stimulation (instead of a single continuous loading of 1 h) might increase the small increase in PGE2 release. The effects of compression were time-dependent, as they were detected 48 h after the end of mechanical loading but not after 24 h. Previous studies have similarly shown cell death and increase in inflammatory mediators as a result of hyperphysiological dynamic compression [8-10].

The novel findings that TRPV4 inhibition attenuates compression-induced LDH and PGE2 release in vitro, and that TRPV4 KO induces IVD degeneration and reduced COX2 expression in vivo, suggest a dual role of TRPV4 in the IVD. On one hand, our data show that TRPV4 pharmacological inhibition significantly reduces cell damage and inflammation induced by hyperphysiological dynamic compression. While these findings are new in NP cells, they find an echo in other studies showing that induced cell death is mitigated by TRPV4 inhibition or knockdown in other organs and tissues such as pancreas, brain and heart [31-34]. Moreover, we previously showed that stretch-induced inflammation (including increased COX2 mRNA expression and PGE2 release) was partially TRPV4-dependent in AF cells [24]. The reduction in PGE2 release caused by TRPV4 inhibition in vitro is in further agreement with our in vivo data showing a decreased COX2 expression in the NP of trpv4-deficient mice. On the other hand, TRPV4

expression is necessary and plays a role in IVD homeostasis. Trpv4 KO murine IVDs displayed mild degeneration compared to WT IVDs. These results align with previous reports of trpv4-deficient mice exhibiting mildly detrimental phenotypes, including a larger bladder capacity due to impaired mechanosensing, thicker bones due to impaired osteoclast differentiation, reduced water intake due to altered osmosensing, and compromised pressure and pain sensing [35]. While the constitutive expression of TRPV4 seems to be essential throughout the body, its temporary inhibition or conditional downregulation in the IVD might counteract exacerbated mechanosensing and pain induced by aberrant mechanical stress during DDD and LBP. Nevertheless, experiments with mechanical loading of trpv4 KO and WT mouse tails should be performed to confirm these results.

Finally, our finding that TRPV4 inhibition during dynamic compression activates the ERK MAPK pathway supports a role of TRPV4 in cell death. In fact, the ERK pathway is known to regulate survival and apoptosis in IVD cells and tissues [18, 36, 37]. Moreover, ERK activation was previously shown to counteract compression-induced apoptosis in the endplate and transitional zone of the AF in mouse IVDs [18, 36]. Our results are in further agreement with previous studies that demonstrate a link between TRPV4 and ERK. In a study showing the contribution of TRPV4 to hypo-osmotic stress in chondrocytes, ERK inhibition prevented increased levels of TRPV4 in cells subjected to hypo-osmotic stress [38]. Moreover, TRPV4 inhibition was previously shown to reduce myocardial ischemia/reperfusion injury in mice by attenuating apoptosis and increasing ERK phosphorylation [34].

The conclusions of this study are limited by several aspects. First, two different animal models were used. While the mouse is an excellent model to investigate mechanical loading, the small size of murine IVDs prevents harvesting a sufficient amount of IVD cells for in vitro experiments. High amounts of NP cells were required for embedding in agarose-collagen hydrogels, and this quantity could also not be achieved by expansion of human NP cells, due their low availability and proliferation rate. Moreover, while female mice were used in compression experiments, male WT and trpv4 KO mice were used later, thus preventing a direct comparison between the two data sets. Finally, although the in vivo and in vitro loading regimes both have a hyperphysiological loading magnitude, a physiological frequency, and the same overall duration, they differ in the fact that the in vivo loading is repetitive and the in vitro loading is continuous. This difference can explain different observations between the two experimental settings.

In summary, we show that TRPV4 regulates COX2/PGE2 in bovine NP cells in vitro and in mouse IVDs in vivo, and that TRPV4 inhibition significantly reduces cell damage and PGE2 release induced by hyperphysiological compression in vitro, possibly via ERK activation. These novel findings thus identify TRPV4 as a promising therapeutic target to treat IVD degeneration, DDD, and LBP. Preclinical and clinical trials examining TRPV4 inhibition in the context of DDD and LBP are currently lacking. However, the administration of the TRPV4 antagonist GSK2798745 to healthy volunteers and heart failure patients was recently shown to be safe [39]. Targeting the mechanosensitive TRPV4 channel may benefit patients with IVD pathologies caused by aberrant mechanical loading. Nevertheless, it should be noted that TRPV4 is polymodal, ubiquitous, and its constitutive expression seems to be necessary. Therefore, a therapy targeting TRPV4

needs to be carefully elaborated in order to maintain its beneficial and necessary roles in homeostasis. A localized and/or temporary inhibition or knockdown (e.g. via the CRISPR-based technology [40]) of TRPV4 in the IVD, via injection of a specific antagonist or inducible gene editing in case of excessive mechanical load, might be desirable therapeutic strategies in the future.

Author contributions

E.C. conceived the project, designed and conducted experiments, analyzed data, and wrote the manuscript. S.H. conducted in vitro experiments. A.C.S. designed and conducted mouse mechanical loading experiments. W.K.T. performed and analyzed FAST histological staining. A.A.K. optimized and analyzed COX2 immunohistochemistry. W.H. performed statistical analysis. V.Y.L. supervised FAST histological staining. R.M. designed and supervised mouse loading experiments. S.J.F. and K.W.-K. provided funding and supervised the project. All authors reviewed and approved the manuscript.

4.6 References

1. M.A. Adams, P.J. Roughley, What is intervertebral disc degeneration, and what causes it?, Spine 31(18) (2006) 2151-2161.

2. P.P.A. Vergroesen, I. Kingma, K.S. Emanuel, R.J.W. Hoogendoorn, T.J. Welting, B.J. van Royen, J.H. van Dieen, T.H. Smit, Mechanics and biology in intervertebral disc degeneration: a vicious circle, Osteoarthritis and Cartilage 23(7) (2015) 1057-1070.

3. O. Airaksinen, J.I. Brox, C. Cedraschi, J. Hildebrandt, J. Klaber-Moffett, F. Kovacs, A.F. Mannion, S. Reis, J.B. Staal, H. Ursin, G. Zanoli, C.B.W.G.G. Ch, Chapter 4 - European guidelines for the management of chronic nonspecific low back pain, European Spine Journal 15 (2006) S192-S300.

4. F. Balague, A.F. Mannion, F. Pellise, C. Cedraschi, Non-specific low back pain, Lancet 379(9814) (2012) 482-491.

5. S.C. Chan, S.J. Ferguson, B. Gantenbein-Ritter, The effects of dynamic loading on the intervertebral disc, Eur Spine J 20(11) (2011) 1796-812.

6. S. Bao, Mechanical stress, Handb Clin Neurol 131 (2015) 367-96.

7. B.V. Fearing, P.A. Hernandez, L.A. Setton, N.O. Chahine, Mechanotransduction and cell biomechanics of the intervertebral disc, JOR Spine 1(3) (2018).

8. A.J. Walsh, J.C. Lotz, Biological response of the intervertebral disc to dynamic loading, J Biomech 37(3) (2004) 329-37.

9. D.L. Wang, S.D. Jiang, L.Y. Dai, Biologic response of the intervertebral disc to static and dynamic compression in vitro, Spine (Phila Pa 1976) 32(23) (2007) 2521-8.

10. S. Illien-Junger, B. Gantenbein-Ritter, S. Grad, P. Lezuo, S.J. Ferguson, M. Alini, K. Ito, The combined effects of limited nutrition and high-frequency loading on intervertebral discs with endplates, Spine (Phila Pa 1976) 35(19) (2010) 1744-52.

11. J.J. MacLean, C.R. Lee, S. Grad, K. Ito, M. Alini, J.C. Iatridis, Effects of immobilization and dynamic compression on intervertebral disc cell gene expression in vivo, Spine (Phila Pa 1976) 28(10) (2003) 973-81.

12. C.T. Ching, D.H. Chow, F.Y. Yao, A.D. Holmes, Changes in nuclear composition following cyclic compression of the intervertebral disc in an in vivo rat-tail model, Med Eng Phys 26(7) (2004) 587-94.

13. C.L. Korecki, C.K. Kuo, R.S. Tuan, J.C. Iatridis, Intervertebral Disc Cell Response to Dynamic Compression Is Age and Frequency Dependent, Journal of Orthopaedic Research 27(6) (2009) 800-806.

14. J.J. Maclean, C.R. Lee, M. Alini, J.C. Iatridis, Anabolic and catabolic mRNA levels of the intervertebral disc vary with the magnitude and frequency of in vivo dynamic compression, J Orthop Res 22(6) (2004) 1193-200.

15. J.J. MacLean, C.R. Lee, M. Alini, J.C. Iatridis, The effects of short-term load duration on anabolic and catabolic gene expression in the rat tail intervertebral disc, J Orthop Res 23(5) (2005) 1120-7.

16. K. Wuertz, K. Godburn, J.J. MacLean, A. Barbir, J.S. Donnelly, P.J. Roughley, M. Alini, J.C. Iatridis, In vivo remodeling of intervertebral discs in response to short- and long-term dynamic compression, J Orthop Res 27(9) (2009) 1235-42.

17. G.J. Kerr, M.A. Veras, M.K. Kim, C.A. Seguin, Decoding the intervertebral disc: Unravelling the complexities of cell phenotypes and pathways associated with degeneration and mechanotransduction, Semin Cell Dev Biol 62 (2017) 94-103.

18. K. Wuertz, N. Vo, D. Kletsas, N. Boos, Inflammatory and catabolic signalling in intervertebral discs: the roles of NF-kappaB and MAP kinases, Eur Cell Mater 23 (2012) 103-19; discussion 119-20.

19. O. Krupkova, J. Zvick, K. Wuertz-Kozak, The Role of Transient Receptor Potential Channels in Joint Diseases, Eur Cells Mater 34 (2017) 180-201.

20. B.A. Walter, D. Purmessur, A. Moon, J. Occhiogrosso, D.M. Laudier, A.C. Hecht, J.C. Iatridis, Reduced tissue osmolarity increases TRPV4 expression and pro-inflammatory cytokines in intervertebral disc cells, Eur Cell Mater 32 (2016) 123-36.

21. A. Franco-Obregon, E. Cambria, H. Greutert, T. Wernas, W. Hitzl, M. Egli, M. Sekiguchi, N. Boos, O. Hausmann, S.J. Ferguson, H. Kobayashi, K. Wuertz-Kozak, TRPC6 in simulated microgravity of intervertebral disc cells, Eur Spine J 27(10) (2018) 2621-2630.

22. T. Kameda, J. Zvick, M. Vuk, A. Sadowska, W.K. Tam, V.Y. Leung, K. Bolcskei, Z. Helyes, L.A. Applegate, O.N. Hausmann, J. Klasen, O. Krupkova, K. Wuertz-Kozak, Expression and Activity of TRPA1 and TRPV1 in the Intervertebral Disc: Association with Inflammation and Matrix Remodeling, Int J Mol Sci 20(7) (2019).

23. A. Sadowska, W. Hitzl, A. Karol, P. Jaszczuk, H. Cherif, L. Haglund, O.N. Hausmann, K. Wuertz-Kozak, Differential regulation of TRP channel gene and protein expression by intervertebral disc degeneration and back pain, Sci Rep-Uk 9 (2019).

24. E. Cambria, M.J.E. Arlt, S. Wandel, O. Krupkova, W. Hitzl, F.S. Passini, O.N. Hausmann, J.G. Snedeker, S.J. Ferguson, K. Wuertz-Kozak, TRPV4 Inhibition and CRISPR-Cas9 Knockout Reduce Inflammation Induced by Hyperphysiological Stretching in Human Annulus Fibrosus Cells, Cells 9(7) (2020).

25. E. Cambria, S. Brunner, S. Heusser, P. Fisch, W. Hitzl, S.J. Ferguson, K. Wuertz-Kozak, Cell-Laden Agarose-Collagen Composite Hydrogels for Mechanotransduction Studies, Front Bioeng Biotechnol 8 (2020) 346.

26. A.C. Scheuren, P. Vallaster, G.A. Kuhn, G.R. Paul, A. Malhotra, Y. Kameo, R. Müller, Mechano-Regulation of Trabecular Bone Adaptation Is Controlled by the Local in vivo Environment and Logarithmically Dependent on Loading Frequency, Frontiers in Bioengineering and Biotechnology 8(1211) (2020).

27. D.J. Webster, P.L. Morley, G.H. van Lenthe, R. Muller, A novel in vivo mouse model for mechanically stimulated bone adaptation--a combined experimental and computational validation study, Comput Methods Biomech Biomed Engin 11(5) (2008) 435-41.

28. V.Y. Leung, W.C. Chan, S.C. Hung, K.M. Cheung, D. Chan, Matrix remodeling during intervertebral disc growth and degeneration detected by multichromatic FAST staining, J Histochem Cytochem 57(3) (2009) 249-56.

29. V. Tam, W.C.W. Chan, V.Y.L. Leung, K.S.E. Cheah, K.M.C. Cheung, D. Sakai, M.R. McCann, J. Bedore, C.A. Seguin, D. Chan, Histological and reference system for the analysis of mouse intervertebral disc, J Orthop Res 36(1) (2018) 233-243.

30. C. Moore, F. Cevikbas, H.A. Pasolli, Y. Chen, W. Kong, C. Kempkes, P. Parekh, S.H. Lee, N.A. Kontchou, I. Yeh, N.M. Jokerst, E. Fuchs, M. Steinhoff, W.B. Liedtke, UVB radiation generates sunburn pain and affects skin by activating epidermal TRPV4 ion channels and triggering endothelin-1 signaling, Proc Natl Acad Sci U S A 110(34) (2013) E3225-34.

31. S. Casas, A. Novials, F. Reimann, R. Gomis, F.M. Gribble, Calcium elevation in mouse pancreatic beta cells evoked by extracellular human islet amyloid polypeptide involves activation of the mechanosensitive ion channel TRPV4, Diabetologia 51(12) (2008) 2252-2262.

32. J.Z. Bai, J. Lipski, Differential expression of TRPM2 and TRPV4 channels and their potential role in oxidative stress-induced cell death in organotypic hippocampal culture, Neurotoxicology 31(2) (2010) 204-214.

33. M. Shi, F. Du, Y. Liu, L. Li, J. Cai, G.F. Zhang, X.F. Xu, T. Lin, H.R. Cheng, X.D. Liu, L.Z. Xiong, G. Zhao, Glial cell-expressed mechanosensitive channel TRPV4 mediates infrasound-induced neuronal impairment, Acta Neuropathol 126(5) (2013) 725-39.

34. Q. Dong, J. Li, Q.F. Wu, N. Zhao, C. Qian, D. Ding, B.B. Wang, L. Chen, K.F. Guo, D.H. Fu, B. Han, Y.H. Liao, Y.M. Du, Blockage of transient receptor potential vanilloid 4 alleviates myocardial ischemia/reperfusion injury in mice, Sci Rep-Uk 7 (2017).

35. B. Nilius, T. Voets, The puzzle of TRPV4 channelopathies, EMBO Rep 14(2) (2013) 152-63.

36. K. Ariga, K. Yonenobu, T. Nakase, N. Hosono, S. Okuda, W. Meng, Y. Tamura, H. Yoshikawa, Mechanical stress-induced apoptosis of endplate chondrocytes in organ-cultured mouse intervertebral discs: an ex vivo study, Spine (Phila Pa 1976) 28(14) (2003) 1528-33.

37. M.V. Risbud, A. Guttapalli, T.J. Albert, I.M. Shapiro, Hypoxia activates MAPK activity in rat nucleus pulposus cells: regulation of integrin expression and cell survival, Spine (Phila Pa 1976) 30(22) (2005) 2503-9.

38. I.M. Hdud, A. Mobasheri, P.T. Loughna, Effect of osmotic stress on the expression of TRPV4 and BKCa channels and possible interaction with ERK1/2 and p38 in cultured equine chondrocytes, Am J Physiol-Cell Ph 306(11) (2014) C1050-C1057.

39. N. Goyal, P. Skrdla, R. Schroyer, S. Kumar, D. Fernando, A. Oughton, N. Norton, D.L. Sprecher, J. Cheriyan, Clinical Pharmacokinetics, Safety, and Tolerability of a Novel, First-in-Class TRPV4 Ion Channel Inhibitor, GSK2798745, in Healthy and Heart Failure Subjects, Am J Cardiovasc Drug 19(3) (2019) 335-342.

40. O. Krupkova, E. Cambria, L. Besse, A. Besse, R. Bowles, K. Wuertz-Kozak, The potential of CRISPR/Cas9 genome editing for the study and treatment of intervertebral disc pathologies, JOR Spine 1(1) (2018) e1003.

Chapter 5

TRPV4 inhibition and CRISPR-Cas9 knockout reduce inflammation induced by hyperphysiological stretching in human annulus fibrosus cells

TRPV4 inhibition and CRISPR-Cas9 knockout reduce inflammation induced by hyperphysiological stretching in human annulus fibrosus cells

Elena Cambria [1], Matthias J. E. Arlt [1,2], Sandra Wandel [1], Olga Krupkova [1,3,4], Wolfgang Hitzl [5,6,7], Fabian S. Passini [1,2], Oliver N. Hausmann [8,9], Jess G. Snedeker [1,2], Stephen J. Ferguson [1] and Karin Wuertz-Kozak [1,10,11]

1 Institute for Biomechanics, ETH Zurich, 8093 Zurich, Switzerland

2 Department of Orthopedics, Balgrist University Hospital, University of Zurich, 8008 Zurich, Switzerland

3 Department of Biomedicine, University of Basel, 4031 Basel, Switzerland

4 Spine Surgery, University Hospital Basel, 4031 Basel, Switzerland

5 Research Office (Biostatistics), Paracelsus Medical University, 5020 Salzburg, Austria

6 Department of Ophthalmology and Optometry, Paracelsus Medical University, 5020 Salzburg, Austria

7 Research Program Experimental Ophthalmology and Glaucoma Research, Paracelsus Medical University, 5020 Salzburg, Austria

8 Neuro- and Spine Center, Hirslanden Klinik St. Anna, 6006 Lucerne, Switzerland

9 Medical Faculty, University of Bern, 3012 Bern, Switzerland

10 Department of Biomedical Engineering, Rochester Institute of Technology, Rochester, NY 14623, USA

11 Spine Center, Schön Klinik München Harlaching, Academic Teaching Hospital and Spine Research Institute of the Paracelsus Private Medical University Salzburg (Austria), 81547 Munich, Germany

5.1 Abstract

Mechanical loading and inflammation interact to cause degenerative disc disease and low back pain (LBP). However, the underlying mechanosensing and mechanotransductive pathways are poorly understood. This results in untargeted pharmacological treatments that do not take the mechanical aspect of LBP into account. We investigated the role of the mechanosensitive ion channel TRPV4 in stretch-induced inflammation in human annulus fibrosus (AF) cells. The cells were cyclically stretched to 20% hyperphysiological strain. TRPV4 was either inhibited with the selective TRPV4 antagonist GSK2193874 or knocked out (KO) via CRISPR-Cas9 gene editing. The gene expression, inflammatory mediator release and MAPK pathway activation were analyzed. Hyperphysiological cyclic stretching significantly increased the IL6, IL8, and COX2 mRNA, PGE2 release, and activated p38 MAPK. The TRPV4 pharmacological inhibition significantly attenuated these effects. TRPV4 KO further prevented the stretch-induced upregulation of IL8 mRNA and reduced IL6 and IL8 release, thus supporting the inhibition data. We provide novel evidence that TRPV4 transduces hyperphysiological mechanical signals into inflammatory responses in human AF cells, possibly via p38. Additionally, we show for the first time the successful gene editing of human AF cells via CRISPR-Cas9. The pharmacological inhibition or CRISPR-based targeting of TRPV4 may constitute a potential therapeutic strategy to tackle discogenic LBP in patients with AF injury.

Keywords: mechanotransduction, cyclic stretching, transient receptor potential channel, gene editing, interleukins, low back pain

5.2 Introduction

Unlocking the mechanisms leading from mechanical stimuli to cellular sensing and response has become necessary to understand and tackle diseases in essentially all medical disciplines [1]. Musculoskeletal disorders are often associated with abnormal mechanical stress applied to load-bearing tissues [2,3]. In the intervertebral disc (IVD), compressive forces from the body weight and spinal motions generate hydrostatic and osmotic pressures in the central gelatinous nucleus pulposus, which in turn increase tensile stresses in the ring-shaped annulus fibrosus (AF) [4]. While physiological mechanostimulation is favorable and even necessary to maintain IVD homeostasis, hyperphysiological mechanical loading is a well known contributor to IVD degeneration [5]. Furthermore, mechanical overloading interacts with inflammation and catabolism to cause degenerative disc disease (DDD) [6,7,8,9]. DDD, characterized by IVD structural failure and nociception [6], is the main cause of discogenic back pain. Low back pain (LBP) is a condition with a lifetime prevalence of 84% and the primary cause of disability worldwide [10,11]. In particular, AF disruption is commonly linked to LBP and disability [12]. Current pharmacological treatments of LBP, such as anti-inflammatory drugs, do not take into account the mechanical aspect of the problem. Moreover, they have low effect sizes and their mechanisms of action remain unclear [10]. A profound knowledge of the

mechanotransductive pathways leading to the degeneration and inflammation of the AF could improve the efficacy of novel pharmaceutical therapies.

Several studies have previously proved the detrimental effects of hyperphysiological mechanical loading on IVD cells at the molecular level. Cyclic stretching of IVD (mostly AF) cells at a high strain from 8 to 20% was shown to induce the downregulation of anabolic markers (ACAN, COL2) [13] and the upregulation of catabolic (MMP1, MMP3, MMP9, MMP13, ADAMTS4, ADAMTS5) [13,14] and (pro-)inflammatory (COX2, PGE2, IL1β, IL6, IL8, IL15, TLR2, TLR4, NGF, TNFα, MCP1, MCP3, MIG) [13,14,15,16,17] mediators. Stretch-induced inflammation in the IVD may be regulated by the NF-κB [13] or the mitogen-activated protein kinase (MAPK: ERK1/2, p38 and JNK) [17] signaling pathways. Nevertheless, the exact mechanosensing and mechanotransductive mechanisms of AF cells remain poorly understood.

Transient receptor potential (TRP) ion channels have emerged as a novel class of cellular sensors and as potential therapeutic targets to treat several diseases [18]. TRP channels are non-selective calcium-permeable transmembrane channels that are sensitive to a variety of stimuli, including temperature, pH, oxidative stress, and importantly, mechanical stress [19]. There are six sub-families of mammalian TRP channels: TRPC (canonical), TRPV (vanilloid), TRPM (melastatin), TRPP (polycystin), TRPML (mucolipin) and TRPA (ankyrin) [19]. The member 4 of the vanilloid subfamily (TRPV4) is of particular interest in the context of joint diseases, due to its ability to transduce mechanical, inflammatory and pain signals [20]. In chondrocytes, similar in many aspects to IVD cells, TRPV4 was shown to mediate the transduction of dynamic compressive loading [21]. Moreover, cartilage-specific TRPV4 knockout in mice reduced age-related osteoarthritis [22]. The exploration of TRP channels in the IVD is at its infancy, with only few published studies [23,24,25,26,27]. Most of the known TRP channel genes are expressed in the IVD [26]. Interestingly, TRPV4 has been associated with reduced osmolarity and pro-inflammatory cytokines in bovine nucleus pulposus cells [23]. Additionally, treatment with IL1β increases TRPV4 gene expression in human IVD cells, thus revealing a potential inflammatory role of the channel in IVDs [27]. Nevertheless, the roles of TRPV4 in mechanosensing and mechanotransduction in the IVD remain to be established.

In this study, we aimed to investigate whether stretch-induced inflammation is signaled through TRPV4 in human primary AF cells. To this end, we modulated the TRPV4 activity and expression through pharmacological inhibition and CRISPR-Cas9 knockout, respectively, in AF cells that were cyclically stretched at a hyperphysiological strain of 20%.

5.3 Materials and methods

Human AF Cell Isolation and Culture

Human IVD biopsies were obtained from patients undergoing spinal surgery for disc herniation or DDD after informed consent. Patient characteristics can be found in **Table 1**.

The study was conducted in accordance with the Declaration of Helsinki, and the protocol was approved by the ethical committee of the Canton of Zurich, Switzerland (2019-00736). AF tissue was intraoperatively excised from the IVD and enzymatically digested overnight at 37 °C, 5% CO_2, using 0.2% collagenase NB4 (17454, Serva) and 0.3% dispase II (04942078001, Roche) in PBS 1X with 5% antibiotic–antimycotic (anti–anti; 15240-062, Gibco, Switzerland). Isolated cells were cultured up to passage 1–2 at 37 °C, 5% CO_2 in a growth medium (Dulbecco's modified Eagle medium/F-12 Nutrient Mixture (DMEM/F12; 31330-038, Gibco, Switzerland), supplemented with 10% fetal calf serum (FCS; F7524, Sigma-Aldrich, Switzerland) and 1% anti–anti).

Table 1. Patient characteristics: F = female; M = male; DDD = degenerative disc disease; L = lumbar; C = cervical.

N°	Age	Sex	Diagnosis	Disc Level	Pfirrmann Grade
1	74	M	Herniation	L4/5	3
2	71	M	Herniation	L4/5	3
3	76	F	DDD	L5/S1	4
4	56	F	DDD	C6/7	3
5	40	F	Herniation	C5/6	2
6	52	F	Herniation	L4/5	3
7	15	M	DDD	L4/5	4
8	75	F	DDD	L3/4	3
9	46	M	Herniation	L4/5	4

Generation of CRISPR-Cas9 TRPV4 Knockout (KO) Cells

The CRISPRdirect online tool (http://crispr.dbcls.jp; [28]) was used to design a single guide RNA (sgRNA) against TRPV4 with a highly specific target site (TRPV4 (hu) 739–761: CGGAGCGCACCGGCAACATG). A non-targeting control sgRNA (Hu Non-Targeting 40: GACTTATAAACTCGCGCGGA) was chosen from the study of Morgens et al. [29]. Low targeting potential was checked by a BLASTN (BLASTN 2.8.0) search. Target sequences' oligos were synthesized with BsmBI restriction site overhangs by Microsynth (Balgach, Switzerland) and then annealed and cloned into the lentiCRISPRv2 transfer plasmid, a gift from Feng Zhang (Addgene plasmid # 52961; [30]), according to the protocol of the Feng Zhang Lab.

HEK293T cells were co-transfected with the lentiCRISPRv2 plasmid with the packaging plasmids pCMV-VSV-G (a gift from Bob Weinberg; Addgene plasmid # 8454; [31]) and psPAX2 (a gift from Didier Trono; Addgene plasmid # 12260) using Lipofectamine 3000 (Invitrogen, Thermo Fisher Scientific) according to the manufacturer's instructions, in order to produce lentiviral particles.

Human AF cells were transduced through incubation with medium containing viral particles and 8 μg/mL polybrene for 24 h. The cells were selected with 4 μg/mL puromycin (A1113803, Gibco) for 7 days and cultured for 8 weeks in growth medium

before being tested. The efficiency of the KOs was tested by RT-qPCR and immunocytochemistry.

Cyclic Stretching

Commercial stretching chambers (10 cm^2, STB-CH-10, STREX) were coated with 50 µg/mL fibronectin (FC010, Merck Millipore) overnight at 37 °C. The human AF cells at passage 1–2 were seeded in the chambers (100,000 cells per chamber in 5 mL growth medium) and cultured for 72 h at 37 °C, 5% CO_2, unless otherwise stated. The cells were serum-starved for 4–12 h in a no-serum medium (DMEM/F12 with 0.1% ampicillin (A0839, AppliChem, Darmstadt, Germany). The chambers were mounted on a commercial stretching bioreactor (STB-140-10, STREX) and subjected to 20% cyclic sinusoidal uniaxial strain at a frequency of 1 Hz at 37 °C and 5% CO_2. Control chambers were kept in identical conditions without stretching.

Time course: Cells were stretched for 1, 2, 4, 8, 12 or 24 h. The stretching started with the chambers that were stretched for 24 h, and shorter duration chambers were added progressively on the device so that the stretching was stopped at the same time for all conditions. Immediately after the mechanical loading, the cells were lysed for gene expression analysis.

TRPV4 inhibition: Cells were pre-treated for 15 min with 0, 20, 50, 100, 200 or 500 nM of the selective TRPV4 antagonist GSK2193874 (1336960-13-4, Sigma-Aldrich). The concentration of the vehicle (DMSO) was equalized in all chambers (0.005%). Cells were subjected to cyclic stretching for 1 h in the presence of the antagonist or vehicle and either immediately lysed for gene expression analysis or cultured in 2 mL of fresh no-serum medium for 24 h for analysis of the conditioned medium.

MAPK activation: Cells were seeded in the chambers (300,000 cells per chamber in 5 mL growth medium), cultured for 24 h at 37 °C, 5% CO_2 and serum-starved. Cells were pre-treated for 15 min with 0, 20, 100, 200 or 500 nM of GSK2193874 and stretched for 15 min in the presence of the antagonist or vehicle. As a positive control, the cells were pre-treated for 15 min with 10 ng/mL recombinant human IL1β (200-01B, PeproTech) and further incubated for 15 min without stretching in the presence of IL1β. Cells were lysed for Western blot immediately after stretching.

TRPV4 knockout: CRISPR-Cas9-transduced non-targeting control (NT) and TRPV4 knockout (KO) cells were subjected to cyclic stretching for 1 h and either immediately lysed for gene expression analysis or cultured in 2 mL of fresh no-serum medium for 24 h for analysis of the conditioned medium.

RNA Extraction and RT-qPCR

Immediately after stretching, the cells were rinsed with cold PBS 1X and lysed on ice with 600 µL per chamber of GENEzol (GZR200, Geneaid) using a cell scraper. The RNA was extracted with chloroform, precipitated with isopropanol, washed in ethanol and resuspended in RNase-free water according to the Geneaid instructions. The RNA yield and purity were measured on a NanoDrop 1000 Spectrophotometer (Thermo Fisher

Scientific). The TaqMan Reverse Transcription kit (N8080234, Applied Biosystems) was used to reverse-transcribe 1 µg of RNA into cDNA in a 30 µL volume. PCR reactions were carried out in a 10 µL total volume containing 20 ng of cDNA, TaqMan primers (TRPV4: Hs01099348_m1; COL1A1: Hs00164004_m1; COL2A1: Hs00264051_m1; ACAN: Hs00153936_m1; MMP1: Hs00233958_m1; MMP3: Hs00968308_m1; MMP13: Hs00233992_m1; IL6: Hs00174131_m1; CXCL8 (IL8): Hs00174103_m1; PTGS2 (COX2): Hs00153133_m1; SDHA: Hs00188166_m1), TaqMan Fast Universal PCR Master Mix (2X) (4352042, Applied Biosystems) and RNase-free water. To measure the TRPV4 mRNA expression of the CRISPR-Cas9 transduced cells, primers (hu TRPV4-652-F: CATCTACGGGGAAGACCTGC; hu TRPV4-768-R: TGAACTCCCTCATGTTGCCG; hu ANXA5-633-F: CCTTCAGGCTAACAGAGACCC; hu ANXA5-728-R: CCCCATTTAAGTTCTCCAGCC) were mixed with 10 ng cDNA, Power SYBR Green Master Mix (2X) (4368577, Applied Biosystems) and RNase-free water in a total volume of 20 µL. The CFX96 Touch Detection System (Bio-Rad) was used to measure the gene expression in duplicates. SDHA (or ANXA5) was used as a reference gene. Results are shown as $2^{-\Delta\Delta Ct}$ values (i.e., relative to SDHA (or ANXA5) and the control condition).

ELISA of Conditioned Medium

ELISA kits were used to quantify the levels of IL6, IL8 (Human IL-6 ELISA set, 555220; Human IL-8 ELISA set, 555244; Reagent set B, 550534, BD OptEIA, BD Biosciences) and PGE2 (RD-PGE2-Ge, Reddot Biotech) in the conditioned medium according to the manufacturer's instructions. The samples used were undiluted.

Western Blot

The cells were rinsed with cold PBS 1X and lysed on ice with 100 µL per chamber of radioimmunoprecipitation assay (RIPA) buffer supplemented with phosphatase and protease inhibitor cocktails (89900, 78428, 78430, Thermo Fisher Scientific) using a cell scraper. The lysates were mixed with 4X Laemmli buffer (1610747, Bio-Rad), heated for 5 min at 95 °C, and loaded onto a 4–20% gradient gel (4568093, Bio-Rad). The proteins were separated by electrophoresis in a Mini-PROTEAN Tetra Cell (Bio-Rad) and transferred to a PVDF membrane (1704156, Bio-Rad). The membranes were washed for 3 × 10 min with Tris buffered saline with 0.05% TWEEN 20 (TBS-T) and blocked for 2 h at room temperature (RT) with 5% skim milk diluted in TBS-T. Primary antibodies (ERK1/2 (ERK): 9102; p-ERK: 9101; p38: 9212; p-p38: 9211; JNK: 9252; p-JNK: 9251; α-tubulin: 2144; Cell Signaling Technology) were applied 1:1000 in 3% bovine serum albumin (BSA) in TBS-T overnight at 4 °C on a rocker. The next day, the membranes were washed for 3 × 10 min with TBS-T and incubated for 1 h at RT on a rocker with the secondary antibody (anti-rabbit IgG HRP: 7074, Cell Signaling Technology) diluted 1:3000 in 5% skim milk in TBS-T. After washing for 3 × 10 min with TBS-T, the proteins were detected with a chemiluminescence substrate (34580, Thermo Fisher Scientific) on a ChemiDocTouch Imaging System (Bio-Rad). The density of the bands was semi-quantified using the ImageLab 6.0 software (Bio-Rad). For each blot, the density of each band was normalized by the one of the non-stretched control (or the stretched 0 nM condition for

JNK and p-JNK, since there were no p-JNK bands for the non-stretched control). Phosphorylated targets were expressed as relative to total targets.

Immunocytochemistry

Two-well chambered coverglasses (155380, Thermo Fisher Scientific) were coated with 10 µg/mL fibronectin for 30 min at 37 °C. The CRISPR-Cas9 transduced cells (NT and KO) were seeded (60,000 cells/well) in growth medium and incubated for 24 h at 37 °C, 5% CO_2. The cells were washed with PBS 1X and fixed for 10 min with methanol at −20 °C. After washing with PBS, the cells were blocked with 5% normal goat serum (G9023, Sigma) in PBS for 1 h at RT. The primary antibody (rabbit polyclonal anti-TRPV4, ACC-034, Alomone Labs) was diluted 1:500 in 1% normal goat serum in PBS and applied overnight at 4 °C with rocking. For the no primary antibody control (negative control), 1% normal goat serum was applied on NT cells. The cells were washed extensively with PBS and incubated for 1 h at RT with the secondary antibody (Cy2 goat anti-rabbit IgG, 111-225-144, Jackson ImmunoResearch) diluted 1:200 in 1% normal goat serum in PBS. After washing with PBS, the samples were mounted with antifade mountant with 4′,6-diamidino-2-phenylindole (DAPI) (P36962, Thermo Fisher Scientific) and cured for 24 h at RT. The samples were imaged with an Olympus IX51 microscope and a 20× objective.

Statistical Analysis

The data were checked for consistency and for normality using skewness, kurtosis and omnibus tests. Due to the small sample sizes, the dependent bootstrap t-test based on 100,000 Monte Carlo samples were used. In addition, the classical dependent t-tests and nonparametric tests (Wilcoxon-Signed test) and the Quantile Sign test were used. All the reported tests were two-sided, and the *p*-values below 0.05 were considered statistically significant. All the statistical analyses were performed with NCSS (NCSS 10, NCSS, LLC. Kaysville, UT) and the PASW 24 (IBM SPSS Statistics for Windows, Version 21.0., Armonk, NY).

5.4 Results

Hyperphysiological Cyclic Stretching Induces Gene Expression of Pro-Inflammatory Mediators in Human AF Cells

In a first step, we analyzed the influence of increasing the duration of cyclic stretching on the gene expression of key mediators such as pro-inflammatory, catabolic and anabolic markers, as well as TRPV4 in human AF cells. A stretching frequency of 1 Hz was chosen to imitate the walking frequency, and a 20% strain was selected as a hyperphysiological magnitude [4]. The shortest duration of 1 h considerably increased the mRNA levels of interleukin 6 (IL6; 2.60-fold), interleukin 8 (IL8; 6.62-fold), cyclooxygenase 2 (COX2; 8.11-fold) and matrix metalloproteinase 1 (MMP1; 3.15-fold) compared to the non-stretched controls (**Figure 1A–D**). The gene expression of matrix metalloproteinase 3 (MMP3) slightly augmented (1.37-fold) after 1 h stretching, but this

change was not significant. Matrix metalloproteinase 13 (MMP13) was detected in only one donor out of three (not shown), and this gene was thus excluded from the statistical analysis. Interestingly, the increase in pro-inflammatory and catabolic mediators at 1 h was then generally dampened with increasing stretching durations (**Figure 1A–E**), suggesting a fast and acute response to mechanical loading. Regarding extracellular matrix genes, while the expression of collagen I (COL1A1) remained unchanged (**Figure 1F**), the collagen II (COL2A1) and aggrecan (ACAN) levels were decreased (0.54- and 0.74-fold, respectively) at a later time point of 2 h stretching compared to the control (**Figure 1G, H**). No significant changes were observed in the TRPV4 gene expression (**Figure 1I**). With the increased gene expression of IL6, IL8, COX2 and MMP1 at 1 h and the reduced expression of COL2A1 and ACAN at 2 h, we established a model of acute pro-inflammatory response to hyperphysiological stretching typical for early-stage AF injury [12].
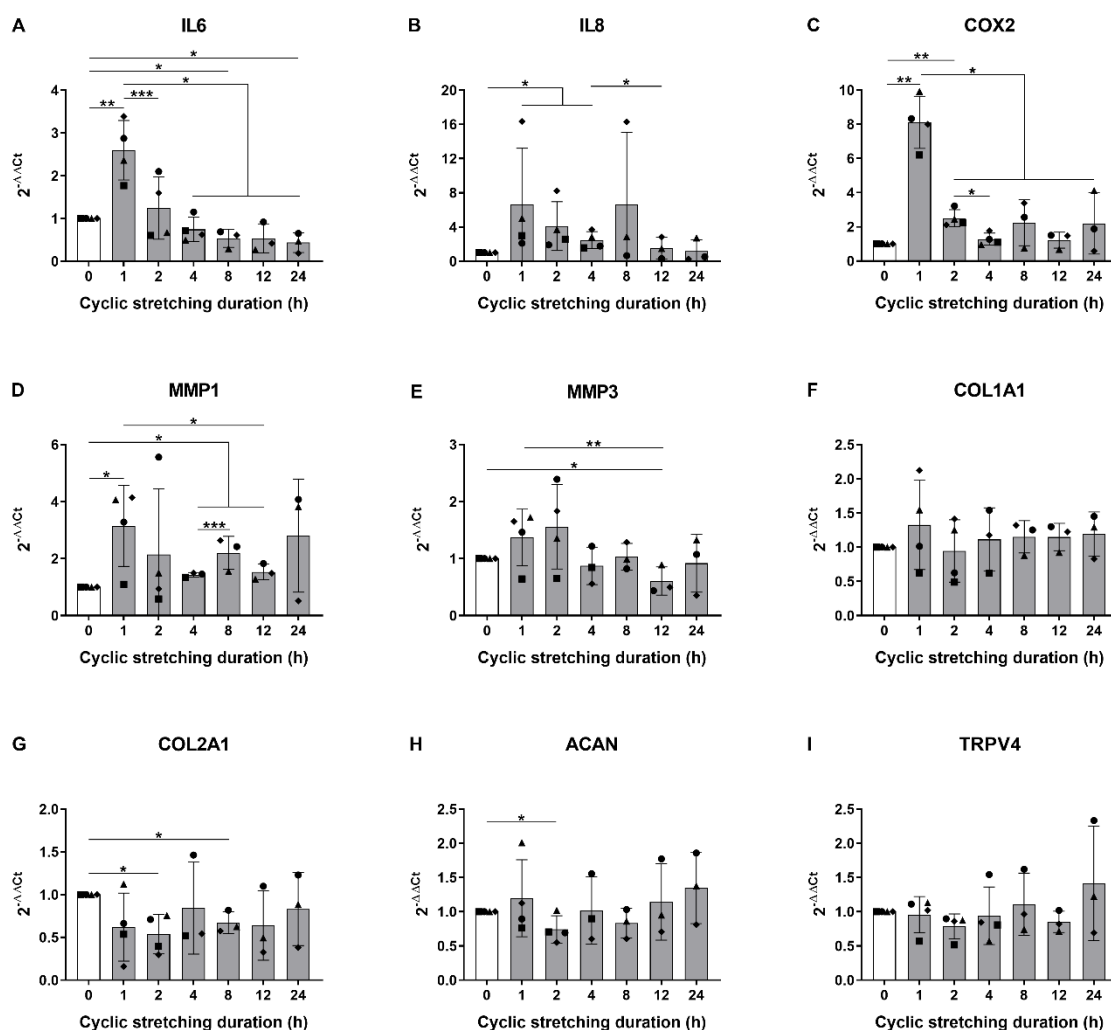
Figure 1. Gene expression of (**A–C**) pro-inflammatory mediators; (**D,E**) matrix metalloproteinases; (**F–H**) extracellular matrix; and (**I**) TRPV4 immediately after 0 (white bar) or from 1 to 24 h (grey bars) of cyclic stretching at 20% strain and 1 Hz. n = 3–4 donors; mean ± SD; * $p < 0.05$, ** $p < 0.01$, *** $p < 0.001$.

Pharmacological Inhibition of TRPV4 Reduces Stretch-Induced Gene Expression of Pro-Inflammatory Mediators

In order to investigate the potential role of the TRPV4 ion channel in the increased expression of IL6, IL8, COX2 and MMP1 induced by hyperphysiological stretching, we selected the stretching duration of 1 h, and further cyclically stretched AF cells in the absence or presence of the selective TRPV4 antagonist GSK2193874 (20 to 500 nM). The non-stretched experimental condition was kept as a benchmark, and the concentration of the vehicle (DMSO) was equalized in all conditions (0.005%). The control cells stretched without antagonist showed a slight augmentation in the TRPV4 mRNA compared to the non-stretched cells in this data set (**Figure 2A**). All the concentrations of GSK2193874 moderately reduced the gene expression of TRPV4 compared to the 0 nM control condition (**Figure 2A**). MMP1 gene expression was only slightly but significantly increased by 1 h stretching compared to the non-stretched cells (**Figure 2B**), but the TRPV4 modulation did not affect this change (**Figure 2B**). The expression of IL6, IL8 and COX2 was confirmed to be significantly increased by 1 h cyclic stretching compared to the non-stretched cells (**Figure 2C–E**). Remarkably, these stretch-induced changes were significantly mitigated by the TRPV4 pharmacological inhibition (at 20 and 100 to 500 nM of GSK2193874 for IL6 and COX2, and 500 nM for IL8; **Figure 2C–E**). These data suggest that TRPV4 partially mediates the stretch-induced gene expression of IL6, IL8 and COX2, but not MMP1.
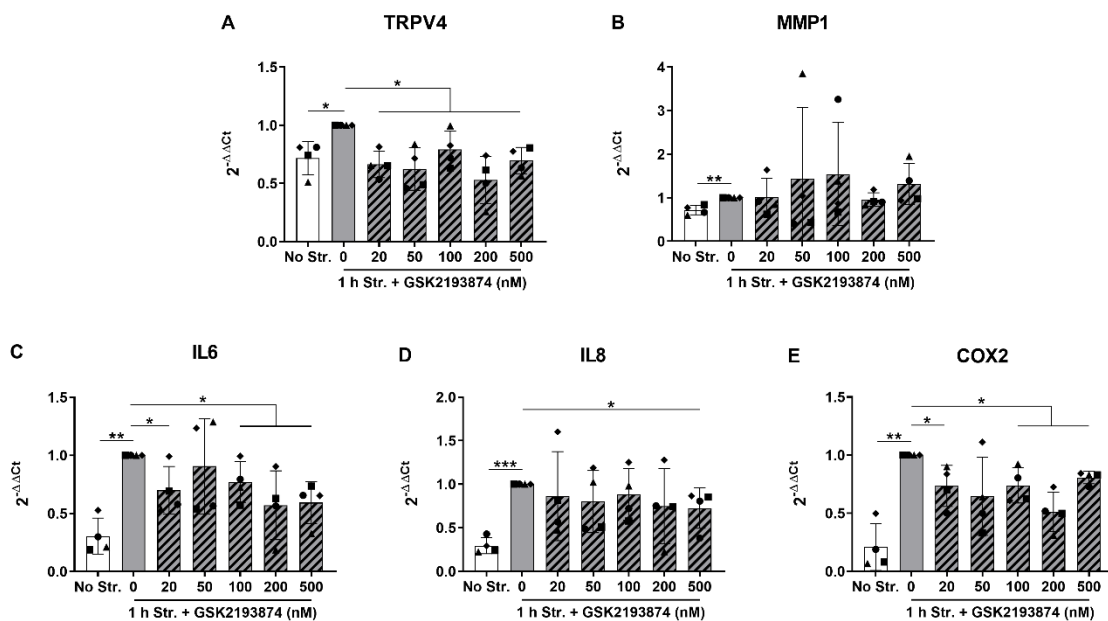
Figure 2. Gene expression of (**A**) TRPV4; (**B**), MMP1; and (**C–E**) pro-inflammatory mediators immediately after no (white bar) or 1 h (grey bars) of cyclic stretching at 20% strain and 1 Hz in the absence or presence (hatched bars) of 20–500 nM of the TRPV4 antagonist GSK2193874. n = 4 donors; mean ± SD; * $p < 0.05$, ** $p < 0.01$, *** $p < 0.001$.

Pharmacological Inhibition of TRPV4 Downregulates the Release of IL8 and PGE2

In a next step, the cells stretched for 1 h with or without GSK2193874, were further cultured for 24 h, in order to measure the release of the pro-inflammatory mediators IL6, IL8 and prostaglandin E2 (PGE2, a product of COX2). The concentrations of these mediators in the conditioned medium of non-stretched samples varied between donors: with a mean of 8.46 ± 11.90 (SD) pg/mL for IL6, 13.50 ± 9.67 pg/mL for IL8, and 9.49 ± 2.22 pg/mL for PGE2. Two donors out of four released concentrations of IL6 below the limit of detection of the assay. Surprisingly, no changes in the IL6 or IL8 release due to stretching were observed (**Figure 3A, B**). Nevertheless, the samples treated with 500 nM GSK2193874 during stretching exhibited a lower release of IL8 compared to the samples stretched in the absence of the antagonist (**Figure 3B**). The release of PGE2 slightly but significantly increased in the stretched samples compared to the controls, and was further attenuated by 100 and 200 nM of the TRPV4 inhibitor (**Figure 3C**). These data thus show that TRPV4 inhibition decreases IL8 release and stretch-induced PGE2 release.
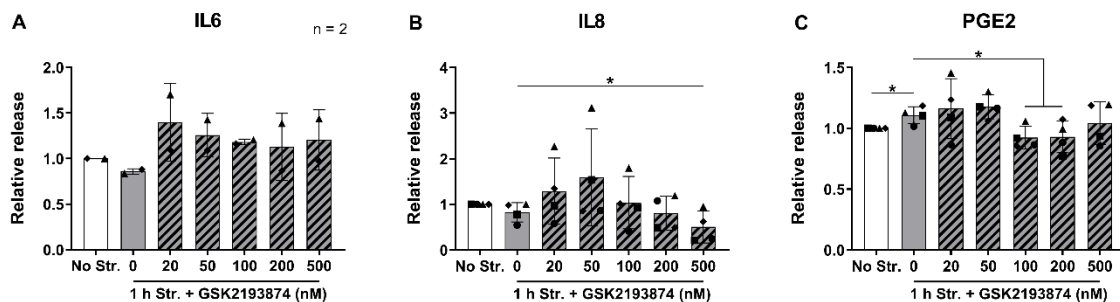
Figure 3. Relative release of (**A**) IL6; (**B**) IL8; and (**C**) PGE2 24 h after no (white bar) or 1 h (grey bars) of cyclic stretching at 20% strain and 1 Hz in the absence or presence (hatched bars) of 20–500 nM of the TRPV4 antagonist GSK2193874. $n = 4$ donors ($n = 2$ for IL6); mean ± SD; * $p < 0.05$, ** $p < 0.01$, *** $p < 0.001$.

Pharmacological Inhibition of TRPV4 Reduces Stretch-Induced p38 Phosphorylation

Cyclic stretching was previously shown to stimulate the gene expression of IL6, IL8 and COX2 via the phosphorylation of the extracellular signal-regulated kinases 1/2 (ERK), p38 and Jun-N-terminal kinase (JNK) in human AF cells [17]. In order to explore whether TRPV4 mediates the stretch-induced activation of MAPKs, we measured the expression of total and phosphorylated MAPKs after 15 min of stretching in the absence or presence of the TRPV4 antagonist. Non-stretched cells were added as a negative control, and the non-stretched cells treated with 10 ng/mL IL1β served as a positive control of the inflammatory response. Treatment with IL1β triggered a strong phosphorylation of ERK, p38 and JNK in all donors (**Figure 4A–C**). On the contrary, the bands for p-ERK and p-p38 were very faint (**Figure 4A, B**), and even absent for p-JNK (**Figure 4C**) in the non-stretched control samples. The expression of the total targets ERK, p38 and JNK remained similar across the conditions (**Figure 4**A–C). The samples cyclically stretched for 15 min without the TRPV4 antagonist displayed denser bands for all the phosphorylated MAPKs compared to non-stretched controls in all donors (**Figure 4A–C**). Upon the analysis of the

densitometry data, even though ERK showed an 8.49-fold increase in activation in stretched samples compared to the controls (**Figure 4D**), only the 2.60-fold upregulation of the p38 phosphorylation was statistically significant (**Figure 4E**). One donor out of three expressed phosphorylated JNK in the positive control, but not in the other experimental conditions, thus preventing statistical analysis (**Figure 4F**). Remarkably, stretch-induced p38 phosphorylation was reduced by 100 nM GSK2193874 (**Figure 4E**). Although the treatment with the TRPV4 antagonist often yielded dimmer bands compared to the 0 nM condition for p-ERK and p-JNK (**Figure 4A, C**), these differences were not significant (**Figure 4D, F**). These experiments show that hyperphysiological cyclic stretching induces the phosphorylation of p38, and this is partially mediated by TRPV4.
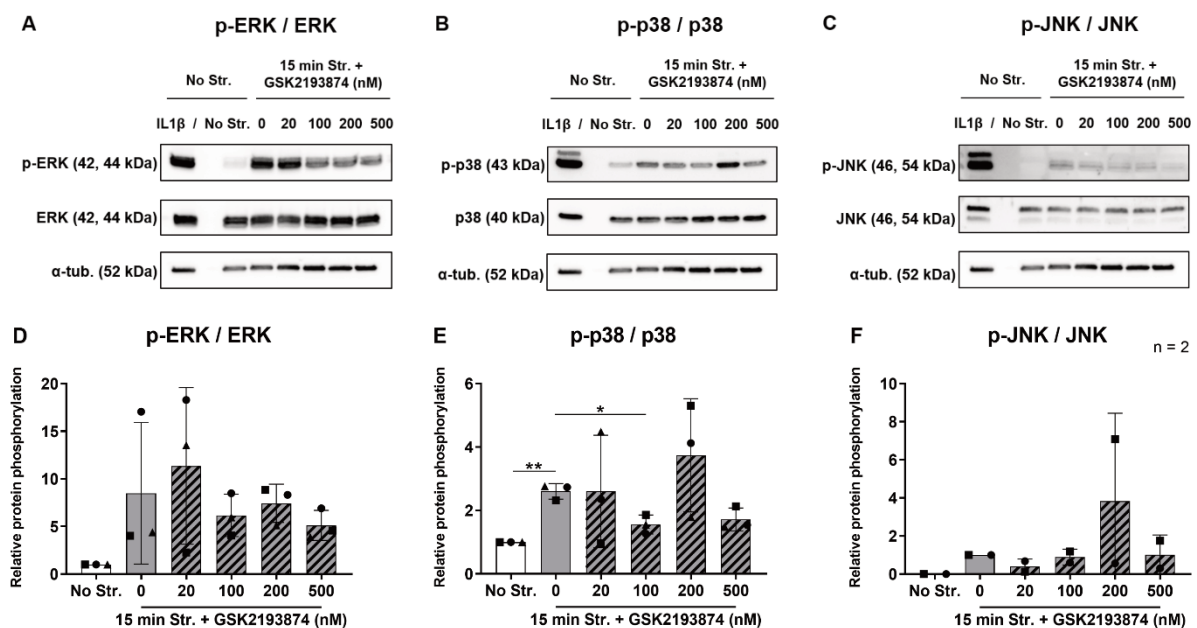
Figure 4. Representative Western blots from one donor (**A–C**) and densitometry analysis (**D–F**) of the phosphorylated and total (**A**, **D**) ERK 1/2; (**B**, **E**) p38; and (**C**, **F**) JNK immediately after no (white bar) or 15 min (grey bars) of cyclic stretching at 20% strain and 1 Hz in the absence or presence (hatched bars) of 20–500 nM of the TRPV4 antagonist GSK2193874. Non-stretched cells treated with IL1β were used as a positive control for the blots. One same blot of α-tubulin is shown three times as a loading control. $n = 3$ donors ($n = 2$ for p-JNK); mean ± SD; * $p < 0.05$, ** $p < 0.01$.

CRISPR-Cas9 Knocks Out TRPV4 in Human Primary AF Cells

In a second part of the study, CRISPR-Cas9 TRPV4 KO cells were generated to further investigate the role of TRPV4 in the stretching-mediated cellular response. Human AF cells were transduced with lentiviral particles containing either a non-targeting sgRNA (NT cells) or a sgRNA against TRPV4 (KO cells). The efficiency of the KOs was tested with RT-qPCR and immunocytochemistry. The gene expression of TRPV4 significantly dropped in the KO cells to 0.13-fold compared to the NT controls, thus revealing a KO efficiency of 87% (**Figure 5A**). While the NT cells stained without primary antibody showed virtually no signal of TRPV4 (**Figure S1**), the NT cells that followed the full immunostaining protocol mostly displayed a robust expression of the ion channel (**Figure 5B**). At the same time, the KO cells expressed TRPV4 at a very low level similar to the no primary antibody control

(**Figure 5C**). We thus show for the first time to our knowledge the gene editing of human AF cells via CRISPR-Cas9. The KO of TRPV4 was successful and confirmed both at the gene and protein levels.
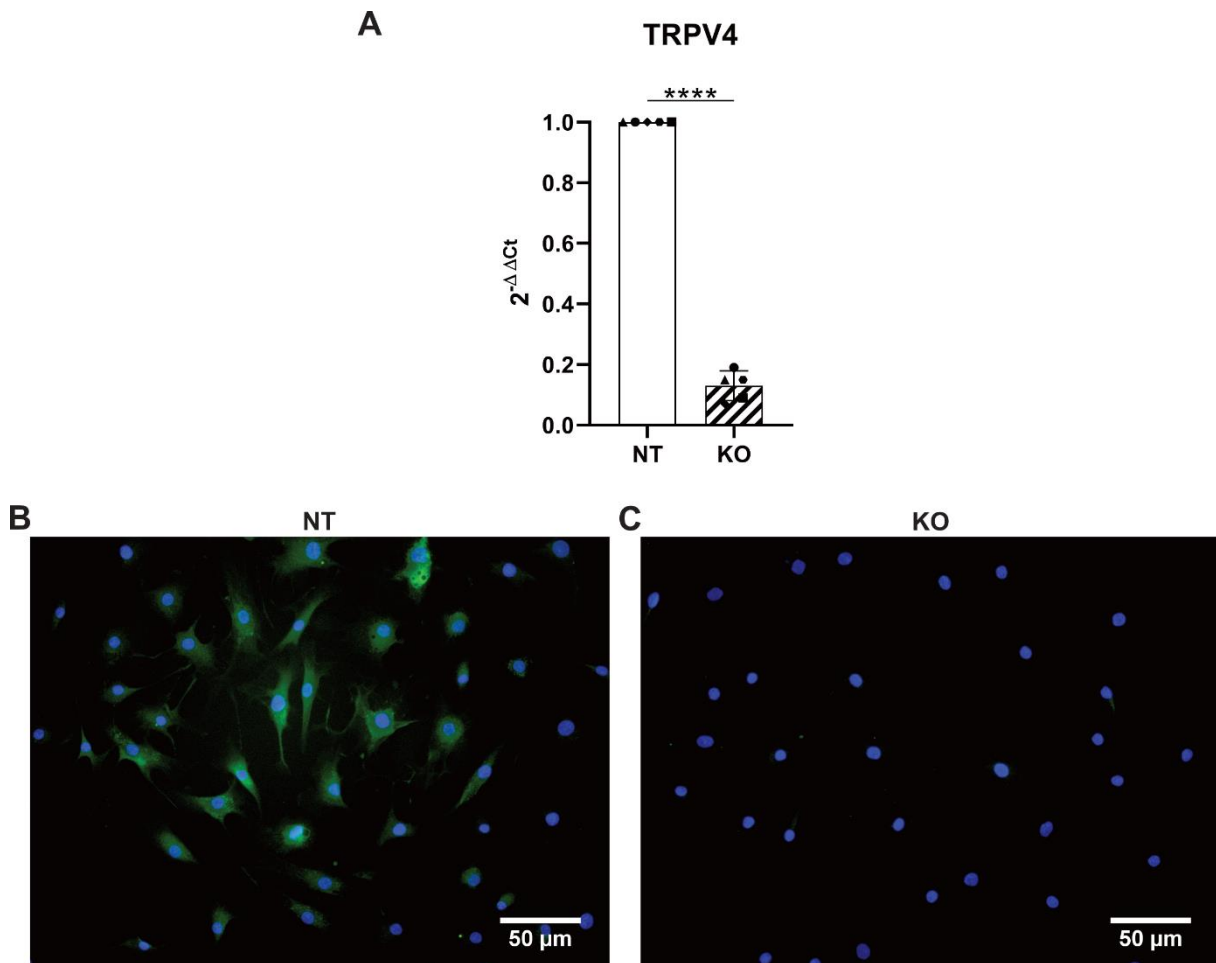
Figure 5. (**A**) Gene expression of TRPV4 in the CRISPR-Cas9-transduced non-targeting control (NT, white bar) and the TRPV4 knockout (KO, hatched bar) cells. n = 5 donors; mean ± SD; **** $p <$ 0.0001. Immunocytochemistry of (**B**) the NT and (**C**) the KO cells; green = TRPV4, blue = DAPI; scale bars = 50 μm.

CRISPR-Cas9 KO of TRPV4 Prevents Stretch-Induced Gene Expression of IL8

Similar to the TRPV4 inhibition experiments, the CRISPR-Cas9-transduced NT and TRPV4 KO cells were subjected to hyperphysiological cyclic stretching for 1 h and immediately lysed for gene expression analysis. The TRPV4 mRNA levels in the NT and KO cells were not affected by mechanical loading (**Figure 6A**). While the MMP1 gene expression was once again significantly augmented (1.52-fold) by stretching compared to the non-stretched controls in the NT cells, this change was not observed in the TRPV4 KO cells (**Figure 6B**). However, TRPV4 KO non-stretched cells showed variable and relatively high levels of MMP1 (**Figure 6B**). As expected, IL6 and IL8 gene expression was significantly upregulated (1.78- and 2.99-fold, respectively) by stretching in NT cells (**Figure 6C, D**). Although IL6 mRNA levels varied among donors in TRPV4 KO non-stretched cells, these were either reduced or remained constant upon stretching (**Figure**

6C). The decrease in IL6 in TRPV4 KO stretched cells compared to NT stretched cells was nonetheless not statistically significant (**Figure 6C**). The stretch-induced upregulation of the IL8 gene expression was completely prevented in TRPV4 KO cells (**Figure 6D**). Surprisingly, the gene expression of COX2 was not significantly altered by stretching in NT cells, and no changes were observed in TRPV4 KO cells (**Figure 6E**). These data support the findings obtained with the TRPV4 inhibition, in that TRPV4 KO prevented the stretch-induced upregulation of IL8 mRNA and tended to reduce the stretch-induced IL6 mRNA.
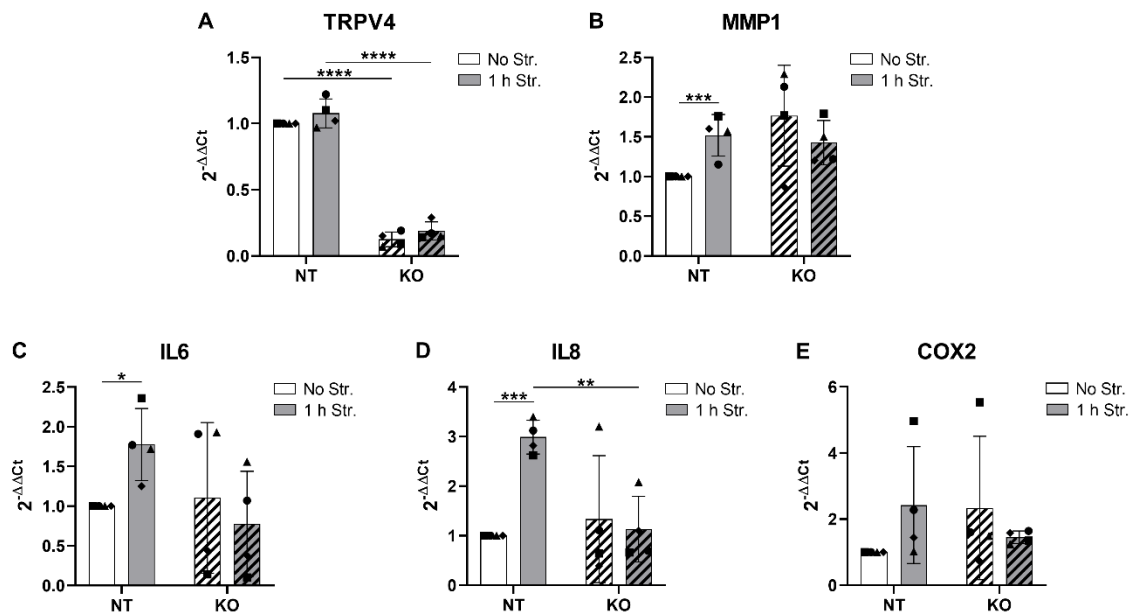
Figure 6. Gene expression of (**A**) TRPV4; (**B**) MMP1; and (**C–E**) pro-inflammatory mediators in the CRISPR-Cas9-transduced non-targeting control (NT, non-hatched bars) and the TRPV4 knockout (KO, hatched bars) cells, immediately after no (white bars) or 1 h (grey bars) of cyclic stretching at 20% strain and 1 Hz. $n = 4$ donors; mean ± SD; * $p < 0.05$, ** $p < 0.01$, *** $p < 0.001$, **** $p < 0.0001$.

CRISPR-Cas9 KO of TRPV4 Downregulates the Release of IL6 and IL8

In a final step, we analyzed the release of IL6, IL8 and PGE2 in the conditioned medium of the NT and TRPV4 KO cells that were cyclically stretched for 1 h and cultured for 24 h. The basal concentrations of IL6, IL8 and PGE2 in the NT non-stretched cells varied between donors: 146.3 ± 145.7 pg/mL, 170.9 ± 160.8 pg/mL, and 12.80 ± 8.01 pg/mL, respectively. One donor out of five released concentrations of IL6 below the limit of detection of the assay. Similar to the TRPV4 inhibition experiment, the stretch-induced upregulation of the IL6 and IL8 genes in NT cells did not result in an increase in IL6 and IL8 release in the conditioned medium (**Figure 7A, B**). Nevertheless, the release of IL6 was significantly lower in the KO stretched cells compared to the NT stretched cells (**Figure 7A**). This effect was not observed for IL8, but the KO non-stretched cells released less IL8 compared to their NT counterparts (**Figure 7B**). No significant changes were observed in the PGE2 release across conditions (**Figure 7C**). These data support the link between TRPV4 and IL8 release, and suggest a role of TRPV4 in mediating IL6 release.
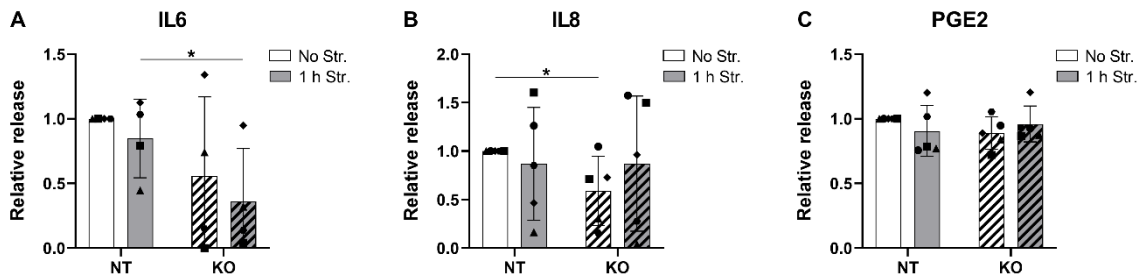
Figure 7. Relative release of (**A**) IL6; (**B**) IL8; and (**C**) PGE2 in the CRISPR-Cas9-transduced non-targeting control (NT, non-hatched bars) and the TRPV4 knockout (KO, hatched bars) cells 24 h after no (white bars) or 1 h (grey bars) of cyclic stretching at 20% strain and 1 Hz. $n = 4$–5 donors; mean ± SD; * $p < 0.05$.

5.5 Discussion

Treating diseases in load-bearing tissues often requires an extensive knowledge of the interaction between the mechanical and inflammatory signals, a concept recently coined as "mechanoflammation" [32]. Understanding the mechanosensing and mechanotransductive pathways at the origin of DDD and LBP would contribute to finding targeted treatments and thus, lightening the immense burden carried by society and the health economy.

In this study, we report novel evidence that mechanoinflammatory responses induced by hyperphysiological stretching are significantly mitigated by TRPV4 inhibition. We also show for the first time, the successful gene editing of human herniated and degenerated AF cells (Pfirrmann grade 2 to 4) via CRISPR-Cas9 for the purpose of knocking out the TRPV4 gene and investigating its role. While the CRISPR-based technology allowed us to confirm the role of TRPV4 in regulating IL6 and IL8, it could be used in future studies to modulate other molecular targets involved in IVD pathologies [33].

Our model exhibits features of stretch-induced low-grade mechanoflammation, representative of early-stage AF injury [12]. In agreement with previous studies [13,14,15,16,17], the hyperphysiological cyclic stretching of AF cells induced an increase in gene expression of IL6, IL8, COX2 and MMP1. This pro-inflammatory response was transient and decreased with increasing stretching durations. Interestingly, Pratsinis and colleagues have similarly reported a bell-shaped expression of pro-inflammatory genes with increasing stretching durations in AF cells [17]. This is compatible with a single continuous loading event, rather than a repetitive loading regime. The reduction of COL2A1 and ACAN mRNA in response to cyclic stretching, also previously reported by another study [13], confirms the degenerative purpose of our hyperphysiological stretching regime. The moderate but significant increase in PGE2 release caused by hyperphysiological cyclic stretching further confirms the COX2 gene expression increase. The lack of augmentation of IL6 and IL8 release in response to stretching could be due to the existence of other rate limiting steps in the involved pathways, or unknown feedback

mechanisms that prevented the translation of the stretch-upregulated IL6 and IL8 mRNAs. In fact, RNA-binding proteins can bind to the adenylate-uridylate (AU)-rich elements in the 3′-untranslated regions of the inflammatory mediators' mRNAs in order to destabilize them, or induce translational silencing to resolve acute inflammation [34,35]. Our finding that hyperphysiological cyclic stretching significantly increased the phosphorylation of p38 is in agreement with the study of Pratsinis et al. [17]. However, in contrast to this report, the activation of ERK and JNK was not statistically significant. With the increased gene expression of IL6, IL8, COX2 and MMP1, the reduced gene expression of COL2A1 and ACAN, the increased PGE2 release and the activation of p38, we established a model of acute pro-inflammatory response to hyperphysiological stretching.

The novel finding that TRPV4 inhibition significantly reduces the stretch-induced gene expression of IL6, IL8 and COX2, but not MMP1, proposes a role of TRPV4 in mediating, at least in part, mechanoflammation in AF cells. It is to be noted that the link between TRPV4 and these pro-inflammatory mediators finds an echo in studies with other organs and tissues. The stretch-induced release of IL6 by mouse lung epithelia cells was modulated by TRPV4 inhibition [36]. In human epidermal keratinocytes, TRPV4 blocking reduced IL6 and IL8 production caused by gamma irradiation [37]. Additionally, the stretch-induced upregulation of COX2 expression was decreased by treatment with a TRPV4 antagonist in human periodontal ligament cells [38]. The reduction of stretch-induced PGE2 release in the presence of the TRPV4 antagonist further confirms the reduction in COX2 gene expression. Moreover, these results are in agreement with a study reporting that the increase in PGE2 release, upon hypo-osmotic stress in porcine chondrocytes, is TRPV4 dependent [39]. Interestingly, stretch-induced p38 phosphorylation was also significantly attenuated by the treatment with the TRPV4 inhibitor. While this finding is new in AF cells, it is corroborated by other studies highlighting the role of p38 in TRPV4-mediated (mechanically induced) inflammation or pain in other organs [36,37,40]. Since we did not analyze the expression of inflammatory mediators in non-stretched cells treated with GSK2193874, it is not possible to know whether their decrease already occurs without stretching. Despite using different concentrations of the TRPV4 antagonist in inhibition experiments, it was not clear whether the observed responses were dose dependent. We attribute this to the moderate effects and variability between different human donors.

In a second part of the study, we conducted experiments with CRISPR-Cas9 TRPV4 KO cells. Although two other research groups have previously reported the gene editing of human nucleus pulposus cells via CRISPR [41,42], we are the first, to our knowledge, to successfully implement CRISPR-Cas9 gene editing in human-degenerated AF cells. TRPV4 KO completely reversed the stretch-induced upregulation of the IL8 gene expression, thus confirming the role of TRPV4 in the mechanoregulation of IL8. TRPV4 KO further tended to reduce the stretch-induced increase in IL6 mRNA, in agreement with the TRPV4 inhibition data. Surprisingly, hyperphysiological cyclic stretching did not upregulate COX2 mRNA and PGE2 release in transduced NT cells. In addition, the basal concentrations of pro-inflammatory mediators were higher in the transduced cells compared to the naive cells, thus suggesting that the used transduction protocol might provoke cellular stress. The fact that TRPV4 KO stretched cells released significantly less IL6 compared to the NT stretched cells strengthens the hypothesis that TRPV4 regulates

IL6 during mechanical loading. Interestingly, TRPV4 KO non-stretched cells also released less IL8 compared to NT non-stretched cells, highlighting again a link between TRPV4 and IL8.

Although in vitro models are well suited to explore molecular and cellular mechanisms, our findings need to be confirmed at the IVD organ scale and in vivo. Many preclinical studies using TRPV4 inhibitors as a treatment for diverse diseases have already been conducted [40,43,44,45]. Recently, the TRPV4 antagonist GSK2798745 was administered to healthy volunteers and heart failure patients without any safety concern [46]. Preclinical and clinical studies investigating TRPV4 inhibition in the context of DDD and LBP are currently lacking. If the mechanoinflammatory role of TRPV4 is further confirmed in vivo, TRPV4 may become a therapeutic target for novel treatments of LBP. This novel type of "mechanomedicine" may benefit patients with IVD pathologies caused by aberrant mechanical loading and hyperphysiological stretching. Mechanical stressors such as impact, heavy lifting, muscle activations, and work/lifestyle factors (e.g., vibration exposure, gait, and posture) [47] are associated with IVD degeneration or injury [2]. In particular, AF disruption is commonly linked to LBP and disability [12]. The healing process following AF injury includes inflammation, the recruitment of immune cells, cell proliferation, the formation of granulation tissue and matrix remodeling [12]. However, if initial inflammation is not resolved, it can become chronic and cause degeneration and pain [12]. The pro-inflammatory mediators investigated in this study downstream of TRPV4 have previously shown to be clinically relevant. Human subjects with LBP were found to display significantly higher levels of IL6 in serum compared to control subjects [48]. Moreover, higher serum levels of IL6 and IL8 mRNA and protein were found in patients with more severe LBP [49,50]. Cytokines can further induce COX2 expression and the subsequent synthesis of PGE2 [51]. Higher levels of COX2 and PGE2 have been found in herniated discs compared to controls [52,53]. Finally, MAPKs are important stress and inflammation regulators in the IVD, and p38 was shown to control the expression of IL6, IL8 and COX2, among other mediators [54]. Currently, p38 inhibitors are being investigated to treat inflammation-related diseases [54]. The mechanisms of action of the current anti-inflammatory treatments of LBP remain unclear [10]. By targeting a specific mechanosensitive marker such as TRPV4, it might be possible to specifically address mechanoflammation and increase effect sizes. Due to its polymodal nature, a targeted and localized silencing of TRPV4 in the AF, e.g., via gene editing, might be desirable in the future. The lentiviruses used in this study randomly integrate in the genome, but they could be replaced in clinical applications by adeno-associated viruses, which integrate into safe harbor regions [55].

5.6 Conclusions

"Mechanoflammation" caused by hyperphysiological cyclic stretching was mitigated by TRPV4 inhibition with the specific GSK2193874 antagonist, thus revealing the novel mechanoinflammatory role of TRPV4 in human primary AF cells. In fact, the stretch-induced upregulation of IL6, IL8 and COX2 gene expression, PGE2 release and p38 phosphorylation were significantly reduced by TRPV4 inhibition. We further report the

use of CRISPR-Cas9 technology to successfully knock out TRPV4 in human AF cells. Remarkably, increases in IL8 mRNA levels caused by hyperphysiological cyclic stretching were completely prevented by TRPV4 KO. TRPV4 KO further reduced the release of IL6 and IL8. Our results thus suggest that TRPV4 mediates stretch-induced inflammation possibly via the activation of the p38 MAPK pathway. Future pharmacological or gene-editing therapies to treat DDD and LBP might thus target TRPV4 or the molecular mediators interacting with it in the signaling pathway.

Author Contributions

E.C. conceived the project, designed and conducted the experiments, analyzed the data and wrote the manuscript. M.J.E.A. designed the sgRNAs, produced the lentiviral particles and transduced part of the human AF cells. S.W. conducted part of the TRPV4 inhibition experiments. O.K. supervised the project. W.H. performed the statistical analysis. F.S.P. helped in establishing and optimizing cell transduction protocols. O.N.H. provided the human AF biopsies. J.G.S., S.J.F. and K.W.-K. provided funding and supervised the project. All authors have read and agreed to the published version of the manuscript.

5.7 References

1. Ingber, D.E. Mechanobiology and diseases of mechanotransduction. *Ann. Med.* **2003**, *35*, 564–577.

2. Bao, S. Mechanical stress. In *The Handbook of Clinical Neurology*; Elsevier: Amsterdam, The Netherlands, 2015; Volume 131, pp. 367–396.

3. Guo, X.E.; Hung, C.T.; Sandell, L.J.; Silva, M.J. Musculoskeletal mechanobiology: A new era for MechanoMedicine. *J. Orthop. Res.* **2018**, *36*, 531–532.

4. Fearing, B.V.; Hernandez, P.A.; Setton, L.A.; Chahine, N. Mechanotransduction and cell biomechanics of the intervertebral disc. *JOR Spine* **2018**, *1*, e1026.

5. Chan, S.C.W.; Ferguson, S.J.; Gantenbein-Ritter, B. The effects of dynamic loading on the intervertebral disc. *Eur. Spine J.* **2011**, *20*, 1796–1812

6. Adams, M.A.; Roughley, P.J. What is intervertebral disc degeneration, and what causes it? *Spine* **2006**, *31*, 2151–2161.

7. Vergroesen, P.-P.; Kingma, I.; Emanuel, K.; Hoogendoorn, R.; Welting, T.; Van Royen, B.J.; Van Dieën, J.H.; Smit, T.H. Mechanics and biology in intervertebral disc degeneration: A vicious circle. *Osteoarthr. Cart.* **2015**, *23*, 1057–1070.

8. Likhitpanichkul, M.; Torre, O.M.; Gruen, J.; Walter, B.A.; Hecht, A.C.; Iatridis, J.C. Do mechanical strain and TNF-alpha interact to amplify pro-inflammatory cytokine production in human annulus fibrosus cells? *J. Biomech.* **2016**, *49*, 1214–1220.

9. Tisherman, R.; Coelho, P.; Phillibert, D.; Wang, D.; Dong, Q.; Vo, N.; Kang, J.; Sowa, J. NF-kappaB signaling pathway in controlling intervertebral disk cell response to inflammatory and mechanical stressors. *Phys. Ther.* **2016**, *96*, 704–711.

10. Balagué, F.; Mannion, A.F.; Pellise, F.; Cedraschi, C. Non-specific low back pain. *Lancet* **2012**, *379*, 482–491

11. Airaksinen, O.; Brox, J.I.; Cedraschi, C.; Hildebrandt, J.; Klaber-Moffett, J.; Kovacs, F.; Mannion, A.F.; Reis, S.; Staal, J.B.; Ursin, H.; et al. Chapter 4. European guidelines for the management of chronic nonspecific low back pain. *Eur. Spine J.* **2006**, *15*, S192–S300.

12. Torre, O.M.; Mroz, V.; Bartelstein, M.K.; Huang, A.H.; Iatridis, J.C. Annulus fibrosus cell phenotypes in homeostasis and injury: Implications for regenerative strategies. *Ann. N. Y. Acad. Sci.* **2019**, *1442*, 61–78.

13. Shengjie, W.; Li, J.; Tian, J.; Yu, Z.; Gao, K.; Shao, J.; Li, A.; Xing, S.; Dong, Y.; Li, Z. High amplitude and low frequency cyclic mechanical strain promotes degeneration of human nucleus pulposus cells via the NF-κB p65 pathway. *J. Cell. Physiol.* **2018**, *233*, 7206–7216.

14. Sowa, G.; Coelho, P.; Vo, N.; Bedison, R.; Chiao, A.; Davies, C.; Studer, R.; Kang, J. Determination of annulus fibrosus cell response to tensile strain as a function of duration, magnitude, and frequency. *J. Orthop. Res.* **2011**, *29*, 1275–1283.

15. Miyamoto, H.; Doita, M.; Nishida, K.; Yamamoto, T.; Sumi, M.; Kurosaka, M. Effects of cyclic mechanical stress on the production of inflammatory agents by nucleus pulposus and anulus fibrosus derived cells in vitro. *Spine* **2006**, *31*, 4–9.

16. Gawri, R.; Rosenzweig, D.H.; Krock, E.; A Ouellet, J.; Stone, L.S.; Quinn, T.M.; Haglund, L. High mechanical strain of primary intervertebral disc cells promotes secretion of inflammatory factors associated with disc degeneration and pain. *Arthritis Res. Ther.* **2014**, *16*, R21.

17. Pratsinis, H.; Papadopoulou, A.; Neidlinger-Wilke, C.; Brayda-Bruno, M.; Wilke, H.-J.; Kletsas, D.; Information, P.E.K.F.C. Cyclic tensile stress of human annulus fibrosus cells induces MAPK activation: Involvement in proinflammatory gene expression. *Osteoarthr. Cartil.* **2016**, *24*, 679–687.

18. Moran, M.M.; McAlexander, M.A.; Bíró, T.; Szallasi, A. Transient receptor potential channels as therapeutic targets. *Nat. Rev. Drug Discov.* **2011**, *10*, 601–620.

19. Krupkova, O.; Zvick, J.; Wuertz-Kozak, K. The role of transient receptor potential channels in joint diseases. *Eur. Cells Mater.* **2017**, *34*, 180–201.

20. McNulty, A.L.; Leddy, H.A.; Liedtke, W.B.; Guilak, F. TRPV4 as a therapeutic target for joint diseases. *Naunyn-Schmiedeberg's Arch. Pharmacol.* **2015**, *388*, 437–450.

21. O'Conor, C.J.; Leddy, H.A.; Benefield, H.C.; Liedtke, W.B.; Guilak, F. TRPV4-mediated mechanotransduction regulates the metabolic response of chondrocytes to dynamic loading. *Proc. Natl. Acad. Sci. USA* **2014**, *111*, 1316–1321.

22. O'Conor, C.J.; Ramalingam, S.; Zelenski, N.A.; Benefield, H.C.; Rigo, I.; Little, D.; Wu, C.-L.; Chen, D.; Liedtke, W.; McNulty, A.L.; et al. Cartilage-specific knockout of the mechanosensory ion channel TRPV4 decreases age-related osteoarthritis. *Sci. Rep.* **2016**, *6*, 29053.

23. Walter, B.; Purmessur, D.; Moon, A.; Occhiogrosso, J.; Laudier, D.; Hecht, A.; Iatridis, J. Reduced tissue osmolarity increases TRPV4 expression and pro-inflammatory cytokines in intervertebral disc cells. *Eur. Cell Mater.* **2016**, *32*, 123–136.

24. Franco-Obregon, A.; Cambria, E.; Greutert, H.; Wernas, T.; Hitzl, W.; Egli, M.; Sekiguchi, M.; Boos, N.; Hausmann, O.; Ferguson, S.J.; et al. TRPC6 in simulated microgravity of intervertebral disc cells. *Eur. Spine J.* **2018**, *27*, 2621–2630.

25. Sadowska, A.; Touli, E.; Hitzl, W.; Greutert, H.; Ferguson, S.J.; Wuertz-Kozak, K.; Hausmann, O. Inflammaging in cervical and lumbar degenerated intervertebral discs: Analysis of proinflammatory cytokine and TRP channel expression. *Eur. Spine J.* **2018**, *27*, 564–577.

26. Sadowska, A.; Hitzl, W.; Karol, A.; Jaszczuk, P.; Cherif, H.; Haglund, L.; Hausmann, O.N.; Wuertz, K. Differential regulation of TRP channel gene and protein expression by intervertebral disc degeneration and back pain. *Sci. Rep.* **2019**, *9*, 18889.

27. Kameda, T.; Zvick, J.; Vuk, M.; Sadowska, A.; Tam, W.K.; Leung, V.Y.-L.; Bölcskei, K.; Helyes, Z.; Applegate, L.A.; Hausmann, O.; et al. Expression and activity of TRPA1 and TRPV1 in the intervertebral disc: Association with inflammation and matrix remodeling. *Int. J. Mol. Sci.* **2019**, *20*, 1767.

28. Naito, Y.; Hino, K.; Bono, H.; Ui-Tei, K. CRISPRdirect: Software for designing CRISPR/Cas guide RNA with reduced off-target sites. *Bioinformatics* **2015**, *31*, 1120–1123.

29. Morgens, D.W.; Wainberg, M.; Boyle, E.; Ursu, O.; Araya, C.L.; Tsui, C.K.; Haney, M.S.; Hess, G.T.; Han, K.; Jeng, E.; et al. Genome-scale measurement of off-target activity using Cas9 toxicity in high-throughput screens. *Nat. Commun.* **2017**, *8*, 15178.

30. Sanjana, N.E.; Shalem, O.; Zhang, F. Improved vectors and genome-wide libraries for CRISPR screening. *Nat. Methods* **2014**, *11*, 783–784.

31. Stewart, S.A.; Dykxhoorn, D.M.; Palliser, D.; Mizuno, H.; Yu, E.Y.; An, N.S.; Sabatini, D.M.; Chen, I.S.; Hahn, W.C.; Sharp, P.A.; et al. Lentivirus-delivered stable gene silencing by RNAi in primary cells. *RNA* **2003**, *9*, 493–501.

32. Vincent, T.L. Mechanoflammation in osteoarthritis pathogenesis. *Semin. Arthritis Rheum.* **2019**, *49*, S36–S38.

33. Krupkova, O.; Cambria, E.; Besse, L.; Besse, A.; Bowles, R.; Wuertz-Kozak, K. The potential of CRISPR/Cas9 genome editing for the study and treatment of intervertebral disc pathologies. *JOR Spine* **2018**, *1*, e1003.

34. Stumpo, D.J.; Lai, W.S.; Blackshear, P.J. Inflammation: Cytokines and RNA-based regulation. *Wiley Interdiscip. Rev. RNA* **2010**, *1*, 60–80.

35. Mazumder, B.; Li, X.; Barik, S. Translation control: A multifaceted regulator of inflammatory response. *J. Immunol.* **2010**, *184*, 3311–3319.

36. Nayak, P.S.; Wang, Y.; Najrana, T.; Priolo, L.M.; Rios, M.; Shaw, S.K.; Sanchez-Esteban, J. Mechanotransduction via TRPV4 regulates inflammation and differentiation in fetal mouse distal lung epithelial cells. *Respir. Res.* **2015**, *16*, 60.

37. Ohsaki, A.; Tanuma, S.I.; Tsukimoto, M. TRPV4 channel-regulated ATP release contributes to gamma-irradiation-induced production of IL-6 and IL-8 in epidermal keratinocytes. *Biol. Pharm. Bull.* **2018**, *41*, 1620–1626.

38. Shen, Y.; Pan, Y.; Guo, S.; Sun, L.; Zhang, C.; Wang, L. The roles of mechanosensitive ion channels and associated downstream MAPK signaling pathways in PDLC mechanotransduction. *Mol. Med. Rep.* **2020**, *21*, 2113–2122.

39. Phan, M.N.; Leddy, H.A.; Votta, B.J.; Kumar, S.; Levy, D.S.; Lipshutz, D.B.; Lee, S.H.; Liedtke, W.; Guilak, F. Functional characterization of TRPV4 as an osmotically sensitive ion channel in porcine articular chondrocytes. *Arthritis Rheum.* **2009**, *60*, 3028–3037.

40. Qu, Y.-J.; Zhang, X.; Fan, Z.-Z.; Huai, J.; Teng, Y.-B.; Zhang, Y.; Yue, S.-W. Effect of TRPV4-p38 MAPK pathway on neuropathic pain in rats with chronic compression of the dorsal root ganglion. *BioMed Res. Int.* **2016**, *2016*, 6978923.

41. Pizzute, T.; He, F.; Zhang, X.; Pei, M. Impact of Wnt signals on human intervertebral disc cell regeneration. *J. Orthop. Res.* **2018**, *36*, 3196–3207.

42. Farhang, N.; Ginley-Hidinger, M.; Berrett, K.C.; Gertz, J.; Lawrence, B.; Bowles, R.D.; Bowles, R.D. Lentiviral CRISPR epigenome editing of inflammatory receptors as a gene therapy strategy for disc degeneration. *Hum. Gene Ther.* **2019**, *30*, 1161–1175.

43. Thorneloe, K.S.; Cheung, M.; Bao, W.; Alsaid, H.; Lenhard, S.; Jian, M.-Y.; Costell, M.; Maniscalco-Hauk, K.; Krawiec, J.A.; Olzinski, A.; et al. An orally active TRPV4 channel blocker prevents and resolves pulmonary edema induced by heart failure. *Sci. Transl. Med.* **2012**, *4*, 159ra148.

44. Dong, Q.; Li, J.; Wu, Q.; Zhao, N.; Qian, C.; Ding, D.; Wang, B.-B.; Chen, L.; Guo, K.-F.; Fu, D.; et al. Blockage of transient receptor potential vanilloid 4 alleviates myocardial ischemia/reperfusion injury in mice. *Sci. Rep.* **2017**, *7*, 42678.

45. Michalick, L.; Erfinanda, L.; Weichelt, U.; Van Der Giet, M.; Liedtke, W.; Kuebler, W.M. Transient receptor potential vanilloid 4 and serum glucocorticoid-regulated kinase 1 are critical mediators of lung injury in overventilated mice in vivo. *Anesthesiology* **2017**, *126*, 300–311.

46. Goyal, N.; Skrdla, P.; Schroyer, R.; Kumar, S.; Fernando, D.; Oughton, A.; Norton, N.; Sprecher, D.L.; Cheriyan, J. Clinical pharmacokinetics, safety, and tolerability of a novel, first-in-class TRPV4 ion channel inhibitor, GSK2798745, in healthy and heart failure subjects. *Am. J. Cardiovasc. Drugs* **2019**, *19*, 335–342.

47. Setton, L.A.; Chen, J. Cell mechanics and mechanobiology in the intervertebral disc. *Spine* **2004**, *29*, 2710–2723.

48. Weber, K.T.; Alipui, D.O.; Sison, C.P.; Bloom, O.; Quraishi, S.; Overby, M.C.; Levine, M.; Chahine, N.O. Serum levels of the proinflammatory cytokine interleukin-6 vary based on diagnoses in individuals with lumbar intervertebral disc diseases. *Arthritis Res.* **2016**, *18*, 3.

49. Khan, A.N.; Jacobsen, H.E.; Khan, J.; Filippi, C.G.; Levine, M.; Lehman, R.A.; Riew, K.D.; Lenke, L.G.; Chahine, N. Inflammatory biomarkers of low back pain and disc degeneration: A review. *Ann. N. Y. Acad. Sci.* **2017**, *1410*, 68–84.

50. Wang, K.; Bao, J.-P.; Yang, S.; Hong, X.; Liu, L.; Xie, X.-H.; Wu, X.-T. A cohort study comparing the serum levels of pro- or anti-inflammatory cytokines in patients with lumbar radicular pain and healthy subjects. *Eur. Spine J.* **2016**, *25*, 1428–1434.

51. Kang, J.D.; Stefanovic-Racic, M.; McIntyre, L.A.; Georgescu, H.I.; Evans, C.H. Toward a biochemical understanding of human intervertebral disc degeneration and herniation. Contributions of nitric oxide, interleukins, prostaglandin E2, and matrix metalloproteinases. *Spine* **1997**, *22*, 1065–1073.

52. Miyamoto, H.; Saura, R.; Doita, M.; Kurosaka, M.; Mizuno, K. The role of cyclooxygenase-2 in lumbar disc herniation. *Spine* **2002**, *27*, 2477–2483.

53. Kang, J.D.; Georgescu, H.I.; McIntyre-Larkin, L.; Stefanovic-Racic, M.; Evans, C.H. Herniated cervical intervertebral discs spontaneously produce matrix metalloproteinases, nitric oxide, interleukin-6, and prostaglandin E2. *Spine* **1995**, *20*, 2373–2378.

54. Wuertz, K.; Vo, N.; Kletsas, D.; Boos, N. Inflammatory and catabolic signalling in intervertebral discs: The roles of NF-kappaB and MAP kinases. *Eur. Cell Mater.* **2012**, *23*, 103–119, discussion 119–120.

55. Henckaerts, E.; Linden, R.M. Adeno-associated virus: A key to the human genome? *Future Virol.* **2010**, *5*, 555–574.

5.8 Supplementary information
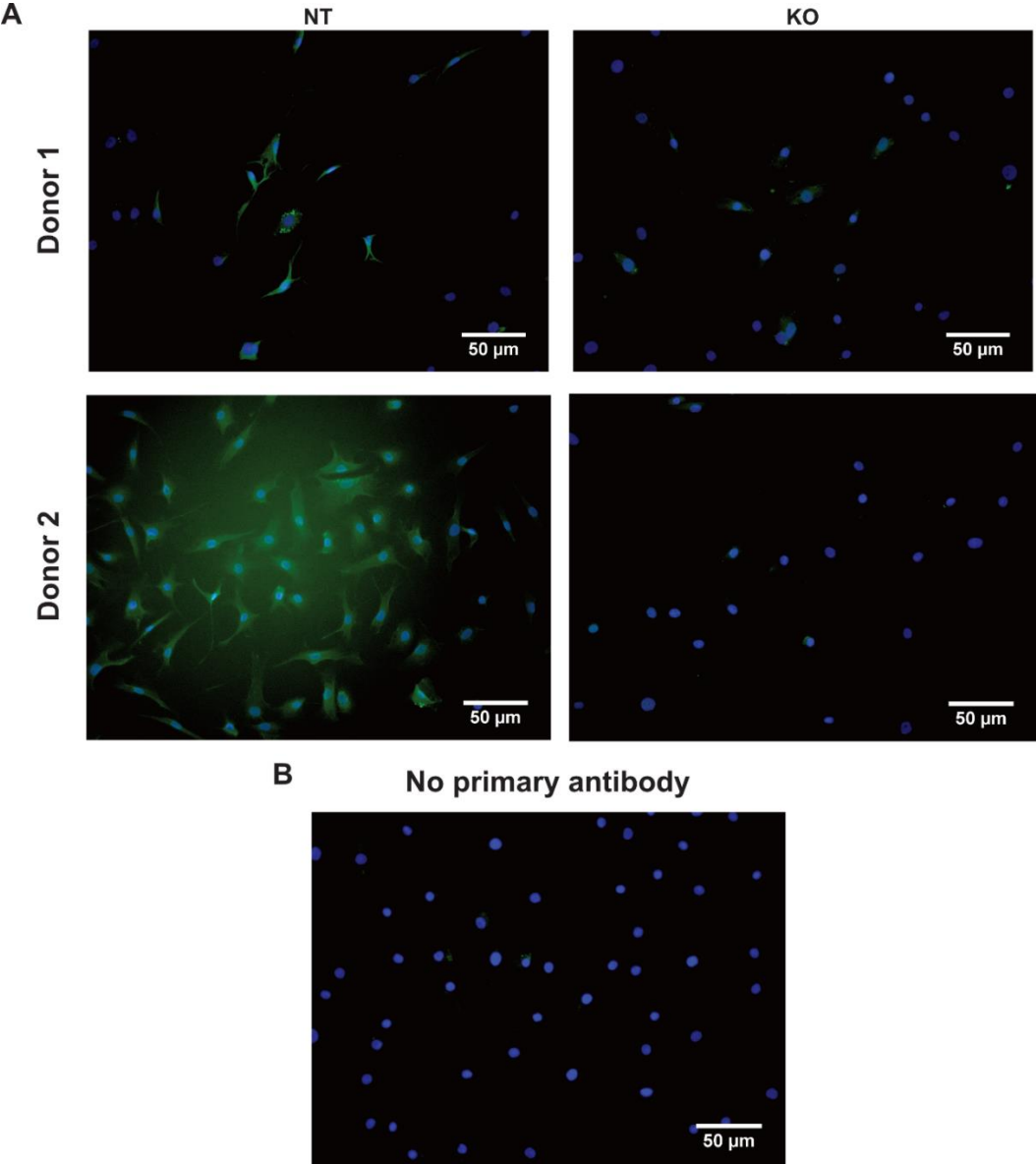
Figure S1. A) Immunocytochemistry of **A**) NT and KO cells from two additional donors; and **B**) NT cells without primary antibody; green = TRPV4, blue = DAPI; scale bars = 50 µm.

Chapter 6

The potential of CRISPR/Cas9 genome editing for the study and treatment of intervertebral disc pathologies

The potential of CRISPR/Cas9 genome editing for the study and treatment of intervertebral disc pathologies

Olga Krupkova[1], Elena Cambria[1], Lenka Besse[2], Andrej Besse[2], Robert Bowles[3,4], Karin Wuertz-Kozak[1,5,6,7]

[1]Department of Health Sciences and Technology, Institute for Biomechanics, ETH Zurich, Switzerland

[2]Department of Oncology and Hematology, Cantonal Hospital St Gallen, St Gallen, Switzerland

[3]Department of Bioengineering, University of Utah, Salt Lake City, Utah

[4]Department of Orthopaedics, University of Utah, Salt Lake City, Utah

[5]Spine Center, Schön Klinik München Harlaching, Munich, Germany

[6]Academic Teaching Hospital and Spine Research Institute, Paracelsus Private Medical University Salzburg, Salzburg, Austria

[7]Department of Health Sciences, University of Potsdam, Potsdam, Germany

6.1 Abstract

The CRISPR/Cas9 system has emerged as a powerful tool for mammalian genome engineering. In basic and translational intervertebral disc (IVD) research, this technique has remarkable potential to answer fundamental questions on pathway interactions, to simulate IVD pathologies, and to promote drug development. Furthermore, the precisely targeted CRISPR/Cas9 gene therapy holds promise for the effective and targeted treatment of degenerative disc disease and low back pain. In this perspective, we provide an overview of recent CRISPR/Cas9 advances stemming from/with transferability to IVD research, outline possible treatment approaches for degenerative disc disease, and discuss current limitations that may hinder clinical translation.

Keywords: CRISPR/Cas9, degenerative disc disease, intervertebral disc, low back pain, targeted genome engineering

6.2 Disc degeneration: the need for novel treatments

Degeneration of the intervertebral disc (IVD) is an age-related process that is characterized by a catabolic shift, leading to matrix breakdown and—ultimately— structural failure. Apparent degenerative changes first occur in the nucleus pulposus (NP) and are associated with a shift from collagen type II to more fibrotic collagen type I as well as with a reduction in proteoglycans and a consequent loss in hydration and disc height [1]. However, the annulus fibrosus (AF) also undergoes degenerative changes as evidenced by disorganization of the lamellar structure, possibly leading to structural defects, such as clefts and tears [2]. The altered biomechanical status during degeneration contributes to the development of tissue damage through the creation of areas of peak stress, exposing the disintegrated tissue to hyperphysiological loading that it cannot withstand [3]. As the IVD possesses little regenerative capacity, and healing can only take place in the outer AF where nutrient supply is greatest, degeneration gradually progresses without treatment.

Although disc degeneration is a main contributor to back pain, only a subpopulation will become symptomatic and experience so-called degenerative disc disease (DDD) that is associated with increased expression of inflammatory molecules, including interleukins IL-1β, IL-8, and IL-6 and tumor necrosis factor (TNF)-α (reviewed in References [4-7]). At the moment, patients suffering from DDD are initially treated conservatively, that is with physiotherapy and analgesic medication, but may have to undergo discectomy if symptoms do not improve. Thus, current therapies only target symptoms but not the underlying molecular processes contributing to disc degeneration and pain development. Accordingly, major effort has been made to design novel, biologically targeted treatment options over the past years, with a focus on 2 approaches:

On the one hand, regenerative therapies to counteract the degeneration process have been attempted but without compelling results thus far. The use of cellular therapies, for example, stem cell treatment, is negatively affected by the harsh microenvironment of

the IVD that is characterized by high mechanical loads, inflammatory cytokines, hypoxia, low glucose levels, acidic pH, and high osmolarity [8]. The application of anabolic substances promoting the production of extracellular matrix (ECM) is hampered by the low cellularity within the IVD (4000 cells/mm^3 in the NP and 9000 cells/mm^3 in the AF) and, furthermore, by the fact that these few cells are metabolically not very active [9, 10]. The outcome of injection of classical anabolic factors such as bone morphogenetic protein (BMP)-7, transforming growth factor (TGF)-β, or growth differentiation factor (GDF)-5 is compromised even more by the short half-life of these growth factors and their rapid diffusion out of the IVD [8].

On the other hand, numerous recent research activities have focused on the means to modulate inflammation in the IVD, mostly via inhibition of the inflammatory cascade (e.g., biologics such as epigallocatechin gallate [EGCG], resveratrol, or piperine)[11 -13] or by neutralization of inflammatory mediators (e.g., infliximab, a TNF-α inhibitor [14]). Although these molecular treatments constitute a novel means for molecular disease modulation, their success is likely not sustained, especially as repeated injection of therapeutics into the IVD is not desired [15]. Novel tools that would allow for safe genetic manipulation of resident cells to modulate the catabolic and inflammatory shift or of therapeutic cells to enhance their robustness, and thus allow them to better withstand the IVD environment, could help to circumvent the limitations of current therapeutic approaches.

6.3 Targeted genome editing by CRISPR/Cas9

Genome editing results in stable phenotype changes and thus can permanently eliminate the underlying causes of diseases. Precise genetic reprogramming techniques have great potential to change traditional "symptomatic" treatments, not only of monogenic diseases but also of age-related and civilization disorders. In addition, these techniques can be implemented in basic and preclinical research to generate disease phenotypes in vitro and in vivo. To date, known genome editing techniques are based on DNA-binding nucleases, namely engineered Zinc Finger Nucleases (ZFN) and Transcription Activator-like Effector Nucleases (TALEN), as well as on RNA-guided nuclease(s), specifically Clustered Regulatory Interspaced Short Palindromic Repeats-associated Cas9 (CRISPR/Cas9) [16]. ZFNs and TALENs have been used to directly correct disease-causing mutations associated with hemophilia B or sickle cell disease. ZFN- and TALEN-based therapies demonstrated success in clinical trials, for example, for HIV, proving the potential of genome editing for applications across basic science, medicine, and biotechnology. However, their main disadvantages are related to the challenges (relatively difficult preparation of functional DNA-binding nucleases) and costs associated with their design and development [17, 18]. Advantages and disadvantages of ZNF and TALENs are reviewed in Reference [18]. Similar to ZFNs and TALENs, CRISPR/Cas9 stimulates a double-strand DNA break (DSB) at a target genomic locus but is easier to prepare and use and is readily programmable. Thus, CRISPR/Cas9 is regarded as a powerful technique for future mammalian genome engineering [19].

The CRISPR/Cas9 system is composed of the bacterial endonuclease Cas9, which can be directed to any DNA sequence by single-guide RNA (sgRNA). sgRNA is a short synthetic RNA composed of a scaffold sequence necessary for Cas9-binding, that is made of crRNA, loop, and trans-activating crRNA (tracrRNA), and a user-defined, variable 17-20 nucleotide spacer that defines the genomic target to be modified [20]. The short nucleotide spacer of sgRNA is complementary to the genomic DNA target sequence in close proximity to the protospacer adjacent motif (PAM) that, in case of Cas9 obtained from *Streptococcus pyogenes,* is a conserved NGG sequence. However, the PAM is not part of gRNA as it is only present downstream of the target DNA (**Figure 1**) [21,22].
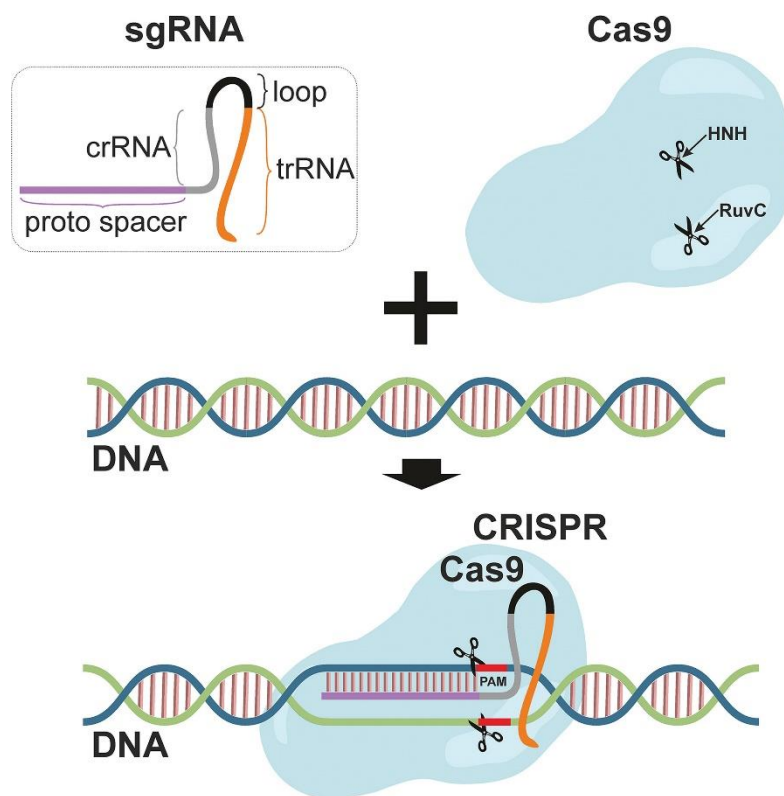
Figure 1: Schematic representation of the CRISPR/Cas9 system. Single-guide RNA (sgRNA) consists of tracer RNA (trRNA); a loop; crispr RNA (crRNA); and protospacer sequence, which is homologous to the target DNA. wtCas9 possess 2 cleavage activities, HNH and RuvC. CRISPR/Cas9 editing tools consist of sgRNA guiding precisely the Cas9 enzyme to the DNA based on the homology between the protospacer motif and DNA. When the heteroduplex between sgRNA and target DNA is formed, Cas9 performs DNA cleavage in close proximity of the PAM sequence and introduces a double-strand DNA break.

The recognition of the target DNA is ensured by heteroduplex formation between the nucleotide spacer of sgRNA and the complementary strand of the target DNA, which is followed by Cas9-mediated DNA cleavage [23]. Typical wild-type Cas9 demonstrates double-stranded DNA cleavage activity provided by 2 domains, RuvC and HNH [24]. Compared to other components guiding the programmable nuclease to the targeted DNA locus, sgRNA design and synthesis are simple and cost effective. However, a

particular concern of CRISPR/Cas9 can be its off-target activity as the sgRNA can still recognize sequences in the genome with a single-base mismatch, causing unwanted DSB and mutations. To mitigate this disadvantage, more precise sgRNA designs, synthetically engineered Cas9, or nickase-Cas9 (Cas9n) with D10A point mutation possessing only single-stranded DNA cleavage activity have been developed [25-27]. CRISPR/Cas9 has been successfully employed to induce single gene mutations, multiple mutations in one cell [28], and to cleave highly methylated regions [29]. Furthermore, a full range of CRISPR/Cas9 library screening platforms, from genome-wide to pathway-specific, is being developed and used to reveal critical biological processes, regulatory genes in development, aging, or drug resistance [25, 30, 31]. As such, CRISPR/Cas9 represents a programmable, versatile, and efficient tool for editing virtually any gene. To date, this system has been exploited to reveal exact gene functions, uncover new drug targets, produce more accurate models of human diseases, and provide potential gene correction therapy [32, 33].

CRISPR/Cas9-based techniques can be used not only to disrupt but also to repair and/or regulate gene expression (**Figure 2**). To generate *CRISPR/Cas9-mediated knockouts*, RNA-guided Cas9 induces DSBs, commonly activating the nonhomologous end-joining (NHEJ) repair pathway. NHEJ produces small random insertions or deletions (indels), resulting in frameshift mutations and loss-of-function phenotypes [34]. *CRISPR/Cas9-mediated gene editing* is achieved in the presence of template DNA, when DSBs are repaired by so-called homology-directed repair (HDR) pathways, which act instead of NHEJ and provide precise insertion of donor DNA into the target site. Apart from site-specific DNA repair, HDR can aid in generating controlled gene knockouts and inserting marker sequences or resistance genes for further selection of cells with desired phenotypes [35]. *CRISPR/Cas9-mediated transcriptional regulation* of gene expression can be achieved by CRISPR interference (CRISPRi) and CRISPR activation (CRISPRa), including CRISPR/Cas9-mediated epigenetic modification of histones. These techniques utilize catalytically inactive RNA-guided Cas9 (so-called dead Cas9, dCas9), fused with transcriptional activators and repressors (VP64 and KRAB, respectively) [36, 37] or with histone-modifying domains (e.g., p300, LSD1) that can regulate transcription by altering chromatin structure [38]. These gRNA-dCas9 complexes can be designed to reversibly target specific regulatory sequences, act as a scaffold for various transcriptional factors, or directly interfere with transcription [17, 33]. In addition, CRISPR technology (particularly CRISPR/Cas13) can be applied to edit RNA by targeting Cas13a protein to RNA, instead of DNA [39]. An overview of possible CRISPR/Cas-based techniques and their specifications is given in **Table 1**. CRISPR/Cas9 can be used in basic IVD research to answer fundamental questions on pathway interactions, to simulate IVD pathologies for research and drug development, and possibly to treat DDD.
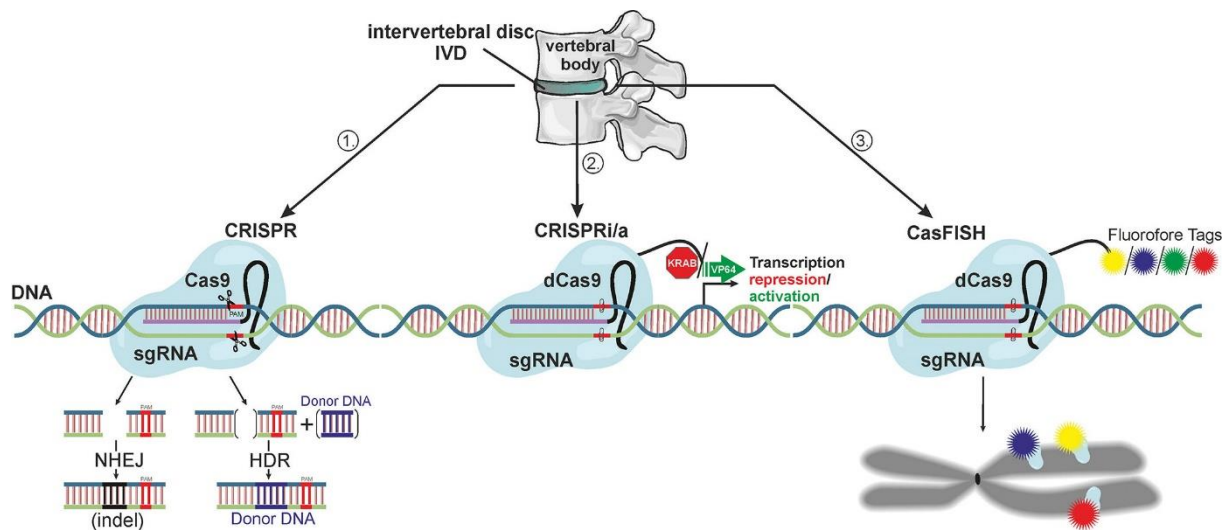
Figure 2: Mechanism of action of CRISPR/Cas9-based techniques. (1) CRIPSPR/Cas9 gene editing: wtCas9 with both cleavage activities is used to create a double-strand break on the target DNA, which can be repaired either by nonhomologous end joining (NHEJ) or by homology directed repair (HDR) in case a template DNA is provided. (2) CRISPR/Cas9 interference (i) or activation (a): deathCas9 (dCas9) without cleavage activity is guided to the DNA site around the transcription start site. dCas9 fused with KRAB domain is used for transcription repression, whereas dCas9 fused with VP64 is used for transcription activation of target gene. (3) CasFISH-mediated chromosome labeling. dCas9 is fused with fluorophore tag and guided in vitro to the target chromosomal DNA that shall be visualized.

Table 1: Specifications of different CRISPR/Cas-based techniques

CRISPR/Cas	Cas form	Target sequence	Application	Vectors
CRISPR/Cas9 DNA application				
CRISPR/Cas9 KO	Cas9 or Cas9n	Early exon or evolutionary conserved region	Gene knockout in vitro, in vivo	Viral transduction for stable delivery, RNP complex electroporation for transient delivery
CRISPR/Cas9 GE	Cas9	Cut site ≤30nt from the proximal ends of the repair template	Gene editing in vitro, in vivo	
CRISPRi	dCas9-KRAB	Targeted to promoters/enhancers	Suppression of gene expression	
CRISPRa	dCAs9-VP64	Targeted to promoters/enhancers	Activation of gene expression	
CASFISH	dCas9-fluorophore	Within the desired exon of the gene	In situ labeling of fixed cells in vitro	RNP electroporation
CRISPR/Cas13a RNA application				
CRISPR/Cas13a KO	Cas13a	Early exon or evolutionary conserved region	RNA knockdown	Viral transduction for stable delivery, RNP complex electroporation for transient delivery
CRISPR/Cas13a GE	Cas13a	Around desired adenosine in spliced RNA	ADAR (adenosine to inosin; A-G) RNA editing	
CRISPR/dCas13a	Cas13a (catalytically inactive)-fluorophore	Region within specific spliced RNA variant	RNA tracking	

CRISPR/Cas9 in IVD research

<u>Genome targeting</u>

CRISPR/Cas9 is a state-of-the-art tool to determine how the genotype influences the phenotype by revealing details on genetic and epigenetic regulation of cell function. IVD research has been historically hindered by slow proliferation and dedifferentiation of IVD cells as well as by a lack of stabilized cell lines. Recently, immortalized rat NP and AF cell lines have been developed using the rho-associated kinase (ROCK) inhibitor Y27632 [40]. As kinase inhibitors often have unspecific effects, precise targeting of the ROCK gene by CRISPR/Cas9 could provide an alternative tool for IVD cell immortalization. Another possible application of CRISPR/Cas9 in primary IVD cells can be to prevent their dedifferentiation, a common issue of in vitro studies [41]. Targeting the expression of dedifferentiation-associated genes, such as collagen II by CRISPRa or collagen I by CRISPRi, could possibly prolong the use of cultured IVD cells in vitro. Collagen II and aggrecan have recently been targeted by CRISPRa in tissue-derived stem cells (ASCs) to shift the cell phenotype toward an IVD phenotype and could also be applied directly in IVD cells [42].

In cartilage research, the Swarm rat chondrosarcoma (RCS) cell line is commonly used to study chondrocyte-specific phenotype due to its similarity to normal rat cartilage and ability to generate cell clones. Recently, an RCS cell line stably expressing Cas9 (RCS-Cas9) was developed and used to investigate the function of the ECM molecules aggrecan and hyaluronan [43, 44]. Aggrecan knockout in RCS-Cas9 cells provided additional knowledge on the role of aggrecan in cell attachment, chondrosarcoma formation, and gene regulation [43], while knockout of hyaluronan synthase-2 revealed the essential role of hyaluronan in the assembly of chondrocyte pericellular matrix [44]. In a chondrogenic mouse teratocarcinoma cell line (ATDC5), CRISPR/Cas9-mediated deletion of the specific binding site of the microRNA miR-322, reduced mitogen-activated protein kinase kinase 1 (MAP2K1 or MEK1) protein levels, and provided new insights into cartilage development [45].

Similar to these cell lines, IVD cells with stably expressed Cas9 could aid in explaining the relationship between IVD genotype and phenotype in the future. Recent studies on IVD biology highlighted the importance of membrane proteins, namely, of cell surface receptors (e.g., toll-like receptor (TLR) TLR2 [46]), channels (e.g., aquaporins [47], transient receptor potential cation channel subfamily V member 4 (TRPV4) [48]), and adhesion molecules (e.g., integrins [49]) as these proteins allow IVD cells to sense their environment and respond to its changes. Although the expression and activity of these molecules are altered during DDD, understanding their exact function has been challenging so far as inhibitors/antagonists and activators/agonists are often nonselective or have short half-lives [50, 51]. The CRISPR/Cas9 system enables the investigation of the exact cell-ECM interactions by functional knockouts, knockdowns, or knockins of receptors, specific subunits, and interaction partners. As an example, gRNA-mediated silencing by dCas9-KRAB-GFP (CRISPRi) was used to study the role of N-cadherin (CDH2) in porcine and human NP cells, revealing that CDH2 regulates juvenile NP cell phenotypes during NP cell cluster formation [52]. Both stable and temporary CRISPR/Cas9 modifications have the potential to uncover the mechanisms involved in

ECM turnover (e.g., matrix metalloproteinases [MMPs], a disintegrin and metalloproteinase with thrombospondin motifs [ADAMTS]), survival, senescence, and mechanotransduction of IVD cells. In addition, CRISPRi has recently been applied to study the role of cytokine receptors TNFR1 and IL1R1 and their downstream proinflammatory signaling in human primary IVD cells [53]. Identification and analysis of noncoding regulatory sequences, such as previously identified enhancers of ECM-degrading enzymes, will also be possible [54].

Moreover, transduction of target cells with pooled lentiviral libraries carrying multiple gRNA and Cas9 protein or only gRNAs-Cas9 for defined sets of genes can allow for the functional screening and identification of molecular pathways involved in various diseases [55-57], possibly including DDD in the future. CRISPR/Cas9 also contributes to the study of genomic regions capable of molecular interactions thanks to the development of CRISPR engineered DNA-binding molecule-mediated chromatin immunoprecipitation (enChIP), where a specific antibody is fused to a dCas9 coexpressed with a gRNA [58]. In IVD research, specifically in studies focusing on IVD oxygenation, enCHiP could, for example, be used to investigate the interaction between hypoxia-responsive elements (HREs) and hypoxia-inducible factors such as HIF-1α [47, 59]. Another use of the CRISPR technology is the visualization of genomic loci in cell nuclei, or so-called Cas9-mediated fluorescence in situ hybridization (CASFISH) [60] (**Figure 1**). By using multicolor dCas9/sgRNAs, several target loci can be labeled simultaneously [60], for example, fibronectin, TGF-β1, and MMPs in human IVDs [61, 62]. Compared to the traditional method, CASFISH could prevent the disruption of the spatial organization of the genetic elements [60].

<u>Disease models</u>

CRISPR/Cas9 systems can be used to generate disease models and thus characterize the functionality of identified therapeutic targets and developed drugs. *In vitro disease models* can be prepared from NP and AF cells or organ cultures intended to simulate the degenerative phenotype. It has been demonstrated that in vitro organ cultures can be more suitable than cells to study IVD biology and therapeutic testing as they retain biological and biomechanical properties similar to the IVD in vivo [63[. However, hallmarks of IVD degeneration are usually not present in organ cultures and have to be induced by nonphysiological insults like injections of proteases [64] or high concentrations of proinflammatory cytokines [65]. Generating organ cultures with multiple edited genes (aggrecan, collagen, MMPs, ADAMTS, ILs) might simulate IVD pathologies more naturally. CRISPR/Cas9 constructs have been delivered into tissues through several methods, including viral vectors [66], nanoparticles [67], or as a gRNA-Cas9 ribonucleoprotein (RNP) complex by nucleoporation, so this option can be feasible [68].

Another approach involves deriving tissues from human-induced pluripotent stem cells (iPSCs) edited with CRISPR/Cas9. This idea has been proposed to develop personalized arthritis therapeutics [69]. Cartilage can indeed be obtained through chondrogenesis of human iPSCs [70]. Deficiencies can first be introduced in iPSCs with CRISPR/Cas9, and the engineered cartilage is then subjected to arthritic stimuli such as proinflammatory cytokines or mechanical loading. Candidate drugs can then be screened

for their potential to rescue the phenotype. Organ cultures with custom modifications in multiple genes and iPSC-derived engineered tissues can serve as an alternative to animal experiments, reducing the need to use animals in research and the initial phases of clinical testing.

CRISPR/Cas9 represents a major asset to generate *in vivo disease models,* such as transgenic mice. Compared to traditional methods, this approach is faster, easier, and more cost effective, and protocols consisting of the injection of a plasmid construct containing the Cas9 and gRNA in mouse zygotes are available [71]. Another approach is to replace the nucleus of an isolated oocyte with the nucleus of a gene-edited somatic cell [72], thus rendering the use of embryonic stem cells obsolete. In addition to single points [73], large domains can also be mutated [74], and multiple genes can be targeted simultaneously, with an efficiency of 95% for single mutants and 80% for double mutants [28]. More recently, in vivo genome editing in specific tissue has been demonstrated by synthetic short-lived gRNA-Cas9 RNP complexes [75]. As genetics is postulated to be a main contributor to disc degeneration and DDD [76], in vivo models expressing Cas9 specifically in the IVD or delivery of short-lived RNP specifically to the IVD will be useful to better understand the role of highlighted candidate genes in disease progression. Such genes include the vitamin D receptor, aggrecan, type IX collagen, asporin, MMP3, IL-1, and IL-6 as polymorphisms in these genes may influence IVD degeneration mechanisms [77]. In vivo inducible systems based on dCas9 have been particularly useful in phenotypic and epigenetic studies in postnatal mammals and in cancer models, allowing the study of gene-level changes [78, 79]. Specifically, induced epigenetic remodeling enabled the amelioration of disease symptoms in mice [80] and thereby represents an interesting approach for the IVD. As such, targeted-induced epigenetic changes have been performed to investigate the effects of TNF-α and IL-1β signaling in primary IVD cells [53].

Mice (and small animals in general) are not the most suitable models to simulate IVD pathologies and therapeutic testing. Unlike human IVDs, their IVDs are too small, contain notochordal cells with self-regenerative potential, and fail to mimic the diffusion limitations of the human IVD. On the other hand, IVDs of larger animals (e.g., sheep or dog) have comparable biology and diffusion distances to humans [81]. CRISPR/Cas9 is not limited to mice but has also been used in domestic species, such as pigs [72, 82], sheep [83], goat [84], and cattle [85], as well as dogs [86] and nonhuman primates [87]. While structural models of IVD degeneration, including injury or chemical treatments, are invasive and unrepresentative of the natural pathophysiology, CRISPR/Cas9 may allow a spontaneous simulation of the disease, for example, by activation of senescence pathways. In the future, large animals with inducible Cas9 in their IVDs can function as programmable translational models for therapeutic testing.

Besides serving the purpose of translational medicine, animal models are also used for research in developmental biology. Notably, notochordal cells are currently of great interest in the IVD scientific community. In the field of spine and cartilage development, the zebrafish is a useful model and a powerful tool for in vivo CRISPR-based screenings [88]. CRISPR/Cas9 *kinesin-I* deletion in zebrafish revealed the role of this gene in cartilage remodeling and chondrocyte maintenance during craniofacial morphogenesis [89], while CRISPR/Cas9 knockout of *cavin1b* in the embryonic notochord showed that caveolae, which are formed by Cavin1b, mediate the mechanoprotection of notochordal cells during

development [90]. Recently, a zebrafish model of idiopathic scoliosis was created by CRISPR/Cas9 deletion of *mapk7*[91].

CRISPR/Cas9 in preclinical testing for IVD therapy

For the efficient treatment of painful IVD degeneration, the pathways that mediate inflammatory and catabolic responses, pain sensing, cell resistance to oxidative stress, and production of ECM should be targeted. For example, CRISPR/Cas9 can enhance the expression of growth factors and ECM proteins, reduce the expression of inflammatory mediators, or correct unfavorable gene polymorphisms in affected individuals, providing patient-specific treatments [77]. To achieve this, precise reprograming of gene expression and repression is needed together with user-friendly protocols that allow for clinical translation. Importantly, it has been demonstrated that CRISPR/Cas9 can simultaneously activate, repress, and knockout several distinct genes in a single cell [92]. This possibility of CRISPR/Cas9 for multiplexing can be a major step forward in the treatment of multifactorial and degenerative diseases such as IVD pathologies.

Another type of Cas protein, Cas13, can be used to edit RNA by targeting CRISPR/Cas13 to RNA instead of DNA [39], for example to correct alternative splicing. It has been shown that certain splicing variants of fibronectin mRNA may be associated with IVD degeneration [93]. Alternative splicing of multiple mRNAs is also involved in chondrogenic differentiation in response to hypoxia, but no such data exist for IVD cells [94]. Specific RNA editing by CRISPR may not only be used to correct false alternative splicing, but also mimic protective alleles, or guide differentiation of stem cells. CRISPR-based genome modification of IVD can be performed directly in vivo or indirectly ex vivo in therapeutic cells that are subsequently transplanted into the IVD. Although targeted CRISPR/Cas9-mediated transgene integration would be ideal, it is not yet completely feasible, and current delivery methods have to be improved.

Ex vivo edited autologous IVD cells

Autologous IVD cells can be obtained from biopsies removed during surgeries. These cells are frequently affected by pre-existing degeneration and suffer from poor expansion rates in vitro [95, 96]. Nevertheless, IVD cells subjected to conventional adenoviral gene delivery of TGF-β, BMP-2, BMP-7, or sex-determining region Y box 2 (SOX2) demonstrated the ability to restore the proteoglycan content and modulate the biological processes in vitro and in vivo [97, 98], suggesting that precise gene targeting in degenerated IVD cells is also possible. Recently, human articular chondrocytes with stable CRISPR/Cas9 knockout of IL1R1 were prepared in vitro and found to have superior properties over nonedited therapeutic cells [99], with recent evidence that TNFR1 and IL1R1 can similarly be targeted via epigenome editing in human primary IVD cells [53]. This suggests that deletion or knockdown of IL1R1 in therapeutic cells may improve the outcome of cell therapies for patients suffering from joint diseases.

Ex vivo edited stem cells

Adult stem cells, such as bone marrow mesenchymal stromal/stem cells (MSCs) or ASCs, can activate hallmarks of IVD regeneration [100, 101]. Some of their advantages

include high proliferation rates, and thus the possibility to expand cells with target modifications. Implantation of adult stem cells in animal models has resulted in the restoration of an IVD-like phenotype, and promising outcomes were found in pilot clinical applications (phase I/III clinical trials) [102]. However, the major drawback of stem cell-based therapies is the poor survival rate of implanted cells due to the pre-existing catabolic and inflammatory environment in the IVD [103-105]. Farhang et al. recently used *CRISPR/Cas9 epigenome editing* to modulate inflammatory responses of human ASCs by repressing the expression of cytokine receptors TNFR1 and IL1R1. Using dCas9-KRAB-induced, site-specific H3K9 methylation of TNFR1 and IL1R1 promoters, resistance of ASCs to inflammatory environments was achieved, thus demonstrating the ability of CRISPR/Cas9 epigenome editing to modulate inflammatory signaling in implantable cells (**Figure 3**) [106]. Although this method does not produce complete knockout of gene expression, these systems have the advantage of being inducible and reversible.
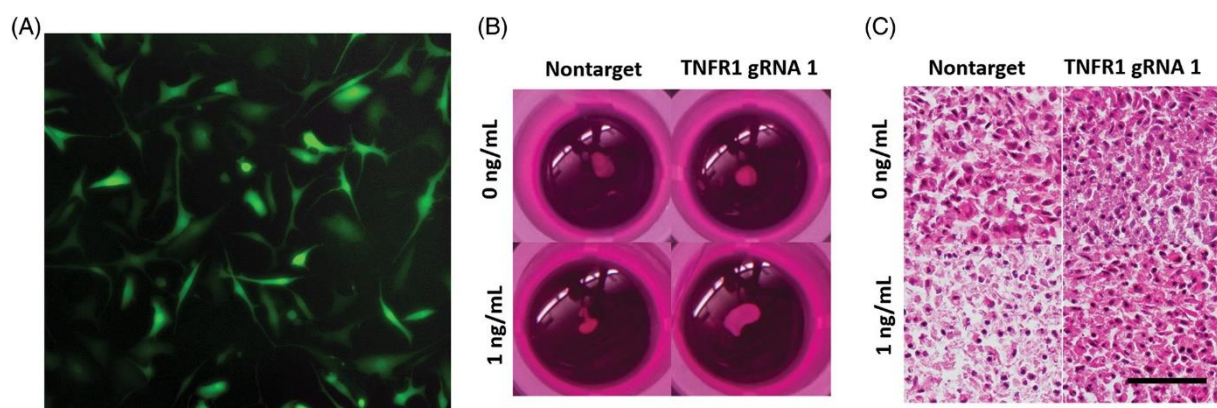
Figure 3: CRISPR epigenome editing in primary IVD cells and stem cells. (A) Lentiviral transduction of primary human IVD cells (69 years, female) expressing CRISPR epigenome editing system [53]. Protection of adipose tissue-derived stem cells from TNF-α after CRISPR epigenome editing of TNFR1, as demonstrated by (B) pellet size and (C) H&E staining of pellets [106].

In murine iPSCs subjected to chondrogenic differentiation, only complete homozygous *CRISPR/Cas9 knockout* of IL1R, but not heterozygous knockout, resulted in a cytokine-resistant cartilage phenotype without chronic inflammation [107]. Taking this approach further, an inflammation-resistant cartilage with the ability to autonomously regulate its own inflammatory responses was recently engineered by *CRISPR/Cas9 gene editing.* In murine iPSCs, sequences for cytokine antagonists IL1Ra and sTNFR1 were targeted to a first exon of the proinflammatory chemokine (C-C) ligand 2 (Ccl2), a common target of TNF-α and IL-1β. In response to cytokine stimulation, the edited cells produced TNF-α and IL-1β antagonists and thus self-inhibited cytokine-mediated signaling [108]. This approach demonstrated the potential of CRISPR/Cas9 gene editing for the autonomous delivery of anti-inflammatory agents involving cellular feedback loops.

Apart from IVD inflammation, therapeutic cells are also subjected to other microenvironmental challenges, such as low pH, nonphysiological loading, hypoxia, or starvation. A possible strategy against the consequences of such a harsh microenvironment could be preventing senescence by regulating the expression of cyclin-dependent kinase inhibitor 2A (p16), cellular antioxidant enzymes, or DNA damage

pathways [109]. CRISPR/Cas9-modified, microenvironment-resistant cells can be edited to coexpress for example sequences of enhanced synthesis of the ECM.

Targeted genome editing in vivo

CRISPR/Cas9-based agents can be delivered directly by local application to protect endogenous cells from chronic inflammation and pain, enhancing their anabolic function and thus counteracting degeneration. As IVD cells are not ideal targets for direct in vivo genetic alterations due to their scarcity and inaccessibility, especially in the adult NP, editing of other cell types can be considered.

Activation of dorsal root ganglion (DRG) neurons and subsequent pain is known to be associated with inflammatory responses of degenerated IVD [5]. A recent in vitro study of Stover et al. explored the potential of DRG-directed *CRISPR/Cas9 epigenome editing* to reduce low back pain (LBP) [110]. Targeted delivery of gRNA-dCas9-KRAB to a promoter of A Kinase Anchor Protein 150 (AKAP150) gene in DRG neurons, stimulated with catabolic IVD-conditioned media, abolished the nociceptive activity of the DRGs while preserving their nonpathological activity. This study demonstrated the potential of CRISPR/Cas9 epigenome editing of pain-related genes in nociceptive neurons as a therapeutic strategy for LBP [110]. Recently, CRISPR/Cas9 adeno-associated virus (AAV)-based delivery into neurons was performed in a rat model of retinal dystrophy for correction of the proto-oncogene tyrosine-protein kinase MER (*Mertk*) gene via homology-independent targeted integration (HITI). Although there was only partial function rescue, the results suggest the feasibility of AAV in vivo-targeted gene therapy in neurons, with possible implications for LBP [111].

Clinical translation of CRISPR/Cas9 gene therapy

CRISPR/Cas9 is already at various stages of clinical trials for a number of disorders due to its wide applicability and ease of customization. The first application of therapeutic genome editing has entered clinical testing for editing of the C-C motif chemokine receptor *CCR5* in CD4 T-lymphocytes of HIV-positive patients [112]. Despite the difficulties, clinical trials based on adenoviral-mediated ZFN gene delivery into T-lymphocytes were completed. A new planned trial investigating the safety of the ex vivo *CCR5* modification in CD34+ hematopoietic stem cells by CRISPR/Cas9 is ongoing in HIV-positive patients to prevent AIDS development (clinicaltrial.gov: NCT 03164135). Another CRISPR/Cas9 application in humans is the ex vivo-programmed cell death protein 1 (*PD1*) gene deactivation in T-lymphocytes of a lung cancer patient and subsequent introduction of the edited cells into the patient, which was based on previous encouraging in vitro results [113, 114]. *PD-1* gene modification is a promising approach that should be clinically trialed for other malignancies, but caution in trial designs with CRISPR/Cas9 needs to be taken when it comes to ethical requirements of scientific validity [115].

The clinical application of CRISPR/Cas9 machinery directly in the human body is envisioned for the treatment of HPV-related cervical intraepithelial neoplasia (clinicaltrial.gov: NCT03057912). A plasmid containing CRISPR/Cas9 is designed to target the gene for viral E6/E7T1 protein and thus eliminate the viral genes from cells infected

by HPV and prevent their malignant transformation. Currently, a major challenge for using CRISPR/Cas9 in vivo is the limitation of viral delivery by vector size, possible immunogenicity, safety concerns, and regulatory hurdles. Integrase-deficient lentiviral vectors (IDLVs) for delivery of CRISPR/Cas9 components have been recently developed [116]. Although progress has been made, developing better delivery systems, together with development of strategies, to systematically minimize off-target effects is necessary for the therapeutic advancement of CRISPR/Cas9 in the future [117].

Although genome editing in the IVD is still far from clinical application, ethical and safety concerns related to the use of CRISPR/Cas9 should be considered now [118]. Off-target effects, which are specifically high in human cells compared to other species, may jeopardize the safety of patients by deregulating other genes with high homology to the intended target DNA sequence. This may cause severe mutations with potentially detrimental consequences, such as cell death. Ethical concerns for CRSIPR/Cas9 are mostly related to heritable genetic engineering, that is, genome editing in the human germline, and the associated possibility that introduced modifications can be transmitted through generations. While techniques for genome engineering thus far were limited to somatic cells and hence restricted to patients accepting the risk of possible side effects after informed consent, CRISPR/Cas9 may lead to unpredictable, possibly dangerous changes in later generations that the consenting patient would be responsible for. However, the extent of the risk depends on the treated cell and tissue type and is likely less pronounced for intradiscal applications.

Clinical translation of CRISPR/Cas9 for IVD pathologies holds promise as this will allow targeting of the underlying molecular processes contributing to disc degeneration and pain development and hence constitute a major improvement compared to current, symptom-driven therapies. While approaches for CRISPR/Cas9-based IVD regeneration may be challenging to translate to clinical practice due to unfavorable risk-benefit ratios [119] (especially when considering that degeneration itself does not always induce suffering or pain), treatments that specifically target disc-related pain have higher chances for translation. Both CRISPR/Cas9-based regulation of inflammatory processes within the IVD and modification of nociception in spinal nerves may have the highest potential for clinical application due to the high socioeconomic burden of LBP [120]. Furthermore, the means to enhance the mechanical stability of the AF through genome editing and thus prevent IVD herniation would be of great significance for the healthcare systems [121], but this approach would strongly rely on (currently not existing) the early identification of patients at risk. However, when designing new CRISPR/Cas9 treatment strategies, the limitations of this technique for patients in whom cells have already undergone alterations in cell number, activity, and phenotype will have to be considered. Hence, appropriate patient selection, depending on the respective target gene, will be an important factor in the clinical translation of genome editing in the IVD.

6.4 Conclusion

While our understanding of the mechanisms of the CRISPR/Cas9 system and its application in the clinical setting are still developing, CRISPR/Cas9 has the potential to induce a paradigm shift in the study and treatment of human diseases, including DDD and LBP. CRISPR/Cas9 systems provide a novel tool to improve the modeling of DDD and allow studying functions from a macroscopic (body) to a microscopic (cell) scale across all mammalian species. Modeling of IVD degeneration has always been a challenge and is a limitation to the field's progression that may be overcome by CRISPR/Cas9. In addition, gene editing, knockout, and endogenous gene expression control represent powerful tools to advance cell engineering in novel and efficient ways, hindered thus far by technological limitations, complexity of applications, and/or the expense/rapidity of development. This will have profound effects on both cell therapeutics and gene therapies for IVD degeneration application. However, the field has much to learn about the delivery and safety of these systems. Despite these challenges, CRISPR/Cas9 represents a promising new tool that has the potential to break through technological barriers that have been impeding the field's progress and therefore change our thinking and treatment of IVD degeneration, DDD, and LBP.

Acknowledgement

Author contribution

All authors have contributed to the manuscript and approved the final version.

6.5 References

1. Urban JPG, Roberts S. Degeneration of the intervertebral disc. Arthritis Res Ther. 2003; 5: 120- 130.

2. Osti OL, Vernon-Roberts B, Moore R, Fraser RD. Annular tears and disc degeneration in the lumbar spine. A post-mortem study of 135 discs. J Bone Joint Surg Br. 1992; 74: 678- 682.

3. O'Connell GD, Vresilovic EJ, Elliott DM. Human intervertebral disc internal strain in compression: the effect of disc region, loading position, and degeneration. J Orthop Res. 2011; 29: 547- 555.

4. Navone SE, Marfia G, Giannoni A, et al. Inflammatory mediators and signalling pathways controlling intervertebral disc degeneration. Histol Histopathol. 2017; 32: 523- 542.

5. Risbud MV, Shapiro IM. Role of cytokines in intervertebral disc degeneration: pain and disc content. Nat Rev Rheumatol. 2014; 10: 44- 56.

6. Wuertz K, Haglund L. Inflammatory mediators in intervertebral disk degeneration and discogenic pain. Global Spine J. 2013; 3: 175- 184.

7. Modic MT, Ross JS. Lumbar degenerative disk disease. Radiology. 2007; 245: 43- 61.

8. Smith LJ, Nerurkar NL, Choi KS, Harfe BD, Elliott DM. Degeneration and regeneration of the intervertebral disc: lessons from development. Dis Model Mech. 2011; 4: 31- 41.

9. Maroudas A, Stockwell RA, Nachemson A, Urban J. Factors involved in the nutrition of the human lumbar intervertebral disc: cellularity and diffusion of glucose in vitro. J Anat. 1975; 120: 113- 130.

10. Risbud MV, Shapiro IM. Microenvironmental control of disc cell function: influence of hypoxia and osmotic pressure. Intervertebral Disc. 2014; 1: 93- 108.

11. Li Y, Li K, Hu Y, Xu B, Zhao J. Piperine mediates LPS induced inflammatory and catabolic effects in rat intervertebral disc. Int J Clin Exp Pathol. 2015; 8: 6203- 6213.

12. Wuertz K, Quero L, Sekiguchi M, et al. The red wine polyphenol resveratrol shows promising potential for the treatment of nucleus pulposus-mediated pain in vitro and in vivo. Spine. 2011; 36: E1373- E1384.

13. Krupkova O, Sekiguchi M, Klasen J, et al. Epigallocatechin 3-gallate suppresses interleukin-1beta-induced inflammatory responses in intervertebral disc cells in vitro and reduces radiculopathic pain in rats. Eur Cell Mater. 2014; 28: 372- 386.

14. Nakamae T, Ochi M, Olmarker K. Pharmacological inhibition of tumor necrosis factor may reduce pain behavior changes induced by experimental disc puncture in the rat: an experimental study in rats. Spine. 2011; 36: E232- E236.

15. Carragee EJ, Don AS, Hurwitz EL, Cuellar JM, Carrino JA, Herzog R. 2009 ISSLS prize winner: does discography cause accelerated progression of degeneration changes in the lumbar disc: a ten-year matched cohort study. Spine. 2009; 34: 2338- 2345.

16. Boettcher M, McManus MT. Choosing the right tool for the job: RNAi, TALEN, or CRISPR. Mol Cell. 2015; 58: 575- 585.

17. Qi LS, Larson MH, Gilbert LA, et al. Repurposing CRISPR as an RNA-guided platform for sequence-specific control of gene expression. Cell. 2013; 152: 1173- 1183.

18. Gaj T, Gersbach CA, Barbas CF III. ZFN, TALEN, and CRISPR/Cas-based methods for genome engineering. Trends Biotechnol. 2013; 31: 397- 405.

19. Hsu PD, Lander ES, Zhang F. Development and applications of CRISPR-Cas9 for genome engineering. Cell. 2014; 157: 1262- 1278.

20. Ran FA, Hsu PD, Wright J, Agarwala V, Scott DA, Zhang F. Genome engineering using the CRISPR-Cas9 system. Nat Protoc. 2013; 8: 2281- 2308.

21. Jinek M, Chylinski K, Fonfara I, Hauer M, Doudna JA, Charpentier E. A programmable dual-RNA-guided DNA endonuclease in adaptive bacterial immunity. Science. 2012; 337: 816- 821.

22. Jinek M, East A, Cheng A, Lin S, Ma E, Doudna J. RNA-programmed genome editing in human cells. Elife. 2013; 2: e00471.

23. Nishimasu H, Ran FA, Hsu PD, et al. Crystal structure of Cas9 in complex with guide RNA and target DNA. Cell. 2014; 156: 935- 949.

24. Jinek M, Jiang F, Taylor DW, et al. Structures of Cas9 endonucleases reveal RNA-mediated conformational activation. Science. 2014; 343:1247997.

25. Doench JG, Fusi N, Sullender M, et al. Optimized sgRNA design to maximize activity and minimize off-target effects of CRISPR-Cas9. Nat Biotechnol. 2016; 34: 184- 191.

26. Slaymaker IM, Gao L, Zetsche B, Scott DA, Yan WX, Zhang F. Rationally engineered Cas9 nucleases with improved specificity. Science. 2016; 351: 84- 88.

27. Ran FA, Hsu PD, Lin CY, et al. Double nicking by RNA-guided CRISPR Cas9 for enhanced genome editing specificity. Cell. 2013; 154: 1380- 1389.

28. Wang H, Yang H, Shivalila CS, et al. One-step generation of mice carrying mutations in multiple genes by CRISPR/Cas-mediated genome engineering. Cell. 2013; 153: 910- 918.

29. Hsu PD, Scott DA, Weinstein JA, et al. DNA targeting specificity of RNA-guided Cas9 nucleases. Nat Biotechnol. 2013; 31: 827- 832.

30. Dong Z, Huang M, Liu Z, et al. Focused screening of mitochondrial metabolism reveals a crucial role for a tumor suppressor Hbp1 in ovarian reserve. Cell Death Differ. 2016; 23: 1602- 1614.

31. Jost M, Chen Y, Gilbert LA, et al. Combined CRISPRi/a-based chemical genetic screens reveal that Rigosertib is a microtubule-destabilizing agent. Mol Cell. 2017; 68: 210- 223. e216.

32. Sun L, Lutz BM, Tao YX. The CRISPR/Cas9 system for gene editing and its potential application in pain research. Transl Perioper Pain Med. 2016; 1: 22- 33.

33. Wang H, La Russa M, Qi LS. CRISPR/Cas9 in genome editing and beyond. Annu Rev Biochem. 2016; 85: 227- 264.

34. Maruyama T, Dougan SK, Truttmann MC, Bilate AM, Ingram JR, Ploegh HL. Increasing the efficiency of precise genome editing with CRISPR-Cas9 by inhibition of nonhomologous end joining. Nat Biotechnol. 2015; 33: 538- 542.

35. Miyaoka Y, Berman JR, Cooper SB, et al. Systematic quantification of HDR and NHEJ reveals effects of locus, nuclease, and cell type on genome-editing. Sci Rep. 2016; 6:23549.

36. Perez-Pinera P, Kocak DD, Vockley CM, et al. RNA-guided gene activation by CRISPR-Cas9-based transcription factors. Nat Methods. 2013; 10: 973- 976.

37. Gilbert LA, Larson MH, Morsut L, et al. CRISPR-mediated modular RNA-guided regulation of transcription in eukaryotes. Cell. 2013; 154: 442- 451.

38. Thakore PI, D'Ippolito AM, Song LY, et al. Highly specific epigenome editing by CRISPR-Cas9 repressors for silencing of distal regulatory elements. Nat Methods. 2015; 12: 1143– 1149.

39. Cox DBT, Gootenberg JS, Abudayyeh OO, et al. RNA editing with CRISPR-Cas13. Science. 2017; 358: 1019- 1027.

40. Oh CD, Im HJ, Suh J, Chee A, An H, Chen D. Rho-associated kinase inhibitor immortalizes rat nucleus pulposus and annulus Fibrosus cells: establishment of intervertebral disc cell lines with novel approaches. Spine. 2016; 41: E255- E261.

41. Kluba T, Niemeyer T, Gaissmaier C, Grunder T. Human anulus fibrosis and nucleus pulposus cells of the intervertebral disc: effect of degeneration and culture system on cell phenotype. Spine. 2005; 30: 2743- 2748.

42. Ede DF, Weston J, Davis B, Lam L, Lawrence B, Bowles RD. Regulating hADSC ECM Phenotype via CRISPR epigenome editing for IVD tissue engineering. Transactions of the

Annual Meeting of the Orthopaedic Research Society, Orthopaedic Research Society, New Orleands, LA; 2018.

43. Yang M, Zhang L, Stevens J, Gibson G. CRISPR/Cas9 mediated generation of stable chondrocyte cell lines with targeted gene knockouts; analysis of an aggrecan knockout cell line. Bone. 2014; 69: 118- 125.

44. Huang Y, Askew EB, Knudson CB, Knudson W. CRISPR/Cas9 knockout of HAS2 in rat chondrosarcoma chondrocytes demonstrates the requirement of hyaluronan for aggrecan retention. Matrix Biol. 2016; 56: 74- 94.

45. Bluhm B, Ehlen HWA, Holzer T, et al. miR-322 stabilizes MEK1 expression to inhibit RAF/MEK/ERK pathway activation in cartilage. Development. 2017; 144: 3562- 3577.

46. Krock E, Currie JB, Weber MH, et al. Nerve growth factor is regulated by toll-like receptor 2 in human intervertebral discs. J Biol Chem. 2016; 291: 3541- 3551.

47. Johnson ZI, Gogate SS, Day R, et al. Aquaporin 1 and 5 expression decreases during human intervertebral disc degeneration: novel HIF-1-mediated regulation of aquaporins in NP cells. Oncotarget. 2015; 6: 11945- 11958.

48. Walter BA, Purmessur D, Moon A, et al. Reduced tissue osmolarity increases Trpv4 expression and pro-inflammatory cytokines in intervertebral disc cells. Eur Cell Mater. 2016; 32: 123- 136.

49. Bridgen DT, Gilchrist CL, Richardson WJ, et al. Integrin-mediated interactions with extracellular matrix proteins for nucleus pulposus cells of the human intervertebral disc. J Orthop Res. 2013; 31: 1661- 1667.

50. Millard M, Odde S, Neamati N. Integrin targeted therapeutics. Theranostics. 2011; 1: 154- 188.

51. Vincent F, Duncton MAJ. TRPV4 agonists and antagonists. Curr Top Med Chem. 2011; 11: 2216- 2226.

52. Hwang PY, Jing LF, Chen J, et al. N-cadherin is key to expression of the nucleus pulposus cell phenotype under selective substrate culture conditions. Sci Rep. 2016; 6:28038.

53. Farhang NL, Bowles RD. Lentiviral CRISPR epigenome editing: a potential gene therapy strategy for disc degeneration. Transactions of the Annual Meeting of the Orthopaedic Research Society, Orthopaedic Research Society, New Orleans, LA; 2018.

54. Meyer MB, Benkusky NA, Pike JW. Selective distal enhancer control of the Mmp13 gene identified through clustered regularly interspaced short palindromic repeat (CRISPR) genomic deletions. J Biol Chem. 2015; 290: 11093- 11107.

55. Gilbert LA, Horlbeck MA, Adamson B, et al. Genome-scale CRISPR-mediated control of gene repression and activation. Cell. 2014; 159: 647- 661.

56. Shalem O, Sanjana NE, Hartenian E, et al. Genome-scale CRISPR-Cas9 knockout screening in human cells. Science. 2014; 343: 84- 87.

57. Wang T, Wei JJ, Sabatini DM, Lander ES. Genetic screens in human cells using the CRISPR-Cas9 system. Science. 2014; 343: 80- 84.

58. Fujita T, Fujii H. Efficient isolation of specific genomic regions and identification of associated proteins by engineered DNA-binding molecule-mediated chromatin

immunoprecipitation (enChIP) using CRISPR. Biochem Biophys Res Commun. 2013; 439: 132- 136.

59. Zeng Y, Danielson KG, Albert TJ, Shapiro IM, Risbud MV. HIF-1α is a regulator of galectin-3 expression in the intervertebral disc. J Bone Miner Res. 2007; 22: 1851- 1861.

60. Deng W, Shi X, Tjian R, Lionnet T, Singer RH. CASFISH: CRISPR/Cas9-mediated in situ labeling of genomic loci in fixed cells. Proc Natl Acad Sci U S A. 2015; 112: 11870- 11875.

61. Nerlich AG, Bachmeier BE, Boos N. Expression of fibronectin and TGF-β1 mRNA and protein suggest altered regulation of extracellular matrix in degenerated disc tissue. Eur Spine J. 2005; 14: 17- 26.

62. Weiler C, Nerlich A, Zipperer J, Bachmeier B, Boos N. 2002 SSE award competition in basic science: expression of major matrix metalloproteinases is associated with intervertebral disc degradation and resorption. Eur Spine J. 2002; 11: 308- 320.

63. Gawri R, Mwale F, Ouellet J, et al. Development of an organ culture system for long-term survival of the intact human intervertebral disc. Spine. 2011; 36: 1835- 1842.

64. Chan SCW, Burki A, Bonel HM, Benneker LM, Gantenbein-Ritter B. Papain-induced in vitro disc degeneration model for the study of injectable nucleus pulposus therapy. Spine J. 2013; 13: 273- 283.

65. Krupkova O, Hlavna M, Amir Tahmasseb J, et al. An inflammatory nucleus pulposus tissue culture model to test molecular regenerative therapies: validation with epigallocatechin 3-gallate. Int J Mol Sci. 2016; 17:1640.

66. Song M. The CRISPR/Cas9 system: their delivery, in vivo and ex vivo applications and clinical development by startups. Biotechnol Prog. 2017; 33: 1035- 1045.

67. Lee K. Nanoparticle delivery of Cas9 ribonucleoprotein and donor DNA in vivo. Mol Ther. 2017; 25: 237- 237.

68. Kim S, Kim D, Cho SW, Kim J, Kim JS. Highly efficient RNA-guided genome editing in human cells via delivery of purified Cas9 ribonucleoproteins. Genome Res. 2014; 24: 1012- 1019.

69. Adkar SS, Brunger JM, Willard VP, Wu CL, Gersbach CA, Guilak F. Genome engineering for personalized arthritis therapeutics. Trends Mol Med. 2017; 23: 917- 931.

70. Craft AM, Rockel JS, Nartiss Y, Kandel RA, Alman BA, Keller GM. Generation of articular chondrocytes from human pluripotent stem cells. Nat Biotechnol. 2015; 33: 638- 645.

71. Henao-Mejia J, Williams A, Rongvaux A, Stein J, Hughes C, Flavell RA. Generation of genetically modified mice using the CRISPR-Cas9 genome-editing system. Cold Spring Harb Protoc. 2016; 2016(2): 150- 159. https://doi.org/10.1101/pdb.prot09070.

72. Zhou XQ, Xin JG, Fan NN, et al. Generation of CRISPR/Cas9-mediated gene-targeted pigs via somatic cell nuclear transfer. Cell Mol Life Sci. 2015; 72: 1175- 1184.

73. Inui M, Miyado M, Igarashi M, et al. Rapid generation of mouse models with defined point mutations by the CRISPR/Cas9 system. Sci Rep. 2014; 4: 5396.

74. Lupianez DG, Kraft K, Heinrich V, et al. Disruptions of topological chromatin domains cause pathogenic rewiring of gene-enhancer interactions. Cell. 2015; 161: 1012- 1025.

75. Staahl BT, Benekareddy M, Coulon-Bainier C, et al. Efficient genome editing in the mouse brain by local delivery of engineered Cas9 ribonucleoprotein complexes. Nat Biotechnol. 2017; 35: 431- 434.

76. Chan D, Song Y, Sham P, Cheung KM. Genetics of disc degeneration. Eur Spine J. 2006; 15(suppl 3): S317- S325.

77. Mayer JE, Iatridis JC, Chan D, Qureshi SA, Gottesman O, Hecht AC. Genetic polymorphisms associated with intervertebral disc degeneration. Spine J. 2013; 13: 299- 317.

78. Lei Y, Zhang X, Su J, et al. Targeted DNA methylation in vivo using an engineered dCas9-MQ1 fusion protein. Nat Commun. 2017; 8: 16026.

79. Braun CJ, Bruno PM, Horlbeck MA, Gilbert LA, Weissman JS, Hemann MT. Versatile in vivo regulation of tumor phenotypes by dCas9-mediated transcriptional perturbation. Proc Natl Acad Sci U S A. 2016; 113: E3892- E3900.

80. Liao HK, Hatanaka F, Araoka T, et al. In vivo target gene activation via CRISPR/Cas9-mediated trans-epigenetic modulation. Cell. 2017; 171(7): 1495- 1507.e15.

81. Alini M, Eisenstein SM, Ito K, et al. Are animal models useful for studying human disc disorders/degeneration? Eur Spine J. 2008; 17: 2- 19.

82. Yang LH, Guell M, Niu D, et al. Genome-wide inactivation of porcine endogenous retroviruses (PERVs). Science. 2015; 350: 1101- 1104.

83. Wu MM, Wei CH, Lian ZX, et al. Rosa26-targeted sheep gene knock-in via CRISPR-Cas9 system. Sci Rep. 2016; 6:24360.

84. Ni W, Qiao J, Hu SW, et al. Efficient gene knockout in goats using CRISPR/Cas9 system. PLoS ONE. 2014; 9: e106718.

85. Wang ZD. Genome engineering in cattle: recent technological advancements. Chromosome Res. 2015; 23: 17- 29.

86. Zou Q, Wang X, Liu Y, et al. Generation of gene-target dogs using CRISPR/Cas9 system. J Mol Cell Biol. 2015; 7: 580- 583.

87. Chen YC, Zheng YH, Kang Y, et al. Functional disruption of the dystrophin gene in rhesus monkey using CRISPR/Cas9. Hum Mol Genet. 2015; 24: 3764- 3774.

88. Shah AN, Davey CF, Whitebirch AC, Miller AC, Moens CB. Rapid reverse genetic screening using CRISPR in zebrafish. Nat Methods. 2015; 12: 535- 540.

89. Santos-Ledo A, Garcia-Macia M, Campbell PD, Gronska M, Marlow FL. Kinesin-1 promotes chondrocyte maintenance during skeletal morphogenesis. PLoS Genet. 2017; 13: e1006918.

90. Lim YW, Lo HP, Ferguson C, et al. Caveolae protect notochord cells against catastrophic mechanical failure during development. Curr Biol. 2017; 27: 1968- 1981.e7.

91. Gao W, Chen C, Zhou T, et al. Rare coding variants in MAPK7 predispose to adolescent idiopathic scoliosis. Hum Mutat. 2017; 38: 1500- 1510.

92. Ousterout DG, Kabadi AM, Thakore PI, Majoros WH, Reddy TE, Gersbach CA. Multiplex CRISPR/Cas9-based genome editing for correction of dystrophin mutations that cause Duchenne muscular dystrophy. Nat Commun. 2015; 6: 6244.

93. Anderson DG, Markova D, Adams SL, Pacifici M, An HS, Zhang Y. Fibronectin splicing variants in human intervertebral disc and association with disc degeneration. Spine. 2010; 35: 1581-1588.

94. Yao Y, Shang J, Song W, Deng Q, Liu H, Zhou Y. Global profiling of the gene expression and alternative splicing events during hypoxia-regulated chondrogenic differentiation in human cartilage endplate-derived stem cells. Genomics. 2016; 107: 170-177.

95. Sakai D, Andersson GB. Stem cell therapy for intervertebral disc regeneration: obstacles and solutions. Nat Rev Rheumatol. 2015; 11: 243-256.

96. Vadala G, Russo F, Di Martino A, Denaro V. Intervertebral disc regeneration: from the degenerative cascade to molecular therapy and tissue engineering. J Tissue Eng Regen Med. 2015; 9: 679-690.

97. Moon SH, Nishida K, Gilbertson LG, et al. Biologic response of human intervertebral disc cells to gene therapy cocktail. Spine. 2008; 33: 1850-1855.

98. Ren S, Liu Y, Ma J, et al. Treatment of rabbit intervertebral disc degeneration with co-transfection by adeno-associated virus-mediated SOX9 and osteogenic protein-1 double genes in vivo. Int J Mol Med. 2013; 32: 1063-1068.

99. Karlsen TA, Pernas PF, Staerk J, Caglayan S, Brinchmann JE. Generation of IL1 beta-resistant chondrocytes using CRISPR-CAS genome editing. Osteoarthritis Cartilage. 2016; 24: S325-S325.

100. Sakai D, Mochida J, Yamamoto Y, et al. Transplantation of mesenchymal stem cells embedded in Atelocollagen gel to the intervertebral disc: a potential therapeutic model for disc degeneration. Biomaterials. 2003; 24: 3531-3541.

101. Ganey T, Hutton WC, Moseley T, Hedrick M, Meisel HJ. Intervertebral disc repair using adipose tissue-derived stem and regenerative cells experiments in a canine model. Spine. 2009; 34: 2297-2304.

102. Blanquer SB, Grijpma DW, Poot AA. Delivery systems for the treatment of degenerated intervertebral discs. Adv Drug Deliv Rev. 2015; 84: 172-187.

103. Sakai D, Grad S. Advancing the cellular and molecular therapy for intervertebral disc disease. Adv Drug Deliv Rev. 2015; 84: 159-171.

104. Huang YC, Urban JPG, Luk KDK. OPINION intervertebral disc regeneration: do nutrients lead the way? Nature Reviews Rheumatology. 2014; 10: 561-566.

105. Urban JPG, Smith S, Fairbank JCT. Nutrition of the intervertebral disc. Spine. 2004; 29: 2700-2709.

106. Farhang N, Brunger JM, Stover JD, et al. CRISPR-based epigenome editing of cytokine receptors for the promotion of cell survival and tissue deposition in inflammatory environments. Tissue Eng Pt A. 2017; 23: 738-749.

107. Brunger JM, Zutshi A, Willard VP, Gersbach CA, Guilak F. CRISPR/Cas9 editing of murine induced pluripotent stem cells for engineering inflammation-resistant tissues. Arthritis Rheumatol. 2017; 69: 1111-1121.

108. Brunger JM, Zutshi A, Willard VP, Gersbach CA, Guilak F. Genome engineering of stem cells for autonomously regulated, closed-loop delivery of biologic drugs. Stem Cell Rep. 2017; 8: 1202-1213.

109. Khatiwala R, Cai CX. Strategies to enhance the effectiveness of adult stem cell therapy for ischemic heart diseases affecting the elderly patients. Stem Cell Rev Rep. 2016; 12: 214- 223.

110. Stover JD, Farhang N, Berrett KC, Gertz J, Lawrence B, Bowles RD. CRISPR epigenome editing of AKAP150 in DRG neurons abolishes degenerative IVD-induced neuronal activation. Mol Ther. 2017; 25: 2014- 2027.

111. Suzuki K, Tsunekawa Y, Hernandez-Benitez R, et al. In vivo genome editing via CRISPR/Cas9 mediated homology-independent targeted integration. Nature. 2016; 540: 144- 149.

112. Tebas P, Stein D, Tang WW, et al. Gene editing of CCR5 in autologous CD4 T cells of persons infected with HIV. N Engl J Med. 2014; 370: 901- 910.

113. Su S, Hu B, Shao J, et al. CRISPR-Cas9 mediated efficient PD-1 disruption on human primary T cells from cancer patients. Sci Rep. 2016; 6:20070.

114. Cyranoski D. CRISPR gene-editing tested in a person for the first time. Nature. 2016; 539: 479.

115. Baylis F, McLeod M. First-in-human phase 1 CRISPR gene editing cancer trials: are we ready? Curr Gene Ther. 2017; 17(4): 309- 319.

116. Ortinski PI, O'Donovan B, Dong XY, Kantor B. Integrase-deficient lentiviral vector as an all-in-one platform for highly efficient CRISPR/Cas9-mediated gene editing. Mol Ther Methods Clin D. 2017; 5: 153- 164.

117. Gori JL, Hsu PD, Maeder ML, Shen S, Welstead GG, Bumcrot D. Delivery and specificity of CRISPR/Cas9 genome editing technologies for Human Gene Therapy. Hum Gene Ther. 2015; 26: 443- 451.

118. Shinwari ZK, Tanveer F, Khalil AT. Ethical issues regarding CRISPR mediated genome editing. Curr Issues Mol Biol. 2017; 26: 103- 110.

119. Cribbs AP, Perera SMW. Science and bioethics of CRISPR-Cas9 gene editing: an analysis towards separating facts and fiction. Yale J Biol Med. 2017; 90: 625- 634.

120. Wieser S, Horisberger B, Schmidhauser S, et al. Cost of low back pain in Switzerland in 2005. Eur J Health Econ. 2011; 12: 455- 467.

121. Guterl CC, See EY, Blanquer SB, et al. Challenges and strategies in the repair of ruptured annulus fibrosus. Eur Cell Mater. 2013; 25: 1- 21.

Chapter 7

Synthesis

Low back pain (LBP) affects up to 84% of people at some point in their life, causing loss of productivity, disability, and a huge global socio-economic burden [1]. One of the main causes of LBP is degenerative disc disease (DDD), a multifactorial syndrome combining intervertebral disc (IVD) degeneration, inflammation, and nociception [2]. Mechanical loading is a well-known contributor to IVD degeneration and DDD [2]. However, the underlying mechanisms of the mechanosensing and mechanotransduction molecular pathways are under-investigated. This partly contributes to the suboptimal design of current pharmacological treatments, which have unclear mechanisms of action, low effect sizes [1], can provoke side effects over the long term [3], and do not take into account the mechanical nature of LBP. From a mechanobiological perspective, transient receptor potential (TRP) channels constitute interesting therapeutic target candidates for the treatment of DDD and LBP. These non-selective calcium-permeable transmembrane channels can sense various stimuli including changes in temperature, pH, osmolarity, as well as oxidative and mechanical stress [4]. The mechanosensitive member 4 of the vanilloid subfamily (TRPV4) is especially intriguing, as it is known to transduce mechanical, inflammatory and pain signals in joint tissues [5]. Nevertheless, TRPV4 has never been studied in the context of IVD mechanotransduction. The overall goal of this thesis was to investigate the potential role of TRPV4 in mediating hyperphysiological mechanical signals in the IVD, and its relevance as a therapeutic target to treat LBP. To this end, the following specific aims were addressed.

Aim 1: To develop a novel 3D hydrogel that combines mechanical strength and biofunctionality for mechanotransduction studies

Aim 2: To investigate the role of TRPV4 in transducing hyperphysiological dynamic compression

Aim 3: To investigate the role of TRPV4 in transducing hyperphysiological cyclic stretching

7.1 Contributions to the field

As a first step in investigating TRPV4 in IVD cell mechanotransduction, we established a suitable in vitro compression model. Mechanotransduction in vivo takes place in a three-dimensional (3D) microenvironment with instructive biochemical cues and specific mechanical stimuli [6]. Conducting mechanotransduction studies with in vivo relevance thus requires advanced 3D culture systems that possess both the biofunctionality of native extracellular matrix proteins, and tunable mechanical properties. To this end, we developed novel agarose-collagen composite hydrogels that: (i) mimic native tissues constituted of non-fibrillar matrix and collagens; (ii) combine the mechanical properties of agarose and the biofunctionality of collagen I; and (iii) allow the exploration of mechanical loading and cellular mechanotransduction. More specifically, we showed that agarose-collagen hydrogels form a homogenous interconnected network of the two polymers that retain strong mechanical properties and dimensional stability over time. Bovine nucleus pulposus (NP) cells embedded in agarose-collagen hydrogels

were viable, displayed a low proliferation rate and a round morphology typical of IVD cells in vivo. Moreover, agarose-collagen scaffolds outperformed agarose hydrogels in terms of matrix production. The gene expression of collagen I and II, as well as aggrecan, increased at day 7 in blended hydrogels, and the glycosaminoglycan content was also increased compared to the agarose hydrogels at this time-point. We finally confirmed our hypothesis that physical blending of collagen I into agarose enhances the biofunctionality of the construct by promoting cell adhesion and mechanotransduction ability, as measured by focal adhesion kinase (FAK) activation. This highly biomimetic and reproducible model system and the developed protocols (e.g. hydrogel fabrication, cellular assays, mechanical loading, RNA and protein extraction, etc.) can further be used to model other native tissues composed of non-fibrillar matrix and collagens and to investigate their mechanotransduction mechanisms.

In a second step, we used our novel agarose-collagen in vitro models, as well as mouse in vivo models to investigate the role of TRPV4 in transducing hyperphysiological dynamic compression in NP cells cultured in the above-described new model, and IVDs. We showed that hyperphysiological dynamic compression induces IVD degeneration in vivo, as well as cell damage and increased inflammation in vitro, as measured by lactate dehydrogenase (LDH) and prostaglandin E2 (PGE2) release. Importantly, we demonstrated for the first time that TRPV4 inhibition via a selective antagonist significantly reduces compression-induced LDH and PGE2 release and activates the extracellular signal-regulated kinases 1/2 (ERK) pathway. Finally, trpv4-deficient mice displayed mild IVD degeneration and a significantly reduced expression of cyclooxygenase 2 (COX2, the enzyme that synthesizes PGE2) compared to wild-type (WT) mice. This study is, to our knowledge, the first to show that TRPV4 regulates COX2/PGE2 and mediates cell damage induced by hyperphysiological dynamic compression, possibly via ERK, in NP cells and IVDs. Our findings suggest that targeted TRPV4 modulation might constitute a promising therapeutic strategy to treat patients suffering from IVD pathologies caused by aberrant mechanical stress.

We finally investigated the role of TRPV4 as a mechanotransducer and potential therapeutic target in a model that was more clinically relevant, as we used human degenerated annulus fibrosus (AF) cells that were cyclically stretched at a hyperphysiological strain. We first developed a model with an inflammatory response to hyperphysiological stretching representative of early-stage AF injury. More specifically, we showed that hyperphysiological cyclic stretching increases the gene expression of pro-inflammatory and catabolic mediators (interleukins 6 and 8 (IL6, IL8), COX2, and matrix metalloproteinase 1); reduces the expression of anabolic genes (collagen II and aggrecan); increases PGE2 release; and activates the p38 mitogen-activated protein kinase (MAPK). TRPV4 pharmacological inhibition and gene editing were then tested as potential therapeutic approaches to rescue the induced mechanoflammation. To this end, we established the first successful gene editing of human herniated and degenerated AF cells via CRISPR-Cas9 to knock out the TRPV4 gene (TRPV4 KO). We demonstrated that TRPV4 pharmacological inhibition significantly reduces the stretch-induced upregulation of IL6, IL8, and COX2 gene expression, PGE2 release, and p38 phosphorylation. Remarkably, increases in IL8 mRNA levels caused by hyperphysiological cyclic stretching were completely prevented by TRPV4 KO. TRPV4 KO further reduced the release of IL6 and IL8.

123

This study thus identifies for the first time TRPV4 as a mediator of stretch-induced inflammation in human AF cells. While the CRISPR-based technology allowed us to confirm the role of TRPV4 in regulating IL6 and IL8, it could be used in future studies to modulate other molecular targets involved in IVD pathologies. Together with our findings on TRPV4-dependent compression-induced cell damage and inflammation, this study highlights a novel link between mechanical hyperphysiological loading and injury mechanisms leading to IVD degeneration and elucidates an important pathway in the complex process that ultimately leads to chronic LBP. This knowledge could be further applied to design novel pharmacological therapies targeting TRPV4 and its molecular partners.

7.2 Limitations

The conclusions of this thesis are limited by several aspects. The sample size used for statistical analysis in our studies typically comprised n = 3-5 biological replicates. Although this rather small sample size is typical for basic in vitro studies, it can limit the statistical power of a study. The choice of the number of biological replicates was dictated by several technical limitations. When working with human primary degenerated cells, we were mainly limited by initially low cell numbers after cell isolation and low proliferation rates in culture. Moreover, cells were cultured only up to passage 2 to avoid cell dedifferentiation due to culture on 2D plastic. This prevented the achievement of high cell numbers via cell expansion. These problems are common in the IVD research field, as IVDs are known to have very low cellularity and cell proliferation rate that decrease even further with IVD degeneration and cell senescence [7]. In the case of bovine NP cells embedded in 3D agarose-collagen hydrogels, the cell number was still a concern, but to a lesser extent. In fact, healthy bovine NP cells proliferate relatively fast compared to degenerated human IVD cells. Nevertheless, in order to achieve a physiological IVD cell density of $4x10^6$ cells/ml in the hydrogels, $6.4x10^5$ cells/gel were required. Therefore, every experiment necessitated a very high initial cell number. Other technical problems that hampered the increase of the sample size for hydrogel studies included the relatively time-consuming hydrogel fabrication process, pre-culture time, and optimized protocols to extract RNA and proteins from 3D scaffolds.

Several in vitro and vivo models were used in this thesis, each with its own advantages and drawbacks. With respect to in vitro models, we either used bovine NP cells embedded in 3D agarose-collagen hydrogels or human degenerated AF cells cultured in 2D. Although whole IVDs are useful models, isolated cells were preferred for three main reasons: (i) intact human IVDs cannot be obtained in Switzerland; (ii) it is challenging and time-consuming to extract RNA from tissues with low cellularity and high proteoglycan content like healthy bovine IVDs [8]; and (iii) isolated cells allow a more standardized investigation of precise molecular mechanisms compared to tissues. Bovine IVD cells are healthy and can be obtained in high numbers for 3D cell culture. However, they do not perfectly recapitulate the human cellular physiology. When possible, we privileged the use of human cells, like in the stretching study in Chapter 5. However, the lack of availability of healthy human disc tissue in Switzerland prompted us to isolate cells from

degenerated and herniated IVD biopsies. While degenerated IVD cells are useful to test therapeutic approaches aiming to revert their pathological phenotype, they do not allow to accurately study mechanisms leading from a healthy to a pathological phenotype. Another aspect to consider is the variability between different human donors, which is reflected in the obtained data. Human patients varied in age, sex, IVD pathology, and grade of degeneration. Moreover, although we aimed to use only AF cells in the stretching study (Chapter 5), it is challenging to separate the NP tissue from the AF tissue, especially in highly degenerated samples with an unclear NP/AF boundary. AF tissue was intraoperatively excised and digested, but cells were not sorted to distinguish between AF and NP cells using NP cell specific markers such as forkhead box F1 (FOXF1), carbonic anhydrase XII (CA12), cytokeratin-19 and paired box-1 (PAX1) [9]. Another disadvantage of the in vitro model of the stretching study (Chapter 5) is its 2D nature, which does not mimic the complex 3D microenvironment of IVD cells. However, this 2D model was chosen because it is one of the best-established ones for cell stretching [10].

We used a mouse in vivo model in preliminary experiments to study the effects of hyperphysiological dynamic compression or TRPV4 KO. The mouse is an excellent in vivo model to investigate mechanical loading via tail compression and offers relative ease of access to preliminary pre-clinical data. However, the small size of murine IVDs prevents harvesting a sufficient amount of IVD cells for in vitro experiments, especially for encapsulation in our agarose-collagen hydrogels. This required the use of the bovine animal model additionally in the compression study in Chapter 4 and prevented the direct comparison between in vivo and vitro experiments.

A final limitation is that our experimental models mostly simulate acute low-grade inflammation reminiscent of early-stage IVD injury or DDD, but not chronic inflammation. By stimulating the cells with a hyperphysiological magnitude and a single short continuous loading, we obtained a transient inflammation that resolved over time. This allowed us to capture the very fast effects of TRPV4. In fact, TRPV4 activation was shown to cause an increase in intracellular calcium influx that was only stable for a few minutes [11]. Moreover, the density of TRPV4 at the plasma membrane decreases within 20 min, as the channels translocate to the recycling endosomes [11]. While our data suggest that TRPV4 transduce hyperphysiological mechanical signals into cell damage and inflammation via the ERK and p38 MAPKs, the short time-frame provided by acute inflammation prevented us to devise a clear and complete mechanism of action of the TRPV4 inhibitor. Future studies should further investigate the mechanisms related to TRPV4 in a model of chronic mechanoflammation that can be obtained by applying repetitive hyperphysiological mechanical loading.

7.3 Future perspectives

This thesis investigated the role of TRPV4 in hyperphysiological mechanical loading and acute inflammation of IVD cells and IVDs. Additionally, the effect of TRPV4 KO was investigated in unloaded mice in a preliminary experiment (Chapter 4). Our findings

suggest a dual role of TRPV4 in the IVD. On one hand, our data show that TRPV4 pharmacological inhibition significantly reduces cell damage and inflammation induced by hyperphysiological dynamic mechanical loading (Chapter 4-5). On the other hand, TRPV4 expression is necessary and plays a role in IVD homeostasis. In fact, trpv4 KO murine IVDs displayed mild degeneration compared to WT IVDs (Chapter 4). Although TRPV4 is a promising therapeutic target to treat DDD and LBP, its potential dual role poses challenges for the design of a novel therapeutic approach. Moreover, TRPV4 is ubiquitous and can be activated by different stimuli [12]. Therefore, a therapy targeting TRPV4 needs to be carefully elaborated in order to maintain the beneficial and necessary roles of TRPV4 in homeostasis.

Follow-up projects should first investigate in vitro the exact mechanism of action of TRPV4 inhibitors in other contexts than hyperphysiological mechanical loading and acute inflammation in the IVD. These experimental settings should include unloaded samples, physiological loading, and repetitive hyperphysiological loading inducing chronic inflammation. Our unpublished preliminary data showed that the selective TRPV4 inhibitor did not cause cellular toxicity at the concentrations and durations used in our experiments in both unloaded bovine and human IVD cells, as measured by the LDH assay. However, we did not measure other biological responses. The mechanism of action should be further verified in a pre-clinical model, such as the mouse tail compression model. Mice would be either intradiscally injected with a TRPV4 antagonist (or saline solution) or genetically modified to have reduced or no TRPV4 expression and mechanically loaded (or not) at different regimes. Several KO mouse models of TRPV4 have already been developed [12].

Following the above-mentioned studies that will lead to a better understanding of the therapeutic potential of TRPV4 modulation, subsequent steps should focus on clinical translation. Clinical trials examining TRPV4 inhibition in the context of DDD and LBP are currently lacking. A phase I clinical trial would first test the safety of TRPV4 inhibitor administration in a small sample of healthy subjects. Interestingly, a selective antagonist of TRPV4 was recently administered to healthy volunteers and heart failure patients without any safety concern [13]. Phase II-III trials would then test the efficacy of this therapeutic approach in a higher number of patients affected by DDD and LBP. Doses as well as drug delivery modes should be further tested. The TRPV4 inhibitor could be locally injected in the IVD or encapsulated in a hydrogel that would be injected in the vicinity of the painful IVD.

Finally, a futuristic approach could entail the knockdown or knockout of TRPV4 via gene editing, e.g. via the CRISPR-based technology as mentioned in Chapter 6. Considering the potential dual role of TRPV4, a conditional gene editing induced in case of excessive mechanical loading might be a desirable therapeutic strategy in the future. Nevertheless, several technical, safety and ethical issues need to be addressed before gene editing can be routinely used to treat DDD and LBP.

7.4 Conclusion

LBP is the leading cause of disability worldwide and a huge global socioeconomic burden. Costs associated with LBP are projected to further increase in the coming decades due to the growth and aging of the global population. Yet, the etiology of LBP is still poorly understood and current treatments are not targeted and have poor efficacy. This thesis investigated mechanical loading as one of the main contributors to IVD degeneration, DDD, and LBP. More specifically, we studied the molecular mechanisms leading from hyperphysiological loading to cell damage and inflammation and identified the TRPV4 ion channel as a mechanotransducer and potential novel therapeutic target to tackle LBP. We first developed 3D composite agarose-collagen hydrogels that combine mechanical strength and biofunctionality as novel tools for mechanotransduction studies. We then applied these hydrogels and a mouse in vivo model to investigate the role of TRPV4 in transducing hyperphysiological dynamic compression. In this compression study, we showed that TRPV4 regulates COX2/PGE2 and mediates cell damage induced by hyperphysiological dynamic compression, possibly via ERK, in NP cells and IVDs. In a final step, we investigated the role of TRPV4 in a model that was more clinically relevant, as we used human degenerated annulus fibrosus (AF) cells that were cyclically stretched at a hyperphysiological strain. For the purpose of this study, the first successful gene editing of human herniated and degenerated AF cells via CRISPR-Cas9 was established to knockout TRPV4. We found that TRPV4 inhibition and CRISPR-Cas9 KO significantly reduce inflammation induced by hyperphysiological stretching. Altogether, this thesis highlights a novel link between mechanical hyperphysiological loading and injury mechanisms leading to IVD degeneration and elucidates an important pathway in the complex process that eventually leads to chronic LBP. Future studies should clarify the exact mechanism of action of TRPV4 inhibition and KO, examine their potential to mitigate chronic inflammation, and further test the safety and efficacy of these therapeutic approaches in translational preclinical and clinical trials. If successful, a therapy specifically targeting TRPV4 to treat LBP would considerably contribute to easing the immense burden carried by patients and society.

7.5 References

1.   Balague, F., et al., Non-specific low back pain. Lancet, 2012. 379(9814): p. 482-91.

2.   Adams, M.A. and P.J. Roughley, What is intervertebral disc degeneration, and what causes it? Spine (Phila Pa 1976), 2006. 31(18): p. 2151-61.

3.   Foster, N.E., et al., Prevention and treatment of low back pain: evidence, challenges, and promising directions. Lancet, 2018. 391(10137): p. 2368-2383.

4.   Krupkova, O., J. Zvick, and K. Wuertz-Kozak, The Role of Transient Receptor Potential Channels in Joint Diseases. European Cells & Materials, 2017. 34: p. 180-201.

5.   McNulty, A.L., et al., TRPV4 as a therapeutic target for joint diseases. Naunyn Schmiedebergs Arch Pharmacol, 2015. 388(4): p. 437-50.

6. Martino, F., et al., Cellular Mechanotransduction: From Tension to Function. 2018. 9(824).

7. Gruber, H.E., et al., Increased cell senescence is associated with decreased cell proliferation in vivo in the degenerating human annulus. Spine J, 2009. 9(3): p. 210-5.

8. Lee, J.T.Y., K.M.C. Cheung, and V.Y.L. Leung, Extraction of RNA from tough tissues with high proteoglycan content by cryosection, second phase separation and high salt precipitation. Journal of Biological Methods; Vol 2, No 2 (2015), 2015.

9. Pattappa, G., et al., Diversity of intervertebral disc cells: phenotype and function. J Anat, 2012. 221(6): p. 480-96.

10. Friedrich, O., et al., Stretch in Focus: 2D Inplane Cell Stretch Systems for Studies of Cardiac Mechano-Signaling. Front Bioeng Biotechnol, 2019. 7: p. 55.

11. Baratchi, S., et al., The TRPV4 Agonist GSK1016790A Regulates the Membrane Expression of TRPV4 Channels. Front Pharmacol, 2019. 10: p. 6.

12. White, J.P.M., et al., TRPV4: Molecular Conductor of a Diverse Orchestra. Physiological Reviews, 2016. 96(3): p. 911-973.

13. Goyal, N., et al., Clinical Pharmacokinetics, Safety, and Tolerability of a Novel, First-in-Class TRPV4 Ion Channel Inhibitor, GSK2798745, in Healthy and Heart Failure Subjects. Am J Cardiovasc Drugs, 2019. 19(3): p. 335-342.

Appendix

TRPC6 in simulated microgravity of intervertebral disc cells

Alfredo Franco-Obregon[1,2,*], Elena Cambria[3,*], Helen Greutert[3], Timon Wernas[4], Wolfgang Hitzl[5,6], Marcel Egli[4], Miho Sekiguchi[7], Norbert Boos[8], Oliver Hausmann[9], Stephen J. Ferguson[3], Hiroshi Kobayashi[3,7,†], Karin Wuertz-Kozak[3,10,11,12,†]

[1] Department of Surgery, Yong Loo Lin School of Medicine, National University of Singapore, Singapore, Singapore

[2] BioIonic Currents Electromagnetic Pulsing Systems Laboratory, BICEPS, National University of Singapore, Singapore, Singapore

[3] Institute for Biomechanics, D-HEST, ETH Zurich, Hönggerbergring 64, 8093 Zurich, Switzerland

[4] School of Engineering and Architecture, Lucerne University of Applied Sciences and Arts, Lucerne, Switzerland

[5] Research Office (Biostatistics), Paracelsus Private Medical University, Salzburg, Austria

[6] Department of Ophthalmology and Optometry, Paracelsus Medical University Salzburg, Salzburg, Austria

[7] Department of Orthopaedic Surgery, School of Medicine, Fukushima Medical University, Fukushima, Japan

[8] Prodorso Center for Spinal Medicine, Zurich, Switzerland

[9] Neuro- and Spine Center, Hirslanden Klinik St. Anna, Lucerne, Switzerland

[10] Spine Center, Schön Klinik München Harlaching, 81547 Munich, Germany

[11] Academic Teaching Hospital and Spine Research Institute, Paracelsus Private Medical University, Salzburg, Austria

[12] Department of Health Science, University of Potsdam, Potsdam, Germany

[*] These authors contributed equally.

[†] These authors contributed equally.

Abstract

Purpose: Prolonged bed rest and microgravity in space cause intervertebral disc (IVD) degeneration. However, the underlying molecular mechanisms are not completely understood. Transient receptor potential canonical (TRPC) channels are implicated in mechanosensing of several tissues, but are poorly explored in IVDs.

Methods: Primary human IVD cells from surgical biopsies composed of both annulus fibrosus and nucleus pulposus (passage 1–2) were exposed to simulated microgravity and to the TRPC channel inhibitor SKF-96365 (SKF) for up to 5 days. Proliferative capacity, cell cycle distribution, senescence and TRPC channel expression were analyzed.

Results: Both simulated microgravity and TRPC channel antagonism reduced the proliferative capacity of IVD cells and induced senescence. While significant changes in cell cycle distributions (reduction in G1 and accumulation in G2/M) were observed upon SKF treatment, the effect was small upon 3 days of simulated microgravity. Finally, downregulation of TRPC6 was shown under simulated microgravity.

Conclusions: Simulated microgravity and TRPC channel inhibition both led to reduced proliferation and increased senescence. Furthermore, simulated microgravity reduced TRPC6 expression. IVD cell senescence and mechanotransduction may hence potentially be regulated by TRPC6 expression. This study thus reveals promising targets for future studies.

Keywords: intervertebral disc, simulated microgravity, senescence, TRP channels, mechanotransduction, gene expression

Introduction

Intervertebral discs (IVDs) show signs of degeneration as early as the second decade of life [1]. As normal physiological ageing and pathological degeneration recruit similar signalling cascades, pathological IVD degeneration can be described as accelerated tissue ageing, contributed to by multimodal stress-induced changes with ultimate tissue failure [2]. Although genetics plays an essential role in the onset of ageing and the progression of degeneration [3], mechanical loading and damage, particularly of the lumbar spine, have been identified as contributing factors [4]. Whereas physiological levels of mechanical stress support the metabolic balance of the IVD [5], hyper-physiological mechanical stresses or mechanical unloading biases the IVD towards catabolism, inflammation and reduced viability, hence promoting degeneration [6]. Mechanical unloading, occurring, e.g. during prolonged bed rest, causes long-lasting changes in IVDs [7, 8]. In fact, the changes in IVD morphology measured by magnetic resonance imaging after 21 days of bed rest in 7 healthy subjects persisted after 5 months [7]. The recovery of the IVDs was still incomplete 2 years after 60 days of bed rest [8]. Moreover, astronauts, who are exposed to microgravity during space flights, exhibit spinal lengthening [9], low back pain [10, 11] and an elevated risk of IVD herniation [12]. In vitro experiments [13] and animal studies conducted during space flight [14, 15] have shown degenerative biomechanical or biochemical effects of microgravity. To study microgravity on Earth, random positioning

131

machines (RPMs) are commonly used [16]. Signs of IVD degeneration were observed in mice discs cultured in a rotary wall vessel bioreactor [17], although this was not the case with rat IVDs [18].

During degeneration, IVD cells acquire numerous pathobiological features, including increased levels of cellular senescence [19, 20]. Affected cells possess a so-called senescence-associated secretory phenotype (SASP), characterized by proliferative dysfunction, unresponsiveness to mitogenic stimulation (and hence hampered cell cycle progression), as well as catabolic and inflammatory behaviour [20]. The molecular mechanisms leading to IVD degeneration and ageing are not yet completely understood. However, high levels of free calcium in the cartilaginous endplates are associated with IVD degeneration [21]. Furthermore, free calcium seems to contribute to IVD degeneration through the calcium-sensing receptor (CaSR) [22]. Recently, the expression of transient receptor potential (TRP) channels, a superfamily of ion channel with relevance in calcium regulation [23], has been demonstrated in the IVD [24,25,26]. The members of the canonical family (TRPC) are especially interesting. A direct correlation between TRPC6 expression and the degree of IVD degeneration has been recently shown [25], highlighting TRPC6 as a candidate for further studies on IVD pathobiology. Aside from TRPC6, the isoform TRPC1 may also be of specific relevance. TRPC1 and TRPC6 are both known to affect cell cycle progression in various cell types [27,28,29], and TRPC6 was shown to modulate cellular senescence [30]. Therefore, their modulation and (dys-) regulation may play a crucial role in IVD health, but also degeneration. Importantly, TRPC1 and TRPC6 have both been described as mechanosensitive [26]. TRP channels are therefore interesting candidates when aiming to link IVD mechanobiology with IVD ageing and degeneration. Interestingly, simulated microgravity was shown to depress TRPC1 expression associated with an accumulation of cells into G2/M, effectively stalling proliferation of mouse myoblasts [28, 31].

The aim of this study was to investigate the effects of simulated microgravity and TRPC channel pharmacological inhibition on human IVD cell proliferation, cell cycle progression and senescence (as key features of IVD degeneration).

Materials and methods

Cell isolation and culture

Primary cells were isolated from human IVD biopsies from patients undergoing spinal surgery (approved by the ethical committees in Zurich and Lucerne, Switzerland, and after informed consent), as previously described [32]. For patient demographics, see **Table 1**. Biopsies were composed of both annulus fibrosus and nucleus pulposus (with different ratio), as it is difficult to distinguish these tissues in degenerated samples. The *n* number in each experiment (between 4 and 6) represents the number of donors used per experimental condition.

Table 1: Patient demographics. F = female; M = male; L4/5 = lumbar 4–5; L5/S1 = lumbar 5-sacral 1; C6/7 = cervical 6–7; DDD = degenerative disc disease; uk = unknown

Patient number	Patient Age	Sex	Disc level	Type of disease	Pfirmann grade
1	62	F	L4/5	Spondylolisthesis	V
2	53	M	L5/S1	Herniation	IV
3	71	F	L4/5	DDD	II
4	42	F	L4/5	Herniation	IV
5	uk	uk	uk	uk	uk
6	46	M	L5/S1	DDD	V
7	43	F	L4/5	Herniation	IV
8	uk	uk	uk	uk	uk
9	41	F	L5/S1	Herniation	IV
10	47	F	L4/L5	Herniation	III
11	56	F	L3/4	Herniation	IV
12	57	M	L5/S1	DDD	IV
13	68	M	L4/5	Herniation	III
14	uk	uk	uk	uk	uk
15	40	F	C6/7	Herniation	III
16	44	M	L4/5	Herniation	IV

Cells were cultured in DMEM/F-12 (Gibco, 31330-038) with 10% FCS (Sigma-Aldrich, F7524) and 1% Anti-Anti (= 50 units/mL penicillin, 50 µg/mL streptomycin and 125 ng/mL ampicillin) (Gibco, 15240-062) at 37 °C and 5% CO_2 up to passage 1–2. For the experimental phase, cells were cultured in reduced-serum DMEM/F12 (5% FCS) without antibiotics to avoid any possible interaction of aminoglycoside antibiotics with TRP channel activity [28].

Cellular treatments

<u>Simulated microgravity</u>

To expose cells to simulated microgravity, a previously described RPM was used (**Figure 1**) [28]. The RPM consists of two gimbal-mounted frames independently moved by motors. Samples are placed at the centre of the frames, where the generated motion pattern is designed to equally distribute the gravity vector spatially and temporally (the gravity mathematically averages zero) [33]. Because the constant reorientation of the gravity vector prevents biological systems to adjust to this force, their response is similar to the one achieved upon real microgravity exposure [16].

In our experiments, the rotation speed of the frames was set to 60° per second. IVD cells (n = 4–5, seeded at 6000 cells/cm^2 in T25 flasks (150,000 cells per flask)) were cultured for 24 h prior to simulated microgravity. Flasks were completely filled with culture medium to avoid air bubbles and closed airtight with a filter-less cap [28]. Flasks were mounted onto the RPM (integrated miniaturized CO_2 incubator), whereas corresponding control samples (1 g) were cultured in the same conditions and

simultaneously kept in a standard CO_2 incubator [28]. Treated cells were analyzed for proliferation (up to 5 days of treatment), cell cycle progression (24 h of treatment), cellular senescence (72 h of treatment) and TRP channel expression (72 h of treatment) and compared to untreated controls.
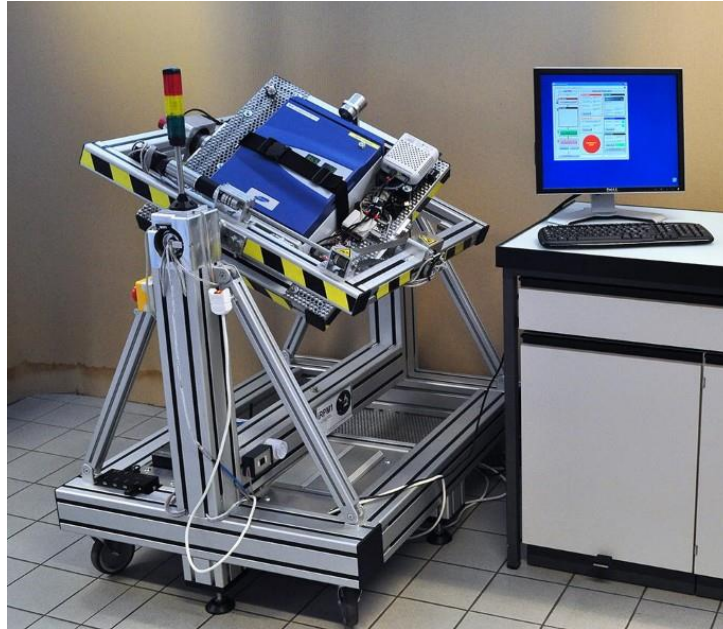
Figure 1: Photograph of the random positioning machine (RPM) used in this study. The samples were mounted in the integrated miniaturized CO_2 incubator in the inner of the two rotating gimbal-mounted frames that are independently moved by motors

Pharmacological TRPC channel inhibition

Twenty-four hours before pharmacological TRPC inhibition with the broad TRPC antagonist SKF-96365 [34] (Sigma-Aldrich, S7809), IVD cells were seeded at a density of ~ 8000 cells/cm^2 in either 24-well plates for subsequent analysis of proliferation ($n = 6$, 15,000 cells per well), 25 cm^2 flasks for cell cycle analysis ($n = 6$, 200,000 cells per flask), or 12-well plates for senescence analysis ($n = 530,000$ cells per well). For cell cycle analysis, cells were exposed to high doses of SKF-96365 (20 μM) for 48 h, whereas proliferation and senescence experiments were conducted for up to 5 days at lower concentrations (1.7 and 2.5 μM) to avoid cell death or complete growth arrest. Treated cells were analyzed as described below and compared to untreated controls.

Cell analysis

Cell proliferation

Manual counting of trypsinized cells was conducted to identify the effects of simulated microgravity and pharmacological TRP inhibition on cell proliferation. Proliferation was analyzed over 5 days (day 0 = seeding cell number, 1, 3 and 5) by counting each replicate twice using a hemocytometer.

Cell cycle

Cell cycle progression was analyzed by flow cytometry analysis as previously described [28]. Cells were fixed in 70% ice-cold EtOH, stored at − 20 °C overnight and then stained with PI/RNase staining buffer (BD Pharmingen, 550825). Cells were analyzed with a FACSCalibur system (BD Biosciences), outfitted with a FL1 channel for PI staining. Appropriate settings for forward- and side-scatter gates were applied to examine 10′000 events/sample. The cell cycle profile was quantified with FlowJo flow cytometry analysis software (TreeStar Inc.), applying the Watson model to fit the histograms of single-gated cells.

Senescence

The level of cellular senescence was assessed by SA-β-galactosidase staining. Cells were washed twice with PBS, fixed with 3% paraformaldehyde in PBS (pH 7.4), washed twice with PBS and incubated overnight at 37 °C with X-gal chromogenic substrate (1 mg/ml) at pH 6.0 [35]. After washing and dehydration with graded ethanol (75–95–99.9%, 1 min each), six images per sample were taken under bright-field illumination (10×). The percentage of senescent cells was determined by manually counting cells with ImageJ.

Gene expression

Gene expression analysis was conducted using a previously described protocol [36]. Briefly, RNA was extracted with TRIzol/chloroform (ThermoScientific, 15596018), the quality and quantity of RNA was determined with the NanodropLite (ThermoScientific) and 1 μg of RNA was reverse-transcribed into cDNA in a 30 μl volume using the High-Capacity cDNA Reverse Transcription Kit (Applied Biosystems, 4374966). For each qPCR reaction, 150 ng cDNA was mixed with TaqMan primers (*TRPC1: Hs00608195_m1; TRPC6: Hs00989190_m1; TBP: Hs00427620_m1*), TaqMan Fast Universal PCR Master Mix (2X) (Applied Biosystems, 4352042) and RNAse-free water to a total volume of 10 μl and gene expression was measured with the CFX96 Touch™ Detection System (Bio-Rad). TATA-binding protein (TBP) was used as a housekeeping gene. Results are shown as $2^{-\Delta\Delta Ct}$ values (i.e. relative to TBP and relative to the untreated control).

Statistical analysis

Data were analyzed for consistency, outliers and for normality. We used normal probability plots for visual inspection of data and Kolmogorov–Smirnov tests to test for normality. Because each donor was measured in the control as well as in the experimental group, samples were dependent (clustered). Data were not normally distributed in any subgroup, and to consider both circumstances, a generalized estimation equation model (GEE) was applied. In detail, we applied a full factorial model with a main, time and interaction effects and used the robust Huber–White sandwich estimator for the covariance matrix (unstructured approach). The lognormal distribution was used to model the underlying distribution. Least significance differences were computed for pairwise comparisons of means. Results are given in terms of means, standard deviations and 95% confidence intervals for means. A significance level of 5% was used. All tests

were two-sided. All analyses were done by using STATISTICA 13 (Hill, T. & Lewicki, P. Statistics: Methods and Applications. StatSoft, Tulsa, OK) and PASW 24 (IBM SPSS Statistics for Windows, Version 24.0., Armonk, NY).

Results

Simulated microgravity and TRPC channel inhibition reduce cell proliferation

Exposing IVD cells ($n = 5$) to simulated microgravity significantly reduced proliferation at days 3 (189 573 cells ± 54 620) and 5 (337 325 cells ± 184 026) compared to cells maintained at 1 g (day 3: 365 600 cells ± 21 637, $p < 0.0001$; day 5: 620 463 cells ± 394 720, $p = 0.0041$) (**Figure 2A**). Similarly, IVD cell proliferation rate ($n = 6$) was slowed at day 3 and day 5 by SKF-96365 (1.7 and 2.5 µM), a non-selective TRPC channel antagonist (**Figure 2B**) [34]. Statistical significance was reached both when comparing each SKF concentration to the control group ($p < 0.0001$ for both concentration at both day 3 and 5) and when comparing the 1.7 µM to the 2.5 µM group ($p = 0.0007$ and $p = 0.002$ for day 3 and 5, respectively), thus proving dose-dependency.
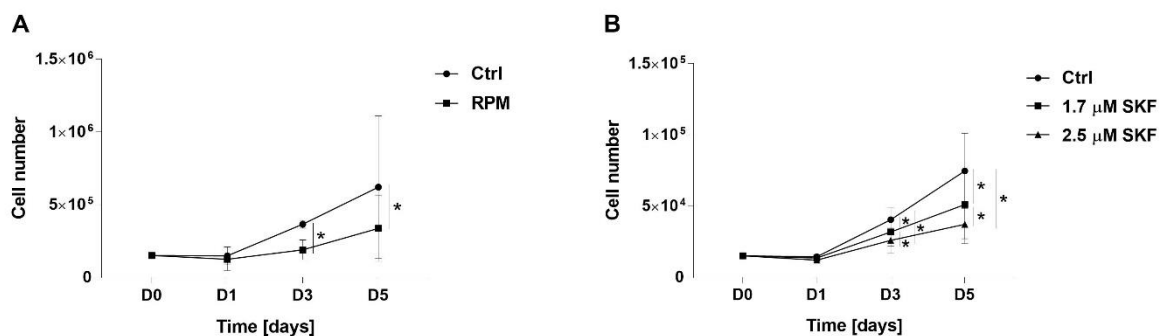
Figure 2: Effects of simulated microgravity and TRPC channel inhibition on proliferation. **A)** Proliferation (total cell number) of human IVD cells at terrestrial gravity (Ctrl) or exposed to simulated microgravity (RPM) up to 5 days ($n = 5$). **B)** Proliferation (total cell number) of human IVD cells with or without TRPC channel inhibition with 1.7 or 2.5 µM SKF-96365 for up to 5 days ($n = 6$). Data are shown as mean with 95% confidence interval, *$p < 0.05$

Simulated microgravity and TRPC channel inhibition affect cell cycle

Although 24 h of simulated microgravity slightly reduced the mean percentage of cells in the G1 phase of the cell cycle from 64.6% ± 8.5 in the controls to 59.0% ± 6.1 and caused an accumulation within the G2/M phase from 11.6 ± 1.9 to 15.2% ± 3.6, these differences were not significant ($p = 0.062$ and $p = 0.076$, respectively) (**Figure 3A**). However, short-term pharmacological blocking of TRPC-mediated calcium entry with SKF-96365 (20 µM, 48 h) resulted in a significant accumulation of IVD cells within the G2/M phase, concomitant with a reduction of cells within the G1 phase ($p < 0.0001$ for both phases) (**Figure 3B**). Specifically, G2/M accumulation increased from 11.4% ± 6.0 (untreated control) to 30.3% ± 8.5, and G1 distribution decreased from 79.7% ± 8.5 to 56.7% ± 11.9.
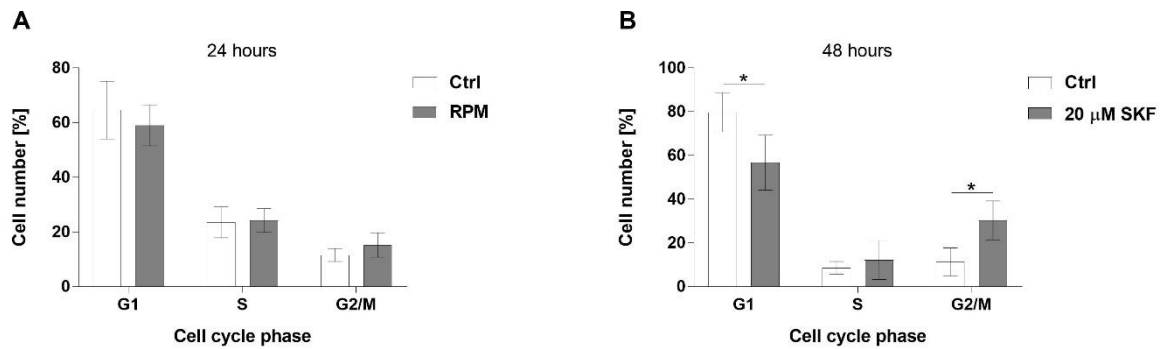
Figure 3: Effects of simulated microgravity and TRPC channel inhibition on cell cycle. **A)** Cell cycle distribution (% of cells in each phase) of human IVD cells at 1 g (Ctrl) or exposed to simulated microgravity (RPM) for 24 h ($n = 5$). **B)** Cell cycle distribution (% of cells in each phase) of human IVD cells with or without TRPC channel inhibition with 20 μM SKF-96365 for 48 h ($n = 6$). Data are shown as mean with 95% confidence interval, *$p < 0.05$

Simulated microgravity and TRPC channel inhibition increase cellular senescence

We found that exposing IVD cells to simulated microgravity for 3 days increased senescence (positive SA-β-galactosidase staining) from $40.0\% \pm 3.6$ (control group) to $50.0\% \pm 6.9$ ($p < 0.0001$) (**Figure 4A**). Similarly, SKF-96365 treatment also augmented the percentage of SA-β-galactosidase-positive cells relative to untreated controls (**Figure 4B**). A significant difference was already observed between the 2.5 μM SKF group and controls at day 1 ($p < 0.0001$), which was maintained at both days 3 and 5 ($p = 0.012$ and $p < 0.0001$, respectively). At these later time points, statistical significance was also reached for the 1.7 μM SKF group ($p = 0.0018$ and $p < 0.0001$) (**Figure 4B**).
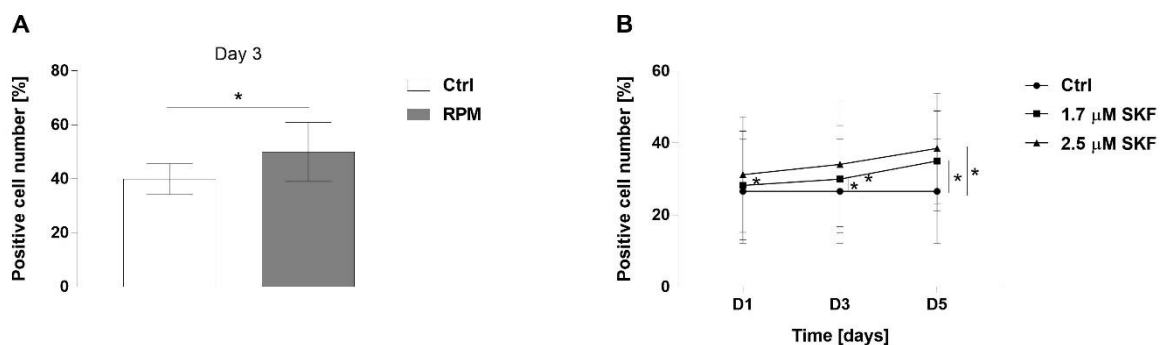
Figure 4: Effects of simulated microgravity and TRPC channel inhibition on senescence. **A)** Percentage of SA-β-galactosidase-positive human IVD cells at 1 g (Ctrl) or exposed to simulated microgravity (RPM) for 3 days ($n = 4$). **B)** Percentage of SA-β-galactosidase-positive human IVD cells with or without TRPC channel inhibition with 1.7 or 2.5 μM SKF-96365 for up to 5 days ($n = 5$). Data are shown as mean with 95% confidence interval, *$p < 0.05$

Simulated microgravity downregulates TRPC6 expression

Motivated by the fact that TRPC channel inhibition had similar effects on proliferation, cell cycle progression and senescence to simulated microgravity, we analyzed the gene expression of the TRPC channel isoforms TRPC1 and TRPC6 under simulated microgravity. While TRPC1 mRNA levels were not affected ($p = 0.14$)

(**Figure 5A**), TRPC6 expression was significantly reduced (mean $2^{-\Delta\Delta Ct}$ value = 0.64 ± 0.19, $p < 0.0001$) (**Figure 5B**).
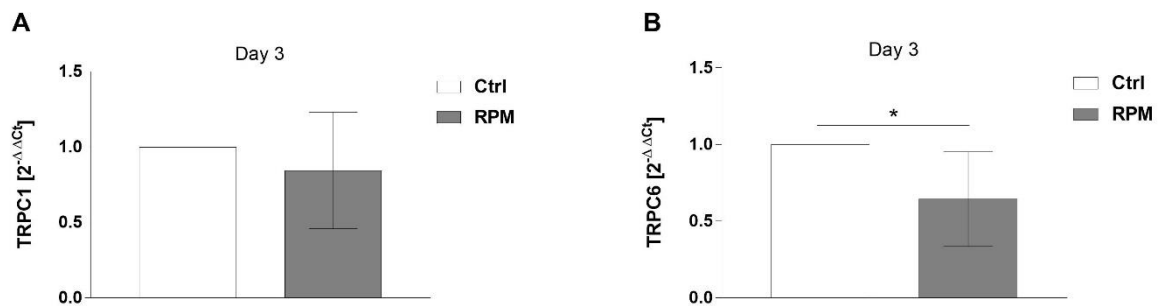
Figure 5: Gene expression of TRPC1 and TRPC6 under simulated microgravity. **A)** Relative gene expression of TRPC1 and **B)** TPRC6 in human IVD cells at 1 g (Ctrl) or exposed to simulated microgravity (RPM) for 3 days ($n = 4$). Results are shown as $2^{-\Delta\Delta Ct}$ values (i.e. relative to TBP and relative to the untreated control) ($n = 4$). Data are shown as mean with 95% confidence interval, *$p < 0.05$

Discussion

In this study, we found that (1) simulated microgravity and pharmacological antagonism of TRPC channels reduced cell proliferation, retarded cell cycle progression and induced cellular senescence, and that (2) simulated microgravity concomitantly inhibited TRPC6 expression (while not affecting TRPC1 expression). TRPC6 may hence potentially play a role in mediating the effects on proliferation and cell cycle distribution that were observed upon simulated microgravity. Further studies including modulation of TRPC6 (with, e.g. activation with CRISPRa or knockout with CRISPRi [37]) are needed to reveal the possible involvement of TRPC6 in IVD mechanotransduction.

Mechanical unloading, as observed in astronauts, para-/tetraplegic patients, bed rest studies [7, 8] or animals undergoing hindquarter suspension, negatively affects IVD metabolism and matrix composition. Here, we simulated microgravity by using an RPM [28] and similarly observed detrimental, degeneration-associated changes. These changes are likely due to the integrated signalling network that couples mechanosensitive receptors and pathways to gene and transcription modulation [38], and may furthermore be associated with structural adjustments on the cell level (e.g. actin cytoskeleton reorganization) [39].

Although constituting a well-accepted method to simulate microgravity, the use of an RPM with its constant reorientation of the samples induces additional forces (e.g. shear stresses) that may create artefacts. These forces present in the culture flasks on the RPM and their effects on the cultured cells were recently thoroughly studied by numerical analysis [40]. Parameters such as rotational velocity of the RPM play a role in the appearance of shear stress [40]. Therefore, additional stressors and artefacts can be prevented by taking the necessary measures for an accurate operation of the RPM [40]. IVD cell culture in flasks on the RPM does not recapitulate the complex three-dimensional disc matrix environment. However, signs of degeneration were similarly observed in

whole mouse discs cultured under microgravity in a rotating wall vessel bioreactor [17]. Compared to studies in the entire human (astronauts and bed rest patients), the RPM represents a simplified in vitro model system, which is nevertheless useful to uncover the underlying molecular mechanisms related to IVD degeneration.

In agreement with our results obtained with human IVD cells, murine myoblasts exposed to simulated microgravity or SKF-96365 exhibited reduced proliferation and cell cycle arrest within the G2/M phase [28, 31]. This reflects the fact that proliferative capacity may concurrently correlate with mechanosensitivity and TRPC function [31]. However, myoblasts seem to rely on modulation of TRPC1 rather than TRPC6, indicating that the exact role of these TRP channels appears to be tissue and/or species dependent. To confirm the specific relevance of TRPC6 for IVD mechanosensing and mechanotransduction, future experiments should not only apply SKF-96365 [34, 41] (which may potentially also affect voltage-dependent calcium channels [42]), but should also target TRPC6 in a more specific manner.

Apart from analyzing cell proliferation and cell cycle progression, we also measured changes in cellular senescence (as assessed by SA-β galactosidase staining), a hallmark of IVD degeneration [43, 44]. TRPC channel inhibition and simulated microgravity both increased cellular senescence in IVD cells. However, variability in the basal levels of senescence (and proliferation capacity) between donors was present, as these differed with respect to age, pathology, degeneration grade and mixture of NP and AF tissue. Senescence in vivo is not only associated with the degree of disc degeneration [45], but also varies between NP and AF [20]. Furthermore, pro-inflammatory cytokines may trigger cell senescence [45], and these may not only be secreted by resident IVD cells, but also by invading immune cells found predominantly in IVD herniation samples [46]. Despite the differences in basal levels of senescence and proliferation capacity stemming from disparities in patient characteristics, we were able to show that microgravity and TRPC channel inhibition both increased cell senescence and decreased cell proliferation. The subsequent gene expression analysis of the TRPC channel isoforms TRPC1 and TRPC6 revealed that TRPC6 was downregulated under microgravity (while TRPC1 expression was not affected). Therefore, TRPC6 could potentially be of importance in the progression of IVD degeneration linked to cell senescence, but further studies are needed. In fact, the role of TRP channels in modulating senescence is also known for other cell types, such as endothelial cells (TRPC5) [47], pancreatic adenocarcinoma cells (TRPM7, TRPM8) [48, 49] and lung fibroblasts (TRPC6) [30].

Mechanistic studies modulating TRPC6 expression/activity are needed to determine whether TRPC6 restricts or reverses progression of a SASP in IVD cells and mitigates the loss of regenerative capacity. This could possibly offer a means to treat IVD degeneration. So far, TRPC6 modulation has been investigated for focal segmental glomerulosclerosis [50], pulmonary hypertension [51] and ischaemia reperfusion-induced lung oedema [52]. TRP channel modulation could be achieved by gene editing, using CRIPSR/Cas9 [37, 53, 54]. However, these approaches are still in an early experimental phase.

Conclusions

In conclusion, we show that human IVD cells subjected to RPM-simulated microgravity or to TRPC channel inhibition display reduced proliferation, retarded cell cycle progression and increased cell senescence. Furthermore, simulated microgravity reduces TRPC6 gene expression. The TRPC6 ion channel may hence be involved in mechanotransduction and in the regulation of cell proliferation and senescence in the IVD. These findings are in agreement with other studies where simulated microgravity induced signs of degeneration in whole mouse IVDs [17] and reduced proliferation in mouse myoblasts by inducing cell cycle arrest [28]. The fact that the effects caused by simulated microgravity (reduced proliferation, retarded cell cycle progression and increased senescence) were recapitulated by TRPC channel inhibition and were accompanied by downregulation of TRPC6 expression suggests that TRPC6 may potentially play a role in the underlying mechanisms. In fact, TRPC6 has also been associated with cell senescence in lung fibroblasts [30], a contributor to pulmonary hypertension [55], consequentially motivating first studies on the therapeutic potential of TRPC6 modulation [55]. This study thus reveals TRPC6 as a potential target for further studies aiming to investigate IVD degeneration.

Ethical approval

All procedures performed in studies involving human participants were in accordance with the ethical standards of the institutional and/or national research committee and with the 1964 Helsinki Declaration and its later amendments or comparable ethical standards.

Informed consent

Informed consent was obtained from all individual participants included in the study.

References

1. Boos N, Weissbach S, Rohrbach H, Weiler C, Spratt KF, Nerlich AG (2002) Classification of age-related changes in lumbar intervertebral discs: 2002 Volvo Award in basic science. Spine 27:2631–2644.

2. Adams MA, Roughley PJ (2006) What is intervertebral disc degeneration, and what causes it? Spine 31:2151–2161.

3. Chan D, Song Y, Sham P, Cheung KMC (2006) Genetics of disc degeneration. Eur Spine J 15:317–325.

4. Wilke HJ, Neef P, Caimi M, Hoogland T, Claes LE (1999) New in vivo measurements of pressures in the intervertebral disc in daily life. Spine 24:755–762

5. Chan SC, Walser J, Kappeli P, Shamsollahi MJ, Ferguson SJ, Gantenbein-Ritter B (2013) Region specific response of intervertebral disc cells to complex dynamic loading: an organ culture study using a dynamic torsion-compression bioreactor. PLoS ONE 8:e72489.

6. Chan SC, Ferguson SJ, Gantenbein-Ritter B (2011) The effects of dynamic loading on the intervertebral disc. Eur Spine J 20:1796–1812.

7. Belavy DL, Bansmann PM, Bohme G, Frings-Meuthen P, Heer M, Rittweger J, Zange J (1985) Felsenberg D (2011) Changes in intervertebral disc morphology persist 5 mo after 21-day bed rest. J Appl Physiol 111:1304–1314.

8. Belavy DL, Armbrecht G, Felsenberg D (2012) Incomplete recovery of lumbar intervertebral discs 2 years after 60-day bed rest. Spine 37:1245–1251.

9. Wing PC, Tsang IK, Susak L, Gagnon F, Gagnon R, Potts JE (1991) Back pain and spinal changes in microgravity. Orthop Clin N Am 22:255–262

10. Kerstman EL, Scheuring RA, Barnes MG, DeKorse TB, Saile LG (2012) Space adaptation back pain: a retrospective study. Aviat Space Environ Med 83:2–7

11. Sayson JV, Hargens AR (2008) Pathophysiology of low back pain during exposure to microgravity. Aviat Space Environ Med 79:365–373.

12. Johnston SL, Campbell MR, Scheuring R, Feiveson AH (2010) Risk of herniated nucleus pulposus among U.S. astronauts. Aviat Space Environ Med 81:566–574

13. Laws CJ, Berg-Johansen B, Hargens AR, Lotz JC (2016) The effect of simulated microgravity on lumbar spine biomechanics: an in vitro study. Eur Spine J 25:2889–2897.

14. Sinha RK, Shah SA, Hume EL, Tuan RS (2002) The effect of a 5-day space flight on the immature rat spine. Spine J 2:239–243

15. Bailey JF, Hargens AR, Cheng KK, Lotz JC (2014) Effect of microgravity on the biomechanical properties of lumbar and caudal intervertebral discs in mice. J Biomech 47:2983–2988.

16. Wuest SL, Richard S, Kopp S, Grimm D, Egli M (2015) Simulated microgravity: critical review on the use of random positioning machines for mammalian cell culture. Biomed Res Int 2015:971474.

17. Jin L, Feng G, Reames DL, Shimer AL, Shen FH, Li X (2013) The effects of simulated microgravity on intervertebral disc degeneration. The Spine J 13:235–242.

18. Stannard JT, Edamura K, Stoker AM, O'Connell GD, Kuroki K, Hung CT, Choma TJ, Cook JL (2016) Development of a whole organ culture model for intervertebral disc disease. J Orthop Transl 5:1–8.

19. Kim KW, Chung HN, Ha KY, Lee JS, Kim YY (2009) Senescence mechanisms of nucleus pulposus chondrocytes in human intervertebral discs. Spine J 9:658–666.

20. Roberts S, Evans EH, Kletsas D, Jaffray DC, Eisenstein SM (2006) Senescence in human intervertebral discs. Eur Spine J 15(Suppl 3):S312–S316.

21. Grant MP, Epure LM, Bokhari R, Roughley P, Antoniou J, Mwale F (2016) Human cartilaginous endplate degeneration is induced by calcium and the extracellular calcium-sensing receptor in the intervertebral disc. Eur Cells Mater 32:137–151

22. Rakan B, AlGarni N, Salem O, Epure L, Habis AA, Antoniou J, Mwale F, Grant M (2015) Free calcium induces degenerative changes in the intervertebral disc through the calcium sensing receptor. Can J Neurol Sci 42:S50–S50.

23. Worley PF, Zeng W, Huang GN, Yuan JP, Kim JY, Lee MG, Muallem S (2007) TRPC channels as STIM1-regulated store-operated channels. Cell Calcium 42:205–211.

24. Walter BA, Purmessur D, Moon A, Occhiogrosso J, Laudier DM, Hecht AC, Iatridis JC (2016) Reduced tissue osmolarity increases TRPV4 expression and pro-inflammatory cytokines in intervertebral disc cells. Eur Cells Mater 32:123–136

25. Sadowska A, Touli E, Hitzl W, Greutert H, Ferguson SJ, Wuertz-Kozak K, Hausmann ON (2018) Inflammaging in cervical and lumbar degenerated intervertebral discs: analysis of proinflammatory cytokine and TRP channel expression. Eur Spine J 27:564–577.

26. Krupkova O, Zvick J, Wuertz-Kozak K (2017) The Role of Transient Receptor Potential Channels in Joint Diseases. Eur Cells Mater 34:180–201.

27. Ichikawa J, Inoue R (2014) TRPC6 regulates cell cycle progression by modulating membrane potential in bone marrow stromal cells. Br J Pharmacol 171:5280–5294.

28. Benavides Damm T, Richard S, Tanner S, Wyss F, Egli M, Franco-Obregon A (2013) Calcium-dependent deceleration of the cell cycle in muscle cells by simulated microgravity. FASEB J Off Publ Fed Am Soc Exp Biol 27:2045–2054.

29. Numata T, Kiyonaka S, Kato K, Takahashi N, Mori Y (2011) Activation of TRP channels in mammalian systems. In: Zhu MX (ed) TRP channels. Boca Raton (FL)

30. Chandrasekaran A, Zhang X, Lee MY, Shapiro R, Trebak M, Melendez JA (2017) 62–H_2O_2 and mTOR control the senescence-associated secretory phenotype by coordinating Ca^{2+} transients through TRPC6 expression and activation. Free Radic Bio Med 112:55–56.

31. Crocetti S, Beyer C, Unternahrer S, Benavides Damm T, Schade-Kampmann G, Hebeisen M, Di Berardino M, Frohlich J, Franco-Obregon A (2014) Impedance flow cytometry gauges proliferative capacity by detecting TRPC1 expression. Cytom Part A J Int Soc Anal Cytol.

32. Krupkova O, Handa J, Hlavna M, Klasen J, Ospelt C, Ferguson SJ, Wuertz-Kozak K (2016) The natural polyphenol epigallocatechin gallate protects intervertebral disc cells from oxidative stress. Oxid Med Cell Longev 2016:7031397.

33. Wuest SL, Richard S, Walther I, Furrer R, Anderegg R, Sekler J, Egli M (2014) A novel microgravity simulator applicable for three-dimensional cell culturing. Microgravity Sci Technol 26:77–88.

34. Song M, Chen D, Yu SP (2014) The TRPC channel blocker SKF 96365 inhibits glioblastoma cell growth by enhancing reverse mode of the Na+/Ca2+ exchanger and increasing intracellular Ca^{2+}. Br J Pharmacol 171:3432–3447.

35. Debacq-Chainiaux F, Erusalimsky JD, Campisi J, Toussaint O (2009) Protocols to detect senescence-associated beta-galactosidase (SA-beta gal) activity, a biomarker of senescent cells in culture and in vivo. Nat Protoc 4:1798–1806.

36. Quero L, Klawitter M, Schmaus A, Rothley M, Sleeman J, Tiaden AN, Klasen J, Boos N, Hottiger MO, Wuertz K, Richards PJ (2013) Hyaluronic acid fragments enhance the inflammatory and catabolic response in human intervertebral disc cells through modulation of toll-like receptor 2 signalling pathways. Arthritis Res Ther 15:R94.

37. Krupkova O, Cambria E, Besse L, Besse A, Bowles R, Wuertz-Kozak K (2018) The potential of CRISPR/Cas9 genome editing for the study and treatment of intervertebral disc pathologies. JOR SPINE 1:e1003.

38. Wong VW, Longaker MT, Gurtner GC (2012) Soft tissue mechanotransduction in wound healing and fibrosis. Semin Cell Dev Biol 23:981–986.

39. Crawford-Young SJ (2006) Effects of microgravity on cell cytoskeleton and embryogenesis. Int J Dev Biol 50:183–191.

40. Wuest SL, Stern P, Casartelli E, Egli M (2017) Fluid dynamics appearing during simulated microgravity using random positioning machines. PLoS ONE 12:e0170826.

41. Cheng H, Curtis AE, Fellingham C, Hancox JC (2016) Multiple ion channel block by the cation channel inhibitor SKF-96365 in myocytes from the rabbit atrioventricular node. Physiol Rep 4:e12819.

42. Zhao H, Simasko SM (2010) Role of transient receptor potential channels in cholecystokinin-induced activation of cultured vagal afferent neurons. Endocrinology 151:5237–5246.

43. Vo NV, Hartman RA, Patil PR, Risbud MV, Kletsas D, Iatridis JC, Hoyland JA, Le Maitre CL, Sowa GA, Kang JD (2016) Molecular mechanisms of biological aging in intervertebral discs. J Orthop Res Off Publ Orthop Res Soc.

44. Feng C, Liu H, Yang M, Zhang Y, Huang B, Zhou Y (2016) Disc cell senescence in intervertebral disc degeneration: causes and molecular pathways. Cell Cycle 15:1674–1684.

45. Wang F, Cai F, Shi R, Wang XH, Wu XT (2016) Aging and age related stresses: a senescence mechanism of intervertebral disc degeneration. Osteoarthr Cartil 24:398–408.

46. Molinos M, Almeida CR, Caldeira J, Cunha C, Gonçalves RM, Barbosa MA (2015) Inflammation in intervertebral disc degeneration and regeneration. J R Soc Interface 12:20141191.

47. Li Z, Guo G, Wang H, Si X, Zhou G, Xiong Y, Li S, Dai R, Yang C (2017) TRPC5 channel modulates endothelial cells senescence. Eur J Pharmacol 802:27–35.

48. Yee NS, Zhou W, Lee M, Yee RK (2012) Targeted silencing of TRPM7 ion channel induces replicative senescence and produces enhanced cytotoxicity with gemcitabine in pancreatic adenocarcinoma. Cancer Lett 318:99–105.

49. Yee NS, Brown RD, Lee MS, Zhou W, Jensen C, Gerke H, Yee RK (2012) TRPM8 ion channel is aberrantly expressed and required for preventing replicative senescence in pancreatic adenocarcinoma: potential role of TRPM8 as a biomarker and target. Cancer Biol Ther 13:592–599.

50. Winn MP, Conlon PJ, Lynn KL, Farrington MK, Creazzo T, Hawkins AF, Daskalakis N, Kwan SY, Ebersviller S, Burchette JL, Pericak-Vance MA, Howel DN, Vance JM, Rosenberg PB (2005) A mutation in the TRPC6 cation channel causes familial focal segmental glomerulosclerosis. Science 308:1801–1804.

51. Pousada G, Baloira A, Valverde D (2015) Molecular and clinical analysis of TRPC6 and AGTR1 genes in patients with pulmonary arterial hypertension. Orphanet J Rare Dis.

52. Weissmann N, Sydykov A, Kalwa H, Storch U, Fuchs B, Schnitzler MMY, Brandes RP, Grimminger F, Meissner M, Freichel M, Offermanns S, Veit F, Pak O, Krause KH, Schermuly RT, Brewer AC, Schmidt HHHW, Seeger W, Shah AM, Gudermann T, Ghofrani HA, Dietrich A (2012) Activation of TRPC6 channels is essential for lung ischaemia-reperfusion induced oedema in mice. Nat Commun.

53. Naldini L (2015) Gene therapy returns to centre stage. Nature 526:351–360.

54. Doudna JA, Charpentier E (2014) Genome editing. The new frontier of genome engineering with CRISPR-Cas9. Science 346:1258096.

55. Noureddine H, Gary-Bobo G, Alifano M, Marcos E, Saker M, Vienney N, Amsellem V, Maitre B, Chaouat A, Chouaid C, Dubois-Rande JL, Damotte D, Adnot S (2011) Pulmonary artery smooth muscle cell senescence is a pathogenic mechanism for pulmonary hypertension in chronic lung disease. Circ Res 109:543–553.

List of abbreviations

2D	Two-dimensional
3D	Three-dimensional
AAV	Adeno-associated virus
ACAN	Aggrecan
ADAMTS	A disintegrin and metalloproteinase with thrombospondin motifs
ADP	Adenosine diphosphate
AEC	Amino-9-ethyl-carbazole
AF	Annulus fibrosus
AKAP 150	A-kinase anchoring protein 150
Anti-Anti	Antibiotic-Antimycotic
ARD	Ankyrin repeat domain
ASCs	Adipose tissue-derived stem cells
ATP	Adenosine triphosphate
AU	Adenylate-uridylate
bFGF	Basic fibroblast growth factor
BMP	Bone morphogenic protein
BSA	Bovine serum albumin
CA12	Carbonic anhydrase XII
CASFISH	Cas9-mediated fluorescence in situ hybridization
CaSR	Calcium-sensing receptor
CDI	Carbonyldiimidazole
CEP	Cartilaginous endplate
COL	Collagen
COX2	Cyclooxygenase 2
CRISPR	Clustered regularly interspaced short palindromic repeats
CRISPRa	CRISPR activation
CRISPRi	CRISPR interference
crRNA	Crispr RNA
Cryo-EM	Cryogenic electron microscopy
Ctrl	Control
DAPI	4′,6-diamidino-2-phenylindole
dCas9	Dead Cas9
DDD	Degenerative disc disease
DMEM	Dulbecco's modified Eagle medium
DMSO	Dimethyl sulfoxide
DNA	Deoxyribonucleic acid
DRG	Dorsal root ganglion
DSB	Double-strand DNA break

ECM	Extracellular matrix
EDC	1-ethyl-3-(3-dimethylaminopropyl) carbodiimide
EDTA	Ethylene-diamine-tetra-acetic acid
EGF	Epidermal growth factor
ELISA	Enzyme-linked immunosorbent assay
enChIP	engineered DNA-binding molecule-mediated chromatin immunoprecipitation
ERK	Extracellular signal-regulated kinases 1/2
FAK	Focal adhesion kinase
FAST	Fast green, alcian blue, safranin-O, tartrazine
FCS	Fetal calf serum
FOXF1	Forkhead box F1
G'	Storage modulus
G''	Loss modulus
GAG	Glycosaminoglycan
GDF5	Growth/differentiation factor 5
GEE	Generalized estimation equation
HDR	Homology-directed repair
HITI	Homology-independent targeted integration
HRE	Hypoxia-responsive element
HTH	Helix-turn-helix
IAF	Inner annulus fibrosus
IDLV	Integrase-deficient lentiviral vector
IGF1	Insulin-like growth factor 1
IHC	Immunohistochemistry
IL	Interleukin
IL1R1	IL 1 receptor 1
IL1Ra	IL1 receptor antagonist
indels	Insertions or deletions
iPSCs	Induced pluripotent stem cells
IVD	Intervertebral disc
JNK	Jun-N-terminal kinase
KO	Knockout
LBP	Low back pain
LDH	Lactate dehydrogenase
MAPK	Mitogen-activated protein kinase
MCP	Monocyte chemoattractant protein
MIG	Monokine induced by gamma interferon

miRNA	MicroRNA
MMP	Matrix metalloproteinase
MRI	Magnetic resonance imaging
MSCs	Mesenchymal stem cells
NBD	Nemo binding domain
NF-κB	Nuclear factor-kappa B
NGF	Nerve growth factor
NHEJ	Nonhomologous end-joining
NP	Nucleus pulposus
NSAIDs	Non-steroidal anti-inflammatory drugs
NT	Non-targeting
OAF	Outer annulus fibrosus
OP1	Osteogenic protein 1
PAM	Protospacer adjacent motif
PAX1	Paired box-1
PBS	Phosphate buffered saline
PCR	Polymerase chain reaction
PEGDA	Poly(ethylene glycol) diacrylate
PGE2	Prostaglandin E2
RCS	Rat chondrosarcoma
RIPA	Radioimmunoprecipitation assay
RNA	Ribonucleic acid
RNAi	RNA interference
RNP	Ribonucleoprotein
ROCK	Rho-associated kinase
RPM	Random positioning machine
RT	Room temperature
RT-qPCR	Quantitative reverse transcription PCR
SA β-gal	Senescence-associated β-galactosidase
SASP	Senescence-associated secretory phenotype
SD	Standard deviation
sg-RNA	Single-guide RNA
siRNA	Small interfering RNA
S-NBC	S-2-nitrobenzyl cysteine
SOX	Sex-determining region Y box
Sulfo-SANPAH	Sulfosuccinimidyl 6-(4'-azido-2'-nitrophenylamino)hexanoate
TALEN	Transcription activator-like effector nuclease
TAZ	Transcriptional coactivator with PDZ-binding motif
TBP	TATA-binding protein
TBS-T	Tris buffered saline with TWEEN 20

TDR	Total disc replacement
TGFβ	Transforming growth factor beta
TLR	Toll-like receptor
TNF-α	Tumor necrosis factor alpha
TNFR1	Tumor necrosis factor receptor 1
tracrRNA	Trans-activating crRNA
TRP	Transient receptor potential
TRPA	TRP ankyrin
TRPC	TRP canonical
TRPM	TRP melastatin
TRPML	TRP mucolipin
TRPP	TRP polycystin
TRPV	TRP vanilloid
trRNA	Tracer RNA
WT	Wild-type
YAP	Yes-associated protein
ZFN	Zinc finger nuclease

Curriculum vitae

Elena Cambria

Personal information

Altstetterstrasse 212

8048 Zurich
ecambria@ethz.ch

Born December 2nd 1989

Citizenships: Swiss and Italian
OrcID: 0000-0001-6896-5421

Scientific interests

Biomaterials, mechanotransduction, organoids, stem cell biology, extracellular matrix, regenerative medicine, tissue engineering, organs-on-a-chip, immunoengineering

Education

ETH Zurich, Swiss Federal Institute of Technology	**Zurich, Switzerland**
Candidate for Doctor of Sciences	Jul. 2016 – Mar. 2021
• Thesis on the role of transient receptor potential ion channels in mechanotransduction of intervertebral disc cells	
• Thesis advisors: Prof. Stephen J. Ferguson and Prof. Karin Wuertz-Kozak	
• External project at the **Fraunhofer** Institute for Interfacial Engineering and Biotechnology. Advisor: Prof. Peter Loskill	**Stuttgart, Germany** Apr. – Oct. 2019
EPF Lausanne, Swiss Federal Institute of Technology	**Lausanne, Switzerland**
Master of Science in Bioengineering	Sept. 2012 – Mar. 2015
• Orientation Regenerative Medicine	
• Master thesis at **Massachusetts Institute of Technology**	**Cambridge, MA, USA**
• Thesis title: "Sortase-mediated ligation of epidermal growth factor to pre-formed PEG hydrogels for in vitro tissue models"	Jan. 2014 – Feb. 2015
• Thesis advisors: Prof. Matthias Lütolf and Prof. Linda Griffith	
EPF Lausanne, Swiss Federal Institute of Technology	**Lausanne, Switzerland**
Bachelor of Science in Life Sciences and Technologies	Sept. 2009 – Jul. 2012
• Thesis title: "Multisensory basis of racial stereotypes"	
• Thesis advisor: Prof. Olaf Blanke	

Employment history

ETH Zurich, Swiss Federal Institute of Technology	**Zurich, Switzerland**
Graduate scientific assistant	Jul. 2016 – Mar. 2021
• Investigated transient receptor potential (TRP) ion channels in simulated microgravity of human primary intervertebral disc (IVD) cells and identified TRPC6 as a potential mechanotransducer	
• Established mechanical loading protocols for human and bovine primary IVD cells cultured in 2D and 3D in stretching and compression bioreactors	
• Developed and characterized agarose-collagen composite hydrogels for dynamic compression and mechanotransduction studies of IVD cells	
• Established the first successful CRISPR-Cas9 knockout in degenerated human annulus fibrosus cells (TRPV4 ion channel knockout)	
• Established a model of inflammatory response to hyperphysiological stretching that mimics annulus fibrosus injury and applied pharmacological inhibition and CRISPR-Cas9 gene editing to identify TRPV4 as mediator of stretch-induced inflammation	
• Identified TRPV4 as a regulator of inflammation and compression-induced cell death in bovine IVD cells cultured in 3D agarose-collagen hydrogels and mouse IVDs	
• Advisors: Prof. Stephen J. Ferguson and Prof. Karin Wuertz-Kozak	

Fraunhofer Institute for Interfacial Engineering and Biotechnology	**Stuttgart, Germany**
Visiting scholar	Apr. – Oct. 2019

- Characterized a cartilage-on-a-chip microphysiological system able to perform dynamic compression on adipose tissue-derived mesenchymal stem cells embedded in agarose-collagen hydrogels
- Established chondrogenesis protocols off- and on-chip and evaluated cell viability, and gene and protein expression of chondrogenic markers
- Advisor: Prof. Peter Loskill

University and University Hospital of Zurich	**Zurich, Switzerland**
Graduate scientific assistant	Sept. 2015 – Apr. 2016

- Investigated bone marrow-derived mesenchymal stem cell spheroids for cardiac stem cell therapy
- Assisted in a pre-clinical trial aiming to transplant a tissue-engineered heart valve in a sheep model
- Advisors: Prof. Maximilian Y. Emmert and Prof. Simon P. Hoerstrup

EPF Lausanne Technology Transfer Office / Laboratory of Signal Processing 2	**Lausanne, Switzerland**
"Enable" program intern	Jun. – Jul. 2015

- Performed prior art search, a market study, and developed a business plan
- Advisors: Dr. André Catana and Prof. Pierre Vandergheynst

Massachusetts Institute of Technology	**Cambridge, MA, USA**
Visiting scholar - Master thesis	Jan. 2014 – Feb. 2015

- Established sortase-mediated ligation as a novel tool to specifically and reversibly modify synthetic hydrogels with bioactive proteins
- Developed quantitative assays to analyze the sortase reaction and the hydrogels
- Evaluated the bioactivity of the tethered growth factor (EGF) by examining the DNA synthesis of primary human epithelial cells seeded on the scaffolds
- Advisors: Prof. Matthias Lütolf and Prof. Linda Griffith

EPF Lausanne, **Swiss Federal Institute of Technology**	**Lausanne, Switzerland**
Laboratory intern	Oct. – Dec. 2013

- Generated and monitored embryoid bodies from induced pluripotent stem cells and murine GFP-reporter embryonic stem cells under different culture conditions (Matrigel/PEG hydrogels, gel stiffness). Advisor: Prof. Matthias Lütolf

Gymetrics	**Lausanne, Switzerland**
R&D engineering intern	Jul. – Aug. 2013

- Optimized and assessed the cytotoxicity of new-generation miniaturized biosensors for cell culture monitoring. Advisor: Dr. Frederic Schmitt

EPF Lausanne, **Swiss Federal Institute of Technology**	**Lausanne, Switzerland**
Laboratory intern	Feb. – Jun. 2013

- Optimized an ex vivo organotypic culture system and a stem cell transplantation device for the regeneration of corneal epithelium. Advisor: Prof. Yann Barrandon

Institutional responsibilities

ETH Zurich, Swiss Federal Institute of Technology	**Zurich, Switzerland**
Scientific staff representative at the Institute for Biomechanics Council	Jun. 2019 – Feb. 2021
Organizer of the annual ski event of the Institute for Biomechanics	Sept. 2016 – Jan. 2017

EPF Lausanne, Swiss Federal Institute of Technology	**Lausanne, Switzerland**
Class representative of Master in Bioengineering	Sept. 2012 – Jun. 2014

Approved research projects

Research grant	**EUROSPINE**
30'000 €, project title: "TRPV4 in intervertebral disc cell death & inflammation"	Jun. 2020 – Jan. 2021

Supervision of students

• **Rahel Friedrich**, Master thesis "Characterization of a novel cartilage-on-a-chip based on adipose tissue-derived stem cell chondrogenesis"	Aug. 2019 – May 2020
• **Sally Heusser,** Master thesis "Characterization of hybrid agarose-collagen hydrogels & the role of TRPV4 in dynamic compression of bovine nucleus pulposus cells"	Oct. 2018 – Apr. 2019
• **Sandra Wandel**, Master thesis "The role of TRPV4 in stretch-induced inflammation of intervertebral disc cells"	Mar. 2018 – Aug. 2018
• **Silvio Brunner**, internship "Characterization of hybrid agarose-collagen hydrogels for dynamic compression of cells"	Mar. 2018 – Jul. 2018
• **Sandra Wandel**, semester project "Optimization of methods to analyse activation of TRP channels in cell-seeded agarose 3D hydrogels after dynamic compression"	Sept. 2017 – Dec. 2017
• **Silvio Brunner**, Master thesis "The expression of TRP channels in dynamic compression of intervertebral disc cells"	Feb. 2017 – Jul. 2017
• **Silvio Brunner**, semester project "Characterization and dynamic compression of cell-seeded agarose gels"	Sept. 2016 – Jan. 2017

Teaching activities

ETH Zurich, Swiss Federal Institute of Technology	**Zurich, Switzerland**
Graduate scientific assistant	Jul. 2016 – Nov. 2019
• Presented in the course "Colloquium in Biomechanics" (once per semester)	

ETH Zurich, Swiss Federal Institute of Technology	**Zurich, Switzerland**
Teaching assistant	Jul. 2016 – Jul. 2019
• Organized a session of the course "Practical Methods in Tissue Engineering" (12 Master students), led 2 assistants, composed protocols and exercise questions, graded homework, led and supervised the session (once per semester)	

Professional activities

Conference session co-chair	TERMIS EU, May 2019, Rhodes, « Microfluidics & Bioreactors » session
Journal reviewer	PLOS ONE, European Spine Journal
Society membership	Tissue Engineering and Regenerative Medicine International Society (TERMIS), European Organ-on-Chip Society (EUROoCS), EUROSPINE
Peer mentoring group	Supported by *Fix the Leaky Pipeline! A career-building program for women in science* at ETH Zurich (Jun. 2019 – Jun- 2020)

Prizes, awards, fellowships

"Early Postdoc.Mobility" fellowship	**Swiss National Science Foundation**
73'500 CHF, project title: "Development of mechanically stimulated and vascularized cancer organoids-on-chip to model tumor growth and invasion"	Apr. 2021- Sep. 2022

"Doc.Mobility" fellowship	**Swiss National Science Foundation**
10'000 CHF, project title: "Intervertebral disc-on-a-chip (IVDoC): a microphysiological system to investigate load-induced calcium regulation and stem cell differentiation"	Apr. – Oct. 2019

Shortlisted for the SYIS oral presentation award Abstract title: "TRPV4 inhibition reduces stretch-induced inflammation in human intervertebral discs"	**TERMIS-EU** May 2019
Travel award 2'000 € to attend the "Basic Biomechanics and Biomechanical Methods for Experimental Research of the Musculoskeletal System" course in Ulm, Germany	**EUROSPINE** Jun. 2018
Travel award 1'000 CHF to attend the ORS PSRS 4th International Spine Research Symposium in Lake Harmony, Pennsylvania, USA	**Swiss Bone and Mineral Society** Oct. 2017
Distinction of excellence Outstanding Master in Bioengineering	**EPF Lausanne** Oct. 2015
Finalist for the Student Award Master thesis title: "Sortase-mediated ligation of epidermal growth factor to pre-formed PEG hydrogels for in vitro tissue models"	**Swiss Society for Biomedical Engineering** Aug. 2015

Personal skills and certifications

Languages	French/Italian (native speaker), English (full proficiency), German (very good proficiency)
Laboratory skills	Primary cell isolation, cell culture, spheroid formation, hydrogel fabrication, mechanical loading bioreactors, experience with organs-on-a-chip, CRISPR-Cas9 KO, cellular assays (viability, proliferation, senescence, adhesion), GAG and DNA quantification, RNA extraction, RT-qPCR, Western Blot, ELISA, immunocytochemistry, widefield and confocal microscopy
Certifications	FELASA B (certification for animal experimentation), "Good Clinical Practice" basic course
Digital skills	Microsoft Office suite, GraphPad Prism, Endnote, basics of C++, Matlab, COMSOL Multiphysics, ImageJ and Affinity Publisher

Research output list

Publications in peer-reviewed scientific journals

*co-first authorship, #corresponding author

- Wuertz-Kozak K*#, Roszkowski M*, **Cambria E**, Block A, Kuhn G, Abele T, Hitzl W, Drießlein D, Müller R, Rapp MA, Mansuy IM, Peters EMJ, Wippert P (**2020**). Effects of early life stress on bone homeostasis in mice and humans. *Internation Journal of Molecular Sciences, 21(18), 663*
https://doi.org/10.3390/ijms21186634

- **Cambria E**#, Arlt M, Wandel S, Krupkova O, Hitzl W, Passini F, Hausmann O, Snedeker J, Ferguson SJ, Wuertz-Kozak K (**2020**). TRPV4 inhibition and CRISPR-Cas9 knockout reduce inflammation induced by hyperphysiological stretching in human annulus fibrosus cells. *Cells*, 9(7), 1736.
https://www.mdpi.com/2073-4409/9/7/1736

- **Cambria E**#, Brunner S, Heusser S, Fisch P, Hitzl W, Ferguson SJ, Wuertz-Kozak K (**2020**). Cell-laden agarose-collagen composite hydrogels for mechanotransduction studies. *Frontiers in Bioengineering and Biotechnology*, 8, 346.
https://www.frontiersin.org/articles/10.3389/fbioe.2020.00346/full

- Franco-Obregón A*, **Cambria E***, Greutert H, Wernas T, Hitzl W, Egli M, Sekiguchi M, Boos N, Hausmann O, Ferguson SJ, Kobayashi H#, Wuertz-Kozak K# (**2018**). TRPC6 in simulated microgravity of intervertebral disc cells. *European Spine Journal*, 27(10), 2621-2630.
  https://link.springer.com/article/10.1007/s00586-018-5688-8

- Krupkova O#, **Cambria E**, Besse L, Besse A, Bowles R, Wuertz-Kozak K (**2018**). The potential of CRISPR/Cas9 genome editing for the study and treatment of intervertebral disc pathologies. *JOR Spine*, 1(1), e1003.
  https://onlinelibrary.wiley.com/doi/full/10.1002/jsp2.1003

- **Cambria E**, Pasqualini FS, Wolint P, Günter J, Steiger J, Bopp A, Hoerstrup SP, Emmert MY# (**2017**). Translational cardiac stem cell therapy: advancing from first-generation to next-generation cell types. *NPJ Regenerative medicine*, 2(1), 17.
  https://www.nature.com/articles/s41536-017-0024-1

- **Cambria E***, Steiger J*, Günter J, Bopp A, Wolint P, Hoerstrup SP, Emmert MY# (**2016**). Cardiac regenerative medicine: the potential of a new generation of stem cells. *Transfusion Medicine and Hemotherapy*, 43(4), 275-281.
  https://www.karger.com/Article/FullText/448179

- Günter J*, Wolint P*, Bopp A*, Steiger J, **Cambria E**, Hoerstrup SP, Emmert MY# (**2016**). Microtissues in cardiovascular medicine: regenerative potential based on a 3D microenvironment. *Stem cells international*, 2016.
  https://www.hindawi.com/journals/sci/2016/9098523/

- **Cambria E***, Renggli K*, Ahrens CC, Cook C, Kroll C, Krueger A, Imperiali B, Griffith LG# (**2015**). Covalent modification of synthetic hydrogels with bioactive proteins via sortase-mediated ligation. *Biomacromolecules*, 16(8), 2316-2326.

https://pubs.acs.org/doi/10.1021/acs.biomac.5b00549

Contributions to international conferences

Presenter underlined, *co-first authorship

- **Cambria E**, Sadowska A, Haglund L, Krupkova O, Passini F, Hitzl W, Snedeker J, Hausmann ON, <u>Wuertz-Kozak K</u> (**2019**). Expression of TRPV4 in human IVDs and its relevance in stretch-induced inflammation. Oral presentation, *EUROSPINE*, Helsinki, Finland.
  https://link.springer.com/content/pdf/10.1007%2Fs00586-019-06101-2.pdf

- **Cambria E**, Sadowska A, Haglund L, Jaszuczuk P, Passini F, Hitzl W, Snedeker J, Hausmann ON, <u>Wuertz-Kozak K</u> (**2019**). Expression of TRPV4 in human IVDs and its relevance in stretch-induced inflammation. Oral presentation, *ISSLS Annual Meeting*, Kyoto, Japan.
  https://www.issls.org/wp-content/themes/isslsweb/issls_pdf/abstract-book-kyoto-2019-latest.pdf

- <u>**Cambria E**</u>, Passini F, Krupkova O, Hitzl W, Snedeker J, Hausmann ON, Ferguson SJ, Wuertz-Kozak K (**2019**). TRPV4 inhibition reduces stretch-induced inflammation in human intervertebral discs. Oral presentation, *TERMIS EU*, Rhodes, Greece. **Shortlisted for the SYIS oral presentation award**
  https://www.ecmconferences.org/abstracts/2019/Collection3/collection3.pdf

- <u>**Cambria E**</u>, Krupkova O, Boos N, Ferguson SJ, Wuertz-Kozak K (**2018**). TRPV4 in stretch-induced inflammation of intervertebral disc cells. Oral rapid fire and poster presentations, *ECMatrix Summer School*, Zurich, Switzerland.
  https://archiveweb.epfl.ch/ecmatrix.epfl.ch/wp-content/uploads/2018/09/ECMatrix2018_booklet.pdf

- **Cambria E**, Krupkova O, Boos N, Ferguson SJ, Wuertz-Kozak K (**2018**). TRPV4 in stretch-induced inflammation of intervertebral disc cells. Poster presentation, eCM 2018, Davos, Switzerland. https://www.ecmconferences.org/abstracts/2018/Collection3/pdf/collection3_poster.pdf

- Franco-Obregón A, **Cambria E**, Greutert H, Wernas T, Egli M, Sekiguchi M, Boos N, Hausmann ON, Ferguson SJ, Kobayashi H, Wuertz-Kozak K (**2017**). TRPC1 and TRPC6 in mechanotransduction and ageing of intervertebral disc cells. Poster presentation, *SSB+RM 2nd Young Scientist Symposium*, Zurich, Switzerland.

- **Cambria E**, Brunner S, Greutert H, Kobayashi H, Wernas T, Krupkova O, Ferguson SJ, Franco-Obregón A, Wuertz-Kozak K (**2017**). The role of TRP channels in mechanical unloading/loading of intervertebral disc cells. Oral presentation, *ORS PSRS 4th International Spine Research Symposium*, Lake Harmony, USA.

- Olga Krupkova O, Kameda T, Zvick J, **Cambria E**, Wuertz-Kozak K (**2017**). The expression of transient receptor potential (TRP) channels in intervertebral disc cells is regulated by pro-inflammatory cytokines. Poster presentation, *ORS PSRS 4th International Spine Research Symposium*, Lake Harmony, USA.

- Franco-Obregón A, Kobayashi H, Greutert H, Wernas T, Egli M, **Cambria E**, Sekiguchi M, Boos N, Hausmann ON, Ferguson SJ, Wuertz-Kozak K (**2017**). The balance of Transient Receptor Potential Channel TRPC6 to TRPC1 determines ageing and mechanotransduction in intervertebral disc cells. Oral presentation, *TERMIS EU*, Davos, Switzerland. https://www.ecmconferences.org/abstracts/2017/Collection2/pdf/collection2_oral.pdf

- Franco-Obregón A*, Kobayashi H*, Greutert H, Wernas T, Egli M, **Cambria E**, Sekiguchi M, Boos N, Hausmann ON, Ferguson SJ, Wuertz-Kozak K (**2017**). The balance of Transient Receptor Potential Channel TRPC6 to TRPC1 determines ageing and mechanotransduction in intervertebral disc cells. Poster presentation, *ORS Annual Meeting*, San Diego, USA. https://www.ors.org/Transactions/63/0869.pdf

- Renggli K*, **Cambria E***, Ahrens CC, Cook C, Imperiali B, Griffith LG (**2015**). Covalent modification of synthetic hydrogels with bioactive proteins via sortase-mediated ligation. Oral presentation, *250th American Chemical Society National Meeting & Exposition*, Boston, USA

- Renggli K, Maurissen TL, **Cambria E**, Imperiali B, Griffith LG (**2015**). Sortase Mediated Ligation to Covalently Tether Bioactive Proteins to 2D and 3D Hydrogel Systems. Poster presentation, *4th TERMIS World Congress*, Boston, USA. http://doi.org/10.1089/ten.tea.2015.5000.abstracts

Outreach activities

- **Cambria E** (**2018**). TRPV4 in stretch-induced inflammation of human intervertebral disc cells. Oral presentation, *ETHZ, Department of Health Sciences and Technology, Research Day*, Zurich, Switzerland.

- Steiger J, **Cambria E**, Günter J, Wolint P, Bopp A, Hoerstrup S, Emmert M. Generation of therapeutic multi-cellular three dimensional (3D) microtissues (MTs) for cardiac regeneration: Evaluation of the in vitro microenvironment of co-culture MTs. Poster presentation (**2016**), *15th Day of Clinical Research, University of Zurich*, Zurich, Switzerland. http://www.ctc.usz.ch/Documents/Abstracts_15th_DOCR_2016.pdf

- Günter J, Wolint P, Steiger J, **Cambria E**, Bopp A, Hoerstrup S, Emmert M. Biobanking of 3D microtissues for future off-the-shelf regenerative therapies (**2016**). Poster presentation, *15th Day of Clinical Research, University of Zurich*, Zurich, Switzerland. http://www.ctc.usz.ch/Documents/Abstracts_15th_DOCR_2016.pdf

- **Cambria E**, Renggli K, Ahrens C, Cook C, Kroll C, Krueger A, Imperiali B, Griffith LG (**2016**). Sortase-mediated ligation of epidermal growth factor to pre-formed PEG hydrogels for in vitro tissue models. Poster presentation, *15th Day of Clinical Research, University of Zurich*, Zurich, Switzerland. http://www.ctc.usz.ch/Documents/Abstracts_15th_DOCR_2016.pdf

- **Cambria E** (**2015**). Sortase-mediated ligation of epidermal growth factor to pre-formed PEG hydrogels for in vitro tissue models. Guest presentation, *AO Research Institute Davos* https://www.aofoundation.org/-/media/project/aocmf/aof/documents/ari-research-innovation/about/ari-activity-reports/ari_activity_report_2015.pdf?la=en&hash=B374D31A13D8FCA09C8F6E7CBF0B82ECAB21A3 E0

Other artefacts with documented use

*co-first authorship, #corresponding author

- Wuertz-Kozak K*#, Roszkowski M*, **Cambria E**, Block A, Kuhn G, Abele T, Hitzl W, Drießlein D, Müller R, Rapp MA, Mansuy IM, Peters EMJ, Wippert P (**2020**). Effects of early life stress on bone homeostasis in mice and humans. *BioRxiv preprint*. https://www.biorxiv.org/content/10.1101/2020.07.21.214122v1

Submitted but not yet accepted/published publications

*co-first authorship, #corresponding author

- **Cambria E**#, Heusser S, Scheuren A, Tam Wai K, Karol A, Hitzl W, Leung V, Müller R, Ferguson SJ, Wuertz-Kozak K (**2020**). TRPV4 mediates cell damage induced by hyperphysiological compression and regulates COX2/PGE2 in intervertebral discs. *In review*

Unpublished work

- **Cambria E** (**2015**). Sortase-mediated ligation of epidermal growth factor to pre-formed PEG hydrogels for in vitro tissue models. Master Thesis, *École polytechnique fédérale de Lausanne.*